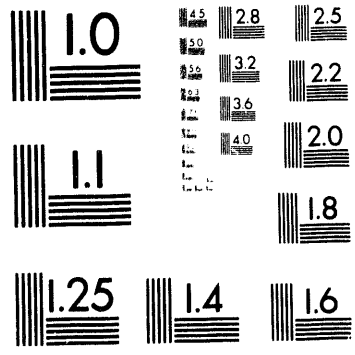
1.0
1.1
1.25
1.4
1.6
1.8
2.0
2.2
2.5
2.8
3.2
3.6
4.0
4.5
5.0
5.6

1 of 3

NUREG/CR-5843
SAND92-0167

CORCON-MOD3: An Integrated Computer Model for Analysis of Molten Core-Concrete Interactions

User's Manual

Manuscript Completed: August 1993
Date Published: October 1993

Prepared by
D. R. Bradley, D. R. Gardner, J. E. Brockmann, R. O. Griffith

Sandia National Laboratories
Albuquerque, NM 87185

Prepared for
Division of Systems Research
Office of Nuclear Regulatory Research
U.S. Nuclear Regulatory Commission
Washington, DC 20555-0001
NRC FIN L1434

ABSTRACT

The CORCON-Mod3 computer code was developed to mechanistically model the important core-concrete interaction phenomena, including those phenomena relevant to the assessment of containment failure and radionuclide release. The code can be applied to a wide range of severe accident scenarios and reactor plants. The code represents the current state of the art for simulating core debris interactions with concrete. This document comprises the user's manual and gives a brief description of the models and the assumptions and limitations in the code. Also discussed are the input parameters and the code output. Two sample problems are also given.

Contents

Contents (continued)

Figures

Tables

Nomenclature

a	Laplace constant ($= [\sigma/g(\rho_l-\rho_g)]^{1/2}$)
A	Area; initial mass concentration of condensing vapor
$[A]$	Aerosol concentration
A_{ij}	Oxide phase interaction parameters
c	Speed of sound in the gas
c_p	Specific heat
C	Cunningham slip correction factor
C_i	Heat capacity of layer i for the new mass at the old temperature
C_{Iwey}	Coefficient used in the boiling heat transfer model
C_{sf}	Coefficient used in the boiling heat transfer model
C_d	Drag coefficient
d	Diameter
D_i	Diffusion coefficient for species i
E	Dimensionless entrainment volume due to bubble bursting
E^*	Dimensionless droplet entrainment flux
f	Fraction of evolved gas entering bubbles
fef_i	Free energy function for species i
g	Gravitational acceleration (= 9.806 m/s^2)
g_i	Gibbs free energy of species i
G	Gibbs free energy
ΔG	Free energy of formation
h	Convective heat transfer coefficient; specific enthalpy
h_{fg}	Enthalpy of vaporization
h_{ij}	Metal phase interaction parameter
H	Total enthalpy
ΔH	Change in enthalpy; latent heat of fusion
ΔH_{abl}	Heat of ablation
j	Superficial velocity (volumetric flux)
Ja^*	Dimensionless variable in Equation (64)
k	Thermal conductivity; Boltzmann's constant
K	Extinction coefficient
$K_{eff,i}$	Effective rate constant for formation of vapor species i
$K_{g,i}$	Gas phase mass transport coefficient
$K_{m,i}$	Rate constant for condensed phase mass transport
$K_{v,i}$	Vaporization rate constant
Ku	Dimensionless number in the Kutateladze correlation
ℓ	Liquid layer thickness
L	Characteristic length; layer thickness; radiation path length
m	Mass
M	Morton number ($= g\mu^4\Delta\rho/\rho^2\sigma^2$)
M_i	Molecular weight of species i
n	Number concentration of aerosol particles
N	Number of size segments used to describe the aerosol particle size distribution
N_A	Avogadro's number (6.023 x 10^{23} atoms/mole)
N_k	Number of moles of species k
$N(\mu_g)$	Dimensionless gas viscosity
Nu	Nusselt number (= hL/k)
p	Pressure

Nomenclature

P	Power
P_i	Partial pressure of species i
P^*	Product of partial pressure times fugacity coefficient
Pr	Prandtl number ($= \mu c_p/k$)
q	Heat flux
Q	Heat flow
Q^*	Heat transfer enhancement factor
r	Radius; radial coordinate
R	Radial melt dimension
R_o	Universal gas constant
Ra	Rayleigh number ($= g\beta\Delta TL^3/\nu\alpha$)
Re	Reynolds number ($= \rho uL/\mu$)
s_i	Specific entropy of species i
$\dot{s}$	Surface recession rate (ablation rate)
S	Volumetric heat source
Sh	Sherwood number ($= K_{m,i}d/D_i$)
t	Time
Δt	Timestep
T	Temperature
δT	Temperature correction
ΔT	Temperature difference; temperature change
u	Flow velocity in the film
U	Velocity of rising bubbles
v_d	Droplet settling velocity
v_i	Molar volume of species i
V	Volume
V_{tr}	Transition gas velocity
W_{ij}	Metal phase interaction parameter
W_j	Weight fraction of species j
We	Weber number ($= U^2 d\rho_f/\sigma_f$)
x	Spatial location
x_s	Position of concrete surface
x_i	Mole fraction of species i
X	Position of solidification and melting fronts; enthalpy change in temperature units
z	Axial (vertical) coordinate

Greek

α	Thermal diffusivity; gas volume fraction; parameter in melt radius solution
α_d	Droplet volume fraction
α_D	Coefficient for aerosol removal by diffusion
α_I	Coefficient for aerosol removal by impaction
α_S	Coefficient for aerosol removal by sedimentation
β	Thermal expansivity
γ	Temperature difference ratio
γ_i	Activity coefficient for species i
δ	Film thickness
ϵ	Emissivity
η	Dimensionless gas velocity
θ	Wall inclination
λ	Melting and solidification constants
μ	Dynamic viscosity; mean particle size
μ_k	Chemical potential of species k
ν	Kinematic viscosity
ξ	Normalized excess bubble volume

ρ	Density
ρ_{molar}	Molar density of the condensed phase
σ	Surface tension; geometric standard deviation of aerosol particle size distribution
σ_B	Stefan-Boltzmann constant (= 5.668 x 10^{-8} $W/m^2 K^4$)
ϕ	Volume fraction solids in a slurry
Φ	Flux
ψ_k	Volume fraction of species k
ω	Dimensionless bubble volume
Ω	Implicitness factor (fully explicit = 0; fully implicit = 1)

Subscripts

a	Based on the Laplace constant; atmosphere
abl	Ablation
A	Atmosphere
b	Bubble
B	Bubbling film; bottom
c	Concrete; convective
cln	Coolant
conv	Convective
crit	Critical
CHF	Critical Heat Flux
d	Droplet
e	Elemental; entrainment; equivalent
eff	Effective
enter	Entering
eq	Equilibrium
f	Fluid
F	Film
fg	Vaporization
g	Gas phase
gas	Gas sparged
i	ith species or layer
in	Incoming
I	Interface
ℓ	Liquid phase
leave	Leaving
liq	Liquidus
L	Laminar; layer; condensed phase
Leid	Leidenfrost (film collapse) point
m	Melting; mixture
max	Maximum
mp	Melting point
o	Overall
out	Outgoing
p	Pool; Aerosol particle
pen	Penetration
r	Radiative; radial
react	Chemical reactions
rel	Relative
rise	Rise
R	Radial
rad_{net}	Net radiation
s	Surface; solidification
sat	Saturation

sol	Solidus
source	Decay heat source
stable	Stable thermal gradient
sub	Subcooled
sur	Surroundings
S	Stokes
tot	Total
T	Turbulent; top
tr	Transition
unstable	Unstable thermal gradient
w	Ablating concrete surface (wall)
z	Axial
0	Initial
1	Initially molten phase; component 1 of binary mixture
2	Substrate; component 2 of binary mixture

Superscripts

k	kth temperature range in thermal equation of state
ℓ	Liquid; liquidus
m	Melting state
n	nth time level
o	Undisturbed or unperturbed state
s	Solid; solidus; slag
xs	Excess
~	Projected
^	Property for new composition at old temperature

1.0 Introduction

A proper assessment of the risks to the public associated with the operation of nuclear power plants requires a realistic evaluation of the important accident sequences. The Reactor Safety Study[1] demonstrated that the risks associated with light water reactors (LWRs) are dominated by core meltdown sequences. In these hypothetical accident sequences, loss of normal and emergency cooling systems leads to melting and slumping of the core. If uninterrupted, this is followed by failure of the pressure vessel and deposition of molten core and associated structural materials onto the concrete floor of the reactor cavity.

The interaction of the resulting pool of debris with the concrete has been identified as an important part of the accident sequence. The debris is maintained at elevated temperatures by decay heat from non-volatile fission products retained in the melt. The temperatures and heat fluxes involved are sufficient to decompose and ablate concrete; such attack could fail containment by basemat penetration. This would result in a release of radioactive materials to the soil underneath the reactor building.

Potentially more important are the various mechanisms which can lead to above-ground failure of containment and release of radioactive materials to the atmosphere. The most obvious of these involve the large amounts of water vapor and carbon dioxide which are produced by the decomposition of concrete. These gases can then be reduced to hydrogen and carbon monoxide in chemical reactions with the core debris. (Small quantities of hydrocarbons and other species are also formed.) All four major gases contribute to the risk of eventual overpressurization of containment. Hydrogen and carbon monoxide are also combustible, presenting an additional risk of sudden overpressurization if they are ignited. Also, ablative attack may cause the failure of internal structures in the containment building such as the reactor pedestal in a boiling water reactor (BWR); the resulting mechanical disruption could fail the containment itself. Finally, heat from the debris may be sufficient by itself to cause the failure of containment. This might happen, for example, by degradation of the containment penetration seals in a BWR or by overheating of the drywell liner in a BWR Mark I containment.

The CORCON-Mod3 computer code was developed to mechanistically model the important core-concrete interaction phenomena, including those phenomena relevant to the assessment of containment failure and radionuclide release. The code is sufficiently flexible that it can be applied to a wide range of severe accident scenarios, and reactor plants. As such, the code represents the current state of the art for simulating core debris interactions with concrete.

1.1 Historical Background

A research program to investigate molten core/concrete interactions was initiated at Sandia National Laboratories in July 1975, under the sponsorship of the Reactor Safety Research Division of the U.S. Nuclear Regulatory Commission. This program was initially experimental, but its scope was soon broadened to include the development of computer models to describe the interactions. A preliminary model, based on limited data and using untested assumptions, was quickly developed by W. B. Murfin in 1977.[2] This model, INTER1, was intended as a qualitative tool, suitable for sensitivity studies; its use for quantitative prediction was specifically discouraged by its author.[2]

Following the release of INTER1, work was begun on development of an improved computer code, CORCON. This program was intended to provide a more detailed--and more mechanistic--description of the physical processes involved in molten core/concrete interactions. The first version of the code, CORCON-Mod1,[3] was released in 1981. It lacked models for the freezing of core debris and for interactions between debris and a coolant (water), which limited its applicability to the early stages of accidents involving dry reactor cavities. Later development work has concentrated on removing these limitations. Also, as experience with the code accumulated, several deficiencies in the existing modeling became apparent and improvements were made to correct them.

It was decided that CORCON-Mod1 would be supported as originally issued. That is, errors which prevented the code from performing as intended (as indicated by the users manual) would be corrected, but improved models would not be issued until an entirely new version of the code was completed. In the second version of the code, CORCON-Mod2,[4] the restrictions mentioned above were removed by the inclusion of freezing and coolant models. Heat transfer and viscosity models were improved, and the code was brought into conformity with the 1977 ANSI standard for FORTRAN programming.[5] CORCON-Mod2 was released in 1984.

Since its release, CORCON-Mod2 has been used extensively to analyze core-concrete interaction experiments, such as SURC-4,[6] and to analyze core-concrete interactions in various severe accident scenarios. It is incorporated in the systems-level codes CONTAIN[7] and MELCOR,[8] which are used to analyze containment response and overall accident progression, respectively.

This experience with CORCON-Mod2 and the improved knowledge of core-concrete interactions gained since the release of the code, have revealed some deficiencies in CORCON-Mod2. For example, the difficulties encountered by core-concrete interaction codes in simulating the results of International Standard Problem 24 (ISP-24),[9] which is based on the SURC-4 experiment,[6] revealed the need to include condensed-phase chemical reactions and improved heat transfer models.

In CORCON-Mod3, many of the deficiencies previously identified have been removed, and several significant new features have been added. A summary of model improvements and additions is provided in Section 1.3 of this report.

1.2 Broad Capabilities of CORCON-Mod3

CORCON is a general computational model describing the interactions between molten core materials and concrete in LWRs. The molten core debris is assumed to lie in an axisymmetric concrete cavity, with gravity acting parallel to the axis of symmetry. Several standard concretes may be used, or the user may specify a non-standard concrete. Coolant (water) may be present. The user also may specify addition of core material and/or coolant as a function of time.

The model includes heat transfer between the corium and the concrete and between the corium and the atmosphere. If coolant is present, then the heat transfer from the corium to the coolant, and from the coolant to the atmosphere, is modeled.

For heat transfer between the corium and the concrete, the user may select to model the interfacial region as a gas film or a slag film. Heat transfer across the gas film is by combined radiation and convection (the models in the code are identical to those used in CORCON-Mod2). The model for heat transfer across the slag film is based on analysis of transient slag and crust growth at the interface during intermittent contact between the corium and the concrete. Convective heat transfer between the bulk melt and the film (gas or slag) is modeled using heat transfer correlations derived for boiling and gas barbotage.

The heat transfer model for the coolant includes a representation of the full pool boiling curve. The effect of ambient pressure is included in the models for film, nucleate, and transition boiling. The effect of coolant subcooling is included in the nucleate boiling model, while the effects of subcooling and gas barbotage are included in the film boiling models. The transition boiling regime is treated using a log-linear interpolation between the critical heat flux and the Leidenfrost points.

Models have been added to simulate the mixing between corium layers which occurs via droplet entrainment. Melt stratification via de-entrainment has been added as well. The user may choose to disable the mixing calculation, forcing the corium to remain stratified into distinct oxidic and metallic layers. Here, as in CORCON-Mod2, the layering configuration is determined by the relative densities of the layers.

Both gas-phase and condensed-phase chemical reactions are modeled. The model assumes chemical equilibrium between the oxides, metals, and gases in each layer containing metals. Chemical reactions between gases and oxides in a purely oxidic layer are not treated. The user may disable the oxide-metal condensed phase reactions if desired.

CORCON-Mod3 models the generation of aerosols and the release of radionuclides using the VANESA model,[10] which has been fully integrated into the code. The VANESA model, which was developed originally as a stand-alone code, treats aerosol generation by vaporization and by mechanical processes (e.g., bubble bursting). Kinetic limitations to the vaporization process are considered. VANESA also models aerosol removal by an overlying water pool.

CORCON-Mod3 includes a much broader range of user options than were available in CORCON-Mod2. Through input the user can modify many of the more important models and parameters in the code. This capability allows the code to be applied to a broader range of accident conditions. It also allows the user greater flexibility in modeling uncertain phenomena.

The features described above allow CORCON-Mod3 to model a wide range of core-concrete interaction phenomena and allow the code to be used to simulate the effects of core-concrete interactions in a wide range of severe accident scenarios. CORCON-Mod3 is a state-of-the-art computer code for simulating the interaction of molten core debris with concrete in LWRs.

1.3 Improvements in CORCON-Mod3

Many improvements have been made to CORCON-Mod2 during the development of CORCON-Mod3. Several of

the phenomenological models in CORCON-Mod2 were improved, and several new models were added.

The model improvements include:

- the debris-concrete heat transfer models now allow either a stable gas film or an unstable gas film with intermittent melt-concrete contact,
- the coolant heat transfer model now includes the enhancement of film boiling heat transfer by gas barbotage and coolant subcooling, and
- the models for bubble phenomena (bubble size, rise velocity, and void fraction) have been upgraded to reflect our improved understanding of bubble behavior.

The new models include:

- an integrated version of the VANESA model[10] that includes models for aerosol generation and radionuclide release from the melt, and scrubbing in overlying water pools.
- the models for condensed phase chemical reactions between oxide and metals,
- activity coefficient models for the condensed phases (used in the aerosol generation and radionuclide release calculation),
- an aerosol scrubbing model for subcooled pools, and
- a parametric treatment of core debris spreading across the concrete floor of the reactor cavity.

In addition to these model changes, CORCON-Mod3 provides the user with the capability of modifying a wide range of models and model parameters. This additional flexibility allows the code to be used in a broader range of applications.

The new and improved models are described briefly in Section 2. A more detailed description of the current phenomenological models will be provided in the forthcoming CORCON-Mod3 models and correlations report.

2.0 Brief Descriptions of the Phenomenological Models

2.1 Overview of CORCON Phenomenology

CORCON-Mod3 is a mechanistic computer model that describes the core-concrete interaction phenomena relevant to the assessment of containment failure and radionuclide release. In this section, we present a brief description of the principal interaction phenomena modeled in the code.

A great deal may be understood about core/concrete interactions from a very simple picture. The attack of core debris on concrete is largely thermal in a light-water reactor. Energy is generated in the core debris from radionuclide decay and from chemical reactions, and may be lost either through its top surface or to the adjacent concrete. (In many experimental studies, externally supplied induction or joule heating is substituted for the reactor decay heat.) In either case, so long as the heat source is sufficiently large, the situation rapidly approaches a quasi-steady state where the losses from the core debris balance the internal sources. The partition of internally generated heat between concrete and surface is determined by the ratio of the thermal resistances of the corresponding paths. In this simple view, pool behavior is dominated by conservation of energy, with heat-transfer relations providing the most important constitutive relations.

Under most circumstances, the heat flux to the concrete is sufficient to decompose it, releasing water vapor (adsorbed and from hydroxides) and carbon dioxide (from carbonates), and to melt the residual oxides. The surface of the concrete is ablated at a rate which is typically several centimeters per hour. The molten oxides and molten steel from reinforcing bars in the concrete are added to the pool. The gases are strongly oxidizing at pool temperatures and will be reduced, primarily to hydrogen and carbon monoxide, on contact with metals in the pool. Ultimately the reacted and unreacted gases enter the atmosphere above the pool. These gases may or may not burn immediately, depending on their temperature and on the relative concentrations of oxygen, steam, and combustible gases. Combustion of these flammable gases are an important consideration in the assessment of containment failure during a severe reactor accident. Modeling of these above-pool phenomena is not included in CORCON-Mod3.

Gas released at the bottom of the melt pool rises through it in the form of bubbles. Gas released at the sides of the melt also form bubbles and rise to the surface. At high gas release rates a stable gas film may form at either the bottom or side surfaces. The presence of gas bubbles in the pool increases the volume of the pool, and increases the interfacial area in contact with concrete.

Vaporization of melt constituents into the rising bubbles leads to aerosol generation when these vapors condense in the cooler atmosphere above the melt. Aerosol particles are generated also when the bubbles rupture at the surface of the melt and are entrained by the rising gases. The aerosols that are produced by these processes include both radioactive and non-radioactive species. Radionuclide release during core-concrete interactions can be an important contributor to the radionuclide source term arising from the accident.

Because the concrete thermally decomposes at depths well below the surface, the thermal response of the concrete is complex. The released gases produce internal pressures which drive flows of carbon dioxide, steam, and liquid water through the pores of the concrete. Experiments have shown that at low incident heat fluxes, the concrete may be heated to substantial depths prior to the onset of ablation. At higher heat fluxes, however, penetration of the thermal front will be minimal prior to the onset of ablation. In either case, a steady temperature profile is eventually attained and ablation assumes a pseudo-steady character. Given the high heat fluxes expected during core-concrete interactions, we have always assumed steady state ablation in CORCON. This is true also of CORCON-Mod3.

Experimental evidence[11a,12] shows that the various oxidic species in the melt are highly miscible, as are the metallic species, but that the two groups are mutually immiscible. In the absence of gas bubbling, the core debris will stratify into distinct layers based on their relative densities. A stratified layer configuration has been assumed in previous versions of CORCON.

Mixing of the immiscible layers can occur at high gas fluxes or when the densities of the layers are close.[13] Mixing occurs when droplets of the lower (denser) layer are entrained by bubbles passing through the interface between the layers. Once entrained into the mixture, the droplets will settle out. Therefore, during a core-

concrete interaction, there may be times in which the molten core debris is mixed and other times in which the debris is stratified. CORCON-Mod3 models both entrainment and droplet settling (deentrainment). The user may disable the mixing calculation and force the core debris to remain fully mixed or fully stratified.

If water is present, it will form an additional layer at the top of the pool. Though explosive interactions have been observed when molten material has been poured through water,[14] recent experiments have shown that explosive interactions are unlikely when water is poured onto melts composed of prototypic LWR core materials.[15,16] (The reader should note that there have been experiments in which energetic events have been observed in this configuration.[17,18] However, these were tests using highly superheated metallic melts under vigorous gas sparging. We do not expect these conditions to exist in LWR accidents.) If the water does not react violently with the molten material underneath it, it will provide an enhanced heat sink. This is likely to cool the top of the melt below the solidification temperature, resulting in a solid crust on the surface. It has been suggested that these crusts will progressively fragment and allow water ingression until the core debris is completely quenched.[19] This progressive quenching of the melt has not been observed in any experiments to date. CORCON-Mod3 treats heat transfer to the coolant using pool boiling correlations. It does not allow for either steam explosions or the progressive quenching of a molten pool to a coolable debris bed.

An overlying coolant pool will also trap aerosols generated during the core-concrete interaction. Depending on the depth of the pool and its degree of subcooling, there may be a factor of ten or more reduction in the amount of aerosol released into the containment atmosphere.[15]

As time progresses, the debris pool grows; its surface area increases, and decay heating decreases. Therefore, pool temperatures and heat fluxes decrease, and the possibility of refreezing arises. Substantial freezing of the metallic phase may occur. However, the large internal heating and small thermal conductivity of the oxidic phase prevent the existence of steady crusts more than a few centimeters thick. The bulk of this phase will remain liquid, probably for weeks.[11f]

Coupling between the molten pool and the rest of containment is rather one-sided; the pool serves as a source of mass and energy while being only weakly influenced by conditions in the containment. Containment pressure affects the properties of gases in the pool and of any water over the molten debris. However, the effects on gas-related heat transfer coefficients, on equilibrium gas compositions, and on the temperature and latent heat of the water are relatively small. Heat loss from the top of the molten debris is dominated by radiation to containment structures or to the overlying water. Because of the fourth-power temperature dependence of the radiative flux, this loss is rather insensitive to containment temperatures (unless they are very high). In the absence of a water layer, the optical properties of the atmosphere may become significant. Molecular absorption by atmospheric gases is a relatively small effect,[11f] but aerosol concentrations may be great enough that the atmosphere is optically thick.[11g]

Because CORCON-Mod3 is not intended to serve as a full containment code, no attempt is made to model above-pool structures. The surroundings, temperature, and atmospheric pressure are user-specified and may be given as functions of time. The decrease in radiative heat transfer from the pool surface to the surroundings, associated with atmospheric attenuation by aerosols, is approximately accounted for. The calculation is based on diffusion theory for gray, infinite parallel plates, and an aerosol concentration is calculated internally for the purpose of determining the atmospheric extinction coefficient during the interaction.

2.2 System Components

The principal components of the CORCON system are the core debris, the concrete, and the atmosphere and surroundings above the debris. The code will also treat an overlying coolant pool if one is present. The composition of each component is specified through user input in terms of a "master list" of chemical species. The list, presented in Table 2.1, is divided into four groups: oxidic compounds, metals and other elements, gases, and miscellaneous compounds. As noted in the table, not all of the species in the master list are available to the user for specification of initial compositions. The aluminates (species 12 to 17) are a hold-over from the viscosity modeling of CORCON-Mod1 and are not used in CORCON-Mod3. The fission-product pseudo species (oxides 24 to 28, metal 47 and gases 82 to 83) are used in the decay-heat generation model. The initial fission product composition is determined within the code from the concentration of fission products in the fuel. The fission product composition is then updated during the calculation to account for addition of core material into the reactor cavity and release in the form of aerosols.

Although we believe that the list of available species is more than ample for describing the physical and chemical processes pertinent to the interaction of molten LWR

Table 2.1 Chemical species included in the CORCON master species list†

	Oxides		Metals and other elements		Gases		Miscellaneous
1	SiO_2	43	Fe	63	C(g)	100	H_2O evap
2	TiO_2	44	Cr	64	CH_4	101	H_2O chem
3	FeO	45	Ni	65	CO	102	$CaCO_3$
4	MnO	46	Zr	66	CO_2	103	$Ca(OH)_2$
5	MgO	47	*FpM	67	C_2H_2	104	H_2O cℓn
6	CaO	48	Mn	68	C_2H_4	105-109	Blank
7	SrO	49	C(c)	69	C_2H_6		
8	BaO	50	Al	70	H		
9	Li_2O	51	U	71	H_2		
10	Na_2O	52	Si	72	H_2O		
11	K_2O	53	UAl_3	73	N		
12	$KAlO_2$	54	UAl_2	74	NH_3		
13	$NaAlO_2$	55	Na	75	N_2		
14	$BaAl_2O_4$	56	Ca	76	O		
15	$CaAl_2O_4$	57	**X	77	O_2		
16	$MgAl_2O_4$	58-62	Blank	78	OH		
17	$MnAl_2O_4$			79	CHO		
18	Fe_2O_3			80	CH_2O		
19	Al_2O_3			81	CrO_3(g)		
20	UO_2			82	*$FpMO_2$(g)		
21	ZrO_2			83	*$FpMO_3$(g)		
22	Cr_2O_3			84	Al_2O_2(g)		
23	NiO			85	Al_2O(g)		
24	*$FpMO_2$(c)			86	AlO(g)		
25	*$FpMO_3$			87	OAlH(g)		
26	*FpOx			88	AlOH(g)		
27	*FpAlkMet(c)			89	OAlOH(g)		
28	*FpHalogn(c)			90	AlO_2(g)		
29	Fe_3O_4			91-99	Blank		
30	Mn_3O_4						
31	PuO_2						
32	UO_3						
33	U_3O_8						
34-42	Blank						

*Pseudo species representing four condensed phase fission product groups.

**Inert oxidic species treated as an element "X" in chemical equilibrium calculation.

Aluminates, species 12-17, not used in CORCON-Mod3.

†Actual species names used in the code have all upper case letters and no subscripts (e.g., SiO_2 = SIO2).

core materials (and coolant) with concrete, blank spaces have been left in the list for future additions. Such additions to the list might be required, for example, for treatment of the sodium chemistry associated with core/concrete interactions in Liquid Metal Fast Breeder Reactor (LMFBR) accidents.

The VANESA model was developed using a somewhat simpler description of the melt, and considers only the major condensed phase species. VANESA focussed primarily on gas phase chemistry and it therefore includes a much more extensive species list for the gas phase. The VANESA species list is shown in Table 2.2.

2.2.1 Debris Pool

CORCON models the debris pool as consisting of a number of layers contained in a concrete cavity. These layers are, from bottom up, a heavy (i.e., dense) oxide phase (HOX), a heterogeneous mixture of heavy oxides and metals (HMX), a metallic phase (MET), a heterogeneous mixture of metals and light oxides (LMX), a light oxide phase (LOX), a coolant (CLN), and the atmosphere (ATM). The three-letter mnemonics are useful in describing the pool structure, and have been used in appropriate variable names throughout the code. Layer volumes, including the swelling effects of gas bubbles, determine the elevations of layer interfaces and of the pool surface.

These seven layers are always present in the data structure but may be "empty" in the sense of containing no material. Note that the coolant (CLN) is treated in the same manner as the debris-containing layers.

Many different layer configurations are possible now that CORCON-Mod3 allows for the existence of mixture layers. Mixing, stratification, and density changes resulting from material addition can lead to changes in the layer orientation during a calculation.

If an overlying coolant layer is present, it will form a layer overlying the core debris. The user may specify the presence of a coolant layer at the start of the calculation or may specify addition of coolant at some later time. Currently, water is the only acceptable coolant.

2.2.2 Concrete Cavity

The concrete cavity containing the core debris is assumed to be axisymmetric. Several simple geometries are available to describe its initial shape. The user may specify a cylinder with either a flat base or a hemispherical base. A general (axisymmetric) initial shape may also be defined by specifying the initial position of each body point. The shape of the cavity is represented and tracked by the position of a number of points, termed "body points," on its surface.

The composition of the concrete must also be specified, and may be chosen as one of the three built-in default concretes. These are referred to as "basaltic aggregate concrete," "limestone aggregate common sand concrete," and "limestone aggregate concrete." The compositions of these concretes are given in Table 2.3; they are based on measured compositions reported by Powers.[11b] The solidus and liquidus temperatures for these concretes, also included in internal data, are given in Table 2.4; the user must specify an ablation temperature somewhere between these limits.

Alternatively, provision is made for the user to define a "non-standard" concrete. In this case, the composition and melting range of the concrete must be user-specified, in addition to the ablation temperature. The concrete composition may be specified either in terms of $CaCO_3$ and $Ca(OH)_2$, or in terms of their decomposition products, CaO, CO_2, and H_2OCHEM (chemically bound water). The latter form is used internally, with the code performing the conversion if necessary.

Steel reinforcing bar in the concrete is also permitted; if present, it is assumed to be pure iron (Fe). Alternatively, CORCON-Mod3 allows the user to specify the composition of the rebar to be something other than iron. This option was included to enable the user to simulate experiments with zirconium rods embedded in the concrete.[20] Concrete, with or without reinforcing rods, is treated as a homogeneous material.

2.2.3 Atmosphere and Surroundings

The atmosphere above the pool and its surroundings serve as sinks for mass (evolved gases) and energy (convection and radiation from the pool surface). CORCON-Mod3 contains very simple models for these components. The atmosphere is described by a specified (constant) temperature and (time-dependent) pressure. The surroundings are described by a specified (time-dependent) temperature and (time- or temperature-dependent) emissivity. Within the code, the pool surface (bottom of the atmosphere) is treated as a major computational interface. Very limited information, restricted to mass flows and (linearized) heat transfer relations, is passed across the interface. Thus, because the interface is well-defined and actively used in the stand-alone code, a more detailed above-pool model--or a full containment response code--could be easily

Table 2.2 Chemical species included in the VANESA species list

J	1	2	3	4	5	6	7	8	9	10
I										
1	H_2O(g)	H_2(g)	H(g)	OH(g)	O(g)	O_2(g)	CO_2(g)	CO(g)	NU*	NU*
2	Fe(c)	FeO(c)	Fe(g)	FeO(g)	FeOH(g)	$Fe(OH)_2$(g)	NU	NU	NU	NU
3	Cr(c)	Cr_2O_3(c)	Cr(g)	CrO(g)	CrO2(g)	CrO_3(g)	H_2CrO_4(g)	CrOH	$Cr(OH)_2$	NU
4	Ni(c)	NiO(c)	Ni(g)	NU	NiOH	$Ni(OH)_2$	NiH	NU	NU	NU
5	Mo(c)	NU	Mo(g)	MoO(g)	MoO_2(g)	MoO_3(g)	H_2MoO_4(g)	$(MoO_3)_2$	$(MoO_3)_3$	MoOH
6	Ru(c)	NU	Ru(g)	RuO(g)	RuO_2(g)	RuO_3(g)	RuO_4(g)	RuOH	$Ru(OH)_2$	
7	Sn(c)	NU	Sn(g)	SnO(g)	SnOH(g)	$Sn(OH)_2$(g)	SnTe(g)	SnH	SnH_4	Sn_2
8	Sb(c)	NU	Sb(g)	NU	SbOH(g)	$Sb(OH)_2$(g)	Sb_2(g)	Sb_4(g)	SbTe(g)	SbH_3
9	Te(c)	NU	Te(g)	TeO(g)	TeO_2(g)	Te_2O_2(g)	TeOH	$TeO(OH)_2$(g)	Te_2(g)	H_2Te(g)
10	Ag(c)	NU	Ag(g)	AgO(g)	AgOH(g)	$Ag(OH)_2$(g)	AgTe	AgH	Ag_2	Ag_3
11	MnO(c)		Mn(g)	MnO(g)	MnH	MnOH(g)	$Mn(OH)_2$(g)	NU	NU	NU
12	CaO(c)	NU	Ca(g)	CaO(g)	CaOH(g)	$Ca(OH)_2$(g)	CaH	Ca_2	Nu	NU
13	Al_2O_3(c)	NU	Al(g)	AlO(g)	AlOH(g)	Al_2O(g)	AlO_2(g)	Al_2O_2(g)	$Al(OH)_2$(g)	AlO(OH)(g)
14	Na_2O(c)	NU	Na(g)	NaOH(g)	NaO(g)	$Na_2(OH)_2$(g)	NaH(g)	Na_2(g)	NU	NU
15	K_2O(c)	NU	K(g)	KOH(g)	KO(g)	$K_2(OH)_2$(g)	KH(g)	K_2(g)	NU	NU
16	SiO_2(c)	NU	Si(g)	SiO(g)	SiO_2(g)	SiOH(g)	$Si(OH)_2$(g)	SiH	SiH_4	Si_2
17	UO_2(c)	NU	U(g)	UO(g)	UO_2(g)	UO_3(g)	H_2UO_4(g)	UOH	$U(OH)_2$	NU
18	ZrO_2(c)	Zr(c)	Zr(g)	ZrO(g)	ZrO_2(g)	ZrOH(g)	$Zr(OH)_2$(g)	ZrH	NU	NU
19	Cs_2O(c)	NU	Cs(g)	CsOH(g)	CsO(g)	$Cs_2(OH)_2$(g)	Cs_2O(g)	Cs_2(g)	CsH	CsO_2
20	BaO(c)	NU	Ba(g)	BaO(g)	BaOH(g)	$Ba(OH)_2$(g)	BaH	NU	Nu	Nu
21	SrO(c)	Nu	Sr(g)	SrO(g)	SrOH(g)	$Sr(OH)_2$(g)	SrH	NU	NU	NU
22	La_2O_3(c)	NU	La(g)	LaO(g)	LaOH(g)	$La(OH)_2$(g)	La_2O	$(LaO)_2$	NU	NU
23	CeO_2(c)	NU	Ce(g)	CeO(g)	CeOH(g)	$Ce(OH)_2$(g)	CeO_2	$(CeO)_2$	NU	NU
24	NbO(c)	NU	Nb(g)	NbO(g)	NbOH(g)	$Nb(OH)_2$(g)	NbO_2(g)			
25	CsI(c)	NU	CsI(g)	I(g)	HI(g)	I_2(g)	IO	NU	NU	NU

*NU = Not Used

Table 2.3 Chemical compositions of default concretes (Values in w/o)

Species	Species no.	Basaltic aggregate concrete	Limestone aggregate - common sand concrete	Limestone aggregate concrete
SiO_2	1	54.84	35.80	3.60
TiO_2	2	1.05	0.18	0.12
MnO	4	0.00	0.03	0.01
MgO	5	6.16	0.48	5.67
CaO	6	8.82	31.30	45.40
Na_2O	10	1.80	0.082	0.078
K_2O	11	5.39	1.22	0.68
Fe_2O_3	18	6.26	1.44	1.20
Al_2O_3	19	8.32	3.60	1.60
Cr_2O_3	22	0.00	0.014	0.004
CO_2	66	1.50	21.154	35.698
H_2O evap	100	3.86	2.70	3.94
H_2O chem	101	2.00	2.00	2.00

Table 2.4 Melting ranges of default concretes

Concrete	Temperature (K) Solidus	Liquidus
Basaltic Aggregate	1350	1650
Limestone Aggregate-Common Sand	1420	1670
Limestone Aggregate	1690	1875

substituted. This is typically what is done when integrating CORCON into integral accident analysis codes such as CONTAIN[7] and MELCOR.[8]

Heat transfer from the pool surface is by convection and radiation with the latter mode ordinarily dominant. Convective heat transfer is calculated using the temperature of the atmosphere while radiative heat transfer uses the temperature of surrounding surfaces. If desired, CORCON-Mod3 computes atmospheric aerosol concentration for the purpose of estimating the optical thickness of the cavity atmosphere above the pool.

2.3 Physical Processes

A number of physical processes are included in the modeling of molten-fuel/concrete interactions; these include internal energy generation, mass and heat transfer, chemical reactions, concrete response, and bubble phenomena. The models are described in the following subsections. The level of detail is intended to be sufficient for understanding of the basic concepts and the code implementation; for details, the reader should consult the references.

In several cases, one or more phenomena are tightly coupled and must be considered simultaneously. For example, concrete response determines gas generation, which affects heat transfer and the heat flux to concrete, which in turn feeds back to determine concrete response. We will note such coupled interactions in the discussion which follows.

2.3.1 Energy Generation

The entire fuel/concrete interaction process is driven by decay heat generated in the pool, including actinides, decay products and irradiated structural materials. Because of the loss of some of the more volatile fission products before the pool is formed (i.e., during the in-vessel core melt progression), use of the ANS Standard decay curve is not appropriate. While decay heating could be calculated using detailed decay chains, as described in the Users' Manual for CONTAIN,[7] the isotopic information is not needed for fission-product tracking in CORCON-Mod3. Therefore, we have included a much simpler decay heat model in the code.

Bennett[a] has shown that the decay power for typical reactor cores in the 1-hour to 10-day time-frame is nearly proportional to operating power and relatively insensitive to burnup. Therefore, a SANDIA-ORIGEN[21] calculation was performed for a reference core representative of a large PWR core at equilibrium burnup (3320 MWt and 33000 MWD/ MTU). From the results of this calculation, we identified 27 elements (excluding noble gases) which account for essentially all the heat production in the reference core in the time-frame of interest. We assume that the initial intact-core inventory is proportional to core operating power, as specified by the user. The initial pool inventory of fission products is then determined by the fraction of the core contained in the melt, as given by the mass of UO_2 and the user-specified core size, multiplied by a "retention fraction" for each element. (Note that as a result of this scheme, UO_2 must be present for decay heat to be represented.) These retention fractions account for partial loss of the more volatile species during the in-vessel melt progression phase. The elements, their assumed chemical forms[b] and concentrations in the core, and the default retention fraction for each species[l] are given in Table 2.5. The retention fractions may be overridden by the user if desired.

The radionuclide release model in the code requires the initial fission product composition of the core debris to be specified. The user has two options for specifying the fission product composition. The default is to use the fission product composition determined for the decay power calculation. As another option, the user may specify the fission product composition. This option is useful when performing experiment simulations since the melt has a given composition of fission product simulants.

The decay power is calculated using the further assumption that the specific decay power (W/g-atom) associated with each element is a simple function of time after SCRAM. The values of the decay power associated with each element (also taken from the reference SANDIA-ORIGEN calculation) are tabulated at eight time points: 0.5, 1.0, 2.0, 4.0, 10.0, 24.0, 72.0, and 240 hours. A power-law interpolation (i.e., log-power is assumed to be linear in log-time) is then used to determine the decay power at intermediate times. If needed, the decay power may be extrapolated to earlier or later times.

[a] Bennett, D. E., "Power Level-Burnup Parametric Study," memorandum to M. Berman, Sandia National Laboratories, Albuquerque, NM, September 10, 1979.
[b] Powers, D. A., private communication, 1980.

Table 2.5 Decay-heat elements and groupings

Pseudo-element	Element	Mass concentration [g-atom/MW (thermal)]	Retention fraction
FpM			
Metals	Mo	.6053	.97
	Tc	.1545	.97
	Ru	.3885	.97
	Rh	.0690	.97
	Sb	.00244	.85
	Te	.0627	.85
FpOx			
Monoxides	Sr	.2155	.90
	Ba	.1915	.90
Dioxides	Zr	.7352	.99
	Ce	.3870	.99
	Np	.0422	.99
	Cm	.00204	.99
	Nb	.01139	.99
	Pu	.7921	.99
	Am	.00593	.99
Sesquoioxides	Y	.1099	.99
	La	.1662	.99
	Pr	.1446	.99
	Nd	.4638	.99
	Sm	.0539	.99
	Eu	.01705	.99
FpAlkMet			
Alkali Metals	Rb	.0819	.19
	Cs	.3776	.19
FpHalogn	Br	.00530	.10
Halogens	I	.0320	.10
UO_2	U	user input	
Zr, ZrO_2	Zr (structural)	user input	

There may be further losses from the melt during the interaction due to further vaporization and to mechanical sparging and aerosol generation driven by concrete decomposition gases. The user has two options for determining release from the melt: a complete radionuclide release and aerosol generation calculation using the VANESA model, or the simple release model employed in CORCON-Mod2 and retained in CORCON-Mod3. The detailed treatment in the VANESA model is described in Section 2.3.14 and will not be discussed here. The simple CORCON-Mod2 model is discussed below.

CORCON-Mod2 considered only vaporization of alkali metals and halogens. It is extremely unlikely that either group will be present in elemental form because the alkali metals boil (at one atmosphere) slightly below 1000 K and the halogens boil below 500 K. The halogens will probably be present as alkali halides (e.g., CsI) with boiling points of 1500 to 1600 K. Under ordinary conditions, the melt will contain more alkali metal than halogen; the excess will most probably occur as hydroxides with boiling points comparable to the halides. However, the retention fractions may be specified such that the amount of halogen present exceeds the amount of alkali metal. If this occurs, the model in CORCON-Mod3 will eliminate the excess halogen during initialization; an appropriate message is written to the output file. The remaining halogens and alkali metals are then removed exponentially in time with an arbitrary but reasonable half-life of 10 minutes. Except in the decay power model, the fission products and actinides are grouped as four pseudo elements, as follows:

FpM - metals which may oxidize, and whose oxides may volatilize

FpOx - chemically inert oxides

FpAlkMet - alkali metals

FpHalogn - halogens.

Thus, the composition of the melt is represented in terms of these four pseudo elements which are resolved into actual elements only for the calculation of decay power.

2.3.2 Melt/Concrete Heat Transfer

Heat transfer between molten core debris and reactor cavity concrete is controlled by the bubbling of concrete decomposition gases through the melt. This process is similar to nucleate boiling or gas barbotage except that at the interface between the core debris and the concrete, gas is being released coincident with melting of the concrete surface. The molten concrete is miscible in molten oxidic core debris, but is immiscible in metallic core debris. At bubble departure, drops of concrete slag are displaced from the surface of the concrete by the buoyancy of the concrete slag in the denser molten core material and the suction caused by the low pressure region in the wake of the rising bubbles.

Coincident with gas bubbling and concrete melting at the interface, the molten core debris may begin to solidify as a crust adjacent to the melting concrete surface. This crust may be stable or unstable depending on its growth rate, its strength properties, and the disruptive forces acting to destabilize it. If the crust is unstable, it will fragment and be carried away by the rising bubbles. If the crust is stable, it will continue to grow at a rate determined by the local energy balance. Eventually, it may provide a barrier to the flow of gases and concrete slag. If this occurs, the flow of gas and slag will then be parallel to the concrete surface.

At extremely high gas generation rates, it may be possible to form a stable gas film at the melt-concrete interface. This is the description assumed in previous versions of CORCON. When a stable film is present, heat transfer across the film is by combined radiation and convection.

In order to adequately represent melt/concrete heat transfer in the cases described above, models are required for bubble-driven heat transfer, slag layer growth and removal, crust growth and stability, and heat transfer across a stable film. Models for bubble-driven convection heat transfer are described in Section 2.3.2.1. The models for interfacial heat transfer phenomena are discussed in Section 2.3.2.2.

2.3.2.1 Bulk Pool Heat Transfer

Heat is removed at the boundaries of the pool, which are its top surface and its interface with concrete.
As discussed in Section 2, the internal temperature of the pool adjusts quickly so that these heat losses balance the internal heat generation, and the heat transfer approaches a steady state. Therefore, we use quasi-steady models for heat transfer in CORCON-Mod3. The principal advantage of quasi-steady models is that heat fluxes at any time depend on the current state of the pool and not on its history. For example, fully developed flow is assumed in convective correlations and the temporal development of boundary layers is not considered.

In CORCON-Mod3 we employ a multi-layered pool model (Section 2.2.1) for which it is convenient to consider heat transfer one layer at a time. Given a trial

set of interfacial temperatures, a solution is found (independently) for each layer. Newton's iteration is then used to revise the interfacial temperatures to satisfy the requirement that the heat flux must be continuous at all interfaces between layers. The solutions for the individual layers are repeated at each step. The heat-transfer model allows for several possible configurations in each layer: the layer may be completely molten, it may have a solid crust on one or more surfaces, or it may be completely solid. In this section, we will address heat transfer in a liquid layer or the liquid portion of a partially-solidified layer. The modifications necessary to account for crusting or freezing will be described in the next section.

Heat transfer coefficients are required from the interior of a liquid layer to its surfaces. If the layer were a right circular cylinder, there would be three such coefficients: to the upper, lower, and radial surfaces. In CORCON-Mod3, these three heat transfer coefficients are evaluated for a cylinder whose thickness and volume match those of the layer. Boundaries with other layers are assumed to be horizontal, and the corresponding heat transfer coefficients employed directly. For the boundary with concrete, an appropriate combination is constructed, as described in Section 2.3.2.2, to account for the actual inclination of the surface.

The analysis includes the effects of the passage of concrete decomposition gases through the liquid. Models are included for gas injection at the bottom surface of the melt, and gas agitation along the sides of the melt. The bulk pool heat transfer model in CORCON-Mod3 has evolved from those used in CORCON-Mod1, and CORCON-Mod2. The model in CORCON-Mod1 was based on the correlation recommended by Blottner[22] which was a modification of a correlation by Konsetov.[23] CORCON-Mod2 retained this model for the radial (vertical) surface, but utilized the empirical correlation developed by Ginsberg and Greene[24] for axial (horizontal) interfaces.

Early comparisons between CORCON-Mod2 predictions and the results from experiments demonstrated very clearly that the heat transfer models in the code were not accurate. Because of this, Bradley[25] initiated a reassessment of the heat transfer models in the code. His recommendations formed the basis for selection of the models implemented into CORCON-Mod3.

For the bottom interface of the melt pool, where gas bubbles may be injected from the incoming concrete, the heat transfer coefficient for a liquid layer is calculated using the correlation devised by Kutateladze. The Kutateladze[26] correlation is given by:

$$Nu_a = 1.5 \times 10^{-3}\, Ku^{2/3}\, f(\eta) \qquad (1)$$

where Nu_a is the Nusselt number based on a characteristic length equal to the Laplace constant a,

$$a = \{\sigma_\ell/[g(\rho_\ell - \rho_g)]\}^{1/2} \quad , \qquad (2)$$

Ku is a dimensionless number defined as

$$Ku = \frac{Pr\ p\ j_g}{g\ \mu} \qquad (3)$$

η is a dimensionless gas velocity defined by

$$\eta = j_g/V_{tr} \qquad (4)$$

and $f(\eta)$ is given by

$$f(\eta) = \begin{cases} 1, & \text{if } \eta \le 1 \\ \eta^{-1/2} & \text{if } \eta > 1 \end{cases} \quad . \qquad (5)$$

In these equations, j_g is the superficial velocity for the gas entering the melt, V_{tr} is a transition velocity correlated by

$$V_{tr} = 4.0 \times 10^{-4}\sigma_\ell/\mu_\ell \qquad (6)$$

σ_ℓ is the surface tension of the liquid, ρ_ℓ is the density of the liquid, ρ_g is the density of the gas, p is the pressure at the interface, and Pr is the Prandtl number for the liquid. For many fluids, the transition velocity calculated using the above equation is comparable to the velocity for transition from bubbly to churn-turbulent flow. The heat transfer correlations have been formulated such that alternate equations for the transition velocity can be easily substituted into the model.

In CORCON-Mod3, a smooth transition for Nu_a through the value $\eta = 1$ is effected by using

$$Nu_a = \frac{Nu_{a1}/\eta + Nu_{a2}\,\eta}{1/\eta + \eta} \qquad (7)$$

where Nu_{a1} and Nu_{a2} are defined as follows:

$$Nu_{a1} = 1.5 \times 10^{-3}\, Ku^{2/3}$$
$$Nu_{a2} = 1.5 \times 10^{-3}\, Ku^{2/3}\, \eta^{-1/2} \quad (8)$$

Results from experiments with gas agitation of heated surfaces suggest that heat transfer along vertical walls is less sensitive to the superficial gas velocity than is indicated by the Kutateladze correlation.[27,c] The experiments show also that at high gas velocities convective heat transfer at horizontal and vertical surfaces is nearly the same. These results suggest that a modified form of the Kutateladze correlation should be used for calculating the heat transfer coefficient to the side of a liquid layer. We have chosen, therefore, to represent convective heat transfer along the vertical sidewalls using only the churn-turbulent (i.e., $\eta > 1$) form of the Kutateladze correlation. This form of the correlation depends on the superficial gas velocity raised to the one-sixth power. This dependence is in the range of literature values which indicate a 0.14 to 0.33 dependence on gas velocity.[22,27]

For liquid layers within the melt pool, a correlation devised by Greene[28] is used to calculate the heat transfer coefficient in each layer, except for the uppermost melt layer. Greene's correlation is

$$h = 1.95\, k\, (Re\, Pr)^{0.72}/r_b, \quad (9)$$

where k is the thermal conductivity, Re is the Reynolds number for the liquid based on the characteristic length r_b and the superficial gas velocity j_g, Pr is the Prandtl number for the liquid, and r_b is the average bubble radius in the layer.

For the uppermost melt layer (adjacent to the atmosphere or coolant), the heat transfer coefficient is calculated using a modified form of the Kutateladze correlation (Equation (1)), which accounts for the greater surface area of the unstable surface. For the upper melt surface, the Kutateladze correlation is simply multiplied by an area enhancement derived by Farmer:[29]

$$A^* = 1 + 4.5\, \frac{j_g}{U_b} \quad (10)$$

At sufficiently low gas velocities, heat transfer in molten debris is dominated by natural convection. This process is modeled in CORCON-Mod3 by conventional Nusselt-Rayleigh correlations in the form:[30]

$$Nu = \max\left(0.54\, Ra^{1/4},\ 0.14\, Ra^{1/3}\right), \quad (11)$$

for axial heat transfer in an unstable thermal gradient, and

$$Nu = \max\left(0.59\, Ra^{1/4},\ 0.10\, Ra^{1/3}\right) \quad (12)$$

for radial heat transfer. Here

$$Nu = h\ell/k \quad (13)$$

is the Nusselt number, based on the layer thickness, ℓ, and

$$Ra = g\beta\Delta T\ell^3/\nu\alpha \quad (14)$$

is the Rayleigh number. ΔT is the temperature difference, fluid to boundary. In Equations (11) and (12), the first expression in parentheses corresponds to laminar (low Rayleigh number) convection and the second to turbulent (high Rayleigh number) convection.

The heat transfer coefficient at a surface where the temperature gradient is stable is calculated directly from Equation (12). If the temperature gradient is stable at one interface but unstable at the other, convective flows driven by the unstable gradient steepen the stable gradient. To account for the resulting increase in heat transfer, the heat transfer coefficient for the stable gradient is then calculated from

$$Nu_{stable} = 1 + \left[1 + 2Nu_{unstable}\frac{|\Delta T_{unstable}|}{|\Delta T_{stable}|}\right]^{1/2} \quad (15)$$

Kulacki and co-workers[31-33] have developed correlations for convective heat transfer in internally heated fluid layers. The model in CORCON-Mod3 reproduces the various correlations with a maximum error of 30 percent and an average error closer to 10 percent.[11d]

The natural convection limit is imposed in CORCON-Mod3 by choosing the greater of the Nusselt numbers calculated for bubble-enhanced and for natural convection. The actual implementation assumes that

[c] Greene, G. A., private communication, March, 1991.

Equation (15) may be applied even when $Nu_{unstable}$ is evaluated for bubble-enhanced convection.

For very thin or very viscous layers, the natural convection correlations above can yield smaller heat fluxes than would result from simple conduction. Therefore, an approximate conduction limit is imposed in CORCON-Mod3, in the form of a lower limit in the Nusselt number. The formulation is based on the average temperature of the liquid layer, T, which is consistent with CORCON usage and is normal practice for convective heat transfer. For convection, there is an (usually unstated) assumption that the boundary layers are thin and that the local temperature is essentially equal to the average temperature. The assumption fails at or near the conduction limit, where the temperature profile is quadratic (for a uniform volumetric source). This is the reason that we have chosen an "approximate" limit rather than an "exact" one. A full discussion is contained in Reference 11e.

In the radial direction, the exact conduction result for a quadratic temperature profile is

$$Nu_R + \frac{q_R \ell}{k(T_\ell - T_R)} = \frac{4\ell}{R} \qquad (16)$$

where Nu_R is the Nusselt number based on layer thickness, and R is the average radius of the layer. This provides the desired lower bound on radial heat transfer.

The exact axial conduction result is

$$q_T = 2k\left[T_\ell - T_T + \left(-T_B + 2T_\ell - T_T\right)\right]/\ell \qquad (17)$$

$$q_B = -2k\left[T_\ell - T_B + \left(-T_B + 2T_\ell - T_T\right)\right]/\ell \qquad (18)$$

where the fluxes are positive up, and subscripts "B" and "T" refer to the bottom and top surfaces, respectively. Note that q_B in Equation (17) does not necessarily have the same sign as $(T_B - T_\ell)$ and similarly for q_T and $(T_\ell - T_T)$ in Equation (18), which would greatly complicate an attempt to impose the "exact" limit. In order to avoid this, we have employed the approximations

$$q_T \approx 2k\{T_\ell - T_T + 2\,[\max\,((T_\ell - T_T)(T_\ell - T_B), 0)]^{1/2}\}/\ell \qquad (19)$$

and

$$q_B \approx -2k\{T_\ell - T_B + 2\,[\max\,((T_\ell - T_T)(T_\ell - T_B), 0)]^{1/2}\}/\ell \qquad (20)$$

which have the desired properties, and the same values as Equations (17) and (18) for the limiting cases of no internal heating ($T = (T_B + T_T)/2$) and of large internal heating ($T_B - T_\ell = T_T - T_\ell$). In fact, as discussed in Reference 11e, the approximation errs only in the temperature at which steady state is achieved for given boundary temperatures and volumetric heating. This error is unavoidable if we wish the heat fluxes to have the same sign as the temperature differences. In any case, if the conduction limit in a liquid is reached, the layer must be relatively thin, and the maximum error in the average temperature, one third of the temperature difference across the layer,[11e] must be relatively small. It represents only a minor error in the sensible heat content of the layer and has no other consequences. Equations (19) and (20), rewritten in the form of Nusselt numbers based on layer thickness, are employed in CORCON-Mod3 as lower bounds in the Nusselt numbers in a liquid layer.

2.3.2.2 Interfacial Heat Transfer

At the time CORCON-Mod2 was released, it was assumed that gas release from the decomposing concrete was sufficient to form a stable gas film between the concrete and the debris pool. There was no convincing experimental evidence to support or disprove this assumption. Consequently, CORCON-Mod2 employed a model for melt/concrete heat transfer that assumed the boundary region was dominated by a stable gas film and that on horizontal and nearly horizontal surfaces the Taylor instability leads to formation of bubbles which enter the melt, while on more steeply inclined surfaces the gas forms a flowing film.

Since that time, the assumption of an initially stable gas film has been shown to be incorrect under most realistic accident conditions.[25] Instead, gas release is usually far less than that required to form a stable gas film, and intermittent debris-concrete contact occurs. This intermittent contact results in periodic growth and removal of slag from the interface, and, depending on the temperature of the molten debris, may also lead to periodic growth and removal of debris crusts. Simplified models for these processes have been developed and implemented in CORCON-Mod3. The stable gas film model implemented in CORCON-Mod2 has been retained, and the user can select either the slag or gas film model at the start of a calculation. No transition from one model to the other is included.

The following is a brief discussion of the slag film and gas film models. For further discussion of the slag film model the reader is referred to Reference 25.

Slag Film Model

Simultaneous concrete melting and molten core debris solidification can be modeled using an analysis similar to that used by Epstein[34] to model freezing of molten reactor fuel on the surface of stainless steel cladding. Epstein's model considers four regions: the initially molten phase, the solid substrate, the solidified molten phase crust, and the layer of melting substrate. The energy equation in each of these regions has the form:

$$\frac{\partial^2 T_i}{\partial x^2} = \frac{1}{\alpha_i} \frac{\partial T_i}{\partial t} \tag{21}$$

where T_i is the temperature in region i, α_i is the thermal diffusivity of region i, x is the spatial location, and t is time. (Note that internal heating of the molten phase due to decay heat has been neglected. It can be easily shown that during a bubble cycle, internal energy generation can be neglected.)

The energy equation is solved subject to the following boundary conditions: continuity of temperature at each interface, continuity of heat flux (including effects of phase change) at each interface, and the temperature of the melt and substrate at "infinity" is fixed at the initial temperature of the region.

Given these boundary conditions, the temperature of each of the four regions has the general form:

$$T_i = A_i + B_i \, \mathrm{erf}\left[\frac{x}{2(\alpha_i t)^{1/2}}\right] \tag{22}$$

with the positions of the solidification and melting fronts given by equations of the following form:

$$X_i(t) = 2 \lambda_i (\alpha_i t)^{1/2} \tag{23}$$

In these equations, A_i, B_i, and λ_i are constants determined by applying the boundary conditions.

Application of the boundary conditions results in a set of algebraic equations for the constants. By algebraic manipulation, this set of equations can be reduced to two simultaneous transcendental equations for λ_1 and λ_2. After λ_1 and λ_2 have been determined, the temperature at the interface between the core debris and concrete can be determined from the following equation:

$$\frac{T_i - T_{2mp}}{T_{1mp} - T_{2mp}} = \frac{\mathrm{erf}(\lambda_2)}{\mathrm{erf}(\lambda_2) - \sigma \, \mathrm{erf}(\lambda_1)} \tag{24}$$

where T_i is the interface temperature, T_{1mp} and T_{2mp} are the melting points of the initially molten phase and solid substrate, and σ is the following function of material properties:

$$\sigma = \frac{k_{2m}}{k_{1s}} \left[\frac{\alpha_{1s}}{\alpha_{2m}}\right]^{1/2} \tag{25}$$

where k and α are the thermal conductivity and thermal diffusivity of the respective regions, and the subscripts 1s and 2m refer to the solidifying molten phase and melting substrate, respectively.

Under some conditions, solidification of the molten phase does not occur. The equation for the interface temperature is then derived following the same procedure but with three regions rather than four. The resulting equation for the interface temperature is

$$\frac{T_{10} - T_i}{T_{10} - T_{2mp}} = \frac{\sigma}{\sigma + \mathrm{erf}(\lambda_2)} \tag{26}$$

where T_{10} is the initial temperature of the molten phase, and σ is now based on the thermal conductivity and thermal diffusivity of the molten phase rather than the crust.

The preceding analysis is implemented in CORCON-Mod3 by treating the transient slag layer growth and removal process as a heat transfer resistance in series with convective heat transfer within the molten pool. At the interface between the slag layer and the molten pool

$$h_p (T_p - T_i) = h_s (T_i - T_c) \tag{27}$$

where h is the convective heat transfer coefficient, and the subscripts p, i, c, and s refer to the debris pool, the interface, the concrete surface, and slag layer. The pool heat transfer coefficient is determined using the equations discussed in the preceding section. The concrete surface temperature is simply the user-specified ablation temperature. The interface temperature is determined using the analysis described above. Solving this equation for the slag heat transfer coefficient yields

$$h_s = h_p \frac{T_p - T_i}{T_i - T_c} = h_p \gamma \quad (28)$$

The overall heat transfer coefficient (between the molten debris and the concrete surface) is given by

$$h_o = \frac{h_s h_p}{h_s + h_p} \quad (29)$$

Substituting for h_s into this equation results in

$$h_o = h_p \left(\frac{\gamma}{\gamma + 1}\right) \quad (30)$$

Bradley[25] found that the value of $\gamma/(\gamma+1)$ is relatively insensitive to the material properties of the core debris. Whether the core debris is metallic or oxidic, $\gamma/(\gamma+1)$ was found to fall within a narrow range of 0.29 ± 0.07. In light of the uncertainty in the heat transfer models, we decided to implement the model assuming a constant value of γ. The value of γ corresponding to a value of $\gamma/(\gamma+1)$ equal to 0.29 is 0.41. Hence, the slag heat transfer coefficient is assumed to be given by

$$h_s = 0.41\ h_p \quad (31)$$

Currently, the code provides a lower limit to the slag heat transfer coefficient of 1000 W/m^2 K. This value simulates conduction-limited heat transfer across a thin (1 mm) slag layer. Calculated results should be relatively insensitive to this value since it is likely to be invoked only when a debris crust exists at the interface with the concrete. Therefore, heat transfer would be controlled by conduction through the crust, and the contribution from the slag thermal resistance would be small.

Stable Gas Film Model

For a stable gas film, two models for heat transfer are used, one for nearly horizontal films in which there is essentially no gas flow parallel to the concrete surface, and one for inclined films in which there is gas flow parallel to the concrete surface. A film is classified as "nearly horizontal" if its inclination is less than 15 degrees.

For a stable gas film on a nearly horizontal surface, heat transfer is computed from a mechanistic model based on momentum balance in a Taylor-instability bubbling cell.[35]

The result may be cast in the form of a Nusselt number based on film thickness as

$$Nu_B \equiv \frac{h_B \delta_B}{k_g} = 0.804 \quad (32)$$

where h_B is the heat-transfer coefficient, δ_B is the film thickness, and k_g is the thermal conductivity of the gas. The factor 0.804 is the fraction of the surface not occupied by bubble sites and, therefore, available for heat transfer. The film thickness satisfies

$$\delta_B^3 = 15.05\ Re_B\ L^3 \quad (33)$$

Here L is a material property

$$L = \left[\frac{\mu_g^2}{g\rho_g(\rho_\ell - \rho_g)}\right]^{1/3} \quad (34)$$

where g is the acceleration of gravity, subscripts ℓ and g refer to pool material and film properties, respectively, and

$$Re_B = \frac{\rho_g j_g a}{\mu_g} \quad (35)$$

is the Reynolds number based on the Laplace constant (defined in Equation (2)), and the superficial velocity j_g with which gas enters the film. Note that if the process modeled were really film boiling, the equations would be closed through the relations

$$q = h_B \Delta T = \rho_g j_g h_{fg}^* \quad (36)$$

where h_{fg}^* is the effective heat of vaporization. Relatively simple manipulation can then be used to reduce the present model to a form similar to Berenson's[36] correlation for boiling on a flat plate,

$$h = 0.68 \left[\frac{k_g^3 h_{fg}^* g \rho_\ell (\rho_\ell - \rho_g)}{\mu_g \Delta T (2\pi a)}\right]^{1/4} \quad (37)$$

This bubble model is used for inclinations less than 15 degrees in CORCON-Mod3. Above 30 degrees we use a flowing-film model, and consider both laminar and turbulent films. The transition model used between 15 degrees and 30 degrees will be described later. The film models are mechanistic, based on momentum balances in

an inclined flowing film, with the Reynolds analogy used for heat transfer in the turbulent case. The results, expressed as Nusselt numbers, are

$$Nu_{LF} = h_{LF}\,\delta_{LF}/k_g = 1 \tag{38}$$

for the laminar case and

$$Nu_{TF} = h_{TF}\,\delta_{TF}/k_g = 0.0325\ Pr^{1/3}\ Re_F^{3/4} \tag{39}$$

for the turbulent case. In these equations, Pr is the Prandtl number for the film, and Re_F is the Reynolds number based on film thickness:

$$Re_F = \rho_g\,\bar{u}\delta/\mu_g \tag{40}$$

with $\bar{u}$ the average flow velocity in the film. The film thicknesses satisfy

$$\delta_{LF}^3 = 5.61\ Re_F\ L^3/\sin\theta \tag{41}$$

$$\delta_{TF}^3 = 0.0469\ Re_F^{7/4}\ L^3/\sin\theta \tag{42}$$

where θ is the inclination of the film from the horizontal.

In CORCON-Mod3, we employ a simple transition between the laminar and turbulent flow regimes which will ensure continuity of film thickness and heat-transfer coefficient with the appropriate limits:

$$\delta_F = \max(\delta_{LF},\ \delta_{TF}) \ , \tag{43}$$

$$Nu_F = \max\ (Nu_{LF},\ Nu_{TF}) \ , \tag{44}$$

$$h_F = Nu_F\ k_g/\delta_F \ , \tag{45}$$

where the various film thicknesses and Nusselt numbers have been defined above.

A transition between the bubbling model and the film-flow model is also required. We have incorporated a mechanistic model[11g] based on a momentum balance with a fraction, f, of injected gas going into bubbles and the rest into establishing the film. The results have the form

$$\delta^3 = \delta_F^3 + f(\sin 15°/\sin\theta)\ \delta_B^3 \tag{46}$$

$$h = \left[fNu_B + (1 - f)Nu_F\right] k_g/\delta \ . \tag{47}$$

A transition is achieved by decreasing f linearly with sin θ from 1 at 15 degrees to 0 at 30 degrees.

Because of the high temperatures involved, heat transfer by radiation across the gas film must also be included. The radiative component accounts for about one half of the total heat flux in many CORCON calculations. We use the form for a transparent gas between infinite parallel gray walls

$$q_{rad_{net}} = \frac{\sigma_B\left(T_A^4 - T_w^4\right)}{\left(1/\varepsilon_p + 1/\varepsilon_w - 1\right)} \ . \tag{48}$$

Here σ_B is the Stefan-Boltzmann constant, T_A and T_w are the temperatures of the pool side of the gas film and of the ablating concrete surface, respectively, and ϵ_p and ϵ_w are the corresponding emissivities.

The convective heat-transfer coefficients above involve the superficial velocity of gas entering the interface region and, in film flow regions, the film-wise mass flow. The latter is determined by the entering gas flow at all upstream points. The superficial gas velocity is determined by the concrete response, which is determined by the total heat flux. This, in turn, involves the heat-transfer coefficients themselves. A self-consistent solution has been found advisable for numerical stability; this is obtained through a simple iteration.

Note that $\rho_g u\delta$ is the mass flow per unit width of film, which satisfies

$$\frac{d}{ds}\left(r\rho_g\bar{u}\delta\right) = r(1 - f)\rho_g j_g \tag{49}$$

where r is the local radius of the cavity, s is the path length measured along the film, and f is the interpolation factor which imposes the transition from bubbling to film flow.

We solve this equation by use of a simple predictor-corrector method. An inner iteration, as described above, is required to solve the non-linear (because of radiation) energy balance at each point. In cases where the spacing between body points is too great to resolve the development of the gas film,

intermediate points are considered by the integration routine.

Numerical Solution Technique

Heat transfer through the (slag or gas) film is formulated in terms of the temperatures of its surfaces. On the melt pool side, this temperature, T_A, is determined implicitly by the requirement that the heat flux be continuous. The subroutine SURFEB is used to perform a surface energy balance at the interface between the melt and the film and to evaluate its temperature at each spatial point. The nonlinear equation

$$q_p = q_{rad_w} + h_f (T_A - T_w) \qquad (50)$$

is solved for T_A using Newton's iteration. (Note that the radiation term disappears if the slag film model is selected by the user. This greatly simplifies the solution for T_A.) A complete solution, including the full evaluation of pool-side heat transfer within the iteration loop, would be extremely expensive in computer time because the energy balance is typically performed at hundreds of points along the pool/concrete interface.

The crust formation model in CORCON-Mod3 was developed originally for CORCON-Mod2. This model introduces a discontinuity in behavior when T_A passes through the solidification temperature, T_s. The qualitative dependence of q_p on T_A is shown in Figure 2.1. When T_A is slightly greater than T_s, no crust exists and the derivative dq_p/dT_A is given by a convective heat-transfer correlation. When T_A is slightly less than T_s, a crust must be present. When a crust is present, the derivative is small because a small change in surface temperature merely changes the (steady) crust thickness with very little change in the heat flux. The discontinuity in slope must be accounted for to prevent unphysical results or failure of the iteration which determines T_A.

As in CORCON-Mod2, CORCON-Mod3 uses a piecewise linear approximation to q_p as a function of T_A. There are two cases, as shown in Figure 2.2, depending on whether or not a crust was present (T_A was less than T_s) when within-pool heat transfer was last evaluated. If so, q_p is evaluated as

$$q_p = q_p^{old} + \frac{dq_p}{dT_A}\left(T_A - T_A^{old}\right) , \qquad (51)$$

for $T_A \le T_s$. For $T_A > T_s$, q_p is extrapolated linearly to zero at $T_A = T_M$, where T_M is currently taken as the temperature of the liquid center of the layer. This isillustrated in Figure 2.2A. If, on the other hand, no crust was previously present (T_A was greater than T_s), Equation (51) is used to evaluate q_p for $T_A > T_s$. For $T_A < T_s$, the heat flux q_p is assumed to be constant as shown in Figure 2.2B.

2.3.3 Coolant Heat Transfer

If a coolant layer is present, CORCON-Mod3 calculates boiling heat transfer. The boiling heat transfer model in the code includes the full boiling curve, based on standard pool boiling correlations as summarized by Bergles.[37] Corrections are made for the effects of gas injection at the melt/coolant interface and coolant subcooling. The various correlations involved are not used directly in CORCON-Mod3. This is possible because the boiling heat transfer coefficient for a given fluid, water in this case, is a function of pressure and temperature only, with all of the detailed dependence of material properties on temperature and pressure contained in the one function. A series of calculations was performed outside the code, using thermal and transport properties from the Steam Tables,[38] to generate tables of values. These were then fit by simple analytic forms which reproduce the tables within 3 percent over the pressure range of 10 kPa to 10 MPa (saturation temperatures from 320 K to 580 K). The principal advantage of using these fits is that extensive libraries of water properties need not be included in the code.

Nucleate boiling is treated by using the Rohsenow[39] correlation for the temperature rise and the Zuber[40,41] correlation (with Rohsenow's coefficient)[42] for the critical heat flux to calculate the values of q_{CHF} and of $T_w - T_{sat}$ at the point of critical heat flux (where T_w, as used here, is the temperature of the debris surface). These are represented as

$$q_{CHF} = \frac{1.50 \times 10^6 (10^{-5}p)^{0.415}}{1.0 + 5.97 \times 10^{-3}(10^{-5}p)^{1.117}} \qquad (52)$$

$$(T_w - T_{sat})_{CHF} = \frac{1.71 \times 10^3 \, C_{sf} \, (10^{-5}p)^{-0.112}}{1.0 + 7.02 \times 10^{-8}(10^{-5}p)^{3.181}} , \qquad (53)$$

where all values are in S.I. units (i.e., q is in W/m^2, p is in Pa, and T is in K) and the surface coefficient, C_{sf}, is taken as 0.01. The nucleate-boiling portion of the boiling curve is then represented as

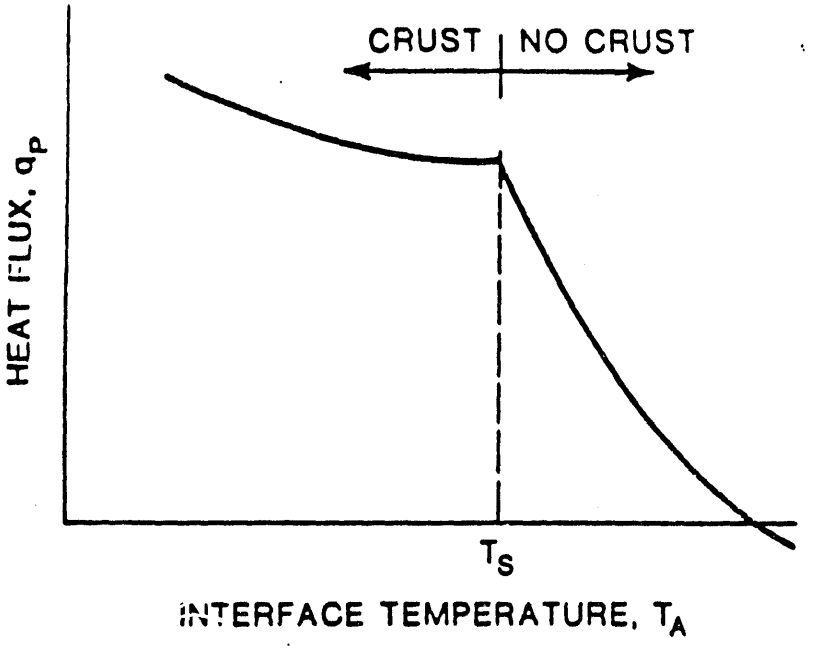

Figure 2.1 Dependence of heat flux on surface temperature

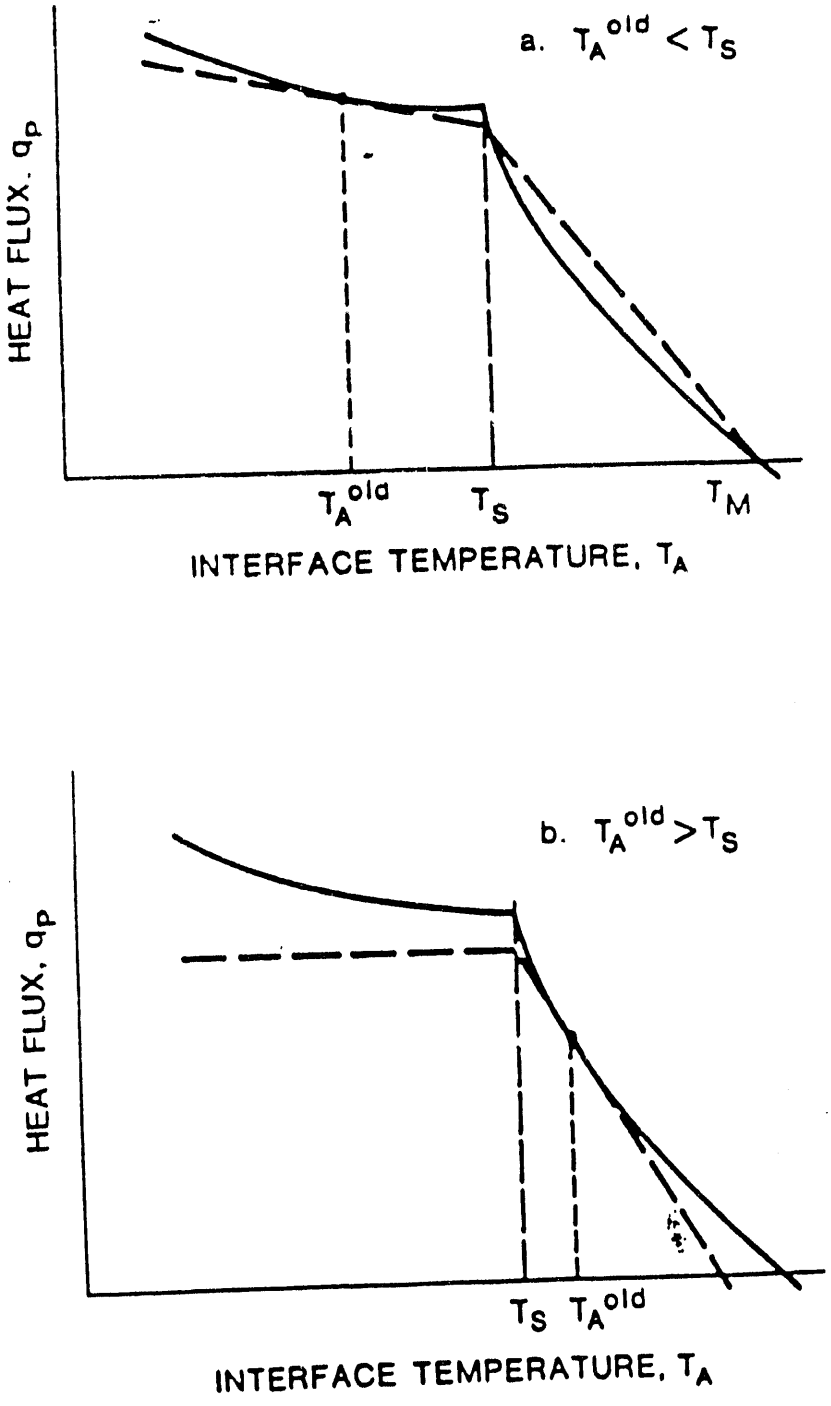

Figure 2.2 Approximation to heat flux as a function of interface temperature

$$q = q_{CHF}\left[(T_w - T_{sat})/(T_w - T_{sat,CHF})\right]^{n} \quad (54)$$

where the exponent is that attributed to Rohsenow in Reference 37.

The effect of subcooling on nucleate boiling is included, using the expression recommended by Ivey:[43]

$$q_{CHF,sub}/q_{CHF,sat} = 1 + C_{Ivey}(T_{sat} - T_b) \quad , \quad (55)$$

where T_b is the bulk temperature of the fluid and the coefficient C_{Ivey} is given by

$$C_{Ivey} = 0.1\left[\frac{\rho_f}{\rho_v}\right]^{3/4}\frac{c_f}{h_{fg}} \quad . \quad (56)$$

This coefficient is calculated as a function of pressure from the fit

$$C_{Ivey} = \frac{4.77 \times 10^{-2}(10^{-5}p)^{-0.683}}{1.0 + 6.29 \times 10^{-3}(10^{-5}p)^{0.862}} \quad . \quad (57)$$

The film boiling regime is based on the Berenson correlations[36] for the heat-transfer coefficient in film boiling and for the temperature difference at the Leidenfrost temperature (minimum film-boiling point). These have been fit for use in CORCON-Mod3 as

$$q_{Leid} = \frac{1.88 \times 10^{4}(10^{-5}p)^{0.894}}{1.0 + 7.58 \times 10^{-3}(10^{-5}p)^{0.956}} \quad (58)$$

and

$$(T_w - T_{sat})_{Leid} = \frac{8.56 \times 10^{1}(10^{-5}p)^{0.848}}{1.0 + 1.38 \times 10^{-1}(10^{-5}p)^{0.750}} \quad . \quad (59)$$

Above the Leidenfrost point, the total heat flux including radiation is represented, in accordance with Reference 37, as

$$q = q_c\,(q_c/q)^{1/3} + q_r \quad . \quad (60)$$

Here q_c is the convective heat flux in the absence of radiation, and the factor $(q_c/q)^{1/3}$ accounts for the fact that the total heat flux contributes to the vaporization rate, which determines the thickness and thermal resistance of vapor film. The heat flux q_c has an explicit variation with temperature as the 3/4 power of $(T_w - T_{sat})$. We assume that this dominates the implicit temperature dependence through material properties, so that q_c may be calculated as

$$q_c = q_{c,Leid}\left[(T_w - T_{sat})/(T_w - T_{sat})_{Leid}\right]^{0.75} \quad . \quad (61)$$

The radiative contribution, q_r, is given for infinite parallel gray walls by

$$q_r = \frac{\sigma_B\left(T_w^4 - T_{sat}^4\right)}{1/\epsilon_w + 1/\epsilon_f - 1} \quad . \quad (62)$$

where ϵ_w is the emissivity of the wall and ϵ_f that of the coolant.

CORCON-Mod3 includes the effects of gas barbotage and coolant subcooling on film boiling heat transfer. Both gas barbotage (i.e., noncondensible gas injection at the interface) and coolant subcooling can greatly increase the film boiling heat flux, while also increasing the temperature at which the vapor film collapses (the Leidenfrost point).

Gas barbotage increases film boiling heat transfer by increasing agitation of the coolant, and by increasing agitation of the melt surface. In CORCON-Mod3, the enhancement to the film boiling heat flux due to gas barbotage is included as a multiplicative factor. The factor used depends on whether the surface underlying the coolant is solid or liquid.

If the surface underlying the coolant is liquid, then the enhancement factor is calculated using a correlation of experimental results advanced by Greene.[d] The experimental results were for freon and water on three different molten metals, bismuth, lead, and Wood's metal. The expression proposed by Greene is

$$Q_f^* = \min\left\{1 + 11.85\left[\frac{j_g^*}{Ja^*}\right]^{0.91}\left(1 + 2j_g^*\right),\ 5\right\} \quad (63)$$

where Q_f^* is the ratio of the measured heat flux to the heat flux calculated using the Berenson correlation, $j_g^* = j_g/U_\infty$, j_g is the superficial gas velocity, U_∞ is the terminal rise velocity of the noncondensible gas bubbles in the liquid metal, and Ja^* is defined by

[d] Greene, G. A., private communication, February, 1990.

$$Ja^* = \frac{c_{p,v}\,\Delta T_{sat}}{h_{fg} + 0.5 C_{p,v}\,\Delta T_{sat}} \quad (64)$$

where ΔT_{sat} is the wall superheat $T_T - T_{sat}$, and $c_{p,v}$ is the specific heat of the vapor at constant pressure.

If the surface underlying the coolant is solid, then the enhancement factor is calculated using a correlation advanced by Duignan.[44] This correlation is based on experiments in which gas was injected through heated, drilled plates in contact with an overlying water pool. The correlation used in CORCON-Mod3 is

$$Q_s^* = 1 + 0.99\left(j_g^*/Ja^*\right)^{0.9} \quad (65)$$

where all variables have been previously defined.

When the temperature of the core debris is calculated to lie between the solidus and liquidus temperatures of the debris mixture, the two enhancement factors shown above are weighted by the surface solids fraction. The solids fraction is estimated using

$$\phi = (T_{liq} - T_T)/(T_{liq} - T_{sol}) \quad (66)$$

where T_{liq} is the liquidus temperature, T_{sol} is the solidus temperature, and T_i is the surface temperature. The gas barbotage enhancement factor is then calculated from

$$Q^* = Q_l^*(1-\phi) + Q_s^*\phi \quad (67)$$

The increased agitation of the melt-coolant interface caused by gas barbotage destabilizes the vapor film, thereby increasing the temperature at which the film collapses. The effect of gas barbotage on the minimum film boiling temperature is accounted for by the equation

$$\Delta T_{Leid,gas} = \Delta T_{Leid,0} + 463.1\, j_g^{0.3953} \quad (68)$$

where $\Delta T_{Leid,gas}$ is the minimum film boiling superheat in the presence of gas barbotage, $\Delta T_{Leid,0}$ is the minimum film boiling superheat in the absence of gas barbotage, and j_g is the superficial gas velocity.

Subcooling of the overlying coolant pool can also enhance heat transfer in the film boiling regime. When the overlying coolant pool is subcooled, energy is removed from the gas film by the overlying subcooled coolant. The net effect of this cooling is a reduction in the thickness of the vapor film. The reduced film thickness permits greater heat transfer by conduction.

The enhancement to heat transfer owing to coolant subcooling in the film boiling regime is included as a multiplicative factor. The factor is calculated using an equation of the form proposed by Siviour and Ede[45] and Dhir and Purohit:[46]

$$Q_{sub}^* = 1 + C\,(\Delta T_{sub})^{5/4}/(\Delta T_{sat})^{3/4} \quad (69)$$

where Q_{sub}^* is the coolant subcooling factor, ΔT_{sub} is the coolant subcooling (i.e., $T_{sat} - T_{sub}$), and C is chosen to be 0.98, based on comparison to experimental results in References 46 and 47

By reducing the thickness of the vapor film, the subcooling of the coolant reduces the stability of the film, and increases the minimum film boiling temperature. The effect of coolant subcooling on the minimum film boiling temperature is calculated using a simple linear correlation of experimental data:[46,47,48]

$$\Delta T_{Leid,sub} = \Delta T_{Leid,0} + 8.0\,\Delta T_{sub} \quad (70)$$

where $\Delta T_{Leid,sub} = T_T - T_{sub}$ is the minimum film boiling superheat in the presence of coolant subcooling, and $\Delta T_{Leid,0} = T_T - T_{sat}$ is the minimum film boiling superheat in the absence of coolant subcooling.

In the absence of experimental data for the combined effects of coolant subcooling and gas barbotage, we have implemented the following simple equations to describe the combined effect of these phenomena on the film boiling heat flux and minimum film boiling temperature:

$$Q_{tot}^* = 1 + \left[\left(Q_{sub}^* - 1\right)^2 + \left(Q_{gas}^* - 1\right)^2\right]^{1/2}, \quad (71)$$

and

$$\Delta T_{Leid} = \Delta T_{Leid,0} + \left[\left(\Delta T_{Leid,sub} - \Delta T_{Leid,0}\right)^2 + \left(\Delta T_{Leid,gas} - \Delta T_{Leid,0}\right)^2\right]^{1/2}. \quad (72)$$

The transition-boiling regime is represented by a simple linear interpolation in ℓn q vs. $\ell n\ \Delta T_{sat}$ between the critical heat flux and the Leidenfrost point. The latter is adjusted to account for the effects of coolant subcooling and gas barbotage.

2.3.4 Crust Formation and Freezing

After some period of interaction, core debris temperatures will fall to the point where solidification begins. In the early stages we assume that crusts will form at one or more interfaces with the interior of the layer remaining liquid. (This is not the only possibility: the crusts may be unstable, or the entire melt may form a slurry.) At later times, considerable freezing may occur. If part or all of a layer becomes frozen, heat can be removed from it by conduction only, which is ordinarily far less effective than convection. Because of internal heating and the fact that cooling cannot continue unless heat losses exceed sources, freezing is largely self-limiting.

For some accident scenarios, the core debris may initially be solid or partially solid. If the degree of solidification is such that internally-generated heat cannot be removed, the debris temperature will rise and material will melt until convective heat transfer is sufficient to allow a balance to be achieved. In general, melting will proceed outward from the center of the debris.

A complete formulation of the problem involves transient, two-dimensional heat transfer with conduction, convection, and change of phase. The spatial resolution must be sufficient to resolve centimeter-thick crusts on layers with dimensions of meters. A numerical solution of the full problem would be very difficult, if not impossible.

A major effect of the presence of solid crusts on heat transfer is the limitation of convective losses because the boundary temperature of the liquid cannot fall below the solidification temperature. Also, a crust provides an additional thermal resistance between the interior of the pool and its surroundings. Both effects tend to reduce heat losses and slow internal cooling rates (or force reheating) so that a steady state is approached. We have retained in CORCON-Mod3 the relatively simple quasi-steady-state model developed for inclusion in CORCON-Mod2.[49] The model is described in the following paragraphs.

The model is formulated in terms of the average temperature of the layer, which is known from its mass and energy content, although it assumes the existence of a temperature profile within the layer. The basic approach is to construct a steady-state solution to the heat-transfer equations in a right circular cylinder whose average temperature, boundary temperatures, thickness, and volume all match those of the actual layer. The resulting heat fluxes at the boundaries are then used at the corresponding boundaries of the actual layer. As described above, the state of a layer will evolve toward a situation where heat losses balance internal heat generation. The average temperature and the boundary heat fluxes at this steady state are determined by the internal heating and the boundary temperatures for the layer.

As a further simplification, the problem is reduced to two independent one-dimensional problems, one axial and one radial, by performing radial and axial averages, respectively, of the full two-dimensional problems. This is a familiar approximation for convective heat transfer in an almost isothermal liquid layer with thin thermal boundary layers, and its accuracy is seldom questioned. It might be expected to be less accurate in the opposite limit of conduction in a solid. Therefore, the model was tested by comparing its predictions with the exact solution for steady-state conduction in a right circular cylinder with uniform volumetric heating and specified surface temperatures.[11h] The agreement between the two calculations was found to be good: differences in the partition of heat and in the effect of boundary temperatures on the average temperature were less than 10 percent, and the calculated temperature rises due to internal heating differed by less than 20 percent. Therefore, we believe that the one-dimensional simplification is sufficiently accurate for use in CORCON-Mod3.

Within a one-dimensional calculation, a layer may be entirely liquid, entirely solid, or liquid with a solid crust. For the axial case, a crust may exist on the top, on the bottom, or both. In liquid regions, heat transfer is by convection (natural or bubble-enhanced) with a conduction limit as described in Section 2.3.2.1. In solid regions, it is by conduction. The all-liquid case employs the results of Section 2.3.2.1 directly, while the all-solid case uses the analytic results for steady-state conduction with a constant volumetric source which follows from

$$q_z = -k dT/dz \tag{73}$$

$$dq_z/dz = S_z \tag{74}$$

$$q_r = -k dT/dr \tag{75}$$

$$d(rq_r)/dr = rS_r \quad . \tag{76}$$

Here the heat flux, q, is positive upward or outward, and S is the volumetric heat source. These relations lead to

familiar quadratic temperature profiles. In terms of boundary and average temperatures, the heat fluxes are

$$q_B = k\left(-4T_B + 6\bar{T} - 2T_T\right)/L \quad , \tag{77}$$

$$q_T = k\left(-2T_B + 6\bar{T} - 2T_T\right)/L \quad , \tag{78}$$

$$q_R = 4k(\bar{T} - R)/R \quad , \tag{79}$$

with subscripts B, T, and R referring to the bottom, top, and radial surfaces. Here $\bar{T}$ is the average temperature of the layer, and L and R are its thickness and radius, respectively. Note that the volumetric source does not appear in these results; the implications of this are further discussed in Reference 11h.

In the case of a liquid with crusts, the liquid sublayer is solved first using assumed values of its average temperature and thickness of radius, T_ℓ and ℓ or R_ℓ, and appropriate boundary temperatures. For any surface at which a crust exists, the boundary temperature is assumed to be the solidification temperature. Conduction in a crust is again governed by Equations (73) through (76), and the temperature profile is again quadratic within the crust. We require continuity of the heat flux at the interface with the liquid and set the volumetric source in the crust equal to that in the liquid,

$$S_z = (q_T - q_B)/\ell \quad , \tag{80}$$

$$S_r = 2q_r/R_\ell \quad , \tag{81}$$

This leads to crust thicknesses and average temperatures of

$$\delta_B = 2k(T_S - T_B)/\left[\left(q_{B\ell}^2 + 2k(T_S - T_B)S_z\right)^{1/2} - q_{B\ell}\right] \tag{82}$$

$$\delta_T = 2k(T_S - T_T)/\left[\left(q_{T\ell}^2 + 2k(T_S - T_T)S_z\right)^{1/2} - q_{T\ell}\right] \tag{83}$$

$$\delta_R = 2k(T_S - T_R)/\left[\left(q_{R\ell}^2 + k(T_S - T_R)S_r\right)^{1/2} - q_{R\ell}\right] \tag{84}$$

$$\bar{T}_B = (2T_S + T_B)/3 + q_{B\ell}\,\delta_B/6k \tag{85}$$

$$\bar{T}_T = (2T_S + T_T)/3 - q_{T\ell}\,\delta_T/6k \tag{86}$$

$$\bar{T}_R = (T_S + T_R)/2 \tag{87}$$

for those crusts which are present. Here T_s is the solidification temperature, $\bar{T}_x$ is the average temperature of crust x, and $q_{x\ell}$ is the heat flux at its interface with the liquid, where "x" may be B, T, or R. In some cases, one or more of Equations (82), (83), and (84) may have no real solution. For this to happen the effective source (divergence of the heat flux) must be negative, which may occur if a layer is being heated by an adjacent layer. The solution is to repeat the calculations with the source made less negative by increasing the assumed liquid temperature and/or dimensions.

In general, neither the total layer thickness (or radius) nor the overall average temperature thus determined will be correct for the layer. This requires an iteration on the thickness and temperature of the liquid sublayer. A two-variable form of Newton's iteration has been found effective for this. A "bound and bisect" backup has been included for reliability.

2.3.5 Bubble Phenomena

Gases that rise through the debris pool as bubbles influence the heat transfer in the pool, as described in Section 2.3.2. The bubble properties and behavior also affect mixing between the layers and the aerosol and fission product release.

Owing to the importance of the bubble properties in the interlayer mixing models developed by Greene[13] and now implemented in CORCON-Mod3, the bubble behavior models have been improved in CORCON-Mod3. The new models are described in this section.

Bubble rise velocities are computed for three regimes based on bubble geometry and size. Regime 1 applies to small spherical bubbles with internal gas circulation. Regime 2 applies to ellipsoidal bubbles with internal gas circulation. Regime 3 applies to spherical cap bubbles.

The equation for bubble rise velocity U_b used in Regime 1 is derived using classical hydrodynamic analysis:[50]

$$U_b = \frac{g\, d_b^2\, \rho_l}{12\mu_l} \tag{88}$$

where g is the acceleration due to gravity, d_b is the bubble diameter, ρ_l is the density of the surrounding liquid, and μ_l is the viscosity of the surrounding liquid.

The equation used for bubble rise velocity in Regime 2 is[51]

$$U_b = \left[\frac{2.14\sigma_l}{\rho_l d_e} + 0.505 g d_e \right]^{1/2} \quad (89)$$

where σ_l is the surface tension of the liquid, and d_e is the equivalent diameter of the bubble.

The equation used for bubble rise velocity in Regime 3 is the Davies-Taylor formula[52]

$$U_b = \sqrt{g r_e} \quad (90)$$

where r_e is the radius of an equivalent spherical bubble with the same volume as the spherical cap bubble.

CORCON-Mod3 determines the appropriate regime by first comparing the rise velocities for regimes 1 and 2. If the regime 1 velocity is greater than the regime 2 velocity, the bubble is not spherical, and is, instead, in either regime 2 or 3. (If the converse is true, the bubble is spherical and the regime 1 value is appropriate.) This logic can be used because there is an inflection in the bubble rise velocity curve at the transition from spherical to ellipsoidal bubbles. Next the regime 2 and 3 velocities are compared. If the regime 2 value is greater than the regime 3 value, the bubble must be a spherical cap, otherwise the bubble is an ellipsoid. The regime 2 value is used for ellipsoidal bubbles, while the regime 3 value is used for spherical cap bubbles.

The volume of the debris pool is inflated by the volume of the gas bubbles, a phenomenon known as "level swell." CORCON-Mod2 used a form of the drift-flux correlation[53] to determine the level swell of the melt. Brockmann[54] found that this correlation overpredicted the level swell for steel melts, and he developed a correlation that appears to be accurate for a wide range of material properties. Brockmann's correlation is

$$\alpha = 0.128 M^{-0.0207} \left(j_g^* \right)^{0.584} \quad (91)$$

where α is the volume fraction, j^*_g is a dimensionless superficial gas velocity, given by

$$j_g^* = \frac{j_g}{\left[\frac{\sigma_l g}{\rho_l} \right]^{1/4}} \quad (92)$$

and M is the Morton number, given by

$$M = \frac{g \mu_l^4 (\rho_l - \rho_g)}{\rho_l^2 \sigma_l^3} \quad . \quad (93)$$

The volume fraction is limited to a maximum of 0.42, as suggested by Blottner.[22]

Accurate prediction of bubble size is critical to the calculation of interlayer mixing (see Section 2.3.6). The bubble model used in CORCON-Mod3 treats three bubble formation mechanisms. In this formulation bubble size depends on the superficial gas velocity through the layer.

At low gas velocities, bubbles form at the surface and then depart when their buoyancy overcomes surface tension. A simple force balance yields the equation for the bubble diameter d_b:[53]

$$d_b = 0.0105\theta \sqrt{\frac{\sigma_l}{g(\rho_l - \rho_g)}} \quad , \quad (94)$$

where θ is the contact angle (in degrees) between the melt and the surface; in CORCON-Mod3, the contact angle is assumed to be 120 degrees.

At higher gas fluxes, bubbles grow to larger sizes before departing from the surface. The bubble size correlation implemented in CORCON-Mod3 is based on the Davidson-Schuler[55] equations for the bubble volume, where both high and low viscosity liquids are considered. For low viscosity liquids,

$$V_{bL} = \frac{\pi}{6} d_b^3 = 4.1369 \times 10^{-5} \left[\frac{j_g^{1.2}}{g^{0.6}} \right] \quad (95a)$$

while for high viscosity liquids,

$$V_{bH} = \frac{\pi}{6} d_b^3 = 0.01094 \left[\frac{j_g \mu_g}{\rho_l g} \right]^{3/4} \quad (95b)$$

where j_g is the superficial gas velocity in m/sec and g is the acceleration of gravity (9.8 m/s^2). The code uses the

maximum of the bubble sizes predicted using these two correlations.

At very high gas fluxes, a stable gas film may form. For a gas film, the equation for bubble radius implemented in CORCON-Mod3 is identical to the one used in CORCON-Mod2:

$$r_b = 3.97 \sqrt{\frac{\sigma_l}{g(\rho_l - \rho_g)}} \quad . \tag{96}$$

where the leading coefficient is based on the experiments of Hosler and Westwater.[56] Literature values for this coefficient range from 2.2 to 4.2.[36,44] The lower values are inconsistent with bubble sizes observed in melt-concrete experiments at Sandia National Laboratories and elsewhere.

CORCON-Mod3 calculates the bubble size for each of the three regimes. The Davidson-Shuler equation is used in most cases. The low gas velocity equation provides a lower bound to the bubble size, while the gas film equation provides an upper bound.

The bubble size is recalculated at each layer interface. The effects of chemistry and changes in temperature and pressure are accounted for, but bubble coalescence is not modeled. The average of the radii of the bubbles entering and leaving the layer is used to calculate a single terminal velocity for the layer.

The gas flux at any elevation is calculated using the local cross-sectional area and the total flow of gas from lower in the pool. A local gas volume fraction is then calculated, and the elevations of layer interfaces are determined from the integral of the non-gas volume

$$\frac{m_L}{\rho_L} = \int_{z_{BOT}}^{z_{TOP}} (1 - \alpha(z))\, A(z)\, dz \tag{97}$$

where m_L is the mass of the non-gas in the layer, ρ_L is the density of the non-gas in the layer, $\alpha(z)$ is the local gas volume fraction at elevation z, A(z) is the debris pool area at elevation z, and z_{BOT} and z_{TOP} are the elevations of the bottom and the top of the layer, respectively.

2.3.6 Interlayer Mixing

Though CORCON-Mod2 included mixture layers in its layer structure, it lacked mechanistic models for mixing between the layers of the debris pool. We have developed and implemented an interlayer mixing model in CORCON-Mod3 based on the experimental and analytical work of Greene.[13,57,58] The mechanistic models and their implementation into CORCON-Mod3 are described below.

Two mixture layers are possible, a layer of "light" oxide with suspended metal drops or a layer of metal with suspended "heavy" oxide drops. Mixture layers can be created in one of two ways. First, a mixture layer can be created by the entrainment of one layer, the denser of the two, into another. A mixture layer can also be created when an overlying layer becomes more dense than the layer beneath it. The latter case was handled in CORCON-Mod2 by assuming that a "layer flip" occurred; in other words, the denser oxide layer was assumed to migrate instantaneously through the metal layer and combine with the overlying oxide layer.

When a mixture layer is formed by an unstable density arrangement, mixing is assumed to occur instantaneously; that is, during a single CORCON time step. The adjacent layers are assumed to merge to form the mixture layer.

When a mixture layer is formed by entrainment, the entrained drops are assumed to be carried to the top of the overlying layer before floating free of the entraining bubble. As a result, the overlying layer immediately becomes a mixture layer, and it is redefined by the code.

CORCON-Mod3 calculates also the creation of single-phase layers due to droplet settling (deentrainment). Therefore, mixture layers may eventually stratify into distinct metal and oxide layers if density differences become greater or the gas flow through the melt decreases.

To illustrate the treatment of interlayer mixing in the code, consider the following example: molten core debris is initially stratified with an oxidic phase on the bottom (HOX layer), and a metallic phase on top (MET layer), and is rapidly ablating concrete. The gas flow rate is assumed to be sufficient to begin entraining the oxide into the metal. Once entrainment begins, droplets of the HOX layer are carried to the top of the MET layer, so the MET layer is redefined as an HMX layer (HMX implying suspended heavy oxide in a less-dense metal layer). There will be a net loss of oxide from the HOX layer until the rate of entrainment equals the rate of droplet settling out of the HMX layer. Complete entrainment of the HOX layer may occur as the HOX density decreases due to the addition of lower density concrete oxides (from ablation). If the density of the suspended oxide in the HMX layer subsequently becomes less than the density of the metals, the HMX layer is redefined as the LMX layer (or is combined with the

LMX layer if one is present). Metals in the LMX layer will then begin to settle out of the mixture Complete stratification may occur as the gas flow rate continues to decrease, resulting in a debris configuration with a metal layer (MET) on the bottom and a less dense oxide layer (LOX) on the top. Note that the beginning and ending debris configurations in this example are the same as what was generally observed using CORCON-Mod2. The evolution of the final configuration is, however, more realistic.

The above example represents just one of many scenarios that may occur depending on the relative densities of the oxide and metal phases, and the gas flow through the melt. (Another example is provided in the BWR sample problem shown in Section 6.0.) The comments provided in subroutines ORIENT and ADDLYR are sufficiently detailed for the user to understand the various cases treated by the code.

As the densities of the metallic and oxidic phases and gas flows change, the orientation of the layers may also change. Coding has been included to handle all possible changes in the layer orientation.

In the entrainment calculation, two criteria are used to determine whether entrainment is possible;[13] these are

$$\frac{\rho_2}{\rho_1} < 3 \quad \text{and} \quad \omega > \frac{V_{b,o}}{V_{b,pen}} \tag{98}$$

where ρ_1 is the density of the material in the upper layer, and ρ_2 is the density of the material in the lower layer. In Equation (98), ω is the dimensionless bubble volume, defined by

$$\omega = V_b/V_{b,pen} \tag{99}$$

where V_b is the bubble volume and $V_{b,pen}$ is the bubble volume required for penetration of the interface, given by

$$V_{b,pen} = \left[\frac{3.9\sigma_{12}}{g(\rho_1 - \rho_g)}\right]^{3/2} \tag{100}$$

in which σ_{12} is the surface tension of the liquid-liquid interface, g is the acceleration due to gravity, ρ_ℓ is the density of the liquid surrounding the bubble, and ρ_g is the density of the gas in the bubble. $V_{b,o}$ in Equation (98) is the minimum bubble volume for entrainment, given by

$$V_{b,o} = \left[\frac{7.8\ \sigma_{12}}{g(3\rho_1 - \rho_2 - 2\rho_g)}\right]^{3/2} \tag{101}$$

If either criterion defined by Equation (98) is not satisfied, then entrainment cannot occur. In practice, the second criterion of Equation (98) is the more restrictive of the two.

If both conditions for entrainment are satisfied, then the entrained drop volume per bubble is calculated using the correlation developed by Greene:[13]

$$\frac{V_e}{V_{e,max}} = \frac{1}{806}\ \xi^{0.152}\ Re_1^{0.119}\ Re_2^{0.380} \quad . \tag{102}$$

In Equation (102), V_e is the entrained drop volume per bubble, and $V_{e,max}$ is the theoretical maximum volume that could be entrained and is given by

$$V_{e,max} = \frac{V_b(\rho_1 - \rho_g) - (\sigma_{12}/g)\left(12\pi^2 V_b\right)^{1/3}}{(\rho_2 - \rho_1)} \tag{103}$$

Re_1 are Re_2 in Equation (102) are the Reynolds numbers (based on bubble diameter) for bubbles rising in the lower and upper fluids, respectively, and ξ is the normalized excess bubble volume above that required for entrainment:

$$\xi = (V_b - V_{b,o})/V_{b,o} \quad . \tag{104}$$

Note that, as defined in Equation (103), $V_{e,max}$ goes to zero at the following value for V_b:

$$V_{b,min} = \left[\frac{4.91\sigma_{12}}{g(\rho_1 - \rho_g)}\right]^{3/2} \tag{105}$$

This value for V_b is more limiting than that given by Equation (100). Therefore, it is used along with Equation (101) to determine whether entrainment is possible.

Given the superficial gas velocity through the surface, j_g, and the bubble volume, V_b, the bubble flux (number of bubbles per unit area per unit time) is calculated as

$$\Phi_b = j_g/V_b \quad . \tag{106}$$

Since each bubble has associated with it an entrained drop of a known volume, the mass flux of entrained

material can be calculated. Multiplying the mass flux of entrained material by the interfacial area and time step gives the mass entrained during the time step. This mass and its associated enthalpy are transferred into the mixture layer. If no mixture layer is available to accept the entrained mass, one is created to contain it.

Deentrainment is calculated by first calculating the drop settling velocity using the droplet drag coefficient correlations proposed by Greene.[13] The correlations follow the drag curve for spherical drops until a critical value for the settling velocity is reached. At the critical settling velocity, Greene observed droplet oscillations with a coincident increase in the drag coefficient.

In the absence of drop oscillations, the drag coefficient is determined from the following set of correlations by Beard and Pruppacher:[59]

$$\frac{C_d}{C_{d,S}} = 1 + 0.102\ Re^{0.955} \qquad (107a)$$

for $0.2 < Re < 2.0$

$$\frac{C_d}{C_{d,S}} = 1 + 0.115\ Re^{0.802} \qquad (107b)$$

for $2.0 < Re < 21.0$

$$\frac{C_d}{C_{d,S}} = 1 + 0.1879\ Re^{0.632} \qquad (107c)$$

for $21.0 < Re < 200.0$. In these equations, $C_{d,S}$ is the drag coefficient for Stokes flow:

$$C_{d,S} = 24/Re_d \qquad (108)$$

and Re_d is the Reynolds number for the droplet based on the droplet diameter.

Greene developed the following criterion for the onset of droplet oscillations:

$$We_{crit}\ Re_{crit}^{0.65} = 165 \qquad (109)$$

In this equation, We_{crit} and Re_{crit} are the Weber and Reynolds numbers, respectively, at which drop oscillations were first observed. Coincident with the oscillations was a dramatic increase in the droplet drag coefficient. The observed drag coefficients are correlated by

$$\frac{C_d}{C_{d,crit}} = \left[\frac{Re_d}{Re_{crit}}\right]^{1.12} \qquad (110)$$

where $C_{d,crit}$ is the drag coefficient at the onset of droplet oscillations.

A consistent droplet settling velocity v_d and drag coefficient are determined by iteration. Given v_d, the volume fraction α_d of drops in the mixture layer, and the density of the drop material ρ_d, the mass flux of settling drops is calculated using the equation

$$\Phi_d = v_d \alpha_d \rho_d \qquad (111)$$

Multiplying the mass flux by the interfacial area and the time step yields the mass of drops settling out of the mixture during the time step. This mass and its associated enthalpy are transferred out of the mixture layer and into the layer below it. If no separated layer exists to accept the deentrained mass, one is created at the start of the next timestep.

In CORCON-Mod3, the user has the option of selecting whether to begin a calculation with a stratified or a fully mixed debris pool, and the user can select whether the code will perform the entrainment and deentrainment calculations. This allows the user the flexibility to begin a calculation in a fully mixed configuration and then allow the code to calculate entrainment and deentrainment, or the user can force the debris pool to remain mixed by bypassing the mixing calculation. Similarly, the user can begin a calculation with a stratified debris pool and then allow the code to calculate entrainment and deentrainment, or the user can force the pool to remain stratified by bypassing the mixing calculation.

Average thermophysical properties (thermal conductivity, viscosity, surface tension, etc.) are calculated using volume fraction or mass fraction weighing of the individual metal and oxide phase properties. Separate liquidus and solidus temperatures are calculated for the metallic and oxidic phases. The mixture layer solidus temperature is assumed to be the lower of the metal and oxide phase solidus temperatures, while the mixture liquidus temperature is chosen as the maximum of the metal and oxide phase solidus temperatures. Crust formation occurs only when the local temperature drops below the solidus temperature. Between the solidus and liquidus temperatures, the mixture is assumed to form a

slurry. The solids fraction for the mixture is determined by mass-weighing the solids fraction of the metal and oxide phases, where the solids fraction of each phase is based on the appropriate solidus and liquidus temperatures for that phase.

2.3.7 Pool Surface Heat Transfer

We anticipate that CORCON-Mod3 will be coupled to integral system codes such as MELCOR[8] and CONTAIN.[7] To simplify such efforts, the pool surface has been treated as a major computational interface in CORCON-Mod3, with limited information passed in a well-defined way between above- and below-surface modules. Otherwise, these modules are quite independent; in particular, the need for simultaneous solution of above-surface and below-surface heat transfer relations has been avoided. The treatment in CORCON-Mod3 is identical to that in CORCON-Mod2.

Each half of the problem (above- and below-surface) defines an upward heat flow, Q_s, as a function of the surface temperature, T_s. An energy balance at the surface of the pool requires finding that T_s for which these heat flows are equal; this generally involves solution of a nonlinear--and perhaps very complicated--equation. This may be viewed somewhat differently: for each half of the problem, the boundary condition at the pool surface is the heat flow vs temperature characteristic of the other half, and the object is to find a simultaneous solution. Each "half-problem" is solved with a boundary condition representing the response of the other half, linearized about the most recently calculated surface temperature. The calculation is described in more detail below.

First, the end-of-timestep response of the pool, linearized about its start-of-timestep value, T_s^n,

$$Q_s = Q_s^\circ|_{Pool} + \frac{dQ_s}{dT_s}|_{Pool} \left(T_s - T_s^n\right) \quad , \qquad (112)$$

is calculated in ENRCN1 and passed to the above-pool module, ATMSUR. This response includes contributions from the implicit terms in the pool energy equation, involving the change in layer temperatures with change in end-of-timestep heat loss from the surface. In ATMSUR, it is used as a boundary condition for the full nonlinear problem involving atmosphere and surroundings, resulting in a provisional end-of-timestep surface temperature, $\tilde{T}_s^{n+1}$. This, together with the linearization of above-surface response about $\tilde{T}_s^{n+1}$,

$$Q_s = Q_s^\circ|_{sur} + \frac{dQ_s}{dT_s}|_{sur} \left(T_s - \tilde{T}_s^{n+1}\right) \quad . \qquad (113)$$

is passed back to the below-surface modules. The linearization ultimately serves as a boundary condition for another nonlinear calculation which results in the final end-of-timestep value T_s^{n+1}. This procedure has advantages with respect to the energy-conservation equations, as will be discussed in Section 2.3.12.

In the version of ATMSUR included in CORCON-Mod3, heat loss from the pool surface includes convective heat transfer to the atmosphere and radiative heat transfer to the surroundings. Thermal radiation is the dominant mechanism. If desired, the radiative effects of aerosols in the atmosphere may be included in the calculation, with an atmospheric opacity determined from calculated aerosol concentrations. Once the optical thickness of the atmosphere is known, the one-dimensional diffusion equation is applied for infinite, parallel, optically gray plates giving

$$q_{rad_{sur}} = \frac{\sigma_B \left(T_s^4 - T_{sur}^4\right)}{1/\varepsilon_s + 1/\varepsilon_{sur} - 1 + 0.75\ KL} \qquad (114)$$

where T_s is the surface temperature, T_{sur} is the surroundings temperature, K is the extinction coefficient, L is the average path length for radiation in the cavity atmosphere, and ε_s and ε_{sur} are emissivities of the surface and surroundings, respectively.

Note that Equation (114) reduces to the transparent atmosphere equation as either the extinction coefficient or the average path length approaches zero.

Convection produces additional heat transfer from the pool surface. Unless the atmosphere is truly transparent, however, convection and radiation are strongly coupled; the radiation tends to increase thermal stability and reduce convection.[60] In most cases, however, we have found the convection contribution to be small. Therefore, we have included only a very simple convection model in CORCON-Mod3. The convective heat transfer from the pool surface to the atmosphere is given by

$$q_{conv} = h_s \left(T_s - T_a\right) \qquad (115)$$

where T_a is the bulk temperature of the atmosphere. The heat transfer coefficient, h_s, is assumed to be constant at 10 W/m^2 K.

The total heat flux from the pool surface is given by

$$q_s = q_{rad_{-}} + q_{conv} \quad (116)$$

This equation is solved for T_s simultaneously with the linearized pool response, Equation (112), to determine the provisional end-of-timestep surface temperature $\tilde{T}_s^{n+1}$.

2.3.8 Concrete Decomposition and Ablation

The response of concrete exposed to high heat fluxes is complex. Concrete is an inhomogeneous material which undergoes changes in composition as it is heated. The most important of these changes are the vaporization of interstitial and adsorbed water at about 400 K, the decomposition of calcium and magnesium hydroxides near 700 K, and the decomposition of calcium and magnesium carbonates between about 1000 and 1100 K. The carbon dioxide, water vapor, and liquid water produced within the solid concrete flow through the pores of the remaining matrix in response to pressure gradients. Finally, the remaining oxide matrix melts, at a temperature which ranges from about 1350 K to 1900 K for representative concretes. In the context of molten-core/concrete interactions, the molten and semi-molten materials are removed from the surface into the pool, as the surface recedes.

We have retained in CORCON-Mod3 the simplified model for the concrete response that was used in CORCON-Mod2. This model is based on a steady-state, one-dimensional energy balance, and is described below.

If a steady temperature profile exists in the concrete, a simple heat balance at the concrete surface yields

$$q = \rho_c \Delta H_{abl} \, dx_s/dt \quad (117)$$

where q is the net heat flux to the concrete, ρ_c is the density of concrete, ΔH_{abl} is the ablation enthalpy of concrete, and x_s is the position of the concrete surface.

The heat flux q must, of course, be reconciled with the interfacial heat transfer model of Section 2.3.2.2. In general, this procedure will involve an iteration to determine the temperature of the pool side of the interfacial film (gas or slag), allowing for the fact that the thermal resistance of that film may depend on the gas generation which results from the ablation. If this temperature is below the ablation temperature, the concrete is treated as an adiabatic boundary with q (and dx_s/dt) set equal to zero.

We emphasize that the pseudo-steady temperature profile, which is used to justify Equation (117), does not appear in the equation. The sensible heat and chemical energy (and changes in these quantities) associated with the temperature profile are ignored. This is not a problem in cases where the pool contains a high temperature liquid melt: studies by ACUREX, using a more complex ablation code, have shown that the ablation process reaches a quasi-steady state within about 1 minute.[61] At very late times, or early times with initially solid debris, the inaccuracies could be greater.

The quasi-steady model is also used to calculate the generation of decomposition gases; that is, the mass generation rate of each gas is taken as its partial density in the concrete times the ablation rate. Gas released in advance of the ablation front is thus ignored; this assumption neglects the initial burst of gases associated with establishing a steady profile in the concrete by a hot molten pool. The model is also in error at early times for solid debris, because no gas is generated before ablation begins, as well as at late times if ablation ceases. The ablation enthalpy for concrete in Equation (117) is calculated internally, and consists of both sensible and chemical energies. The sensible energy is computed as described in Section 2.4.1. It includes the energy necessary to raise gaseous decomposition products to the concrete ablation temperature to account for the so-called "transpiration cooling" effect. The chemical energy is included using experimentally determined heats of decomposition for three reactions: evaporation of free water (11 kcal/mole), release of chemically bound water from hydroxides (25 kcal/mole), and release of CO_2 from carbonates (40 kcal/mole). The enthalpy of limestone aggregate/common sand concrete (including decomposition products where appropriate) is illustrated in Figure 2.3 as a function of temperature.

The ablation temperature of concrete is not precisely defined because ablated material may not be completely molten. In CORCON-Mod3, we consider a melting range defined by the concrete liquidus and solidus temperatures, with the ablation temperature ordinarily chosen by the user to lie between them. The choice affects the calculated heat of ablation, as may be seen from Figure 2.3. Concrete decomposition products enter the interfacial film or the pool at the ablation temperature, with the enthalpy appropriate to that temperature. Therefore, because all enthalpies are computed from the same data base, the choice of ablation temperature has no effect on overall conservation of energy.

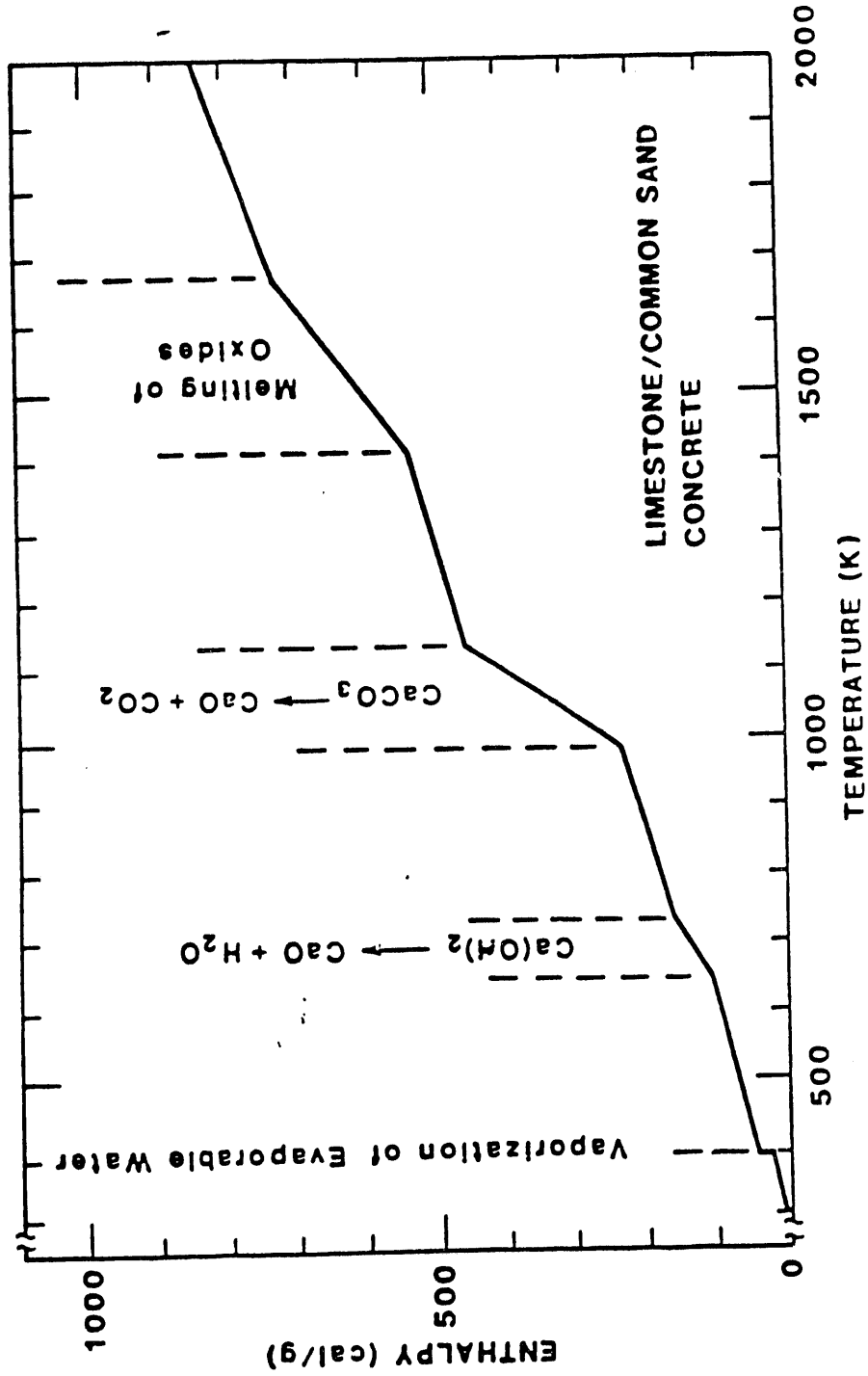

Figure 2.3 Enthalpy of concrete and its decomposition products

If the concrete contains reinforcing steel, the energy necessary to raise it to the concrete ablation temperatures included in the "concrete" ablation enthalpy.

2.3.9 Time-Dependent Melt Radius

In previous versions of CORCON, it was assumed that the melt pool, comprising the core debris, coolant, ablated concrete decomposition products, and ablated materials from the surroundings, completely fills the bottom of the reactor cavity. The assumption limits the utility of the code and may cause numerical problems if small masses of core material are required to be spread thinly over the surface concrete. For example, it is not possible, under this assumption, to simulate the transient events accompanying the initial pour of core debris onto a concrete basemat and the subsequent spreading of the molten debris across the basemat floor. CORCON-Mod3 allows the user to specify a time-dependent radius of the melt that is less than the dimension of the confining cavity. This feature extends the range of severe accident scenarios that can be simulated.

The spreading of a viscous liquid across a solid surface is a complex physical process. If the liquid begins to solidify while flowing, this compounds the complexity of the process. If a crust begins to form on the upper surface of the spreading liquid, the crust may be stable or may be broken up and mixed into the liquid. In the latter case, the resulting slurry has a high viscosity and a high surface tension. Ultimately, the shear stresses required to maintain the flow are greater than those driving the flow, and the flow stops. The molten material continues to solidify in place and may attack the substrate.

Mechanistic modeling of the spreading process described above is not attempted in implementation of the time-dependent melt radius option in CORCON-Mod3. Instead, the user enters a table of times and corresponding radii, and values of maximum and minimum allowable melt thickness. This approach allows considerable flexibility in mimicking the spreading process delineated above, but also allows the user to specify physically unreasonable melt configurations. The option, as currently implemented, will adjust the melt radius to keep the melt thickness between the maximum and minimum thicknesses specified by the user. Alternatively, by setting the maximum and minimum melt thicknesses to be equal, a constant melt thickness can be specified, and the appropriate melt radius will be determined at each time step. A rudimentary criterion is included to determine when the melt contains too much solid material to allow the melt to continue to spread: when the total crust thickness is greater than a half of the melt thickness, spreading stops.

Each layer of the melt pool is assumed to have the same radius until the melt reaches the sidewall. Mass may be added to the melt pool, either additional core debris or concrete ablation products. With the option, it is possible to fix the radius at a particular value, and to have the melt repose on the concrete floor as a non-spreading glob. As currently implemented, the time-dependent melt radius feature is restricted to cylindrical cavities with flat floors (IGEOM = 2).

Coolant may be present in the cavity when the time-dependent melt radius option is invoked. The coolant is treated correctly as long as the quantity of coolant is sufficient to cover the melt. Program execution stops when the coolant no longer covers the melt. Treating the case where the coolant does not fully cover the melt would necessitate extensive modifications to CORCON to add a radial layer structure and allow simultaneous heat transfer from the melt to a radial water layer and the surroundings. We believe that such modifications are not warranted at this time.

Additions to the energy equations to account for the exposed melt edges are described in Section 2.3.12.

2.3.10 Chemical Reactions

In CORCON-Mod2 it was assumed that the principal chemical reaction involved in core/concrete interactions is the oxidation of metals in the pool by concrete decomposition gases. These gases, water vapor and carbon dioxide, are reduced in the process, primarily to hydrogen and carbon monoxide. It is possible to further reduce carbon monoxide to atomic carbon. This is predicted by CORCON-Mod2 in many cases involving metallic zirconium.

In CORCON-Mod3 we treat not only the reactions of metals with gases from the concrete, but also condensed phase reactions between oxides and metals. The latter were added to the code based on the results of the SURC-4 experiment.[5] In this experiment, a vigorous interaction was observed between metallic zirconium and a silicious concrete with low gas content. This interaction could only be explained by considering condensed phase chemical reactions between the zirconium and molten oxides from the concrete. The driving chemical reaction was

$$Zr + SiO_2 \rightarrow Si + ZrO_2 + 2.1\ MJ/kg\ Zr$$

Condensed phase reactions are particularly important for core debris interactions with high silica, low gas, concretes such as the one used in the SURC-4 experiment. They are much less important for calcareous

concretes that have a low silica content and high gas content. The user enables condensed phase chemistry using the input flag, ICHEM.

To include condensed phase chemical reactions, it was necessary to expand the master species list to include uranium, aluminum, calcium, and silicon metals. These and other additions to the master species list are shown in Table 2.1.

CORCON-Mod3 assumes that chemical equilibrium is achieved between the reactants during each timestep. The chemical equilibrium solver minimizes the Gibbs free energy for 56 chemical species and 15 elements. These species, which are shown in Table 2.6, include all relevant condensed species (the metals, their oxides, and condensed carbon), the principal gaseous species of water vapor, hydrogen, carbon dioxide, and carbon monoxide, and a variety of less-important gases such as light hydrocarbons. The subroutine employed, MLTREA, has evolved from an implementation by Powers[11c] of the method of Van Zeggeren and Storey.[62] It performs a simple first-order steepest descent minimization of the Gibbs function subject to constraints on mass conservation and on non- negativity of concentrations. The version included in CORCON-Mod3 is essentially the same as that included in the third correction set for CORCON-Mod2.[63] For a more detailed discussion of the equilibrium solver, the reader is referred to References 11f and 62.

The solution procedure has a number of significant advantages: (1) it is extremely general; (2) reactions need not be specified; (3) convergence does not require a good initial guess (although it is much faster if one is available); and (4) the resulting FORTRAN code is relatively small for the number of species considered. The condensed phase reactants and oxidic products are

Table 2.6 Chemical species included in the CORCON chemical equilibrium solution

Oxides	Metals and Other Elements	Gases
FeO	Fe	C(g)
MnO	Cr	CH_4
Al_2O_3	Ni	CO
UO_2	Zr	CO_2
ZrO_2	FpM*	C_2H_2
Cr_2O_3	Mn	C_2H_4
NiO	C(c)	C_2H_6
$FpMO_2$*	Al	H
$FpMO_3$*	U	H_2
Fe_3O_4	Si	H_2O
Mn_3O_4	UAl_3	N
SiO_2	UAl_2	NH_3
U_3O_8	Ca	N_2
CaO	X**	O
		O_2
		OH
		CHO
		CH_2O
		CrO_3(g)
		$FpMO_2$(g)*
		$FpMO_3$(g)*
		Al_2O_2(g)
		Al_2O(g)
		AlO(g)
		OAlH(g)
		AlOH(g)
		OAlOH(g)
		AlO_2(g)

*Pseudo-species representing condensed phase and gas phase fission product groups
**Inert oxide species treated as element "X" in the chemical equilibrium calculation

treated as ideal solutions in MLTREA; that is, entropy-of-mixing terms are included in their chemical potentials, and the activity of each species is equal to the mole fraction in the phase.

It should be noted that non-ideal solution chemistry has been included in the vaporization release model in VANESA. (See the discussion in Section 2.3.14.) This information could be made available to the MLTREA subroutine, but this has not yet been done. Although non-ideal solution chemistry is important for calculation of vaporization release from the core debris, we currently do not believe it to be important for the calculation of flammable gas production or energy generation, which are the primary results from the MLTREA calculation.

The ICHEM flag, which is used to enable the condensed phase chemistry calculation, is also used to disable the production of condensed carbon (C(c)) during the reaction of carbon dioxide with reactive metals such as zirconium or aluminum. This reaction, which is often referred to as "coking" or "carburization," is predicted by CORCON-Mod2, but has not been observed to any significant extent in previous melt-concrete experiments. To disable the coking reaction, the chemical potentials of C(c) is artifically set to a large value (currently 10^{15} cal/g-mole). With this change in place, the code was found to predict substantial production of acetylene (C_2H_2). Since significant acetylene production also has not been observed in any past experiments, we have suppressed the formation of acetylene by setting the chemical potential of C_2H_2 to a large value (also 10^{15} cal/g-mole) whenever the coking reaction is disabled.

As with earlier versions of CORCON, CORCON-Mod3 contains coding to calculate the reduction of oxides at the pool surface by the oxygen-poor atmosphere above the melt. This feature was implemented and tested during development of CORCON-Mod1, but was bypassed in released versions of the code because of the incomplete treatment of the atmosphere. We have retained it, still bypassed, in CORCON-Mod3.

The thermodynamic-properties package (Section 2.4.1) employs the standard thermochemical reference point of separated elements in their standard states. With this reference point, heats of formation of all species are automatically included, and all heats of reaction are implicitly contained in the enthalpy data. In fact, they are calculated only for edit purposes.

2.3.11 Mass and Energy Transfer

Processes involving mass transfer are of considerable importance in the modeling of molten core/concrete interactions. These include injection of concrete decomposition products (condensed and gaseous) into the pool and further additions of core materials, structural materials, or coolant entering from above. It is convenient to include chemical reactions in the same calculational structure, because these reactions affect the nature of transferred masses.

These transport processes modify both the mass inventories and the energy contents of the various pool layers. The corresponding terms in the mass and energy equations are evaluated in subroutine MHTRAN. The structure of this routine closely mirrors our picture of the physical processes it models, as described in the following paragraphs.

The masses and enthalpies of all pool layers are updated for mass transfer and associated heat transfer in two passes. (Note that a calculation will not begin until there is some debris present in the pool.) The first pass, upward through the pool, follows the rising gases and rising condensed-phase materials from concrete decomposition or concrete/melt/gas reactions. The direction of motion is determined by the density relative to the local layer material and/or the driving forces for entrainment. The compositions and enthalpies of these rising materials are followed and modified for chemical reactions. The materials are thermally equilibrated with any layers they pass through, and their energy is ultimately added to the layer where they remain. Any heat of reaction remains with the layer where the reaction occurred.

The second calculational pass, the downward pass, is similar to the first: it follows any material entering the pool from above in addition to sinking reaction products, concrete ablation products, and droplets settling out of mixture layers. Entering metallic species are added to the first layer of the core debris containing metals. If no layer with metals is present, a metallic layer is created. Addition of oxides and coolant is treated in a similar fashion. As with other material movements in CORCON, mass added to the cavity is assumed to equilibrate thermally with each layer through which it passes or eventually resides. Figures 2.4 through 2.6 show this in more explicit detail. In these figures, Q denotes thermal equilibration, O/M/G refers to the oxide/metal/gas oxidation reaction, and MX denotes interlayer mixing. The total heat capacity of a layer is assumed to be much greater than that of materials passing through it so that thermal equilibration takes place at the

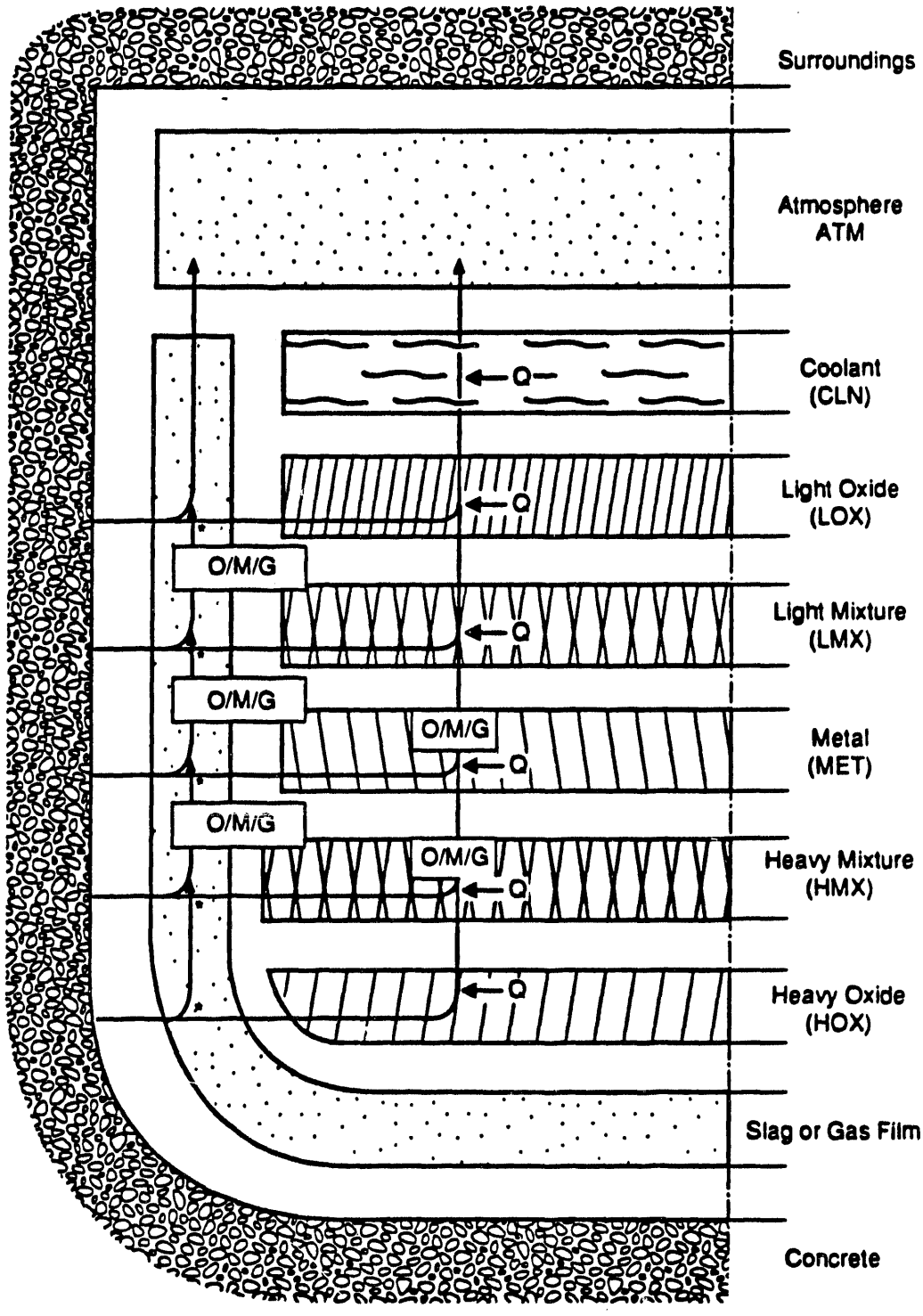

Figure 2.4 Path of gas through pool

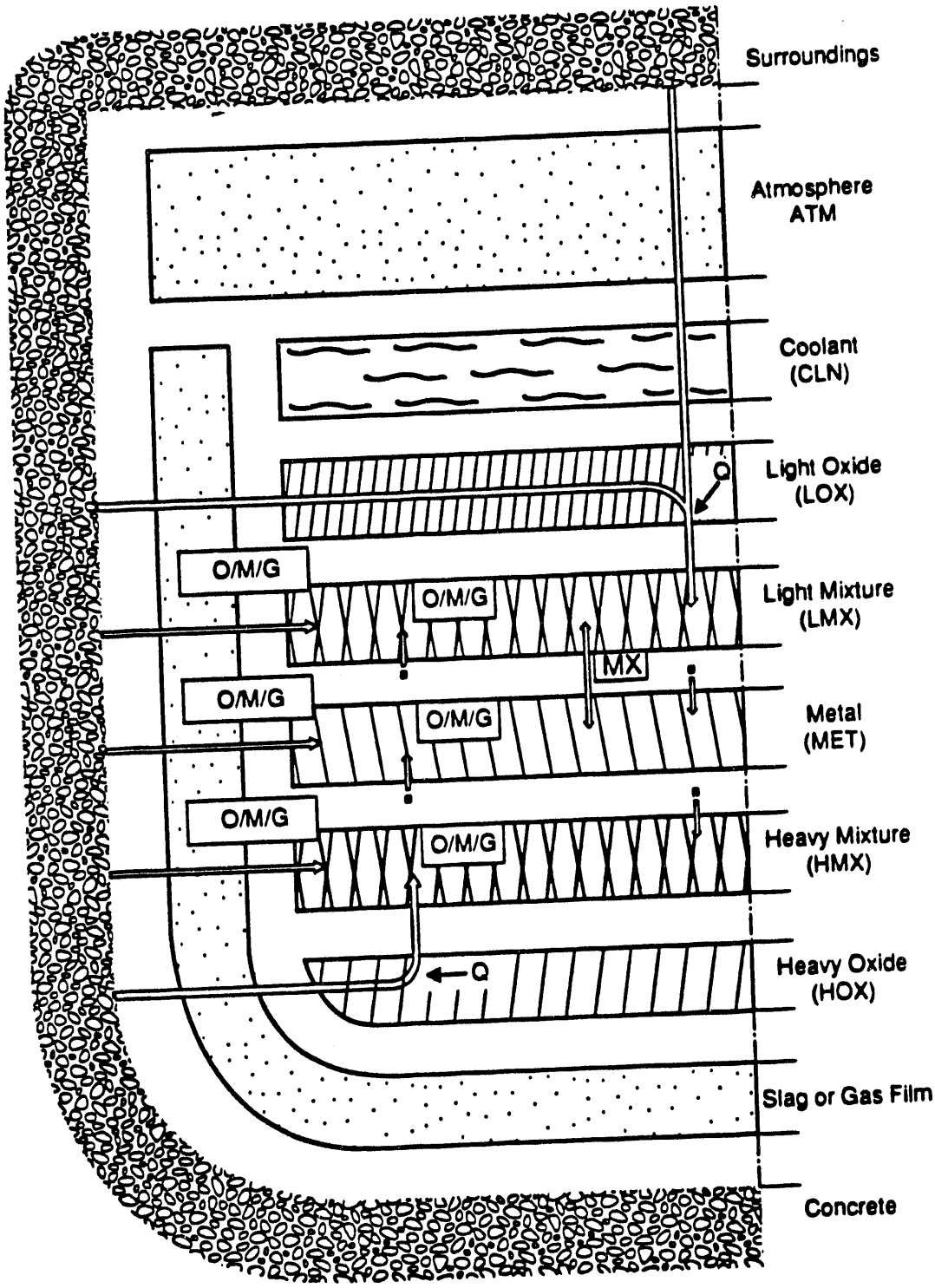

Figure 2.5 Path of metal through pool

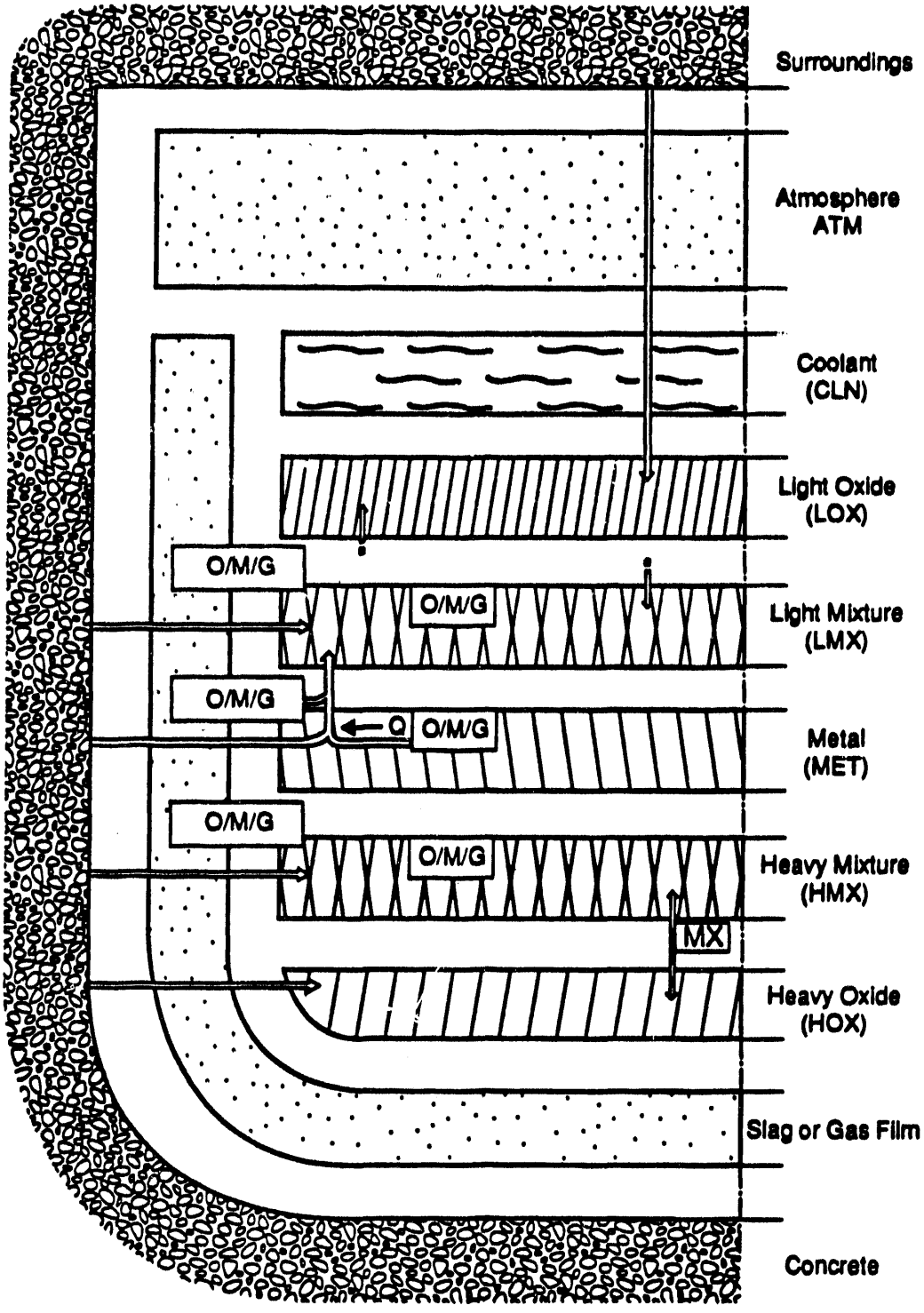

Figure 2.6 Path of oxide through pool

start-of-timestep layer temperature. The associated change in layer enthalpy is given by

$$\Delta H_L = H(m_{in}, T_{in}) - H(m_{out}, T_{out}) \quad (118)$$

where H is enthalpy, T is temperature, m is mass (including composition), and the subscripts "L", "in", and "out" refer to the layer, to material entering it, and to material leaving it, respectively.

Because the enthalpy package employs the standard thermochemical reference point of separated elements in their standard states, this equation will also hold including the effects of chemical reactions. If, for example, the composition of the gas which leaves the layer differs from that of the gas which entered, the entire energy effect is accounted for through the different compositions associated with m_{out} and m_{in}.

2.3.12 Energy Conservation

The energy equation to be solved for each layer of the pool is given by

$$\begin{aligned} H_i^{n+1} = {} & H_i^n + \Delta H_{enter\ i} - \Delta H_{leave\ i} \\ & + \Delta H_{react\ i} + \Delta H_{source\ i} \\ & - Q_{abl\ i} + Q_{Bi} - Q_{Ti} - Q_{Ri} \end{aligned} \quad (119)$$

where

H_i^n = the total enthalpy of layer i at time level n

$\Delta H_{enter\ i}$ = the enthalpy of materials entering during the time-step

$\Delta H_{leave\ i}$ = the enthalpy of materials leaving during the time-step

$\Delta H_{react\ i}$ = the enthalpy gain from chemical reactions

$\Delta H_{source\ i}$ = the enthalpy gain from decay heat sources

$Q_{abl\ i}$ = the heat loss to ablate concrete

Q_{Bi} = the heat transferred from the bottom surface (zero for the bottom layer where this is part of Q_{abl}), and

Q_{Ti} = the heat transferred to the top surface.

Q_{Ri} = the heat transferred to the exposed melt edges if the time-dependent melt radius option is used.

As discussed in Section 2.3.11, the "entering," "leaving," and "reaction" terms are naturally associated. The "reaction" term is included implicitly in the other two for the thermochemical reference point employed. These terms are calculated in subroutine MHTRAN as discrete changes, involving all of the material which moves during a time-step. Residence times are not considered. In other words, all materials which result from ablation are assumed to be completely relocated during the same timestep.

Energy generation from radionuclide decay power changes slowly. Therefore, the corresponding term in the energy equation is evaluated explicitly (in the numerical methods sense) as a beginning-of-timestep power multiplied by Δt. The remaining three terms in Equation (119) involve heat flows which are driven by temperature differences. The heat loss to concrete is also evaluated explicitly, but the remaining terms are treated using a linearized-implicit algorithm. These terms involve the axial heat flows to the upper and lower surfaces of the layer (with the exception of the bottom layer for which the lower surface is adjacent to concrete), and are taken as weighted averages of the values at time n and the linearly-projected values at time n + 1. This results in the equation

$$\begin{aligned} H_i^{n+1} = {} & H_i^{n+1(explicit)} + \Omega\Delta t\Big[\left(\tilde{Q}_{Bi}^{n+1} - Q_{Bi}^n\right) \\ & -\left(\tilde{Q}_{Ti}^{n+1} - Q_{Ti}^n\right) - \left(\tilde{Q}_{Ri}^{n+1} - Q_{Ri}^n\right)\Big] \end{aligned} \quad (120)$$

where the tilde "~" denotes the linearized projection described below, and, of course, $H_i^{n+1(explicit)}$ includes the terms $(Q_{B\ i}^n - Q_{T\ i}^n)\Delta t$. The implicitness factor Ω is programmed as a variable, but is set equal to 1.

The following discussion of the terms in the energy balance is divided in two sections. The discussion in the first section applies for cases in which the time-dependent melt radius option is not invoked. The second section applied if the user chooses to invoke the time-dependent melt radius option.

Melt Radius Option Not Invoked

When the time-dependent melt radius option is not invoked, $Q_{Ri} = 0$, and the terms in the energy equation are determined as in CORCON-Mod2.

We calculate the projected end-of-timestep heat fluxes from

$$\begin{aligned}\tilde{Q}_{Ti}^{n+1} - Q_{Ti}^{n} &= A_i \left[\frac{\partial q_T}{\partial T_L}\Big|_i \tilde{\Delta T}_i + \frac{\partial q_T}{\partial T_T}\Big|_i \tilde{\Delta T}_i \right] \\ &= \tilde{Q}_{Bi+1}^{n+1} - Q_{Bi+1}^{n} \\ &= A_i \left[\frac{\partial q_B}{\partial T_B}\Big|_{i+1} \tilde{\Delta T}_i + \frac{\partial q_B}{\partial T_L}\Big|_{i+1} \tilde{\Delta T}_{i+1} \right] .\end{aligned} \tag{121}$$

if i is not the top layer in the pool, or from

$$\begin{aligned}\tilde{Q}_{Ti}^{n+1} - Q_{Ti}^{n} &= A_i \left[\frac{\partial q_T}{\partial T_L}\Big|_i \tilde{\Delta T}_i + \frac{\partial q_T}{\partial T_T}\Big|_i \left(\tilde{T}_s^{n+1} - T_s^n\right) \right] \\ &= Q_s^n + \frac{dQ_s}{dT_s}\Big|_{sur} \left(\tilde{T}_s^{n+1} - T_s^n\right)\end{aligned} \tag{122}$$

if it is. Here $q_{T(B)i}$ is the upward heat flux at the top (bottom) of layer i, T_i is the temperature of layer i, T_I is the temperature of the interface, A_i is its area, and Q_s^n and $(dQ_s/dT_s)_{sur}$ define the linearization of above-pool heat transfer described in Section 2.3.7. The subscripts B, T, and L refer to the bottom and top of a layer, and to the layer average, respectively. It is important to note that dq_{Ti}/dT_{Ti} may not equal $-dq_{Ti}/dT_i$. An example of this occurs for a primarily molten layer with a thin crust. An increase in the average temperature increases the liquid temperature and the heat flux to the crusted surface, while an increase in the surface temperature merely decreases the crust thickness with little change in heat flux (under the quasi-steady assumptions of CORCON-Mod3).

The temperatures of the interfaces (other than the top surface) are eliminated, and the change in the temperature of layer i during the timestep approximated in terms of the change in enthalpy by

$$\tilde{\Delta T}_i \approx X_i \equiv \left(H_i^{n+1} - \hat{H}_i\right)/\hat{C}_i \ . \tag{123}$$

Here $\hat{H}_i$ is the total enthalpy at temperature T_i^n of the contents of the layer at time n+1, and C_i is the corresponding heat capacity. When coolant is present, Equation (123) is valid only so long as the coolant remains subcooled. When boiling occurs, T_i^{n+1} must be the saturation temperature T_{sat}, and the final enthalpy of the coolant will determine what fraction of it has vaporized during the time-step. This is handled initially by treating $H_{c\,1\,n}^{n+1}$ and $T_{c\,1\,n}^{n+1}$ as independent variables.

Equations (120) through (123) result in a set of linear equations for the layer enthalpies at time n+1. As coded in subroutine ENRCN1, the equations are written in terms of the X's (which may be thought of as enthalpy changes in temperature units) in the form

$$\begin{aligned}\sum_j A_{ij} X_j = b_i^{(1)} &+ b_i^{(2)} \left(\tilde{T}_s^{n+1} - T_s^n\right) \\ &+ b_i^{(3)} \tilde{\Delta T}_{cln}\end{aligned} \tag{124}$$

They are solved as

$$X_i = X_i^{(1)} + X_i^{(2)} \left(\tilde{T}_s^{n+1} - T_s^n\right) + X_i^{(3)} \tilde{\Delta T}_{cln} \tag{125}$$

with $(T_s^{n+1} - T_s^n)$ and ΔT_{cln} left undetermined.

If no coolant is present, so that all the $X_i^{(3)}$ are 0, the heat flow at the top surface, including the effects of all implicit terms in the energy equation, now has the form

$$Q_s^{n+1} = Q_s^n + \frac{dQ_s}{dT_s}\Big|_{pool} \left(\tilde{T}_s^{n+1} - T_s^n\right) \ . \tag{126}$$

This is the linearized pool response mentioned in Section 2.3.7. Specifically, the derivative is

$$\frac{dQ_s}{dT_s}\Big|_{pool} = \frac{dQ_T}{dT_T}\Big|_{top\ i} + \frac{dQ_T}{dT_L}\Big|_{top\ i} X_{top\,i}^{(2)} \tag{127}$$

This equation is solved simultaneously with the above-pool thermal response in subroutine ATMSUR to determine $\dot{T}_s^{n+1}$. The final evaluation of layer enthalpies and the corresponding layer temperatures is then performed in subroutine ENRCN2. This allows the implicit nature of the equations to be maintained across the pool surface even though above- and below-surface heat transfer are not evaluated simultaneously. It is the stabilizing effect of the implicit algorithm which makes possible the relatively long timesteps routinely employed in the code.

If coolant is present but remains subcooled $H_{c\,1\,n}^{n+1}$ and ΔT_{cln} are related through Equation (123), and ΔT_{cln} may be eliminated from both Equations (125) and (126) through the relationship

$$\tilde{\Delta T}_{cln} = \frac{X_{cln}^{(1)} + X_{cln}^{(2)} \left(\tilde{T}_s^{n+1} - T_s^n\right)}{1 - X_{cln}^{(3)}} \tag{128}$$

This possibility is tested, using the above-pool thermal response from the beginning of the timestep

$$Q_s^{n+1} = Q_s^n + \left.\frac{dQ_s}{dT_s}\right|_{sur} \left(\bar{T}_s^{n+1} - T_s^n\right) \qquad (129)$$

to close the set of equations. If this results in a T_{cln}^{n+1} below saturation, the elimination of ΔT_{ch} is accepted, and the solution proceeds as for the no-coolant case. If, on the other hand, this calculation results in a T_{cln}^{n+1} above saturation, we assume that sufficient boiling occurred during the time-step to hold the temperature to saturation and set T_{cln}^{n+1} equal to T_{sat}. In this case, we use the above-pool thermal response from the start of the timestep, Equation (129), to complete the solution in subroutine ENRCN1. The resulting enthalpy of the coolant corresponds to a liquid/vapor mixture at the saturation temperature. The partition of mass between the two phases is evaluated, and the vapor component is added to the gases which left the pool during the timestep. As before, the calculation is completed through ATMSUR and ENRCN2, but with the derivative dQ_S/dT_S set very large (negative). This procedure assures that ATMSUR will determine a value for T_s^{n+1} very near to T_{sat}.

A special case arises when the coolant layer is totally depleted during a timestep, and the calculation just described results in a layer enthalpy greater than that for saturated vapor. In this case, we assume that all vapor was generated at saturation and decrement the mass and energy of the coolant layer accordingly, but we do not update the enthalpies of other layers at this time. The entire calculation is repeated, with the coolant layer now absent. Because of the detailed balance of heat-flow terms in Equation (120), energy is conserved exactly. Although the total enthalpy of the coolant is not zero at the start of the recalculation, its final enthalpy must be zero. Inspection of the equation will show that the result of the implicit calculation is to force the net heat delivered to the coolant layer during the timestep to be exactly sufficient to vaporize it at its saturation temperature.

The major approximation in this treatment of the coolant is the use of saturation conditions at the beginning of the timestep rather than at the end. This could result in an apparently super-heated liquid coolant or in one which is apparently subcooled but boiling. In practice, no significant problems have been observed.

Melt Radius Option Invoked

Consider now the case when a time-dependent melt radius is used. We must account for heat transfer from the melt edges to either the atmosphere or the coolant. First, we consider the case where coolant is absent.

The interface temperatures are determined in routine INTEMP. Temperatures of horizontal interfaces within the melt are determined as in the previous section. The temperature of the uppermost interface, between the melt and the atmosphere, is also determined as before. Since the heat flux to the atmosphere is known, this flux can be used to determine the temperatures of the exposed layer edges as follows. The linearized atmosphere response q_a is

$$q_a = q_a + \frac{dq_a}{dT_s}\left(T_{Ri} - T_S\right) \ , \qquad (130)$$

where T_{Ri} is the temperature of the edge of layer i and T_s is the provisional surface temperature (assumed known). q_a must match the heat flux at each layer edge,

$$q_{Ri}\left(T_{Ri}^* + \delta T_{Ri}, T_{Li}\right) = \alpha\left\{ q_a + \frac{dq_a}{dT_s}\left(T_{Ri}^* + \delta T_{Ri} - T_s\right)\right\} \ , \qquad (131)$$

where T_{Ri}^* is the current temperature of the edge of layer i, δT_{Ri} is the change in temperature required to produce equality of the fluxes, T_{Li} is the fixed temperature of layer i, and α is a parameter. The value of $\alpha=0$ corresponds to an adiabatic edge, while $\alpha=1$ matches the fluxes. Then linearizing, with

$$\begin{aligned} q_{Ri}^* &= q_{Ri}\left(T_{Ri}^* \ T_{Li}\right) \\ q_a^* &= q_a + dq_a/dT_s\left(T_{Ri}^* - T_s\right) \ , \\ q_{Ri}^* &+ \frac{\partial q_{Ri}}{\partial T_{Ri}}\,\delta T_{Ri} = \alpha q_a^* + \alpha\,\frac{dq_a}{dT_s}\,\delta T_{Ri} \ . \end{aligned} \qquad (132)$$

Solving for the temperature correction δT_{Ri},

$$\delta T_{Ri} = \frac{\alpha q_a^* - q_{Ri}^*}{\dfrac{\partial q_{Ri}}{\partial T_{Ri}} - \alpha\dfrac{dq_S}{dT_S}} \ . \qquad (133)$$

The new edge temperature of layer i is then

$$\min\left(T_{Ri}^{*} + \delta T_{Ri},\ T_{Li}\right) \quad . \tag{134}$$

this constraint is imposed so that the radial heat transfer is always outward (i.e., positive).

The procedure described above is implemented at the end of the main interface temperature iteration loop in INTEMP. Following convergence of the interface temperatures, new values of the average surface temperature T_s and the constant flux q_s are required. The new values are given by

$$T_s = \frac{1}{A}\left[A_T T_T + \sum_{i=1}^{icln-1} A_{Ri} T_{Ri}\right] \tag{135}$$

and

$$q_s = \frac{1}{A}\left[A_T q_T + \sum_{i=1}^{icln-1} A_{Ri} q_{Ri}\right] \tag{136}$$

where T_T is the temperature of the horizontal interface between the melt and the atmosphere, A_T is the area of the interface, and q_T is the flux from the uppermost melt layer to the atmosphere through the top interface. A_{Ri} is the area of the edge of layer i, and A is the total melt area exposed to the atmosphere.

The layer temperatures are updated in routine ENRCN1. To account for the energy loss from the melt to the atmosphere, the energy equation for each layer becomes

$$H_i^{n+1} = H_i^{n+1}(\text{explicit}) + \Omega \Delta t \left\{\left(\tilde{Q}_{Bi}^{n+1} - Q_{Bi}^{n}\right) - \left(\tilde{Q}_{Ti}^{n+1} - Q_{Ti}^{n}\right) - \left(\tilde{Q}_{Ri}^{n+1} - Q_{Ri}^{n}\right)\right\} , \tag{137}$$

where the last term on the right-hand side of the equation accounts for heat transfer from the melt edge, H_i^{n+1} is the enthalpy of layer i at the time step n+1, H_i^{n+1} (explicit) is the explicit part of the update, Ω is the implicitness factor (set equal to 1), and Δt is the length of the time step. Q_{Bi}, Q_{Ti}, and Q_{Ri} are the bottom, top, and radial heat transfer, respectively, of layer i at the appropriate timestep indicated by the superscript. The term, $Q_{Ri}^{n+1} - Q_{Ri}^{n}$, is given by

$$\tilde{Q}_{Ri}^{n+1} - Q_{Ri}^{n} = A_{Ri}\left\{\frac{\partial q_{Ri}}{\partial T_{Ri}}\left(T_s^{n+1} - T_s^{n}\right) + \frac{\partial q_{Ri}}{\partial T_{Li}}\Delta T_{Li}\right\} \tag{138}$$

Equation (135) is then solved in the same way as Equation (120).

Once the layer temperatures T_{Li} at the new time have been determined, the new provisional surface temperature T_s^{n+1}, the new provisional heat flux q_s^{n+1} and derivative dq_s/dT_s and the surface emissivity are updated using area averages over the exposed surface of the melt.

Consider now the case in which the time-dependent melt radius option is invoked and coolant is present. The interface between the melt and the coolant now includes contributions from all the exposed layers. The temperatures of the layer edges are determined in the following way. The temperatures of the horizontal interfaces within the melt are determined as in the case with no time-dependent melt radius. At the melt-coolant interface, we have the energy conservation equation

$$\begin{aligned} &A q_c\left(T_{Bc}^{*},\ \delta T_{Bc},\ T_{Lc},\ T_{Tc}^{*} + \delta T_{Tc}\right) \\ &= A_T\, q_{Tt}\left(T_{Bt}^{*} + \delta T_{Bt},\ T_{Lt},\ T_{Tt}^{*} + \delta T_{Tt}\right) \\ &\quad + \sum_{i=1}^{icln-1} A_{Ri} q_{Ri}\left(T_{Ri}^{*} + \delta T_{Ri},\ T_{Li}\right) \end{aligned} \tag{139}$$

where T_{xy}^{*} is the current temperature of the bottom (x=B), layer (x=L), top (x=T), or edge (x=R) of layer y, which may be coolant (y=c), the top layer of the melt (y=t), or the layer i (y=i). A_T is the area of the top horizontal interface of the melt, A_{Ri} is the exposed area of the edge of layer i, and A is the total exposed area of the melt. Equation (138) is solved by first setting $\delta T_{Bc} = \delta T_{Tt}$ and $T_{Bc}^{*} = T_{Tt}^{*}$, and initially setting $\delta T_{Ri} = 0$. Then linearizing,

$$\begin{aligned} &A\left\{q_c^{*} + \frac{\partial q_c}{\partial T_{Bc}}\delta T_{Tt} + \frac{\partial q_c}{\partial T_{Tc}}\delta T_{Tc}\right\} \\ &= A_T\left\{q_{Tt}^{*} + \frac{\partial q_{Tt}}{\partial T_{Bt}}\delta T_{Bt} + \frac{\partial q_{Tt}}{\partial T_{Tt}}\delta T_{Tt}\right\} \\ &\quad + \sum_{i=1}^{icln-1} A_{Ri} q_{Ri}^{*} \quad , \end{aligned} \tag{140}$$

where $q_c^{*} = q_c\,(T_{Bc}^{*}, T_{Lc}, T_{Tc}^{*})$, etc.

The coolant overlying the melt is treated as a layer, and the appropriate heat fluxes are determined as described in Section 2.3.3. The quantities q_c^* and $\partial q_c/\partial T_{Bc}$ are then used to determine the edge temperature of each melt layer by matching heat fluxes as

$$q_{Ri}^* + \frac{\partial q_{Ri}}{\partial T_{Ri}} \delta T_{Ri} = \alpha \left\{ q_c^* + \frac{\partial q_c}{\partial T_{Bc}} \delta T_{Ri} \right\} , \quad (141)$$

where $\alpha=0$ implies an adiabatic edge, and $\alpha=1$ matches the heat fluxes. Thus

$$\delta T_{Ri} = \left(\alpha q_c^* - q_{Ri}^*\right) \Big/ \left\{ \frac{\partial q_{Ri}}{\partial T_{Ri}} - \alpha \frac{\partial q_c}{\partial T_{Bc}} \right\} , \quad (142)$$

and the new edge temperature for layer i is

$$\min\left(T_{Ri}^* + \delta T_{Ri}, T_{Li}\right) . \quad (143)$$

where the minimum constraint is imposed so that the heat transfer is radially outward (i.e., positive). The parameter α is programmed as a variable but is currently set equal to 0.0 in the code.

The layer temperatures are updated in routine ENRCN1. The energy equation for each melt layer is Equation (137), as in the case with no coolant. When coolant is present, however,

$$\tilde{Q}_{Ri}^{n+1} - Q_{Ri}^n = A_{Ri} \left\{ \frac{\partial q_{Ri}}{\partial T_{Ri}} \Delta T_{Ri} + \frac{\partial q_{Ri}}{\partial T_{Li}} \Delta T_{Li} \right\} \quad (144)$$

where ΔT_{Ri} is the change in the edge temperature over the timestep, and ΔT_{Li} is the change in the layer temperature. By analogy with the expression for ΔT_I, the change in the temperature of the horizontal interface I, the expression for ΔT_{Ri} is

$$\Delta T_{Ri} = \frac{\frac{\partial q_{Ri}}{\partial T_{Li}} \Delta T_{Li} - \alpha \frac{\partial q_{Bc}}{\partial T_{Lc}} \Delta T_{Lc}}{\alpha \frac{\partial q_{Bc}}{\partial T_{Bc}} - \frac{\partial q_{Ri}}{\partial T_{Ri}}} . \quad (145)$$

The energy equation for the coolant layer is then

$$H_c^{n+1} = H_c^{n+1}(\text{explicit}) + \Omega \Delta t \left\{ \left(Q_{Bc}^{n+1} - Q_{Bc}^n\right) - \left(Q_{Tc}^{n+1} - Q_{Tc}^n\right) + \sum_{I=1}^{icln-1} \left(Q_{Ri}^{n+1} - Q_{Ri}^n\right) \right\} , \quad (146)$$

where the summation on the right-hand side accounts for the heat transfer from the exposed edges of the melt layers. Equation (146) with Equation (137) for the non-coolant layers are then solved in the same way as Equation (120).

As noted in Section 2.3.9, the time-dependent melt radius is limited to cases where the coolant completely covers the melt. When the coolant is insufficient to cover the melt, the code reports an error and execution stops.

2.3.13 Cavity Shape Change

The shape of the cross-section of the cavity is defined for computational purposes by a series of "body points." These are the intersections of a fixed series of rays with the cavity surface as shown in Figure 2.7. Given the cavity geometry at the start of a timestep, the shape change procedure provides a new cavity shape at the end of the timestep. The normal recession rate is used at each body point, as calculated by the concrete ablation model. The methods used in CORCON-Mod3 are the same as those developed for CORCON-Mod2. The shape change procedure evolved from the CASCET model written for CORCON-Mod1 by ACUREX/Aerotherm Corporation,[61] under contract to Sandia. We first assume that the concrete recession follows the local normal at each body point and then project the resulting surface points back onto the rays. The projection is performed by passing a circle through each normally receded point and its two nearest neighbors, and defining the new body point as the intersection of this circle with the corresponding ray as shown in Figure 2.8. A solution will exist so long as no body point is allowed to cross the neighboring ray during a timestep. In fact, there are two solutions, and we pick the one which is nearer to the normally receded point.

With one exception, the rays emanate from an origin on the vertical axis of symmetry of the cavity. We have retained the so-called "tangent ray" from CASCET. This is a single ray, parallel to the axis, which defines the edge of the flat bottom of the cavity. Because the

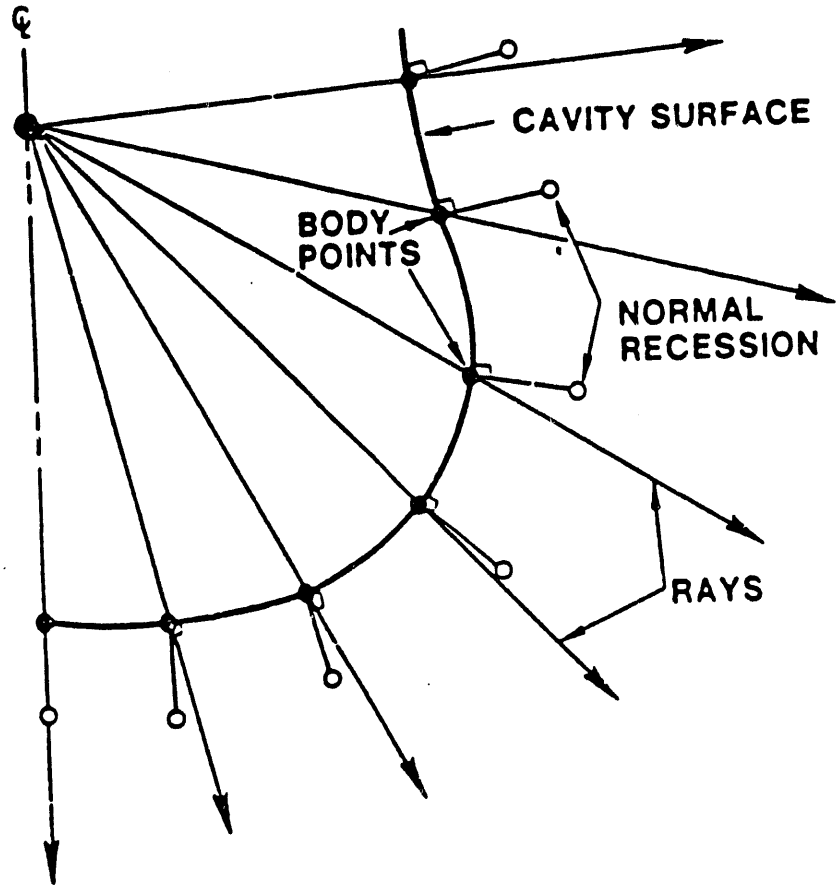

Figure 2.7 Normal surface recession

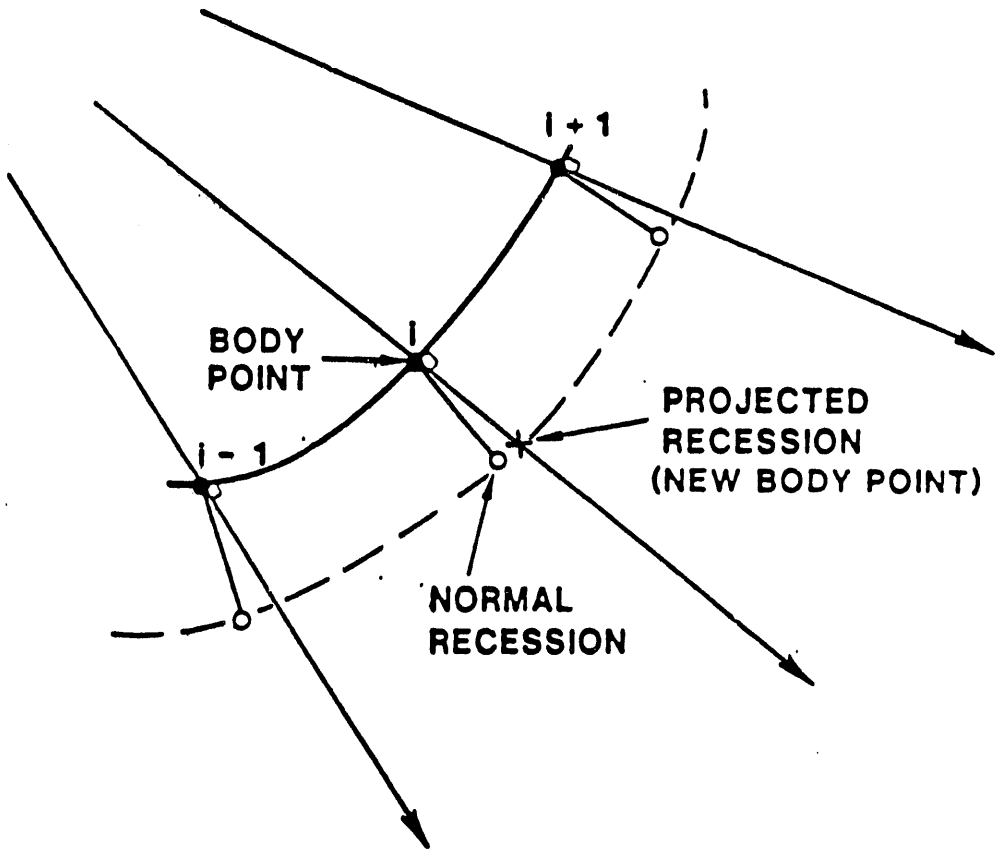

Figure 2.8 Circle intersection projection method

corresponding body point moves vertically, the bottom is constrained to remain flat as is required by the ablation model. When the cavity surface passes through a point where the tangent ray crosses an ordinary ray, the ordering of the body points is changed appropriately.

In these calculations, the "normal" at each body point is chosen as the bisector of the angle formed by lines from the body point to its nearest neighbors on each side. Another modification was made to prevent numerical sharpening of corners projecting into the cavity. In this case, shown in Figure 2.9, if the normal ablation during a timestep is $\Delta s = \dot{s}\Delta t$, the point defining the corner moves $\Delta s/\cos(\gamma/2)$. (Projection back onto the ray system is not included in this Figure.) In CORCON-Mod3, the correction is made for recession of all body points for which $\gamma > 0$.

2.3.14 Aerosol Generation and Radionuclide Release

As gases from decomposition of concrete pass through the melt and leave the pool, aerosols are generated by mechanisms such as vaporization/condensation and bubble bursting. These aerosols were observed in early experimental work, and were hypothesized to be an important mechanism for radionuclide release from the core debris. The VANESA model[10] was developed to predict aerosol generation and radionuclide release during core-concrete interactions. VANESA has now been integrated into CORCON-Mod3.

The VANESA model is called from CORCON-Mod3 as part of the upward pass in subroutine MHTRAN (see discussion in Section 2.3.11). VANESA requires information on: the composition, temperature, and material properties of the core debris; the flow rate and composition of gases sparging the melt; the depth and temperature of any overlying coolant; and the ambient pressure. This information is provided by the remainder of CORCON and is passed to VANESA after first being converted to the form required by VANESA. The following conversions are made in subroutine CVFAC:

- CORCON's debris composition (including fission products) is converted to a VANESA composition by storing CORCON's oxide, metal, and fission product masses in the VANESA composition array XM.
- Average metal and oxide debris temperatures are determined for VANESA by mass-weighting the temperatures of the metals and oxides in the CORCON layers.
- The metal and oxide material properties used in VANESA are calculated by mass-weighting the properties of the metals and oxides in the CORCON layers. The same is true for the bubble properties used by VANESA. All material and bubble properties are converted to c.g.s units for use in VANESA.
- The gas flow rate and composition used in VANESA are determined from the gases exiting the surface of the melt. In other words, VANESA uses the results from the chemical equilibrium solution performed in the CORCON calls to MLTRHA from REACT. (Note that subroutine SRG, which is used in the stand-alone version of VANESA has been eliminated in the integration of VANESA into CORCON.) CORCON gas species that are not tracked by VANESA are included in the total flow rate, but are not included in the VANESA gas composition. These gases are effectively treated as inert in the vaporization release calculation performed in VANESA.
- The coolant depth and temperature, and ambient pressure are passed to VANESA after first converting the depth and pressure to units required by VANESA (i.e., centimeters and atmospheres).

It should be noted that because VANESA is called during the upward pass in MHTRAN, the debris composition passed to VANESA does not include any debris added by user-specified mass addition. Since this mass is added as part of the downward pass in MHTRAN, it is added after the call to VANESA. Consequently, the CORCON and VANESA debris compositions printed in the output will be slightly different whenever the mass is being added to the core debris.

The implementation of the VANESA model included in CORCON-Mod3 calculates the following features of radionuclide release and aerosol generation:

- The rate and total mass of aerosol generated.
- The concentration of aerosols in the evolved gases.
- The composition of the aerosol, including the contributions of non-radioactive materials, as well as those of radionuclides.
- The mean size and size distribution of the aerosols.
- The material density of the aerosol.
- The effects of coolant pools overlying the core debris on the production and nature of the aerosols.

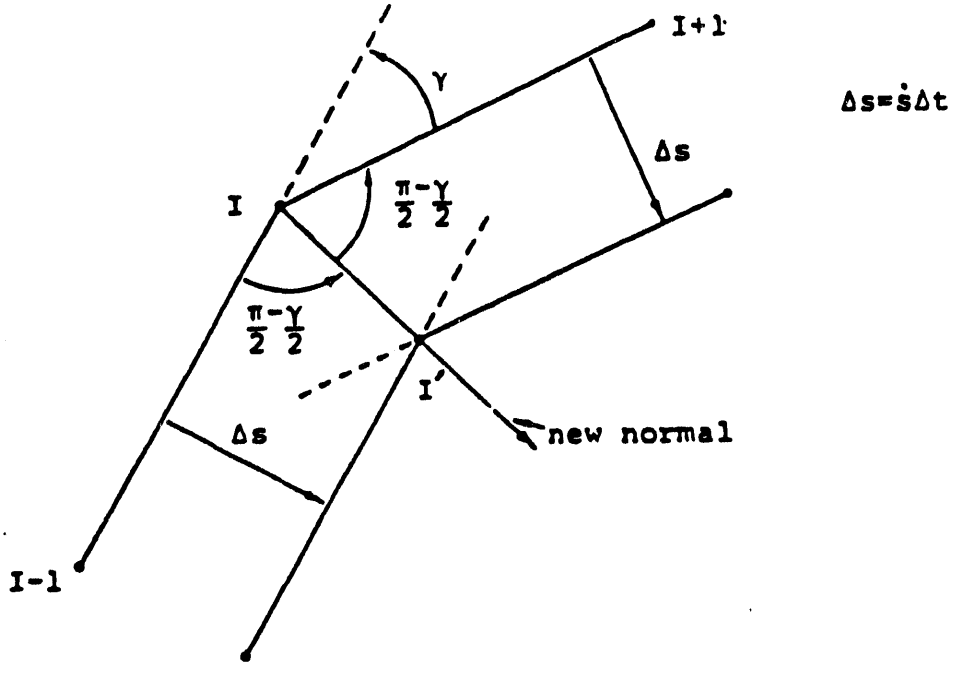

Figure 2.9 Enhanced recession for inside corner point

After completing the above calculations, VANESA passes the calculated results for the mass and composition of the released aerosols back to the rest of CORCON-Mod3. CORCON-Mod3 uses these results to adjust the mass, composition, and enthalpy of each layer. The fission product content of each layer is also adjusted in order to correct the decay power generation for fission product release during the timestep. It should be noted that changes to the gas composition resulting from the vaporization reactions treated by VANESA (see discussion below) are not passed back to CORCON. As a result, the VANESA gas composition reported in the output is slightly different from the gas composition reported by the rest of CORCON.

The VANESA models for aerosol generation, radionuclide release, and water pool scrubbing are briefly described below. The reader is referred to Reference 10 for a more detailed discussion of the models.

Model for Vaporization Release

Vaporization is the most important of the release mechanisms. This is especially true during the early phases of the interaction when the temperatures are the highest and the oxygen potential of the core debris is the lowest. The VANESA model includes both a thermochemical analysis of vaporization and an analysis of the kinetic factors which may prevent the equilibrium limit from being reached.

Vapor formation processes can be quite complex. Consider, for example, the formation of vapor from a condensed phase species MO_x. Vapor formation may occur by unary vaporization, which is described by the following simple stoichiometry:

$$[MO_x] \rightleftarrows MO_x(g)$$

Vaporization may also result from reactions between the condensed phase and the adjacent gas phase. For example, the following reaction stoichiometries may occur:

$$[MO_x] + H_2O \rightarrow MO_{x+1}(g) + H_2$$

$$[MO_x] + xH_2 \rightarrow M(g) + xH_2O$$

A general reaction stoichiometry for vaporization into a steam/hydrogen atmosphere can be written as

$$[MO_x] + (w\text{-}x)\, H_2O \rightarrow MO_wH_y + (w\text{-}x\text{-}y/2)\, H_2 \ .$$

For this reaction, the equilibrium pressure of the vapor species MO_wH_y is given by:

$$\frac{-\Delta G(rxn)}{R_oT} = \ln\left\{ \frac{P^*(MO_wH_y)[P^*(H_2)]^{\left(w-x-\frac{y}{2}\right)}}{X^*(MO_x)[P^*(H_2O)]^{(w-x)}} \right\} \qquad (147)$$

where $P^*(i)$ and $X^*(i)$ are given by:

$$^*(i) = P(i)\phi(i) \text{ and } X^*(j) = x(j)\gamma(j)$$

where $P(i)$ and $\phi(i)$ are the partial pressure and fugacity coefficient for vapor species i, $x(j)$ and $\gamma(j)$ are the mole fraction and activity coefficient for condensed phase species j, and $\Delta G(rxn)$ is given by

$$\begin{aligned} \Delta G(rxn) = {} & \Delta G_f(MO_wH_y) - \Delta G_f(MO_x) \\ & + (w-x-y/2)\ \Delta G_f(H_2) \\ & - (w-x)\ \Delta G_f(H_2O) \end{aligned} \qquad (148)$$

and $\Delta G_f(i)$ is the free energy of formation for species i.

Expressions of this type must be written for each of the vapor species involved in the vaporization process. The event of vaporization of the condensed phase species, MO_x, is then determined by the partial pressures of all vapor species composed of element M. As is shown in the above equation, vaporization release is a strong function of temperature and composition of evolved gases. Because the rising bubbles provide the surface area available for vaporization, release depends also on the gas flow rate through the melt.

The current implementation of VANESA assumes that the fugacity coefficients for all vapor phase species are equal to 1.0. In other words, the vapor phase is assumed to be ideal. Non-idealities are, however, considered for the condensed phase. The code calculates the activity coefficients of metallic species using a subregular solution model. For oxidic species, an associated solution model is used.

In the subregular solution model, the activity coefficient of the metal phase constituents is determined from

$$\ln \gamma_i = \frac{1}{R_oT}\left\{ G^{xs} + \frac{\partial G^{xs}}{\partial x_i} - \sum_{k=1}^{N} x_k \frac{\partial G^{xs}}{\partial x_k} \right\} \qquad (149)$$

where the excess Gibbs free energy is given by

$$G^{xs} = \sum_{i=1}^{N-1} \sum_{j=i+1}^{N} \frac{x_i x_j}{x_i + x_j} \left[W_{ij} x_i + h_{ij} x_j \right] \quad (150)$$

where W_{ij} and h_{ij} are the interaction parameters that describe the chemical interaction between metallic constituents i and j. The interaction coefficients are assumed to be linear functions of temperature; therefore two parameter values are needed to specify each i,j coefficient. Tabulated values for these parameters are included in BLOCK DATA INTCOF. The tabular entry was simplified by making use of the following relationships between W_{ij} and h_{ij}:

$$W_{ij}(T) = h_{ji}(T) \text{ and } h_{ij}(T) = W_{ji}(T)$$

Thus, it was only necessary to enter values into the upper (or lower) diagonal of each array.

The associated solutions model for the oxide phase has not yet been completed. It takes into account a richer chemistry with more constituents than are currently treated in VANESA. The chemical equilibrium of the oxide phase is solved and the associated solution model applied to this richer chemistry. Effective activity coefficients for the species treated in VANESA are then calculated and returned to VANESA. Although the data necessary to use the model are not yet completely available, the model has been formulated and the framework for its solution is included in VANESA. Until the implementation is complete, CORCON-Mod3 should be run with the user flag IDEAL set equal to 1. The model is briefly described below.

The associated solution model adopted for the oxidic phase is based on a model suggested originally by Bottinga and Richert.[63] In this model, the chemical potentials of species in the system are derived by assuming regular solution interactions between pairs of species, and recognizing that the molar volumes of the constituents can be very different. Given this basis, the following equation is derived:

$$\mu_k = \mu_k^{\circ} + R_o T \left\{ \ln \psi_k + \sum_{i=1}^{N} \psi_i \left[1 - \frac{v_k}{v_i} \right] \right. \quad (151)$$
$$\left. + v_k \sum_{i=1}^{N} \sum_{j=1}^{N} \left\{ A_{kj} - \frac{A_{ij}}{2} \right\} \psi_i \psi_j \right.$$

where μ_k° is standard state of the pure liquid species k, ψ_k is the volume fraction of species k in the mixture, v_k is the molar volume of species k in the liquid phase, and A_{kj} is the interaction coefficient for species k-j interactions. The volume fraction of species k is determined from

$$\psi_k = \frac{N_k v_k}{\sum_{i=1}^{N} N_i v_i} \quad (152)$$

where N_i is the number of moles of i in the mixture. Equation (151) can be written in terms of the activity coefficient:

$$\ln \gamma_k = \ln \left[\frac{v_k \sum_{j=1}^{N} N_j}{\sum_{i=1}^{N} N_i v_i} \right] + \sum_{i=1}^{N} \psi_i \left[1 - \frac{v_k}{v_i} \right] + \frac{v_k}{R_o T} \sum_{i=1}^{N} \sum_{j=1}^{N} \left[A_{kj} - \frac{A_{ij}}{2} \right] \psi_i \psi_j \quad (153)$$

Tables of the oxide phase interaction coefficients, A_{ij}, will be included in a later update.

The VANESA model also considers kinetic limitations to the vaporization release. The model treats the following three processes:

- Transport of the volatile constituent of the condensed phase to the free surface.
- Conversion of the condensed phase constituents to the vapor phase
- Gas phase mass transport of vapor species away from the free surface

The following equation for the molar flux is solved for each vapor species:

$$\frac{1}{A} \frac{dN_j}{dt} = K_{eff,j} (P_{eq,j} - P_j) \quad (154)$$

where the $K_{eff,j}$ is the effective rate constant for formation of vapor species j, $P_{eq,j}$ is the equilibrium partial pressure of j over the condensed phase, and P_j is the partial pressure of j in the bulk gas phase. The effective rate constant, $K_{eff,j}$, is given by

$$K_{eff,j} = \frac{1}{\frac{P_{eq,j}}{K_{m,i}\,\rho_{molar}\,x_i} + \frac{1}{K_{v,ij}} + \frac{R_o T}{K_{g,j}}} \qquad (155)$$

where $K_{m,i}$ is the rate constant for condensed phase mass transport, ρ_{molar} is the molar density of the condensed phase, x_i is the mole fraction of constituent i in the bulk condensed phase, $K_{v,ij}$ is the vaporization rate constant, and $K_{g,j}$ is the gas phase mass transport coefficient of vapor species j. In this equation, the subscripts i and j refer to the condensed and vapor phases, respectively.

The rate constant for condensed phase mass transport is calculated in the VANESA model using

$$K_{m,i} = \frac{Sh\ D_i}{d} \qquad (156)$$

where Sh is the Sherwood number, D_i is the condensed phase diffusion coefficient, and d is the diameter of the rising bubbles. The condensed phase diffusion coefficient is determined using the Scheibel[64] modification of the Wilke-Chang[65] correlation:

$$D_i = 8.2\text{x}10^{-10}\ T \left[\frac{1 + \left[\frac{3\ v_L}{v_i} \right]^{2/3}}{\mu_L\ v_i^{1/3}} \right] \qquad (157)$$

where v_L is the molar volume of the condensed phase, v_i is the molar volume of i, and μ_L is the viscosity of the condensed phase. The Sherwood number is determined from one of several different correlations depending on the bubble geometry (e.g., size, shape, etc.). For a discussion of these correlations the reader is referred to Reference 10.

The vaporization rate constant is calculated using a form of the Hertz-Knudsen equation.[66] In this model, $K_{v,ij}$ is determined from

$$K_{v,ij} = \frac{\alpha_i}{\sqrt{2\ \pi\ M_i\ R_o\ T}} \qquad (158)$$

where α_i is the condensation coefficient (currently set equal to 1.0 in the code), M_i is the molecular weight of species i, and T is the vapor phase temperature (assumed equal to the temperature of the melt).

The gas phase mass transport coefficient is calculated from

$$K_{g,j} = \frac{2\ D_j}{d_e} \qquad (159)$$

where D_j is the gas phase diffusion coefficient for vapor species j, and d_e is the equivalent spherical bubble diameter. The gas phase diffusion coefficient is calculated using the equation proposed by Singh and Singh:[67]

$$D_j = \frac{0.00279\ T^{1.622} \left[\frac{M_j + M_g}{M_j\ M_g} \right]^{1/2}}{P \left(v_j^{1/3} + v_g^{1/3} \right)^2} \qquad (160)$$

where M_j and M_g are the molecular weights of species j and the gas phase mixture, v_j and v_g are the molar volumes of species j and the gas mixture, and P and T are the pressure and temperature of the gas phase.

Model for Mechanical Release

Mechanical generation of aerosols by entrainment and bubble bursting is important late in a reactor accident, when the core debris temperature has fallen such that aerosol generation by vaporization is minimal. Both droplet entrainment and bubble bursting are modeled in the code.

Droplet entrainment is modeled using a correlation developed by Kataoka and Ishii:[68]

$$E^* = 0.002\ (j_g^*)^3\ [N(\mu_g)]^{1/2} \left\{ \frac{\rho_l - \rho_g}{\rho_g} \right\} \qquad (161)$$

where E^* is the dimensionless entrainment flux

$$E^* = \frac{\rho_l\ j_l}{\rho_g\ j_g} \qquad (162)$$

j_g^* is the dimensionless gas velocity

$$j_g^* = \frac{j_g}{\left[\frac{\sigma_l\ g\ (\rho_l - \rho_g)}{\rho_g^2} \right]^{1/4}} \qquad (163)$$

and $N(\mu_g)$ is a dimensionless gas viscosity

$$N(\mu_g) = \frac{\mu_g}{\left[\frac{\rho_g \sigma_l^{3/2}}{g^{1/2}(\rho_l - \rho_g)^{1/2}}\right]^{1/2}} \quad (164)$$

The VANESA model calculates aerosol generation by bubble bursting using the following correlation by Azbel:[69]

$$E = \frac{3 K_1}{2 \pi \rho_g d_b} \left\{\frac{NUMER}{DENOM}\right\}^{1/2} \quad (165)$$

where NUMER is

$$NUMER = \left[1 - \frac{d_b^2}{2K_2} + \frac{9}{16}\frac{d_b^4}{K_2^2}\right]^{1/2} + \left[\frac{d_b^2}{4K_2} - 1\right] \quad (166)$$

DENOM is

$$DENOM = 1 + \frac{3}{4}\frac{d_b^2}{K_2} - \left[1 - \frac{d_b^2}{2K_2} + \frac{9}{16}\frac{d_b^4}{K_2^2}\right]^{1/2} \quad (167)$$

the dimensionless entrainment volume, E, is

$$E = \frac{\rho_l V_a}{\rho_g V_b} \quad (168)$$

where V_a and V_b are the volume of the entrained aerosol and bubble, K_1 and K_2 are

$$K_1 = \frac{1.15\pi \sigma_l}{c^2}, \qquad K_2 = \frac{6 \sigma_l}{g(\rho_l - \rho_g)} \quad (169)$$

d_b is the diameter of the bubble, and c is the speed of sound in the gas.

If the user chooses to bypass the VANESA calculation, but still wishes to consider the effects of aerosol generation on radiant heat loss from the upper debris surface, the empirical correlation used in CORCON-Mod2 is used. This correlation is given by:[11d]

$$[A] = (33 + 240 j_g) \exp(-19000K/T) \quad (170)$$

where [A] is the concentration (g/m^3 STP) of aerosol in the evolved gas, T is the temperature of the melt (K), and j_g is the superficial gas velocity through the melt (m/s STP). Note that both the superficial velocity and the concentration in this expression have been reduced to standard temperature and pressure (STP).

The temperature T in Equation (170) is assumed to be the temperature of the top layer of the melt. The gas flow (in bubbles) through the pool is converted to a superficial velocity at STP, and the aerosol concentration is adjusted to the temperature and pressure directly above the pool, with the temperature taken as that of the top layer. If coolant is present, we assume that it is effective in scrubbing aerosols from the evolved gases, and set the concentration in the atmosphere equal to zero.

The empirical aerosol concentration is calculated solely for the purpose of determining the radiative properties of the atmosphere; no composition is calculated for it, and its mass is not charged against the pool inventory.

2.3.15 Aerosol Removal By Overlying Water Pools

The VANESA model also treats the decontamination of aerosol-laden gases passing through an overlying water pool. Aerosol removal is assumed to be due to the following mechanisms: sedimentation of aerosol particles within gas bubbles, impaction and adherence of aerosol particles on the bubble walls, and diffusion of aerosol particles to the bubble walls. If the water pool is subcooled, a fourth mechanism is assumed to be active: collapse of bubbles due to steam condensation in the subcooled pool. This model assumes that either the steam condenses completely immediately after the bubble forms in the subcooled water pool or that steam condensation is just complete when the bubble reaches the water-atmosphere interface.

The VANESA model for aerosol removal is based on the model formulated by Fuchs.[70] The aerosol removal rate is given by:

$$\frac{dm(d_p,x)}{dt} = -[\alpha_s(d_p) + \alpha_l(d_p) + \alpha_D(d_p)]\, m(d_p,x) \quad (171)$$

where $m(d_p,x)$ is the mass of aerosol having diameter d_p at elevation x above the debris surface; and $\alpha_s(d_p)$,

$\alpha_I(d_p)$, and $\alpha_D(d_p)$ are the coefficients for removal by sedimentation, impaction, and diffusion.

The sedimentation coefficient is given by Fuchs:[70]

$$\alpha_s(d_p) = \frac{1.5\ J(d_p)}{d_b\ U_{rise}} \quad (172)$$

where $J(d_p)$ is given by

$$J(d_p) = \frac{g\ \rho_p\ d_p^2\ C}{18\ \mu_g} \quad (173)$$

D_b is the diameter of the bubbles, U_{rise} is the rise velocity of the bubbles in the water pool, ρ_p is the material density of the aerosol particles, μ_g is the viscosity of the gas, C is the Cunningham slip correction factor

$$C = 1 + \frac{2\lambda}{d_p}\left[1.257 + 0.4\ \exp\left[\frac{-0.55\ d_p}{\lambda}\right]\right] \quad (174)$$

where λ is given by

$$\lambda = \frac{1}{\sqrt{2}\ \pi\ d_g^2\ N_A\ (P/82.06\ T)} \quad (175)$$

d_g is the diameter of a gas molecule, P is the local pressure, and N_A is Avogadro's number. The equation for the sedimentation coefficient neglects the effects of water condensation on the aerosol particles. This would increase the effective particle diameter, and thereby increase aerosol removal by sedimentation. Note, however, that this effect would be compensated to some extent by the reduction in the material density of the aerosol.

The coefficient for particle diffusion is also given by Fuchs:[70]

$$\alpha_D(d_p) = 1.8\left[\frac{8\ \theta}{U_{rise}\ d_b^3}\right]^{1/2} \quad (176)$$

where θ is given by

$$\theta = \frac{k\ T\ C}{3\pi\ \mu_g\ d_p} \quad (177)$$

and k is Boltzmann's constant. The equation for the particle diffusion coefficient neglects the effect of steam production on the bubble surface. A flux of steam from the surface would, of course, reduce diffusion of particles to the surface.

The impaction coefficient describes loss of aerosol from the bubbles due to impaction on the bubble wall. This occurs because the particles cannot stay within the internally circulating gas flow. This mechanism is affected by many different processes; consequently, many of the correlations in the literature are quite complex. The VANESA model uses the relatively simple correlation shown below:

$$\alpha_I(d_p) = \frac{8\ U_{rise}\ \tau}{d_b^2}\left[\frac{U_{rel}}{U_{rise}}\right]^2 \quad (178)$$

where τ is given by

$$\tau = \frac{\rho_p\ d_p^2\ C}{18\ \mu_g} \quad (179)$$

and U_{rel} is the relative velocity of the particles. The ratio U_{rel}/U_{rise} is a parameter that depends on many variables such as bubble shape, internal circulation velocity, etc. The user may supply a value through input or may select the default value of 1.5. Values from 1.5 to 4.2 are reasonable. (The upper end of this range corresponds to spherical cap bubbles. For spherical bubbles, the geometrical basis for the impaction model is probably invalid.) Figure 2.12 illustrates the sensitivity of the pool decontamination factor (DF) to variations in this ratio.

As the above equations illustrate, the aerosol removal is sensitive to many factors including: particle size, bubble size, bubble rise velocity, and pool depth. The sensitivities of the calculated pool DF to these variables are shown in Figures 2.10 through 2.13.

The figures show a significant dependence of the pool DF on the size of the aerosol particles. Small particles ($< 1\mu m$) are trapped efficiently because they diffuse quickly to the bubble wall. Large particles ($> 1\ \mu m$) are trapped efficiently because of efficient sedimentation and impaction. It is important, therefore, that the code use accurate models for calculating the particle diameter of the aerosols. These models are described below.

Aerosol formation and growth processes are extremely complex. Important processes include: homogeneous

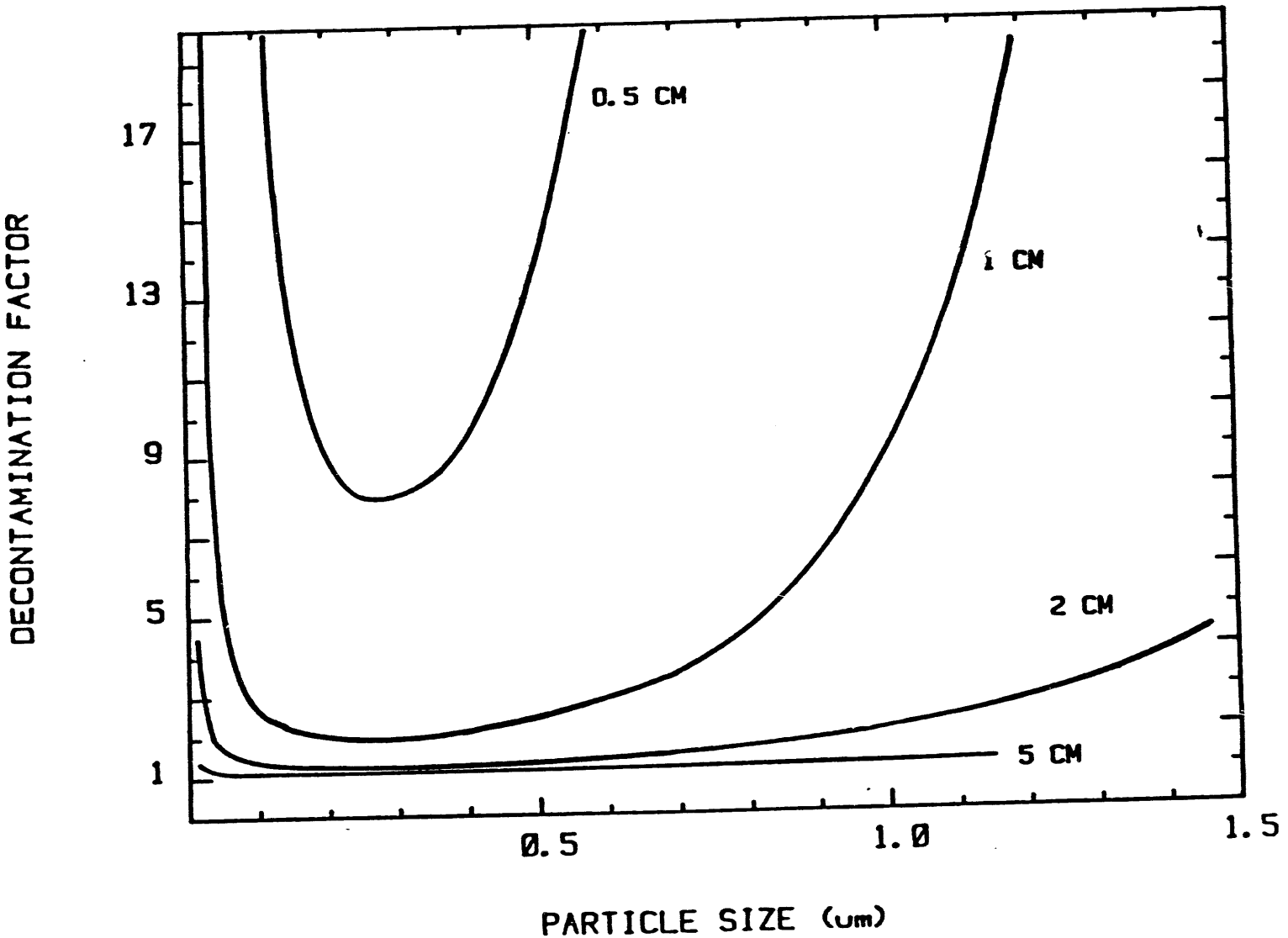

Figure 2.10 Sensitivity of the decontamination factor to bubble size (pool depth is 3 m, V(rel)/V(rise) is 1.5)

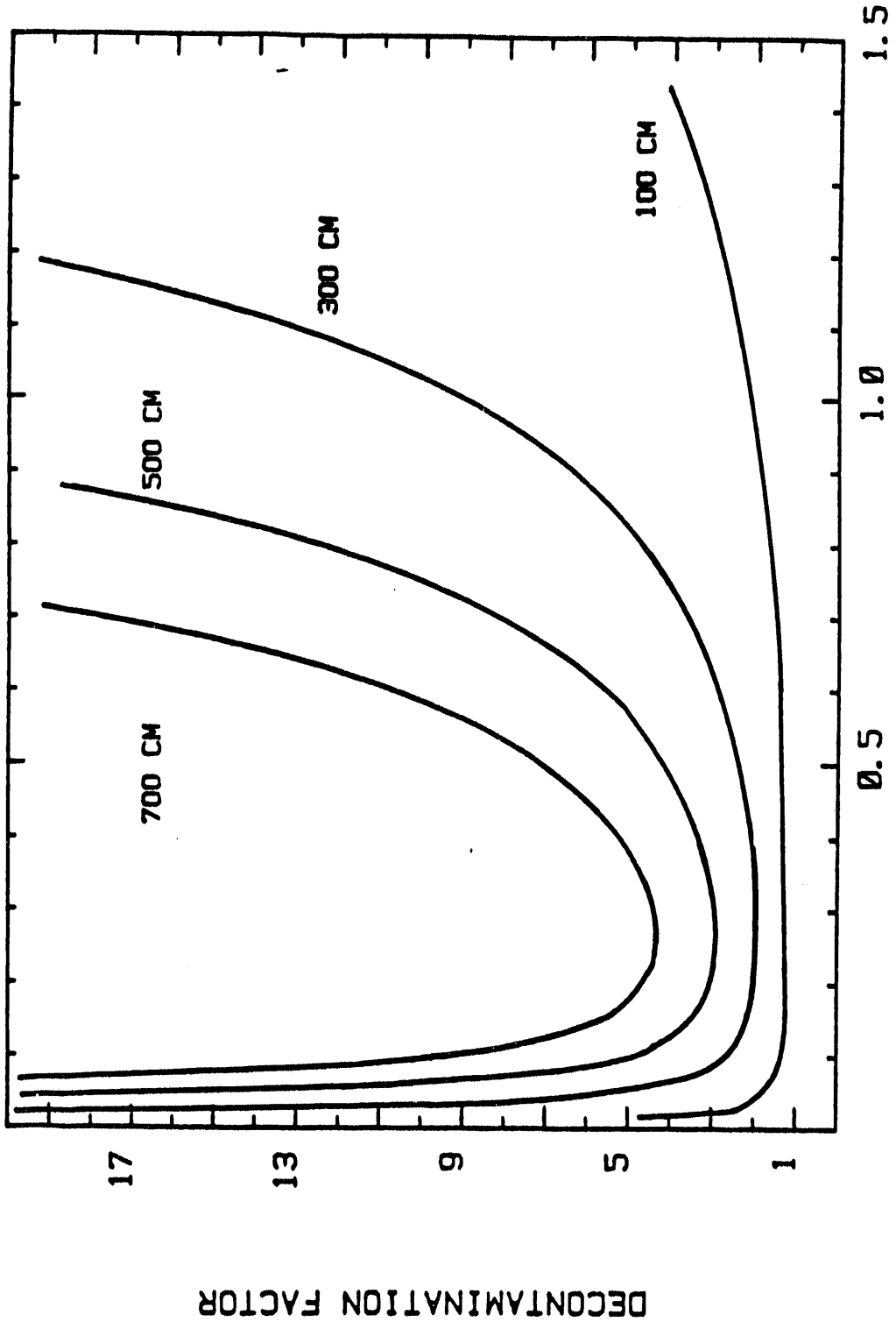

Figure 2.11 Sensitivity of the decontamination factor to pool depth (bubble diameter is 1 cm, V(rel)/V(rise) is 1.5)

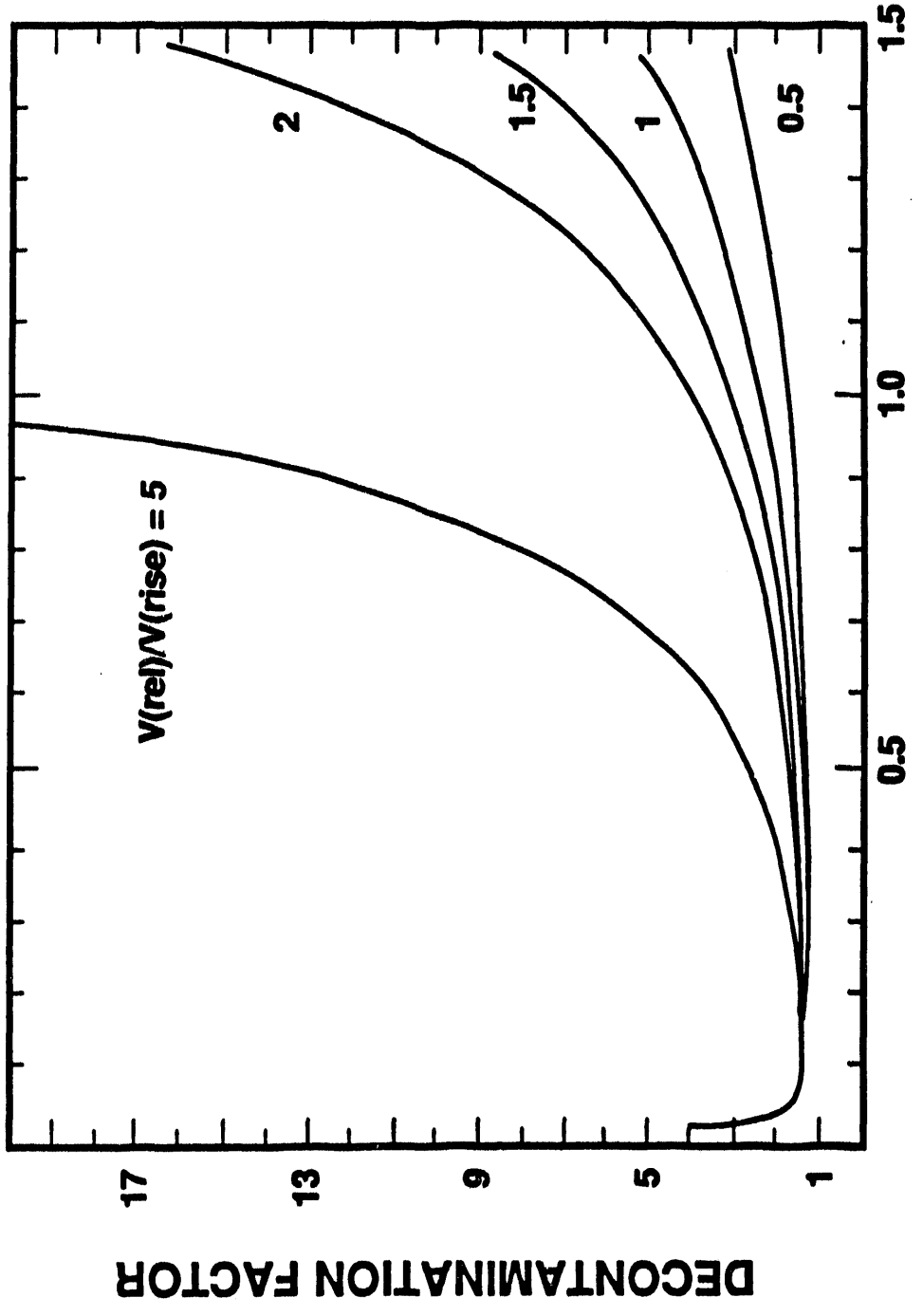

Figure 2.12 Sensitivity of the decontamination factor to the velocity ratio (pool depth is 2 m, bubble diameter is 1 cm)

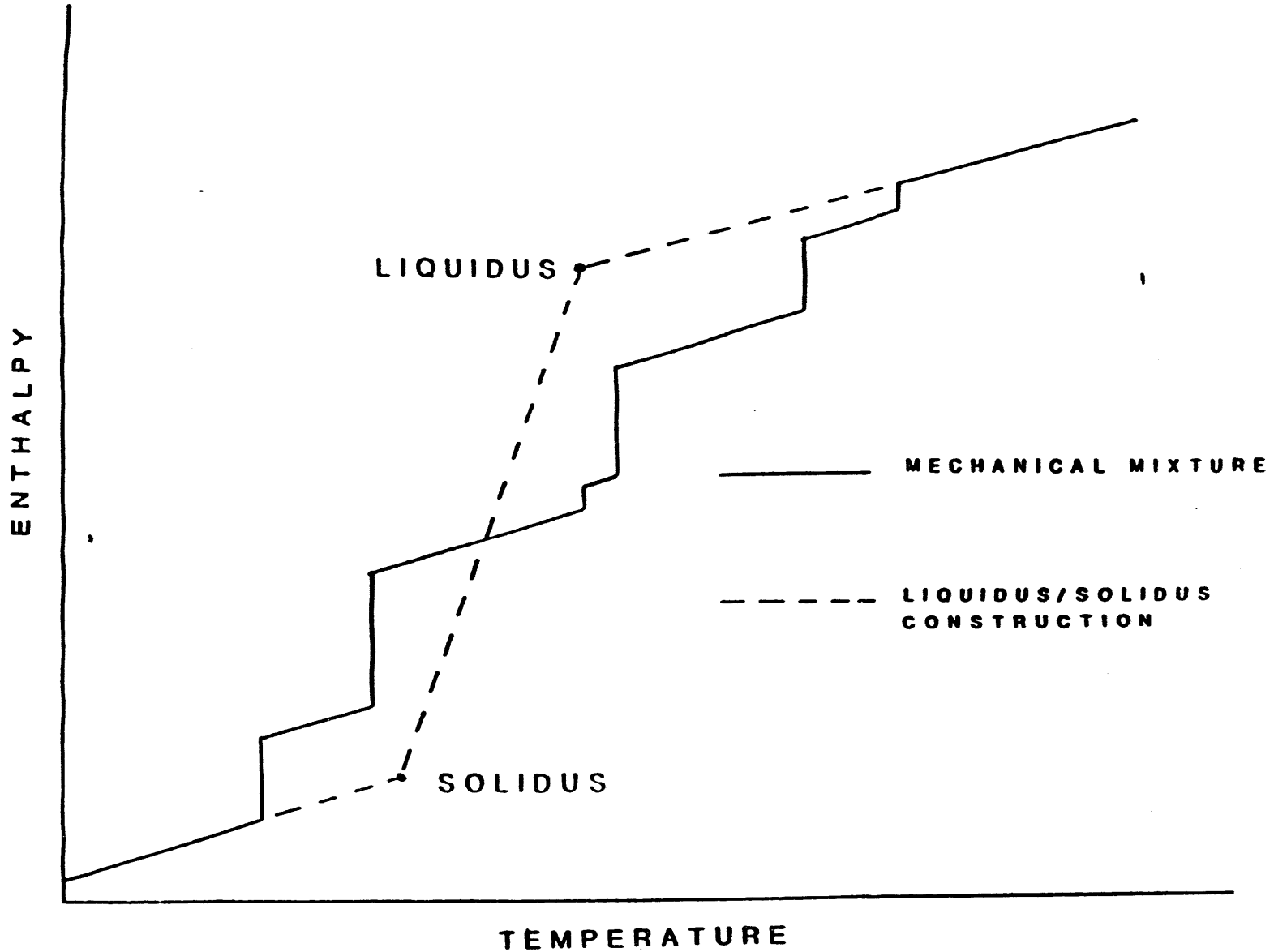

Figure 2.13 Two-phase construction for mixture

nucleation in the vapor phase, condensation of vapor on nucleated particles and other surfaces, and coagulation of particles in the vapor stream. The VANESA manual[10] provides an excellent summary of the models proposed to analyze these processes.

Given the complexity of the required models and the uncertainty associated with these models, the developers of the VANESA model decided to adopt an empirical approach to the calculation of the particle size. This model begins with the assumptions that a.) particle size is dictated by condensation of vapors on nucleated and coagulated particles, and b.) the temperature of the gas stream is low enough that essentially all of the vapor will condense. Given these assumptions, the mean particle size is

$$d_p = \left[\frac{6\ A}{\pi\ \rho_p\ n(t)} \right]^{1/3} \qquad (180)$$

where A is the initial mass concentration of the condensing vapors (g/m^3 gas), ρ_p is the material density of the particles (g/cm^3), and n(t) is the number concentration of the particles (particles/cm^3). Based on experimental results which indicate a mass-weighted mean particle size of 1.2 μm at vapor concentration of 50 to 150 g/cm^3, the number density of the aerosol particles is estimated to be 10^8 particles/cm^3. Thus, the mean particle size in micrometers is calculated by

$$d_p = 0.266 \left[\frac{A}{\rho_p} \right]^{1/3} \qquad (181)$$

For calculations, such as pool decontamination, that require a particle size distribution, a log normal distribution is assumed with a geometric standard deviation of 2.3. (The user may specify alternate values for the particle size and/or geometric standard deviation if desired.)

The aerosol scrubbing model divides the supplied aerosol size distribution into size classes containing equal fractions of the total mass. The upper limit to the particle size in each class is determined from

$$\frac{1}{N} = 0.5 \left[1 + \mathrm{erf} \left[\frac{\ln(D_{i+1}/\mu)}{\sqrt{2}\ \ln(\sigma)} \right] \right] \qquad (182)$$

where N is the number of size segments, D_{i+1} is the upper limit to the size in class i, μ is the mean particle size, and σ is the geometric standard deviation. Within each class, the characteristic size is determined such that half the mass lies above the characteristic size and half lies below.

The code solves for the aerosol removal as a function of position in the pool, and integrates the position-dependent removal to determine the total aerosol removed from the gas stream. Since particle removal is size dependent, the code tracks the changes in the size distribution with position in the water pool.

2.4 Material Properties

Calculation of the physical processes described in the preceding sections requires values for a wide range of thermodynamic and transport properties. These properties are treated as functions of composition and of temperature. However, the dependence is not always explicitly included in the CORCON-Mod3 model; for example, the values used for surface tensions are independent of temperature.

In most cases, properties are required for the mixtures of species which make up the components of the CORCON system, although the calculation of chemical equilibrium requires the chemical properties of the individual species. With a few exceptions, such as the viscosity of oxide mixtures with large silica contents, mixture properties are calculated from those of the constituent species.

The property models described below are the same as those used in CORCON-Mod2 with a few exceptions. A user option for specifying the phase diagrams of the metallic and oxidic phases is now provided in CORCON-Mod3. Also, properties used by the

CORCON-Mod3 implementation of the VANESA model have been included.

2.4.1 Thermodynamic Properties

The thermodynamic properties calculated are density, specific heat, enthalpy, and chemical potential.

Density - ρ (kg/m^3)

Condensed phases:

Mixture densities are computed from

$$\rho_m = 10^3\ m_m / \Sigma_i\ (m_i v_i / M_i) \qquad (183)$$

where the molar volumes of the individual species are given by

$$v_i = v_i^\circ \left[1 + c_i(T - 1673\ K)\right] \quad . \tag{184}$$

Values for v_i° and c_i applicable to the liquid phase are stored in subroutine DENSTY for all condensed species.[71-73] The temperature range of the data from which this relationship was generated varies considerably for the different species. For many of the oxides, it is from 1200 to 1800°C, while for others it covers the entire range from melting to boiling. However, Equation (184) is applied at all temperatures. This disregards the change in density which accompanies freezing.

Separate tables of densities and molecular weights are stored (in BLOCK DATA XNDAR) and used in the VANESA model. The tables include values for both condensed phase species and gas phase species. For the species considered by VANESA, the molar volume is calculated from these values by

$$v_i = \frac{M_i}{\rho_i} \tag{185}$$

where M_i is the molecular weight of species i. The molecular weight of a mixture is calculated by molar weighing of the species molecular volumes.

Gaseous phase:

Densities are computed from the ideal gas relationship

$$\rho_m = 10^3 p M_m / R_o T \tag{186}$$

where M_m is the mixture molecular weight:

$$M_m = \sum_i x_i M_i \quad . \tag{187}$$

Specific Heat - c_p (J/kg K)

The specific heat of any species, condensed or gaseous, is represented in the form

$$c_{p_i} = A_i + 10^{-3}B_i T + 10^{-6}C_i T^2 + 10^5 D_i/T^2 \quad . \tag{188}$$

Within the calculation, units are cal/mol K, reflecting the original data sources; a conversion to S.I. (J/kg K) is made before return from the calculational package. Values of the constants A_i, B_i, C_i, and D_i are tabulated in subroutine CONFND, with one or more temperature ranges for each species. A single range is used for all gaseous species, and the fits are valid from 298.15 to 6000 K. The fits for condensed species include both the liquid and one or more solid phases; in some cases, two ranges are defined for a single phase. Thus, each species requires from two to five sets of coefficients. The upper limit of validity is above 2500 K in most cases, although it is as low as 2000 K in others.[73-77]

In any case, the data for the highest temperature range included are used for all temperatures above the minimum for this range. Mixture specific heats are computed by mass averaging as

$$c_{p_m} = 4186.8 \sum_i \left(m_i c_{p_i}\right)/m_m \quad . \tag{189}$$

where the constant provides the conversion to S.I. units. Specific heats are computed in subroutine CPENTH.

Enthalpy - h (J/kg)

Species enthalpies are computed from integrals of the corresponding specific heats. The conventional thermochemical reference point of separated elements in their standard states (25°C, 1 atm) is employed; i.e., the enthalpies correspond to the JANAF tables. The result may be expressed in the form

$$\begin{aligned} h_i(T) &= h_i(T^1) + \int_{T^1}^{T} dT' c_{p_i}(T') \\ &= K_{hi}^k + A_i^k \left(T - T_i^k\right) \\ &\quad + 10^{-3}B_i^k \left(T^2 - T_i^{k2}\right)/2 \\ &\quad + 10^{-6}C_i^k \left(T^3 - T_i^{k3}\right)/3 \\ &\quad - 10^5 D_i^k \left(1/T - 1/T_i^k\right) \end{aligned} \tag{190}$$

for T in the kth temperature range for species i (i.e., $T_i^k < T < T_i^{k+1}$). The $\{T_i^k\}$ are the break points in the specific heat fits. The first is 298.15 K and the last is treated as infinite. Thus, the first integration constant, K_{hi}^1, is the standard enthalpy of formation of species i. Any others required are computed internally, subject to the condition that the discontinuity in enthalpy at T_i^k be the appropriate heat of transition, $\Delta H_{i,TR}^k$, if a phase change occurs at T_i, and zero otherwise. Subroutine CONFND contains tables of these heats of formation and of transition. The integration constants are evaluated internally during an initial call to CONFND from routine SETUP in order to assure full-word accuracy on machines of different word length. This is done to avoid the possibility of negative discontinuities in h(T), which

could cause numerical problems. At this time, the discontinuities in enthalpy are also replaced by smooth transitions over an arbitrary temperature range of 10 K. As with specific heat, the enthalpy of a mixture is computed by mass averaging:

$$h_m(T) = 4186.8 \sum_i [m_i h_i(T)]/m_m \quad . \qquad (191)$$

Mass averaging of specific heats and enthalpies is really appropriate only for mechanical mixtures in which each species is unaffected by the others. Because of mutual solubilities, actual mixtures of metallic or oxidic species form one or more phases. The principal effect is a change in melting behavior; rather than the individual species melting independently at their own melt points, the entire mixture melts over a range of temperatures.

We account for this effect--at least partially--in CORCON-Mod3. The melting range, defined by the liquidus and solidus temperatures, is prescribed by external models for mixtures of condensed species. Specific heat and enthalpy are calculated in three ranges:

1. For $T < T^s$, the calculation is as described above with the exception that extrapolated solid properties are used for any species which would ordinarily be liquid. This is simply accomplished by ignoring the presence of the sets of coefficients and integration constants for temperature ranges in which the species is liquid, so that the last set describing a solid continues to be used above the melting point.

2. For $T^l < T$, extrapolated liquid properties are used for any species which would ordinarily be solid by ignoring the presence of data for the solid.

3. For $T^s < T < T^l$, linear interpolation in enthalpy is used between the liquidus and solidus. The constant slope is returned as the specific heat. The effect of this construction is indicated in Figure 2.13.

Enthalpies are computed in subroutine CPENTH.

Chemical Potential - g (J/kg K)
Chemical potentials for the species are required in the calculation of chemical equilibrium and are computed from the molar Gibbs function

$$g_i = h_i - Ts_i \quad , \qquad (192)$$

where s is the entropy and may be computed at temperature T and at the reference pressure of one atmosphere from

$$\begin{aligned} s_i(T) &= S_i(T') + \int_{T'}^{T} dT' c_{p_i}(T')/T' \\ &= K_{si}^k + A_i^k \ln\left(T/T_i^k\right) + 10^{-3} B_i^k \left(T - T_i^k\right) \\ &\quad + 10^{-6} C_i^k \left(T^2 - T_i^{k2}\right)/2 \\ &\quad - 10^5 D_i^k \left(1/T^2 - 1/T_i^{k2}\right)/2 \end{aligned} \qquad (193)$$

for T in the kth temperature range for species i (i.e., $T_i^k < T < T_i^{k+1}$). The first integration constant, K_{si}^1, is the standard entropy of formation of species i and, as with the enthalpy, any others required are computed internally, subject to the condition that the discontinuity in enthalpy at T_i^k be the appropriate entropy transition of $\Delta H_{i,TR}^k/T_i^k$, if a phase change occurs at T_i^k and zero otherwise. Again, subroutine CONFND contains the necessary data tables and calculates integration constants during the initial call from SETUP. The chemical potentials, evaluated in subroutine CHEMPO, are used only as internal variables in the chemical equilibrium subroutine MLTREA, which employs chemists' units of cal/mole. Therefore, no conversion to S.I. is made. MLTREA itself converts the standard chemical potentials for pure gases at one atmosphere pressure to mixture conditions using the ideal gas result

$$g_i(p,T) = g_i^\circ(p,T) + R_o T \ln(p_i) \qquad (194)$$

where p_i is the partial pressure of gaseous species i. No pressure correction is made for condensed species.

Free Energy Function - fef (cal/gmole K)

The VANESA model tabulates and uses free energy data in the form of free energy functions. The free energy functions are related to the gibbs function and enthalpy by

$$fef_i = -\frac{g_i(T) - h_i(298.15)}{T} \qquad (195)$$

where $h_i(298.15)$ is the enthalpy of species i at the reference temperature, 298.15 K. The data for the species free energy functions were fit to an equation of the following form

$$\begin{aligned} fef = {} & a_{i,1} + a_{i,2} x + a_{i,3} x^2 + a_{i,4} x^3 \\ & + a_{i,5} \ln(x) + a_{i,6}/x + a_{i,7} x \ln(x) \end{aligned} \qquad (196)$$

where x = T/10000. The seven coefficients for each VANESA chemical species are tabulated in BLOCK DATA BARRAY.

2.4.2 Transport Properties

The transport properties computed in CORCON-Mod3 are the dynamic viscosity, the thermal conductivity, the surface tension, and the emissivity. Detailed models are included for condensed-phase species and mixtures only. Gas-phase viscosity and thermal conductivity (required for calculation of heat-transfer coefficients at the melt/concrete interface) are treated as constants using representative values defined in subroutine GFLMPR.

Dynamic Viscosity - μ (kg/m/s)

Oxidic phase:

The viscosity of molten oxides is quite complex, particularly when significant amounts of silica (SiO_2) are present. For low-silica mixtures, the viscosity is computed from the Kendell-Monroe expression.[72,78]

$$\mu_m = \left[\sum_i X_i \mu_i^{1/3} \right]^3 \quad . \tag{197}$$

The viscosities of the species are determined using an Andrade form[77]

$$\mu_i = \mu_i^\circ \exp\left[\alpha_i/T\right] \quad , \tag{198}$$

where the constants μ_i° and α_i are determined by empirical correlation.

Values of these coefficients are included (in subroutine VISCTY) for only a limited number of species. The values for FeO, Al_2O_3, and UO_2 are based on published data;[72,75] that for CaO is based on our own unpublished theoretical estimate. The values for ZrO_2 and Cr_2O_3 are based on analogy with UO_2 and FeO respectively. These are important contributors to the viscosity because they may be dominant species in either the fuel-oxide layer or the light-oxide (slag) layer. Only these species are considered in the Kendell-Monroe calculation, and the resulting composition is renormalized.

For mixtures with a higher silica content, the viscosity can be greatly increased by the formation of strongly bonded chains of SiO_4 tetrahedra. The viscosity is calculated from a model proposed by Shaw.[79] This was originally generated as a fit to the correlation developed by Bottinga and Weill based on geologic data,[80] and was shown to give good agreement with it within the original data base. Shaw's model has an extremely simple form, for which good extrapolation properties are built in:

$$\mu_m = \exp\left[s\ (10^4/T - 1.50) - 6.40\right] \quad . \tag{199}$$

Here the viscosity, μ, is in poise (1.0 poise = 0.1 kg/m-s) and s is a function of mixture composition given by

$$s = \left(\sum_i n_i x_i s_i^\circ / \sum_i n_i x_i \right) x_{SiO_2} \quad . \tag{200}$$

Data are included in subroutine VISCTY for TiO_2, FeO, MgO, CaO, Li_2O, Na_2O, K_2O, Fe_2O_3, and Al_2O_3; these values are taken from Shaw's paper. Also included are data for UO_2 and ZrO_2 based on an assumed analogy with TiO_2, and for Cr_2O_3 based on an assumed analogy with Fe_2O_3. Again, the composition in terms of these species is renormalized for use in Equation (199).

The Shaw model is restricted to mixtures with relatively high silica contents; it is matched to the low-silica Kendell-Monroe form by simply accepting the greater of the two values calculated from Equations (197) and (199). The transition, where the two values are equal, is typically at a composition of 20 to 30 percent silica.

The maximum viscosity is limited to that for basalt, which is computed from

$$\mu(\text{basalt}) = 1.94 \times 10^{-5} \exp\left[20950/T\right]$$

where μ(basalt) is the viscosity in kg/m-s and T is in Kelvins.

Metallic Phase:

We assume that the viscosity of the metallic phase can be represented by the viscosity of iron (the major constituent) as given by the expression[72]

$$\mu_m = 1.076 \times 10^{-3} \exp(3313/T) \quad . \tag{201}$$

Coolant:

The coolant viscosity is computed from[77]

$$\mu_{coolant} = 2.414 \times 10^{-5}\ 10^{\alpha}$$
$$\alpha = 247.8/(T-140) \quad . \tag{202}$$

Two-Phase, Solid-Liquid Slurry:

CORCON-Mod3 contains a model for the enhancement of viscosity by suspended solids, in the form

$$\mu_{sl} = \mu_m \left[\frac{1 + \phi/2}{(1 - \phi)^4} \right] \quad (203)$$

where μ_{sl} is the slurry viscosity, μ_m is the viscosity of the pure liquid mixture, and ϕ is the volume fraction of solids.

This form was suggested by Kunitz[77] for slurries containing less than 50 percent solids by volume. In CORCON-Mod3, the expression is assumed to apply up to 50 percent solids. The solids fraction is computed by linear interpolation between the mixture liquidus, T^l, and the mixture solidus, T^s, as

$$\phi(T) = \frac{T^l - T}{T^l - T^s}. \quad (204)$$

This equation is applied whenever the temperature is between the liquidus and solidus points.

Recent experiments[c] suggest that the slurry viscosity predicted using the above equation may be significantly smaller than the true viscosity of prototypic mixtures of fuel and concrete oxides. However, these are only preliminary results, so we have made no code modifications in this area.

Thermal Conductivity - k (W/m K)

Values for thermal conductivity[72,73,75,77,82] for condensed-phase species are stored in subroutine THKOND. No temperature dependence is included. Mixture values are computed from the species values by mole-fraction averaging.

It should be mentioned that CORCON uses the same thermal conductivity for both the solid and liquid phases -- literature values for the solid phase thermal conductivity are tabulated in the code. While this is a fairly reasonable assumption for the oxide phase, it may be in error for the metal phase. For example, aluminum at 900 K (33 K below the melting point) has a thermal conductivity of 210 W/m K, while at 1000 K, the thermal conductivity is only 93 W/m K.[83] Most other metals have thermal conductivities in the solid phase that are approximately twice their thermal conductivities in molten phase. To help correct for this potential problem, we have provided the user with the option of specifying a multiplier to be applied in the calculation of the metal phase thermal conductivity. It should be noted, however, that this modified thermal conductivity would still be applied to both the solid and liquid phases.

Surface Tension - σ (N/m)

Values of surface tension[73,74,76,78] for condensed-phase species are stored in subroutine SIGMY. No temperature dependence is included. Mixture values are computed from the species values by mole-fraction averaging.

Emissivity - ε (-)

The calculation of radiative heat transfer requires emissivities for the radiating surfaces. In the CORCON-Mod3 code, only the emissivity of water (coolant) is stored as internal data. Values are input by the user for the ablating concrete surface, for the oxidic and metallic melt phases, and for the surroundings above the pool. The first is specified as a constant, while the last three may be input as functions of either surface temperature or time.

Emissivities are computed in subroutine EMISIV.

2.4.3 Liquid-Solid Phase Transition

In order to model solidification effects, we must be able to determine the liquidus and solidus temperatures for metallic and oxidic mixtures. Melting temperatures and latent heats of fusion are readily available for a wide range of materials. Values for all the condensed-phase species in the CORCON Master List (Table 2.1) are contained in the thermodynamic property tables described in Section 2.4.1. The situation is quite different for the mixtures encountered in melt/concrete interactions; data are lacking, and the mixtures are too complex for detailed analysis. Therefore, we have developed relatively simple procedures for estimating the liquidus and solidus temperatures of the various mixtures encountered in CORCON-Mod3. These temperatures are also used in the construction of a single melt transition in the enthalpy of such mixtures, as described in Section 2.4.1.

[c]Roche, M. Presentation at the ACE Technical Advisory Committee Meeting, Argonne National Laboratory, June 1991.

Concrete:

The melting of concrete is strongly influenced by the presence of trace species such as alkali oxides. However, melting ranges for typical concretes have been determined experimentally, and are included as part of the internal data in CORCON-Mod3 for the three built-in concrete varieties. For user-specified concretes, the liquidus and solidus temperatures must also be input by the user: the values for the built-in concretes, Table 2.4, should provide some guidance.

Metallic Mixtures:

For metallic mixtures (at least late in the accident when solidification is likely) the principal constituents should be Cr, Fe, and Ni from stainless steel. Therefore, we have constructed a simple fit to the iron-chromium-nickel ternary phase diagram,[84] with due consideration to the associated binary phase diagrams. The liquidus and solidus temperatures are fit as

$$T^{l} = \max \begin{cases} 2130 - 510W_{Fe} - 1140W_{Ni}, \\ 1809 - 90W_{Cr} - 440W_{Ni}, \\ 1728 - 200W_{Cr} - 40W_{Fe}, \\ 1793 - 230W_{Cr} - 130W_{Ni}) \end{cases} \quad (205)$$

and

$$T^{s} = \max \begin{cases} 2130 - 730W_{Fe} - 3310W_{Ni}, \\ 1809 - 90W_{Cr} - 560W_{Ni}, \\ 1728 - 250W_{Cr} - 100W_{Fe}, \\ 1783 - 310W_{Cr} - 140W_{Ni}, \\ 1613) \end{cases} \quad (206)$$

where W_{Cr}, W_{Fe}, and W_{Ni} are the weight fractions of Cr, Fe, Ni, respectively. These expressions agree with the original curves within a few tens of degrees. The corresponding contour maps are shown in Figure 2.14. As implemented in CORCON-Mod3, the presence of other elements is ignored, and the weight fractions of chromium, iron, and nickel are renormalized so that

$$W_{Cr} + W_{Fe} + W_{Ni} = 1.0.$$

Other metals such as zirconium or silicon, which may be present in significant amounts at various times during the interaction, may substantially depress the melting temperature of the metal phase. We currently do not account for this effect in CORCON-Mod3. We have, however, provided the user with the option of specifying the solidus temperature for the metal phase. If this option is invoked, the liquidus temperature is set at 10 K above the user-defined solidus temperature.

Oxidic Mixtures:

The melting behavior of oxidic mixtures is far more complicated than that of the metals. The major constituents of concrete, CaO, SiO_2, and Al_2O_3, form a complicated ternary system (see, e.g., Reference 73). The fuel oxides, UO_2 and ZrO_2, appear to form a relatively simple system, but it is really a single-line in the far more complicated uranium-oxygen-zirconium ternary system. Because consideration of the complete phase diagram for concrete oxides plus fuel oxides seems to be out of the question, the melting behavior of oxidic mixtures is treated in an approximate manner.
The user may select from two different representations of the oxide phase diagram: one that assumes an ideal solution for the solid phase, and one that assumes eutectic interactions also occur. In both cases, the oxidic mixture is treated as a pseudo-binary system in which the fuel oxides form one "component" with concrete and steel oxides forming the other.

If the two components are assumed to form ideal solutions in both liquid and solid phases, the following equations for the liquidus and solidus temperatures are applicable:

$$x_1 \exp\left[-\frac{\Delta H^1}{R_o}\left(\frac{1}{T_1^m} - \frac{1}{T^\ell}\right)\right] + x_2 \exp\left[-\frac{\Delta H^2}{R_o}\left(\frac{1}{T_2^m} - \frac{1}{T^\ell}\right)\right] = 1 \quad (207)$$

$$x_1 \exp\left[\frac{\Delta H^1}{R_o}\left(\frac{1}{T_1^m} - \frac{1}{T^s}\right)\right] + x_2 \exp\left[\frac{\Delta H^2}{R_o}\left(\frac{1}{T_2^m} - \frac{1}{T^s}\right)\right] = 1 \quad (208)$$

where x_i is the mole-fraction of component i, T_i^m is its melting temperature, and ΔH_i is its heat of fusion.

This formalism may be applied to a mixture of mixtures by treating T_i^m as T_i^ℓ, the liquidus temperature of mixture

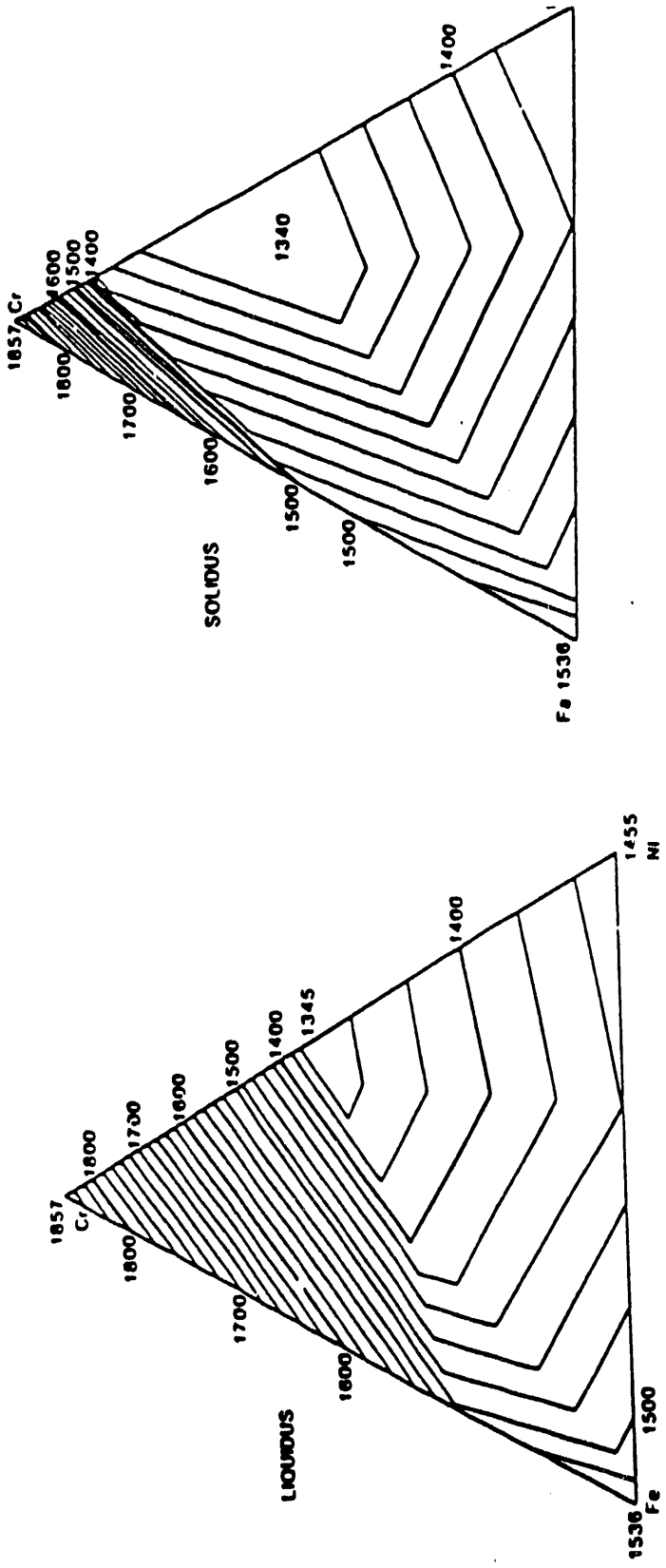

Figure 2.14 Liquidus and solidus temperature fits for Cr-Fe-Ni system

i, in the liquidus equation, and as T_i^s, the solidus temperature of mixture i, in the solidus Equation (207).

The melt properties for the fuel oxides (UO_2 + ZrO_2) are taken as[24]

$$\Delta H = 20800x + 17700\,(1 - x) - 5050\,x\,(1 - x) \quad (209)$$

and

$$T^s = T^l = \Delta H/(20800x/2950 + 17700\,(1 - x)/3123) \quad (210)$$

where ΔH is the component latent heat in cal/mole, T^s and T^l are in K, and x is the mole fraction of ZrO_2 in the UO_2 + ZrO_2 mixture.

For the second mixture, concrete oxides + steel oxides, we use concrete properties with T^s and T^l from either built in data (for the three default concretes) or from user input data (for a nonstandard concrete). The mixture latent heat, ΔH, is internally calculated from built-in enthalpy data as

$$\Delta H = \bar{h}^l\,(\bar{T}) - \bar{h}^s\,(\bar{T}) \quad , \quad (211)$$

where

$$\bar{T} = (T^s + T^l)/2 \quad (212)$$

and

$$\bar{h}^{\ell,s}(\bar{T}) = \Sigma_i m_i \bar{h}_i^{\ell,s}\,(\bar{T})/m \quad (213)$$

Here $\bar{h}_i^{\ell,s}\,(\bar{T})$ are the enthalpies of the liquid and solid phases of the constituent species, extrapolated, if necessary, as described in Section 2.4.1.

An example of the resulting phase diagram, for UO_2 + 35 mol/o ZrO_2 and Limestone Aggregate/Common Sand Concrete is shown in Figure 2.15).

Recent experiments[f] have shown that the phase diagram calculated assuming ideal solution interactions may be significantly in error for the LWR debris compositions of interest. These experiments clearly show that eutectic interactions occur in the oxide mixture. As a result, the solidus temperature of the oxide phase decreases much more rapidly with the addition of concrete oxides than shown in the figure. The experiments show that at only about 10 or 20 mole percent concrete, the solidus temperature of the mixture has fallen to near the concrete solidus temperature.

As one of the user flexibility options in CORCON-Mod3, the user may choose the ideal solution phase diagram (the default selection) or select an alternate parametric representation that accounts (at least approximately) for the observed melting behavior. In the latter, the liquidus temperature is assumed to be the same as for the ideal solution model. The solidus temperature, which is the more critical value, is calculated assuming that the solidus temperature decreases linearly with concrete addition to a user-specified concrete mole fraction. At higher concrete concentrations the solidus temperature is fixed at the concrete solidus. (The resulting phase diagram is shown in Figure 2.16.) While extremely simple, this parametric model provides a fairly accurate representation of the experiment data.

[f]Roche, M. Presentation at the ACE Technical Advisory Committee Meeting, Argonne National Laboratory, June 1991.

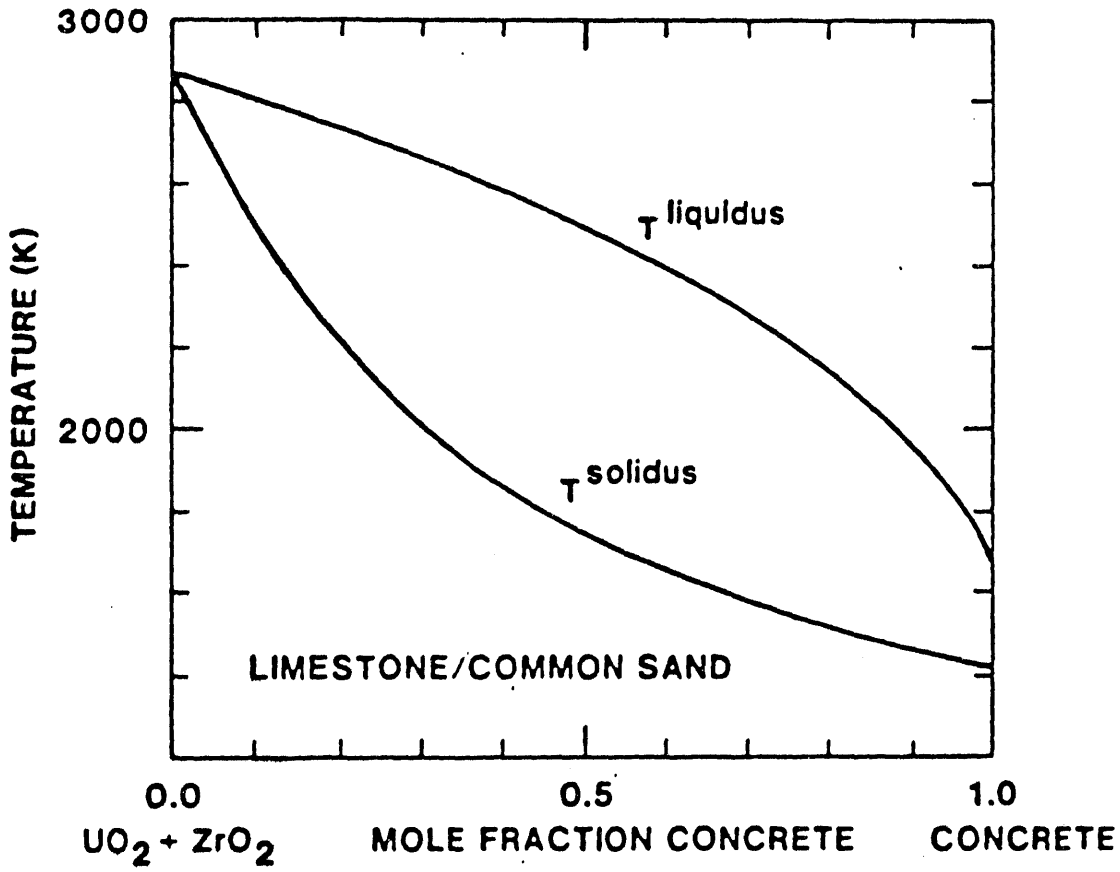

Figure 2.15 Example liquidus and solidus temperatures for oxidic mixtures

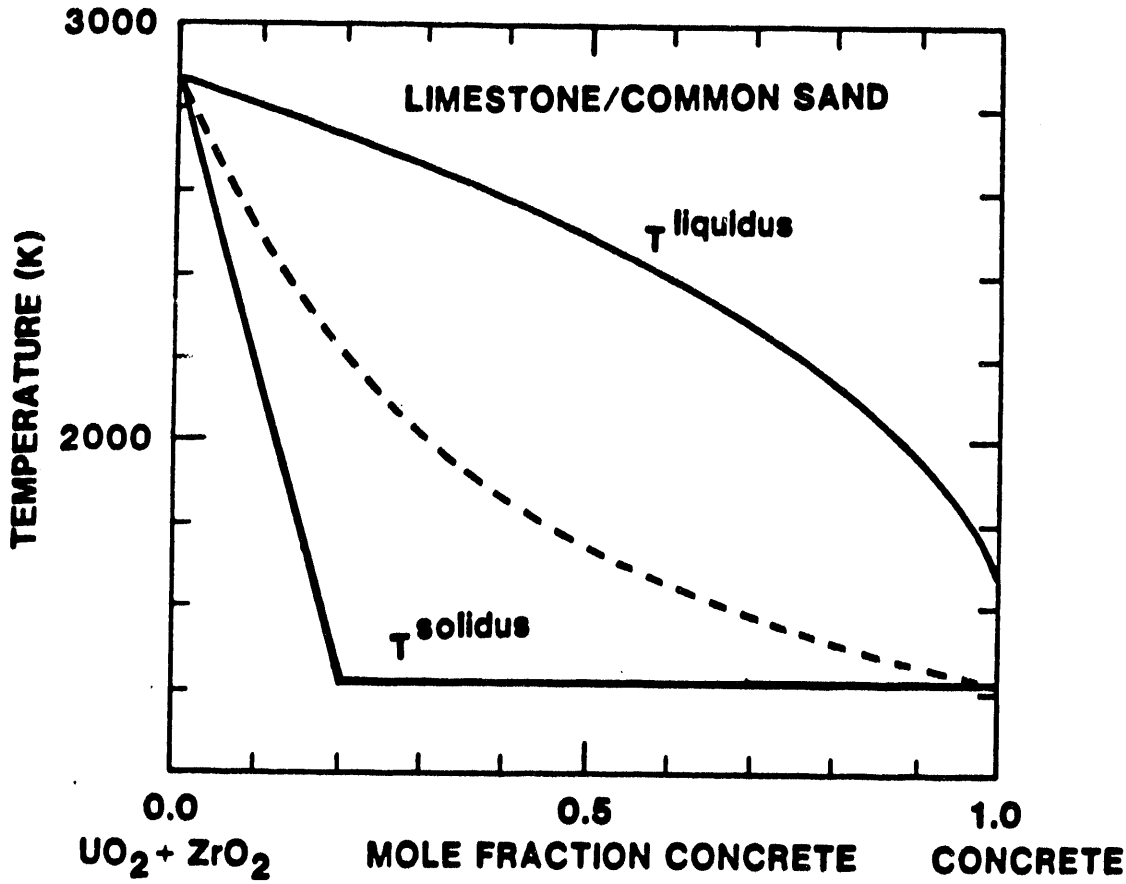

Figure 2.16 Alternate phase diagram for the oxide phase

2.4.4 Coolant Saturation Line

If a coolant is present, CORCON-Mod3 considers the possibility that it may vaporize. The calculational procedure, described in Section 2.12, requires knowledge of the saturation line for the coolant--that is, the temperature at which it boils at any given pressure. The data in the Steam Tables[38] were fit by a nonlinear optimization program as

$$p_{sat}(T) = 1.292 \times 10^{10} \exp\left[\frac{-3880.4}{T-43.15}\right] \quad (214)$$

in S.I. units (pressure p in Pa, temperature T in K). This simple expression reproduces the original data within 0.5 percent for $T < 573$ K, corresponding to $p_{sat} < 8.5$ MPa (which is far in excess of containment failure pressures), and is in error by only 5 percent at the critical point. This accuracy seems more than adequate for a code such as CORCON-Mod3. In addition to its extremely compact and efficient form, Equation (213) has the virtue of an exact analytic inverse:

$$T_{sat}(p) = 43.15 - \frac{3800.4}{\ln\left(p/1.292 \times 10^{10}\right)} \quad . \quad (215)$$

3.0 Assumptions and Limitations

The CORCON-Mod3 code has been designed to be used for the analysis of both reactor accident sequences and melt/concrete interaction experiments. The code input, described in Section 5.0, is sufficiently flexible to allow a user to describe problems of either type. Accident calculations provide information for assessment of the risks of operation of LWR's. Calculations of experiments are useful both for planning and for interpretation of results. The comparison of experiment and calculation is valuable for guiding further efforts in both areas.

The user, however, should be aware of a number of assumptions, approximations, and simplifications employed in the modeling which may affect the accuracy (or at least the interpretation) of CORCON-Mod3 calculations. It is also worth noting that a number of sensitivity parameters are available through input to allow the user to readily explore the extent of importance of some of the approximations noted below. These parameters are listed and briefly discussed in Table 4.1. Among the more important of these are:

1. The atmosphere and surroundings above the pool surface serve only to provide boundary conditions for heat and mass transfer from the pool, as CORCON does not include calculational procedures to update the temperature, pressure, or composition of the atmosphere or the temperature of the surroundings. (However, if these quantities are updated by other code modules coupled to CORCON, the current values will be used.) The calculation of radiative heat loss from the pool surface is based on a one-dimensional model, and the convective loss is calculated using a constant heat transfer coefficient.

2. The calculated concrete response is based on one-dimensional steady-state ablation, with no consideration given to conduction into the concrete or to decomposition in advance of the ablation front. This assumption is probably not a source of serious error in the analysis of reactor accidents, at least for the sequences with long-term interactions between core materials and concrete. The heat fluxes involved are sufficiently large that quasi-steady ablation is approached within the first few minutes of interaction if the pool is molten; the process continues for a period of hours to days, sustained by decay heat from the fission products in the melt. The steady-state ablation assumption makes it difficult to apply the code to transient interactions that occur in the first few minutes following reactor vessel failure. The code may also be inaccurate for analysis of very long-term interactions where the debris temperature may be close to the concrete ablation temperature.

3. The solidification model is preliminary. It assumes that a crust forms on any surface whose temperature falls below the solidification temperature. The mechanical stability of the crusts is not considered. We believe that both the mechanical strength of the crust and the loads imposed on it by concrete decomposition gases are important in determining the true solidification behavior of the core debris.

   The code assumes also that the crust has the same properties as the bulk liquid phase. This may not be true if the liquid phase composition is changing with time. Consider for example the formation of an oxide crust early in the interaction (before significant concrete ablation). This crust material will have a solidus temperature near that of the fuel oxide mixture. As concrete is incorporated into the molten phase, the molten phase solidus temperature will decrease. The code assumes that the same change in the solidus occurs for the crust. Clearly, this is not correct.

4. If the gas-film model is used, it is used for radial heat transfer even after the melt solidifies, even though the assumptions on which the model is based are no longer valid. In particular, no radial gap develops around a layer of the melt which has completely solidified. Thus, radial ablation continues with the "solid" layer continuing to conform to the changing shape of the cavity rather than behaving as a rigid penetrator. As coded, the model also assumes that the frozen material remains gas-permeable. Because the total amount of concrete eroded is largely determined by energy considerations (the available decay energy), the effect of these modeling assumptions is primarily on the calculated shape of the cavity.

5. There is no treatment of chemical reactions between the melt and the atmosphere, or of reactions in the atmosphere. We do not consider these to be significant limitations. Melt-atmosphere interactions are probably insignificant due to the limited surface area and relatively low temperature of the surface. Reactions in the atmosphere do not affect the progress of the core-concrete interaction and so can be

neglected in a computer model such as CORCON. Modeling of atmosphere reactions would, however, be useful when comparing code predictions to experiment results, since the gas stream in the experiments is sampled at some distance from the melt surface.

6. The code assumes ideal chemistry when calculating bulk phase chemical reactions.

7. The code uses flat plate pool boiling correlations to model heat transfer to an overlying coolant pool. Recent experiments show that heat transfer is greatly enhanced during the initial pour of coolant. This enhanced heat transfer may lead to rapid cooling of the melt surface, and a transition to nucleate boiling. The code predicts lower early heat fluxes than in the experiments, and long-term heat transfer by film boiling. Interestingly, the code predicts well the longer term (steady state) coolant heat fluxes measured in the experiments.

8. The time-dependent melt radius model allows the user to mimic the spreading of a melt across a horizontal floor, but it is not a mechanistic model of spreading.

9. The code uses the same Fe-Cr-Ni phase diagram for the metal phase that was in CORCON-Mod2. This treatment neglects important metallic components such as Zr, Si, or Al that may be present in the melt at various times during a core-concrete interaction. In general, these constituents will reduce the melting range of the metal phase relative to the range predicted by the code. Through input the user can modify the phase diagram for the metal phase by specifying a constant solidus temperature. The liquidus temperature is then assumed to be 10 K greater than the specified solidus.

4.0 User Information

In this chapter we describe a typical calculational cycle of the CORCON-Mod3 computer code. We discuss the input parameters and describe the output. Finally, we provide general programming information for the code.

4.1 A Typical Calculational Cycle in CORCON-Mod3

We have designed the calculational cycle in CORCON to reflect our view of the interrelationships of the various physical and chemical phenomena described in Chapter 2. The description of a typical calculational cycle in CORCON will aid user in understanding how the phenomena are modeled in the code.

At the start of a timestep, CORCON has a complete "snapshot" of the problem, that is, it has current values of all the relevant computational variables, including the cavity geometry; the physical, chemical, and thermal state of the melt pool; and the transport properties for the pool. For the first timestep, the "snapshot" comes from the initialization procedure. For later timesteps, the "snapshot" comes from the results of the preceding timestep.

The variables describing the state of the melt pool are advanced to their values at the end of the timestep by the calculational procedure described below. The basic logic is also given in Figure 4.1, which is a flow chart of the main program in CORCON-Mod3.

1. Calculate a timestep. This may be either constant or variable, as specified by the user.

2. Calculate the internal mass transport, melt/gas and condensed phase chemical reactions, and the associated energy terms.

   Injection rates of concrete decomposition products (already known) are assumed to remain constant over the timestep, and the calculation proceeds in two passes.

   The first pass follows rising gases and condensed phase materials (e.g., concrete slag or entrained material), layer by layer. If the material should remain in the current layer, its mass and energy are added to that of the layer; otherwise, it is equilibrated thermally with this layer and passed on to the next. Gas passing through a metal-containing layer is equilibrated chemically with the metal, and the oxidic reaction products are added to the rising oxides, with any heat of reaction remaining in the layer. When the surface of the pool is reached, the rising gases are passed to an interface routine which disposes of them and initializes any downward mass flows, such as added coolant or additional core material falling into the pool. It is in the first pass that the VANESA subroutine is called. The VANESA model calculates radionuclide release and aerosol generation, which are included in the upward flow of material exiting the pool.

   In the second pass, falling condensed-phase materials are followed downward layer by layer, being equilibrated in each layer, until they are added to the appropriate layer.

3. Finish the explicit time-advancement of the layer energy equations.

   This step includes the addition of decay heat and subtraction of heat lost to the concrete. It also accounts for interlayer heat transfer and loss from the pool surface based on rates at the start of the timestep. If coolant is present and is boiling, the calculation is completed at the step; otherwise, the matrix equations for an implicit calculation of the interlayer and surface energy terms is set up. A linearized representation of the pool thermal response, surface heat flux vs surface temperature, is constructed.

4. Determine a provisional end-of-timestep value for the temperature of the surface of the pool by matching heat fluxes to and from this surface. Construct a linearized representation of the above-pool thermal response, as surface heat flux vs surface temperature.

   In matching the heat fluxes, the linearized pool response and the "exact" relationships for the above-pool heat transfer are used. If desired, the change of temperature in the atmosphere and surroundings during the timestep are included here and made consistent with the heat flux. The simple routine provided could easily become part of the interface to a more general model.

5. Complete the solution of the implicit interlayer heat transfer equations, using the provisional end-of-timestep surface temperature, to determine the final layer enthalpies. Reconcile these with the known layer masses and compositions to determine the new layer temperatures.

6. Calculate the new cavity shape, using the ablation rates at the start of the timestep. These ablation rates, are treated as constant over the timestep.

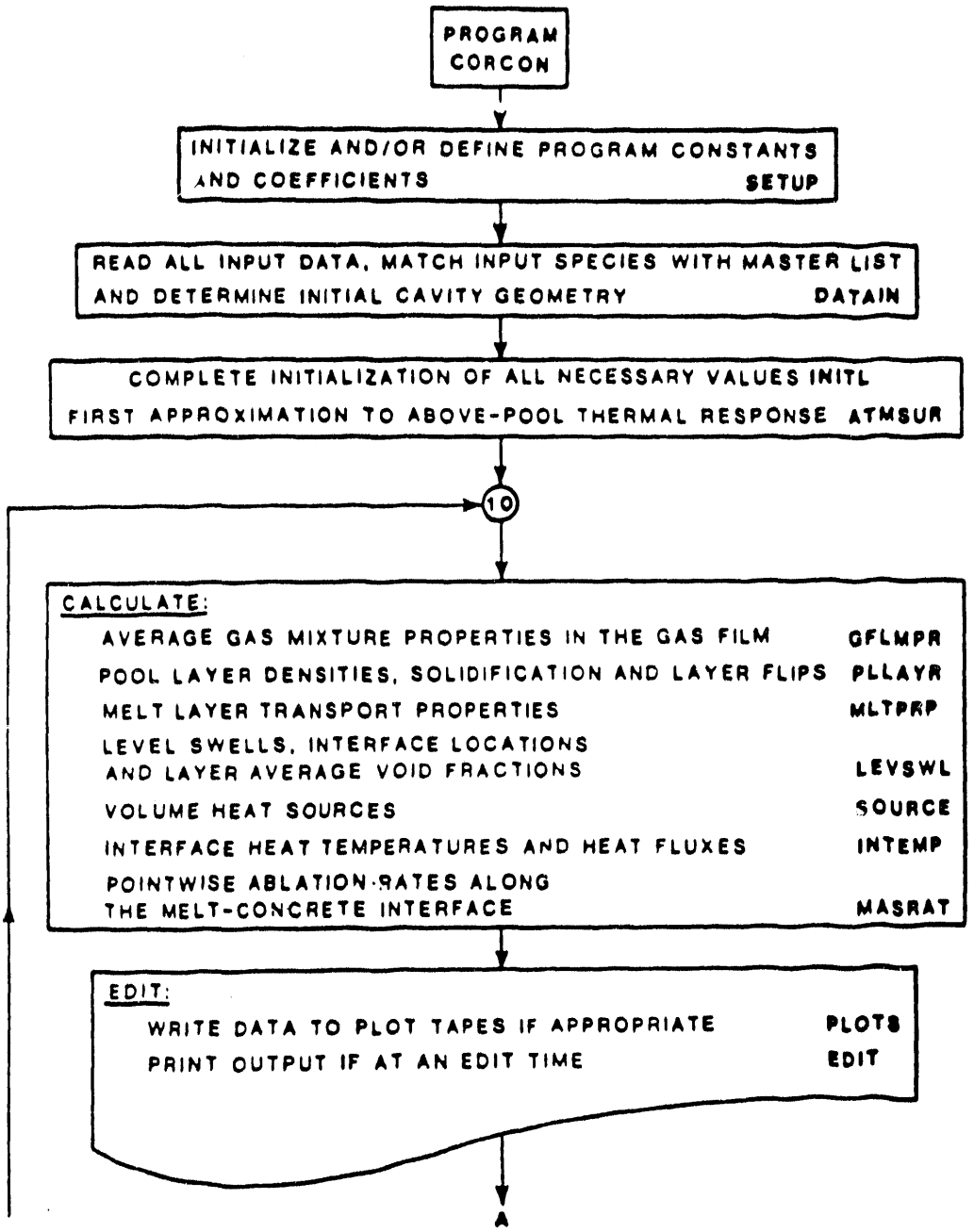

Figure 4.1 Flow diagram for CORCON-Mod3

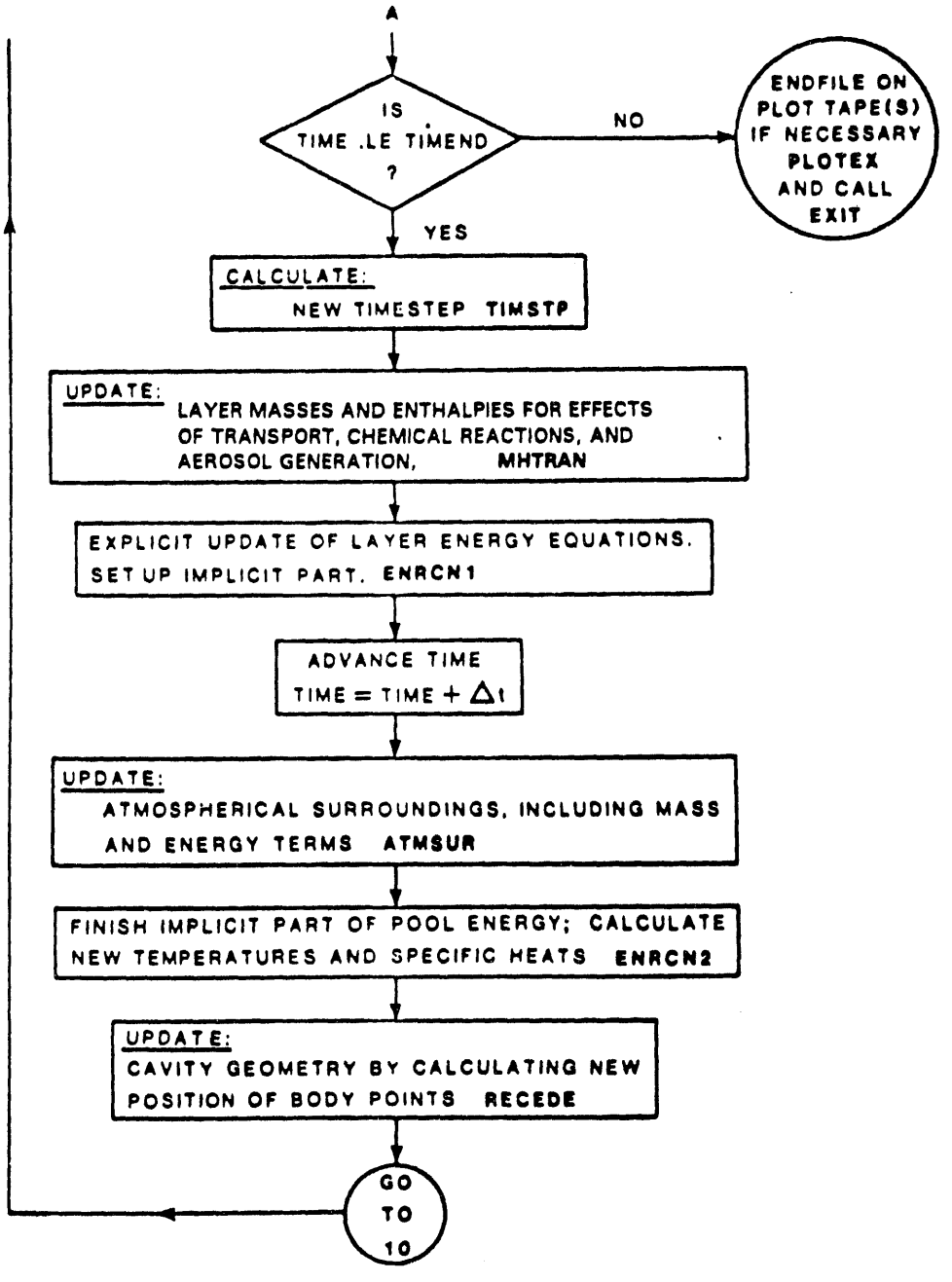

Figure 4.1 Flow diagram for CORCON-Mod3 (continued)

7. Calculate the new layer densities. Determine if the previous layer ordering is still appropriate. If it is not, reorient the layer configuration. Layer flips occur in this step as well as creation of mixture layers.

8. Calculate new layer transport properties (viscosity, thermal conductivity, etc.) from the new compositions and temperatures.

9. Calculate bubble-rise velocities and (from known gas-flow rates) pointwise void fractions in the pool. From the void fractions, the known volume of condensed phases in each layer and the cavity shape determine the elevation of each layer interface.

10. Evaluate decay or externally-imposed heat sources.

11. Evaluate heat transfer between layers and the resulting interlayer heat fluxes.

    The linearized above-pool response which was calculated in Step 4 is used in this calculation. The final temperature of the pool surface determined here will differ slightly from the provisional value calculated in Step 4.

12. Calculate pointwise ablation rates along the melt-concrete interface.

    The thermal resistance of the gas film, if it exists, is calculated based on the local conditions of gas flow and the rate at which gas is entering the film. This rate is made consistent with the local heat flux and ablation rate.

At this point, CORCON once again has a complete "snapshot" of the problem, for the end of the timestep. At this point in the calculational cycle, all the calculated variables have been evaluated at the same time level, allowing the generation of a consistent printed edit of the state of the system, if this is desired.

In the main program, the above steps are executed in the order 7-12, edit if required, check for end of problem, 1-6, and repeat. This order is used because steps 7-11 are also required as part of the initialization.

4.2 Description of the Input Parameters

CORCON-Mod3 expects input to be provided in a file called "ccmod3.in" (Unit 5). The data cards needed for input by the code are described in Table 4.1. Note that the input is compatible with the inputs used for CORCON-Mod2, in the sense that any input deck used for CORCON-Mod2 will also be accepted by CORCON-Mod3. There are, of course, numerous data cards that have been added to the input for the many additional features in CORCON-Mod3. Also, some models that were inactive in CORCON-Mod2 have been activated in CORCON-Mod3 (e.g., time-dependent mass addition). Finally, the reader should note that the user may now include comments within the input deck to explain a particular entry, or to provide a short description of the calculation. Comment lines are assumed by the code if a "$" appears in the first column.

A given problem will not require all the data cards and fields described. In fact, some fields and cards are not yet operational and these are indicated by **[...]** in the table. This has been done to reserve space for further upgrades of the code, and to provide the adventurous code modifier with information concerning partially implemented features.

Data cards are initially read in subroutine DATAIN, and are echoed to the output file, and to a scratch file called "echo.fil" (Unit 7). The cards are subsequently read from the scratch file by routines CONPRP, DATAIN, DCYINT, INCOOL, INGEOM, INPCON, INPGAS, MELTRD, and BCLTOV which interpret the actual data fields.

4.2.1 Discussion of Selected Input Quantities

Most of the input for CORCON is fairly self-explanatory, especially to the user who is familiar with the type of problems it solves. However, experience has shown that some portions of the input require further discussion.

Edit and Timestep Control

The parameter TPRIN (card 3) provides the user with detailed printout after time has passed TPRIN. This is of interest primarily in the diagnosis of code problems; the additional information is printed in terms of FORTRAN variables and requires detailed knowledge of the internal working of the code for its interpretation.
For routine calculations, TPRIN should be set greater than the problem end time TIMEND.

For both the variable timestep control (card group 3A) and the variable edit control (card group 3B), the last specification is assumed to apply to the end of the problem if TIMEND is greater than the last TEND or TED, respectively. Each group is terminated by a blank card rather than by a specified count. This facilitates the insertion of additional control intervals at significant or

Table 4.1 Input instructions for CORCON-Mod3

Card/ Group#	Field	Format	Variable Name	Description
SECTION 1. PROBLEM IDENTIFICATION, COMPUTATIONAL OPTIONS AND CONTROL PARAMETERS				
		PROBLEM TITLE		
1	1-80	A80	ITITL	80 Column run identification
		COMPUTATIONAL OPTIONS INDICES		
2	1-5	I5	ILYR	Index specifying number of initial melt layers: 0 -- 1 oxidic layer & 1 metallic layer 1 -- 1 metallic layer 2 -- 1 oxidic layer 3 -- 1 heterogenous mixture layer **[4 -- 2 oxidic layers & 1 metallic layer]** >10 -- Mixing models enabled; Initial layer configuration set by ones digit (e.g., ILYR=10 indicates two layers with mixing on)
	6-10	I5	ICOOL	Coolant index: 0 -- no coolant 1 -- coolant
	11-15	I5	IGEOM	Cavity geometry index: 1 -- Cylinder with hemispherical base 2 -- Cylinder with flat base **[3 -- Cylinder with spherical-segment base]** 4 -- Arbitrary shape
	16-20	I5	ICON	Concrete composition index: 0 -- Nonstandard concrete 1 -- Basaltic aggregate concrete 2 -- Limestone aggregate; common sand concrete 3 -- Limestone aggregate concrete
	21-25	I5	ICHEM	Coking and condensed phase chemistry (CPC) index: 0 -- Coking off & CPC off 1 -- Coking off & CPC on 10 -- Coking on & CPC off 11 -- Coking on & CPC on
	26-30	I5	IFP	Decay Heat (power) generation index: 0 -- Decay power computed internally 2 -- Power deposited into oxidic and metallic layers input versus time
	31-35	I5	ISUR	Index specifying surface temperature history of atmosphere surroundings: **[0 -- Surface temperature history computed internally] 1 -- Surface temperature input versus time
	36-40	I5	**[IABL]	Index specifying mass addition to pool due to ablation of surroundings 0 -- No mass addition **[1 -- Mass addition rates computed internally]**

Table 4.1 Input instructions for CORCON-MOD3 (continued)

Card/ Group#	Field	Format	Variable Name	Description
	41-45	I5	ISPLSH	Melt/coolant splashout index: 0 -- No splashout from pool **[1 -- Metallic and oxidic phase splashout mass flow rates input versus time]**
	46-50	I5	IPINC	Print increment index: > 0 -- Print output every IPINC time steps ≤ 0 -- Print controlled by Card Group 3B
	51-55	I5	IFILM	Melt-concrete heat flow index: 0 -- Bottom and side use slag film correlations 1 -- Bottom uses slag film & side uses gas film 10 -- Bottom uses gas film & side uses slag film 11 -- Bottom and side use gas film correlations
	56-60	I5	IRSTRT	Restart option index: 0 -- Run starts from beginning **[1 -- Restart calculation based on previously computed results]**
	61-65	I5	IMOV	Cavity shape plot index: 0 -- No plots desired 1 -- Plots are desired
	66-70	I5	IPG	Index specifying plots of prescribed variables versus time: 0 -- No plots desired 1 -- Plots desired
	71-75	I5	ISRABL	Index specifying mass addition to pool 0 -- No mass addition 1 -- Mass addition rates input versus time
	76-80	I5	IAOPAC	Index specifying radiative treatment of atmosphere: 0 -- Treated as transparent 1 -- Opacity due to aerosols computed & included
2A	1	A1	'&'	The ampersand specifies the inclusion of this card.
	2-5	I5	ITIMR	Time dependent melt radius (TDMR) index: 0 -- TDMR option not used 1 -- TDMR option in use (IGEOM = 2 only)
	6-10	I5	IFVAN	Index specifying that a complete VANESA calculation is to be performed 0 -- No VANESA calculation 1 -- Perform complete VANESA calculation
	11-15	I5	IVANFP	Index specifying form of fission product information used by VANESA: 0 -- Fission product composition from CORCON 1 -- Fission product composition to be specified
	16-20	I5	IUSER	Index specifying inclusion of additional user flexibility input: 0 -- No user flexibility input 1 -- User flexibility input to be provided

Table 4.1 Input instructions for CORCON-MOD3 (continued)

Card/ Group#	Field	Format	Variable Name	Description
		CONTROL PARAMETERS		
3	1-10	E10.0	DELTIM	Time-step control: > 0.0 -- DELTM is the time step (s) ≤ 0.0 -- Time step controlled by Card 3A
	11-20	E10.0	TIMEO	Initial time at which calculations are to begin (s)
	21-30	E10.0	TIMEND	Final time at which calculations are to cease (s)
	31-40	E10.0	DPRIN	**[Diagnostic print interval -- print diagnostic messages every DPRIN seconds starting at TIME = TPRIN (s)]**
	41-50	E10.0	TPRIN	Time at which diagnostic output is to begin (s)
Variable time-step control. Include Card 3A only if DELTIM ≤ 0.0				
3A	1-10	E10.0	DTMN	Minimum time step for interval (s)
	11-20	E10.0	DTMX	Maximum time step for interval (s)
	21-30	E10.0	TEND	End time for interval (s)
		Repeat Card 3A for a maximum of 10 intervals, terminate with DTMN ≤ 0.0		
Variable edit control. Include Card/Group 3B only if IPINC ≤ 0.0				
3B	1-10	E10.0	DED	Time between edits for interval (s)
	11-20	E10.0	TED	End time for interval (s)
		Repeat Card 3B for a maximum of 10 intervals, terminate with DED ≤ 0.0		
		SECTION 2. PROBLEM INITIAL CONDITIONS		
		CONCRETE CRUCIBLE INITIAL GEOMETRY		
4	1-5	I5	NRAYS	Number of rays (maximum of 100)
	6-15	F10.0	RO*	R-coordinate of center of ray system (m)
	16-25	F10.0	ZO	Z-coordinate of center of ray system (m) Measured positive downward. Reference is arbitrary.
	*Only permitted value is 0.0			
Cylinder with hemispherical base -- see Section 4.1.1 (Figure 4.1). Include card 5 only if IGEOM = 1.				
5	1-10	F10.0	RS	Radius of hemispherical base (m)
	11-20	F10.0	HC	Height of cylindrical top section (m)
	21-30	F10.0	RW	External radius of concrete crucible (m)
	31-40	F10.0	HBC	Height from external base of crucible to base of cylindrical section (m)

Table 4.1 Input instructions for CORCON-MOD3 (continued)

Card Group#	Field	Format	Variable Name	Description
Cylinder with flat base -- see Section 4.1.1 (Figure 4.2). Include card 6 only if IGEOM = 2.				
6	1-10	F10.0	ZT	Z-coordinate of cylinder top edge (m)
	11-20	F10.0	RAD	Radius of cylinder (m)
	21-30	F10.0	HIT	Height of cylinder (m)
	31-40	F10.0	RADC	Radius of corner (m)
	41-50	F10.0	RW	External radius of concrete crucible (m)
	51-60	F10.0	HBB	Height from external base of crucible to base of cavity (flat bottom) (m)
	61-65	I5	NBOT	Number of ray points equally spaced along flat bottom of cavity
	66-70	I5	NCORN	Number of ray points equally spaced around corner (not including tangent points)
[Cylinder with spherical-segment base -- NOT OPERATIONAL. No input for IGEOM = 3.]				
Arbitrary shape -- see Section 4.1.1 (Figure 4.3). Include cards 7, 8 and 9 only if IGEOM = 4.				
7	1-5	I5	NBOT	Number of ray points equally spaced along flat bottom of cavity
	6-15	F10.0	RTANG	R-coordinate of tangent point (m)
	16-25	F10.0	RW	External radius of concrete crucible (m)
	26-35	F10.0	HTOTL	Height from external base to top of crucible (m)
8	1-10	F10.0	R(1)	R-coordinate of body point #1 (m)
	11-20	F10.0	Z(1)	Z-coordinate of body point #2 (m)
9	1-10	F10.0	R(I)	R-coordinate of body point I (m) for (I = NBOT + 2, NRAYS)
	11-20	F10.0	Z(I)	Z-coordinate of body point I (m) for (I = NBOT + 2, NRAYS)
	(There will be (NRAYS - NBOT - 1) cards in Card Group 9)			
	CONCRETE COMPOSITION AND PROPERTIES			
10	1-10	E10.0	TIC	Initial temperature of concrete (K)
	11-20	E10.0	TW	Temperature of concrete surface (K) (Ablation temperature)
	21-30	E10.0	EW	Emissivity of concrete surface (-)
	31-40	E10.0	RBR	Mass fraction of reinforcing steel in the concrete (mass fraction: kg_FE/kg_concrete)

Table 4.1 Input instructions for CORCON-MOD3 (continued)

Card/ Group#	Field	Format	Variable Name	Description
Include card/group 11, 12 and 13 only if ICON = 0.				
11	1-5	I5	NINP	Number of species in concrete mixture; only species available in the Master Species List may be included.
12	1-8	A8	NAMSP	Name of concrete species (left justified)
	11-20	E10.0	SM	Mass fraction of concrete species (kg/kg_CONC)
		(There will be NINP cards in group 12.)		
13	1-10	E10.0	RHOC	Density of concrete (kg/m3)
	11-20	E10.0	TSOLCT	Concrete solidus temperature (K)
	21-30	E10.0	TLIQCT	Concrete liquidus temperature (K)
		Include card/group 13A and 13B only if RBR <0.0		
13A	1-5	I5	NRBRSP	Number of metallic species in rebar
13B	1-8	A8	NAMSP	Name of rebar species
	11-20	E10.0	SM	Mass fraction of rebar species (kg/kg rebar)
		CORE MELT CONSTITUENTS		
		INITIAL MASSES, COMPOSITIONS, AND TEMPERATURES		
14	1-5	I5	NOSI	Number of melt oxidic species to be input; only species available in the Master Species List may be included
	6-10	I5	NMSI	Number of melt metallic species to be input; only species available in the Master Species List may be included
	11-20	E10.0	TOI	Initial oxidic melt temperature (K)
	21-30	E10.0	TMI	Initial metallic melt temperature (K)
15	1-8	A8	NAMSP	Name of oxidic species (left justified)
	11-20	E10.0	SM	Mass of oxidic species (kg)
		(There will be NOSI cards in card/group 15.)		
16	1-8	A8	NAMSP	Name of metallic species (left justified)
	11-20	E10.0	SM	Mass of metallic species (kg)
		(There will be NMSI cards in card/group 16.)		

Table 4.1 Input instructions for CORCON-MOD3 (continued)

Card/ Group#	Field	Format	Variable Name	Description
				INTACT CORE SIZE AND POWER, AND NUMBER OF RETENTION FRACTIONS TO BE MODIFIED
Include card/groups 17 and 18 only if IFP = 0.				
17	1-10	E10.0	XMTU	Core size (metric tons of uranium)
	11-20	E10.0	XMWTH	Core operating power (MW thermal)
	21-25	I5	NUM	Number of radioactive species in the intact core inventory for which the retention factor will be modified (NUM ≤ 27)
18	1-4	A4	IFP1	Name of radioactive species whose retention factor is to be modified (left justified)
	11-20	E10.0	RET1	Retention factor of radioactive species IFP1
				(There will be NUM cards in card/group 18.)
				COOLANT INITIAL MASS, COMPOSITION, AND TEMPERATURE
Include card/groups 18A and 18B only if ICOOl = 1.				
18A	1-10	E10.0	TCI	Initial coolant temperature (K)
18B	1-8	A8	NAMSP	Name of coolant species (left justified) (H2O or H2OCLN)
	11-20	E10.0	FMCI	Mass of coolant species ()
				ATMOSPHERE INITIAL VOLUME, PRESSURE, TEMPERATURE, AND COMPOSITION
19	1-10	E10.0	VA	Initial gas volume (m**3)
	11-20	E10.0	PA	Initial gas pressure (N/m**2) >0 -- Constant for problem ≤ 0 -- Gas pressure specified by card/groups 20A & 20B
	21-30	E10.0	TA	Initial gas temperature (K)
	31-35	I5	NGSINP	Number of gaseous species in the atmosphere; only species available in the Master Species List may be included (NGSINP ≤ 18).
20	1-8	A8	NAMSP	Name of gaseous species (left justified)
	11-20	E10.0	SM	Mole fraction of gaseous species (-)
				(There will be NGSINP cards in group 20.)
Include card/groups 20A and 20B only if PA ≤ 0.				
20A	1-5	I5	NATMPR	Number of points in table of pressure of gas atmosphere versus time (1 ≤ NATMPR ≤10)

Table 4.1 Input instructions for CORCON-MOD3 (continued)

Card/ Group#	Field	Format	Variable Name	Description
20B	1-10	E10.0	TPA(1)	Table of gas pressure (PA) versus time (s); alternating values
	11-20	E10.0	PAT(1)	of time, TPA (J) and pressure,
	21-30	E10.0	TPA(2)	PAT(J) for J = 1, NATMPR.
	31-40	E10.0	PAT(2)	If NATMPR = 1, pressure is constant at PAT (1).
	•	•		
	•	•		
	•	•		
		E10.0	TPA(NATMPR)	Up to four pairs per card. May require up to 2 cards to complete the table.
		E10.0	PAT(NATMPR)	

SECTION 3. MELT INTERNAL HEAT GENERATION

DECAY POWER FOR OXIDIC AND METALLIC PHASES

Include card/group 21 only if IFP = 2.

21	1-5	I5	NDECO	Number of points in table of oxidic phase power versus time (0 ≤ NDECO ≤ 30)
	6-10	I5	NDECM	Number of points in table of metallic phase power versus time (0 ≤ NDECM ≤ 30)

Include card/group 22 only if NDECO > 0.

22	1-10	E10.0	TI0(1)	Table of oxidic phase power (W) versus time (s);
	11-20	E10.0	PIO(1)	alternating values of time, TIO(J) and power, PIO(J) for
	21-30	E10.0	TIO(2)	J = 1, NDECO.
	31-40	E10.0	PIO(2)	If NDECO = 1, power is constant at PIO(1).
	•	•		
	•	•		
	•	•		
		E10.0	TIO(NDECO)	Up to four pairs per card. May require up to 8 cards to complete table.
		E10.0	PIO(NDECO)	

Include card/group 23 only if NDECM > 0.

23	1-10	E10.0	TIM(1)	Table of metallic phase power (W) versus time (s);
	11-20	E10.0	PIM(1)	alternating values of time, TIM(J) and power, PIM(J) for
	21-30	E10.0	TIM(2)	J = 1, NDECM.
	31-40	E10.0	PIM(2)	If NDECM = 1, power is constant at PIM(1).
	•	•		
	•	•		
	•	•		
		E10.0	TIM(NDECM)	Up to four pairs per card. May require up to 8 cards to complete table.
		E10.0	PIM(NDECM)	

Table 4.1 Input instructions for CORCON-MOD3 (continued)

Card/ Group	Field	Format	Variable Name	Description
	SECTION 4. BOUNDARY CONDITIONS OF PROBLEM ATMOSPHERE SURROUNDINGS			
	SURROUNDING TEMPERATURE HISTORY			
Include card/groups 24 and 25 only if ISUR ≠ 0.				
24	1-5	I5	NTP	Number of points in table of surroundings temperature versus time (NTP ≤ 10)
25	1-10	E10.0	TTS(1)	Table of surroundings temperature (K) versus time (s); alternating values of time, TTS(J) and temperature, TMPS(J) for J = 1, NTP.
	11-20	E10.0	TMPS(1)	
	21-30	E10.0	TTS(2)	
	31-40	E10.0	TMPS(2)	
	•	•		
	•	•		
	•	•		
		E10.0	TTS(NTP)	Up to four pairs per card. May require up to 3 cards to complete table
		E10.0	TMPS(NTP)	
	RATES OF SPECIES MASS ADDITION TO POOL			
Include card/groups 26, 27, 28 and 29 only if ISRABL ≠ 0.				
26	1-5	I5	NSPG	Number of species in mass addition table; only species available in the Master Species List may be included (NSPG ≤ 20).
	6-10	I5	IFPOPT	Option flag for input of fission product mass addition 0 -- fission product composition calculated internally 1 -- fission product composition specified by user
27	1-8	A8	NAMSP	Names of species in mass addition table (left justified)
	(There will be NSPG cards in card/group 27.)			
28A	1-5	I5	NMP(1)	Number of points in table of mass flow rate versus time for first species as defined in card/group 27.
	6-10	I5	NMP(2)	Number of points in table of mass flow rate versus time for second species as defined in card/group 27.
	•	•		
	•	•		
	•	•		
		I5	NMP(NSPG)	Number of points in table of mass flow rate versus time for last species as defined in card/group 27. (NMP(I) ≤ 10, I = 1, NSPG)

Table 4.1 Input instructions for CORCON-MOD3 (continued)

Card/ Group#	Field	Format	Variable Name	Description
28B	1-10	E10.0	TMS(1,1)	Tables of mass flow rate (kg/s) of species I versus
	11-20	E10.0	FMS(1,1)	time (s) for each species as defined in card/group 27;
	21-30	E10.0	TMS(2,1)	alternating values of time, TMS(I,J) and rate, FMS(I,J) for (I
	31-40	E10.0	FMS(2,1)	= 1, NMP(J)) and (J = 1, NSPG).
	•	•	•	
	•	•	•	
	•	•	•	
	•	E10.0	TMS(NMP(1),1)	
	•	E10.0	FMS(NMP(1),1)	
	1-10	E10.0	TMS(1,2)	Start a new card 28B for each new species.
	11-20	E10.0	FMS(1,2)	May require more than one card for each species.
	•	•	•	
	•	•	•	
	•	•	•	
	•	E10.0	TMS(NMP(NSPG),NSPG)	
	•	E10.0	FMS(NMP(NSPG),NSPG)	
29A	1-5	I5	NOTS	Number of points in table of temperature versus time for added oxide phase.
	6-10	I5	NMTS	Number of points in table of temperature versus time for added metallic phase.
	11-15	I5	NCTS	Number of points in table of temperature versus time for added coolant phase.
29B	1-10	E10.0	TIOTS(1)	Tables of time (s) versus temperature (K) for added
	11-20	E10.0	TOTS(1)	oxide phase;
	21-30	E10.0	TIOTS(2)	alternating values of time, TIOTS(I) and temperature,
	31-40	E10.0	TOTS(2)	TOTS(I) for (I = 1, NOTS)
	•	•	•	
	•	•	•	
	•	•	•	
	•	E10.0	TIOTS(NOTS)	
	•	E10.0	TOTS(NOTS)	
29C	1-10	E10.0	TIMTS(1)	Tables of time (s) versus temperature (K) for added
	11-20	E10.0	TMTS(1)	metal phase;
	21-30	E10.0	TIMTS(2)	alternating values of time, TIMTS(I) and temperature,
	31-40	E10.0	TMTS(2)	TMTS(I) for (I = 1, NOTS)
	•	•	•	
	•	•	•	
	•	•	•	
	•	E10.0	TIMTS(NOTS)	
	•	E10.0	TMTS(NOTS)	

Table 4.1 Input instructions for CORCON-MOD3 (continued)

Card/ Group#	Field	Format	Variable Name	Description
29D	1-10	E10.0	TICTS(1)	Tables of time (s) versus temperature (K) for added
	11-20	E10.0	TCTS(1)	coolant phase;
	21-30	E10.0	TICTS(2)	alternating values of time, TICTS(I) and temperature,
	31-40	E10.0	TCTS(2)	TCTS(I) for (I = 1, NOTS)
	•	•	•	
	•	•	•	
	•	•	•	
	•	E10.0	TICTS(NOTS)	
	•	E10.0	TCTS(NOTS)	
		EMISSIVITIES FOR RADIATION HEAT TRANSFER COMPUTATIONS		
30	1-4	A4	IREO	Variable name (either TIME or TEMP) for table of oxidic phase emissivity versus IREO.
	5-8	A4	IREM	Variable name (either TIME or TEMP) for table of metallic phase emissivity versus IREM.
	9-12	A4	IRES	Variable name (either TIME or TEMP) for table of surroundings emissivity versus IRES.
31	1-5	I5	NEO	Number of values in table of oxidic phase emissivities versus IREO ($1 \leq NEO \leq 5$).
	6-10	I5	NEM	Number of values in table of metallic phase emissivities versus IREM ($1 \leq NEM \leq 5$).
	11-15	I5	NS	Number of values in table of surroundings emissivities versus NS ($1 \leq NS \leq 5$).
32	1-10	E10.0	TORT(1)	Table of oxidic phase emissivity (-) versus time (s) or
	11-20	E10.0	EO(1)	temperature (K);
	21-30	E10.0	TORT(2)	alternating values of emissivity, EO(I) and time or
	31-40	E10.0	EO(2)	temperature, TORT(I) for I = 1, NEO.
	•	•	•	
	•	•	•	If NEO = 1, emissivity is constant at EO(1).
	•	•	•	
	•	E10.0	TORT(NEO)	May require up to 2 cards to complete table.
	•	E10.0	EO(NEO)	
33	1-10	E10.0	TORT2(1)	Table of metallic phase emissivity (-) versus time (s)
	11-20	E10.0	EMM(1)	or temperature (K);
	21-30	E10.0	TORT2(2)	alternating values of emissivity, EMM(I) and time or
	31-40	E10.0	EMM(2)	temperature, TORT2(I) for I = 1, NEM.
	•	•	•	
	•	•	•	If NEM = 1, emissivity is constant at EMM(1).
	•	•	•	
	•	E10.0	TORT2(NEM)	May require up to 2 cards to complete table.
	•	E10.0	EMM(NEM)	

Table 4.1 Input instructions for CORCON-MOD3 (continued)

Card/ Group#	Field	Format	Variable Name	Description
34	1-10	E10.0	TORT6(1)	Table of surroundings emissivity (-) versus time (s) or
	11-20	E10.0	ES(1)	temperature (K);
	21-30	E10.0	TORT6(2)	alternating values of emissivity, ES(I) and time or
	31-40	E10.0	ES(2)	temperature, TORT6(I) for I = 1, NS.
	•	•	•	
	•	•	•	If NS = 1, emissivity is constant at ES(1).
	•	•	•	
	•	E10.0	TORT6(NS)	May require up to 2 cards to complete table.
	•	E10.0	ES(NS)	
Include card/group 34A only if IAOPAC ≠ 0.				
34A	1-10	E10.0	RADLEN	Characteristic path length (m) for atmospheric opacity calculation.

SPLASHOUT OF POOL CONSTITUENTS

[Include card/groups 35, 36 and 37 only if ISPLSH ≠ 0.]

SECTION 5. TIME-DEPENDENT MELT RADIUS

Include card/groups 38 and 39 only if IGEOM = 2 and ITIMR =1.

38	1-5	I5	NORAD	Number of points in table of melt radius versus time (0 ≤ NORAD ≤ 12)
	6-15	F10.0	HTMIN	Minimum allowable melt thickness (cm). (HTMIN ≥ 0.1 cm)
	16-25	F10.0	HTMAX	Maximum allowable melt thickness (cm). (HTMAX ≤ 10^5 cm)

Table 4.1 Input instructions for CORCON-MOD3 (continued)

Card/ Group#	Field	Format	Variable Name	Description
39	1-10	F10.0	TIMRAD(1)	Table of melt radius (m) versus time (s);
	11-20	F10.0	RADTIM(1)	alternating values of time, TIMRAD(I) and melt radius,
	21-30	F10.0	TIMRAD(2)	RADTIM(I) for I = 1, NORAD
	31-40	F10.0	RADTIM(2)	
	•	•	•	
	•	•	•	
	•	•	•	
	•	F10.0	TIMRAD(NORAD)	May require up to 3 cards to complete table.
	•	F10.0	RADTIM(NORAD)	
	SECTION 6. USER FLEXIBILITY			
	Include card/group 40A and 64 only if IUSER = 1.			
40A	1-5	I5	IBHTB	Index specifying modification of the bulk heat transfer coefficient for the bottom surface
	6-10	I5	IBHTS	Index specifying modification of the bulk heat transfer coefficient for the side surface
	11-15	I5	IIHT	Index specifying modification of the interlayer heat transfer coefficient
	16-20	I5	ICHT	Index specifying modification of the coolant heat flux calculation
	21-25	I5	ITMFB	Index indicating modification of the minimum film boiling temperature
	26-30	I5	IEON	Index for modification of the entrainment onset criteria
	31-35	I5	IERT	Index for modification of the entrainment rate calculation
	36-40	I5	IDRT	Index for modification of the droplet settling calculation
	41-45	I5	ICDC	Index for modification of the condensed phase diffusion coefficient
	46-50	I5	IVDC	Index for modification of the vapor phase diffusion coefficient
	51-55	I5	ICNCD	Index for modification of the condensation rate coefficient
	56-60	I5	IMU	Index for specification of the mean aerosol particle size
	61-65	I5	IBR	Index for modification of the bubble size models
	66-70	I5	IKM	Index for modification of the metal phase thermal conductivity
	71-75	I5	IKO	Index for modification of the oxide phase thermal conductivity

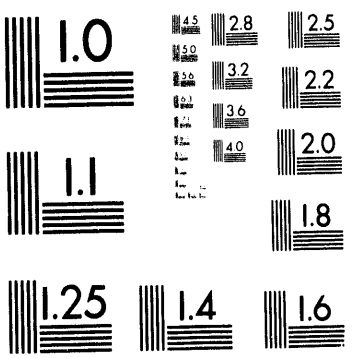
1.0
1.1
1.25
1.4
1.6
1.8
2.0
2.2
2.5
2.8
3.2
3.6
4.0
4.5
5.0
5.6

2 of 3

Table 4.1 Input instructions for CORCON-MOD3 (continued)

Card/ Group#	Field	Format	Variable Name	Description
40B	1-5	I5	IVSM	Index for modification of the metal phase viscosity
	6-10	I5	IVSO	Index for modification of the oxide phase viscosity
	11-15	I5	ISTM	Index for modification of the metal phase surface tension
	16-20	I5	ISTO	Index for modification of the oxide phase surface tension
	21-25	I5	IRHOM	Index for modification of the oxide phase density
	26-30	I5	IRHOO	Index for modification of the metal phase density
	31-35	I5	IPHM	Index for modification of the metal phase diagram
	36-40	I5	IPHO	Index for modification of the oxide phase diagram
	41-45	I5	IZIP	Index for modification of the chemical equilibrium cutoff
			Include card/group 41A only if IBHTB = 1.	
41A	1-10	E10.0	AHTB	Coefficients A,B, and C in:
	11-20	E10.0	BHTB	$Nu = A\ Re^B\ Pr^C$
	21-30	E10.0	CHTB	
			Include card/group 41B only if IBHTB <0.	
41B	1-10	E10.0	XBM	Multiplier applied to bulk convective heat transfer coefficient for the bottom surface of the melt
			Include card/group 42A only if IBHTS = 1.	
42A	1-10	E10.0	AHTS	Coefficients A, B, and C in:
	11-20	E10.0	BHTS	$Nu = A\ Re^B\ Pr^C$
	21-30	E10.0	CHTS	
			Include card/group 42B only if IBHTS <0.	
42B	1-10	E10.0	XSM	Multiplier applied to bulk convective heat transfer coefficient for the radial (side) surface of the melt
			Include card/group 43A only if IIHT =1.	
43A	1-10	E10.0	AI	Coefficients A, B, and C in:
	11-20	E10.0	BI	$Nu = A\ Re^B\ Pr^C$
	21-30	E10.0	CI	
			Include card/group 43B only if IIHT <1.	
43B	1-10	E10.0	XIM	Multiplier applied to interlayer heat transfer coefficient
			Include card/group 44A only if ICHT = 1.	
44A1	1-5	I5	NCHT	Number of entries in table for coolant heat flux vs. ΔT_{sat} (NCHT ≤ 20)

Table 4.1 Input instructions for CORCON-MOD3 (continued)

Card/ Group#	Field	Format	Variable Name	Description
44A2	1-10	E10.0	DTCHT(1)	Table of coolant heat flux (w/m^2) vs. ΔT_{sat}; alternating values of ΔT_{sat} and heat flux
	11-20	E10.0	CHT(1)	
	•			
	•	E10.0	DTCHT (NCHT)	
			CHT (NCHT)	
	•	E10.0		
			Include card/group 44B only if ICHT <0.	
44B1	1-5	I5	NCHT	Number of entries in table for the coolant heat flux vs. ΔT_{sat} (NCHT ≤ 20)
44B2	1-10	E10.0	DTCHT(1)	Table of coolant heat flux multiplier vs. ΔT_{sat}; alternating values of ΔT_{sat} and heat flux multiplier
	11-10	E10.0	CHT(1)	
	•			
	•	E10.0	DTCHT (NCTH)	
	•	E10.0	CHT(NCHT)	
			Include card/group 45 only if ITMFB = 1.	
45	1-10	E10.0	TMFB	Minimum film boiling temperature (K)
			Include card/group 46 only if IEON = 1.	
46	1-10	E10.0	ECRIT	Critical bubble size for entrainment
			Include card/group 47 only if IERT = 1.	
47	1-10	E10.0	XEM	Multiplier applied to calculated entrainment rate
			Include card/group 48 only if IDRT = 1.	
48	1-10	E10.0	XDM	Multiplier applied to calculated droplet settling flux
			Include card/group 49 only if ICDC = 1.	
49	1-10	E10.0	CDM	Multiplier applied to the condensed phase diffusion coefficient
			Include card/group 50 only if IVDC = 1.	
50	1-10	E10.0	VDM	Multiplier applied to vapor phase diffusion coefficient
			Include card/group 51 only if ICNDC = 1.	
51	1-10	E10.0	CNDM	Multiplier applied to the condensation rate coefficient
			Include card/group 52 only if IMU = 1.	
52	1-10	E10.0	PSDMU	Mean aerosol particle size (micrometers)
			Include card/group 53A only if IBR = 1.	
53A	1-10	E10.0	BR1	Multiplier for the Fritz bubble size

Table 4.1 Input instructions for CORCON-MOD3 (continued)

Card/ Group#	Field	Format	Variable Name	Description
	11-20	E10.0	BR2	Multiplier for the Davidson-Schuler bubble size
	21-30	E10.0	BR3	Multiplier for the gas film bubble size
			Include card/group 53B only if IBR < 0.	
53B	1-10	E10.0	BRFIX	Fixed bubble radius (m)
			Include card/group 54 only if IKM = 1.	
54A	1-5	I5	NKMM	Number of entries in the table of thermal conductivity multiplier vs. temperature (NKMM ≤ 10)
54B	1-10	E10.0	TKMM(1)	Table of thermal conductivity multiplier vs. temperature (K); alternating values of temperature and thermal conductivity multiplier
	11-20	E10.0	XKMM(1)	
	•			
	•	E10.0	TKMM (NKMM)	
	•	E10.0	XKMM (NKMM)	
			Include card/group 55 only if IKO = 1.	
55A	1-5	I5	NKOM	Number of entries in table of thermal conductivity multiplier vs. temperature (NKOM ≤ 10)
55B	1-10	E10.0	TKOM(1)	Table of thermal conductivity multiplier vs. temperature (K); alternating values of temperature and thermal conductivity multiplier
	11-20	E10.0	XKOM(1)	
	•			
	•	E10.0	TKOM (NKOM)	
	•	E10.0	XKOM (NKOM)	
			Include card/group 56 only if IVSM = 1.	
56A	1-5	I5	NVSMM	Number of entries in the table of viscosity multiplier vs. temperature (NVSMM ≤ 10)
56B	1-10	E10.0	TVSMM(1)	Table of viscosity multipliers vs. temperature (K); alternating values of temperature and viscosity multiplier
	11-20	E10.0	VSMM(1)	
	•			
	•	E10.0	TVSMM (NVSMM)	
	•	E10.0	VSMM (NVSMM)	
			Include card/group 57 only if IVSO = 1.	

Table 4.1 Input instructions for CORCON-MOD3 (continued)

Card/ Group#	Field	Format	Variable Name	Description
57A	1-5	I5	NVSMO	Number of entries in table of viscosity multiplier vs. temperature (NVSMO ≤ 10)
57B	1-10	E10.0	TVSMO(1)	Table of viscosity multiplier vs. temperature (K); alternating values of temperature and viscosity multiplier
	11-20	E10.0	VSMO(1)	
	•			
	•	E10.0	TVSMO (NVSMO)	
	•	E10.0	VSMO (NVSMO)	
			Include card/group 58 only if ISTM = 1.	
58	1-10	E10.0	STMM	Multiplier applied to the metal phase surface tension
			Include card/group 59 only if ISTO = 1.	
59	1-10	E10.0	STMO	Multiplier applied to the oxide phase surface tension
			Include card/group 60 only if IRHOM = 1.	
60	1-10	E10.0	RHOMM	Multiplier applied to the metal phase density
			Include card/group 61 only if IRHOO = 1.	
61	1-10	E10.0	RHOOM	Multiplier applied to the oxide phase density
			Include card/group 62 only if IPHM = 1.	
62	1-10	E10.0	TSOLMT	Constant value for the metal phase solidus temperature (K)
			Include card/group 63 only if IPHO = 1.	
63	1-10	E10.0	XEUT	Mole fraction of concrete oxides at which the oxide phase solidus temperature has decreased to the concrete solidus
			Include card/group 64 only if IZIP = 1.	
64	1-10	E10.0	ZIP	Value of the ZILCH parameter in MLTREA = cutoff for inclusion in the chemistry solution (default: 1.E-5 moles)

Table 4.1 Input instructions for CORCON-MOD3 (continued)

Card/ Group#	Field	Format	Variable Name	Description
	SECTION 7. VANESA INPUT			
		VANESA INPUT OPTIONS		
65	1-5	I5	IBUB	Bubble diameter option index 0 -- Fixed bubble diameter is user specified 1 -- Bubble diameter is calculated internally
	6-10	I5	KATIS	Mechanical release option index 0 -- Fixed release 1 -- Azbel, Ishii & Kataoka correlations are calculated internally.
	11-15	I5	INOPL	INOPL option 0 -- No pool calculation 1 -- Pool calculation activated
	16-20	I5	IDEAL	Non-ideal chemistry index 0 -- Calculate activity coefficient for use in VANESA 1 -- Assume ideal chemistry
		BCL COMPOSITION		
Include card/groups 66A, 66B and 66C only if IVANFP = 1.				
66A	1-10	E10.0	CES	Mass of Cesium melt constituent (kg).
	11-20	E10.0	IOD	Mass of Iodine melt constituent (kg).
	21-30	E10.0	XEN	Mass of Xenon melt constituent (kg).
	31-40	E10.0	KRY	Mass of Krypton melt constituent (kg).
	41-50	E10.0	TE	Mass of Tellurium melt constituent (kg).
	51-60	E10.0	BA	Mass of Barium melt constituent (kg).
	61-70	E10.0	SN	Mass of Tin melt constituent (kg).
	71-80	E10.0	RU	Mass of Ruthenium melt constituent (kg).
66B	1-10	E10.0	MO	Mass of Molybdenum melt constituent (kg).
	11-20	E10.0	SR	Mass of Strontium melt constituent (kg).
	21-30	E10.0	RB	Mass of Rubidium melt constituent (kg).
	31-40	E10.0	Y	Mass of Yttrium melt constituent (kg).
	41-50	E10.0	TC	Mass of Technetium melt constituent (kg).
	51-60	E10.0	RH	Mass of Rhodium melt constituent (kg).
	61-70	E10.0	PD	Mass of Palladium melt constituent (kg).
	71-80	E10.0	LA	Mass of Lanthanum melt constituent (kg).
66C	1-10	E10.0	CE	Mass of Cerium melt constituent (kg).
	11-20	E10.0	PR	Mass of Praseodymium melt constituent (kg).
	21-30	E10.0	ND	Mass of Neodymium melt constituent (kg).
	31-40	E10.0	SM	Mass of Samarium melt constituent (kg).
	41-50	E10.0	PU	Mass of Plutonium melt constituent (kg).
	51-60	E10.0	AG	Mass of Silver melt constituent (kg).
	61-70	E10.0	SB	Mass of Antinomy melt constituent (kg).
	71-80	E10.0	NB	Mass of Niobium melt constituent (kg).
Include card/group 67 only if INOPL $\neq$ 0.				

Table 4.1 Input instructions for CORCON-MOD3 (continued)

Card/ Group#	Field	Format	Variable Name	Description
67	1-10	I10	I1=NOSC	Number of size segments used to describe the aerosol size distribution ($4 \leq$ NOSC ≤ 50) (If I1 < 0, use default: NOSC = 20.)
	11-20	F10.0	F1=GSD	Geometric standard deviation of size distribution of aerosols entering water pool (If F1 < 0, use default: GSD = 2.3)
	21-30	I10	I2=IDMF	Switch that controls the diffusion mechanism for aerosol entrapment by the water pool. 0 -- Diffusion mechanism inactive $\neq 0$ -- Diffusion mechanism active
	31-40	I10	I3=IMPF	Switch that controls the impaction mechanism for aerosol entrapment by the water pool. 0 -- Impaction mechanism inactive $\neq 0$ -- Impaction mechanism active
	41-50	F10.0	F2=BSIZI	Diameter of gas bubbles at base of the water pool (cm) (If F2 < 0, use default: BSIZI = 1.0 cm)
	51-60	F10.0	F3=VROVR	V(rel)/V(rise), the ratio of gas velocity within the bubble to the rise velocity of the bubble. (If F3 < 0, use default: VROVR = 1.0)

interesting points in the development of the calculation, without providing unneeded detail during the remainder of the problem. The actual timesteps employed may differ from those specified, if necessary, to produce edits at the requested times.

Edits are produced at times which are integral multiples of the edit interval DEDIT(I), rather than a DEDIT(I) from the previous edit. This minimizes the effect of the insertion of additional edits, which is valuable if one must compare the outputs from several calculations at the same times. To clarify this, consider as an example a calculation performed with edit controlled by an input card such as

```
1200.0      21600.0
```

This will produce printed output every 1200.0 s (20 minutes), at times of 1200.0 s, 2400.0 s, 3600.0 s, etc. Suppose that some interesting phenomenon is observed at about 3000 s, and that more frequent output is desirable to study it. The set of input cards

```
1200.0      3000.0
  60.0      3300.0
1200.0     21600.0
```

will produce additional printed output at 3000.0 s, 3060.0 s, ..., 3300.0 s. However, the later edits will still be written at times of 3600.0 s, 4800.0 s, etc., rather than being shifted to 4500.0 s, 5700.0 s, etc.

If variable timestep control is specified (DELTIM < 0) but no intervals are specified, then the calculation will be terminated following input.

If variable edit control is specified (IPINC < 0) but no intervals are specified, then the calculation will be run but no printed output will be generated. This might be desired by a user who is interested only in plots of the output data.

Tables

All input tables are automatically linearly interpolated during execution. This is true for tables given as a function of time and those specified as a function of temperature.

Initial Cavity Geometry

The definitions of most of the variables used to describe the initial cavity geometry (cards 5 to 9) should be apparent from Figures 4.2 through 4.4, or from the definitions of the variables in Section 5.2. However, the variables NBOT and ITANG warrant further discussion.

The cavity-shape description introduces a "tangent ray" parallel to the cavity axis through the tangent point between the flat bottom of the cavity and the curved sides. This ray is used in the shape-change calculation to maintain the flat bottom of the cavity as required by the models.

For the flat-bottomed cylinder, IGEOM = 2, or the arbitrary cavity shape, IGEOM = 4, there is already a normal ray through this tangent point, which is numbered NBOT. The tangent ray, numbered ITANG =NBOT + 1, defines an additional body point which initially coincides with that defined by the ray NBOT, but which diverges from it as the surface recedes. The number of the rays is changed as the calculation proceeds, to reflect their actual ordering along the cavity surface. (Note that "normal" points can cross over the tangent ray.)

In the case of a hemispherically based cavity, IGEOM = 1, a flat bottom is assumed to exist with a radius that is one percent of the sphere radius RS, and only a single point is defined with the number ITANG = NBOT = 2.

The Size and Power of the Intact Core

The size and power of the intact core (card 17) is used to determine the concentration of fission products in the fuel if IFP = 0. This concentration, as modified by retention factors for each element included, together with the UO_2 mass in the pool, is used to evaluate the initial fission-product inventory of the melt. If the initial mass exceeds the size of the intact core, a warning is issued.

4.2.2 Recommended Values and Default Values for Input Quantities

Recommended values for some of the input quantities are described below. Except for the default concrete compositions listed in Table 2.2, default values are not used in CORCON. That is, if a required input value is not defined, then in general code execution is terminated with an appropriate warning or error message.

Timestep Values

The timestep for CORCON is controlled by user input (card 3 and, optionally, group 3A). In selected values for the timestep, the user should remember that the CORCON model is explicit in time for the calculation of ablation rates and convective mass and energy flows. Therefore, if the timesteps employed are too large,

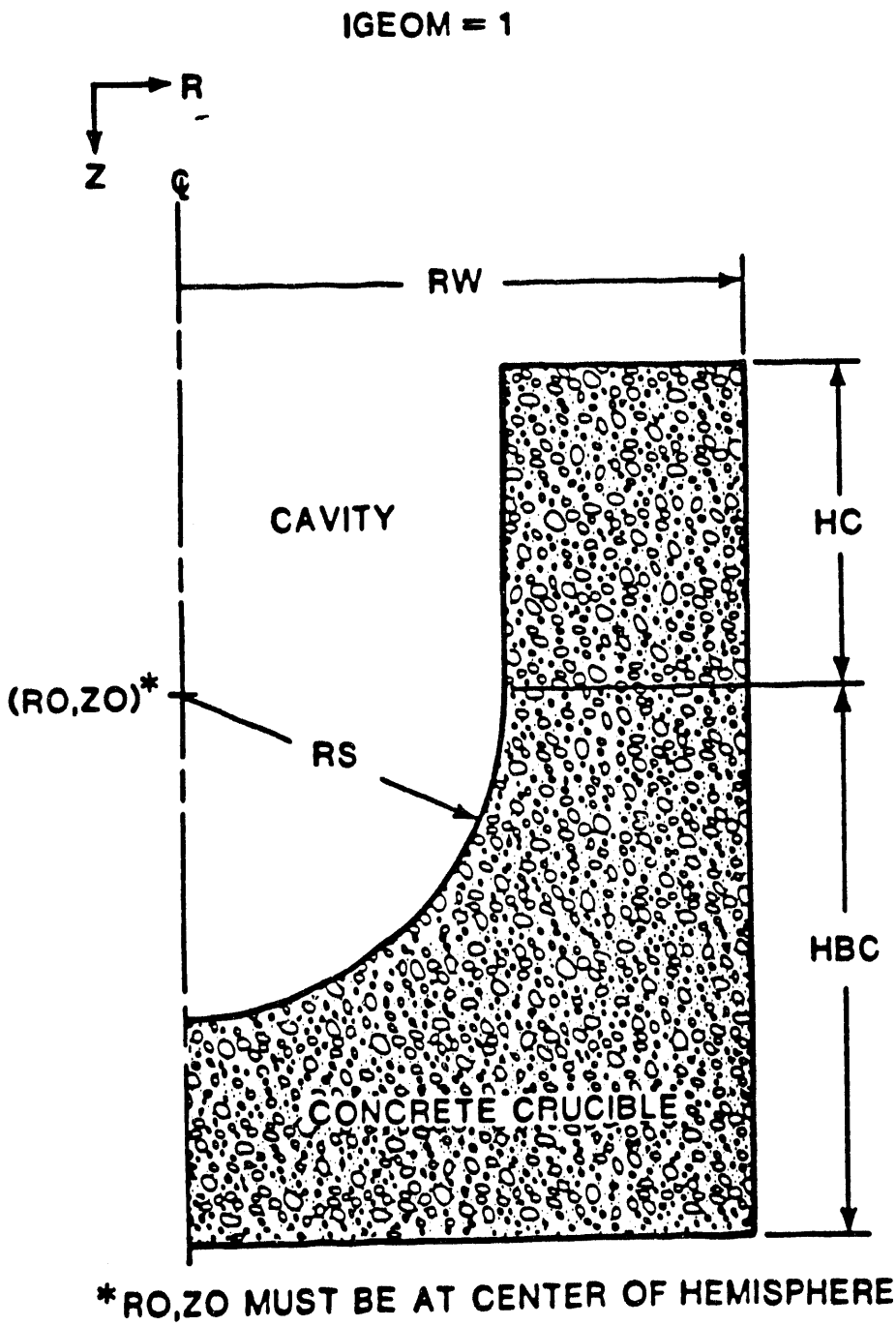

Figure 4.2 Initial cavity geometry - cylinder with hemispherical base

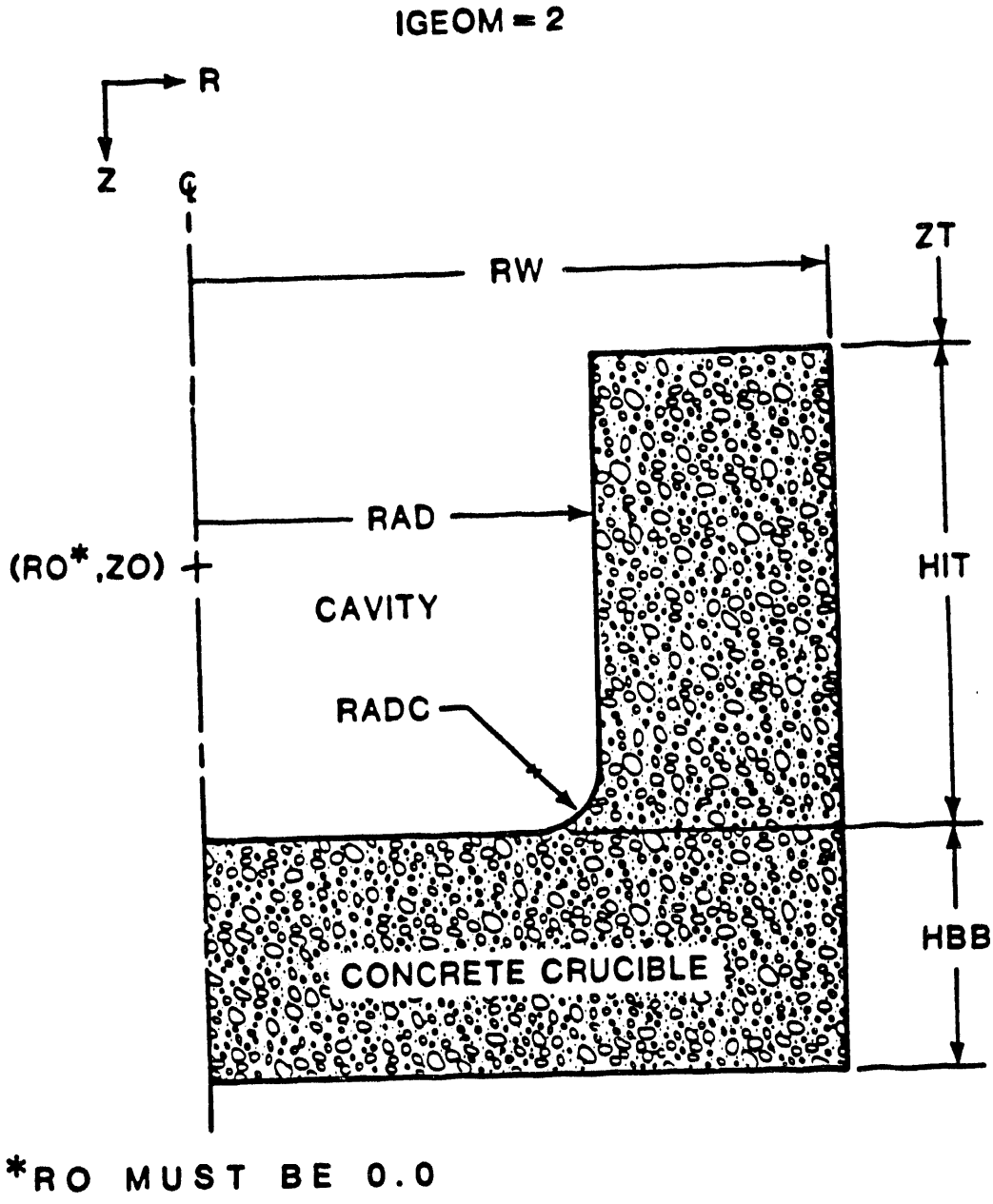

Figure 4.3 Initial cavity geometry - arbitrary shape

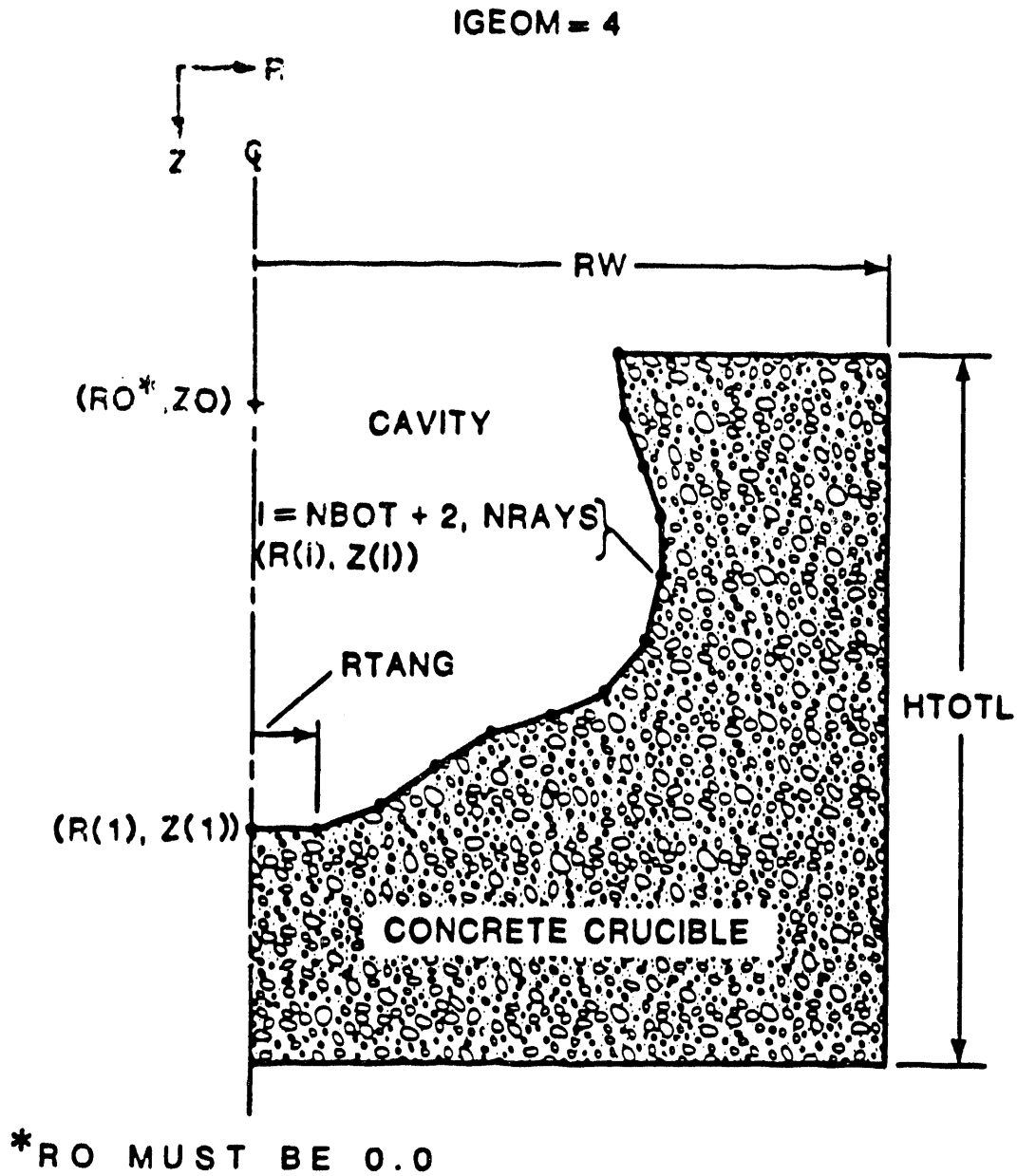

Figure 4.4 Initial cavity geometry - cylinder with flat base

unphysical results may be generated or the calculation may fail completely

Based on experience during the development and testing of CORCON-Mod3 and on experience with previous versions of CORCON, we recommend timestep values in the range of 10 to 60 s. Short timesteps should be used whenever conditions are changing rapidly such as during periods of high heat transfer (rapid concrete ablation), vigorous exothermic chemical reactions, or rapid interlayer mixing. Conditions such as these are most likely to occur at early times. At later times, it may be possible to increase the timestep without incurring numerical problems. Timestep control is accomplished using card group 3A.

Concrete Ablation Temperature

The ablation temperature for concrete, TW, is not clearly defined and must be specified by the user. The user is limited to values between the liquidus and solidus temperatures for the concrete selected. Based on past experience in simulating experiments with CORCON-Mod3, we currently recommend that the ablation temperature be selected at or near the liquidus temperature for the concrete. This selection implies that concrete is not displaced from the interface until it is almost completely molten. The liquidus and solidus temperatures for the default concretes are listed in Table 2.3.

Initial Problem Time

When using the internally calculated decay heat generation, the initial time, TIMEO, corresponds to the time following reactor shutdown (SCRAM) that the melt is deposited into the reactor cavity. If a specific time is not known, a value of TIMEO in the range of two to five hours would be reasonable.

Cavity Coordinate System

In the specification of the ray system (card 4), the origin must lie on the axis of symmetry (R0 = 0.0). Based on sensitivity calculations, we recommend that Z0 be chosen to maximize the number of rays whose intersection with the cavity surface is close to perpendicular, which avoids small-angle intersections. In any case, the origin must lie above the bottom of the cavity. The ray spacing should be chosen so that the separation between body points (i.e., intersections of rays with the cavity surface) is initially in the range of three to 30 cm. Although up to 100 rays may be specified, most applications will require fewer than 60 rays. (Given the uncertainty in modeling heat transfer to the concrete, there is no real benefit to using a greater number of rays to achieve better definition of the cavity shape.)

4.3 Description of the Output

4.3.1 Numerical Output

The output from CORCON-Mod3 is stored in the file, CCMod3.OUT. This file contains several major sections.

The first section is an echo of the input data; it is an uninterpreted reproduction of the records comprising the input stream. This provides a compact, permanent record of the data used in a particular calculation, and is useful for finding input errors.

The second section contains the input data as interpreted in CORCON. It contains a description of the concrete cavity, the composition of the concrete (either default or user-specified), the fission product inventory for the melt and the initial conditions for the melt, the identity and quantity of the coolant (if any), the composition of the atmosphere above the melt pool, the type of boundary conditions, the composition and mass flow rate of material entering the melt pool, and the radiative boundary conditions for the melt pool. Error messages are printed in this section if errors are detected. If errors are detected, code execution continues to the end of this section, and then terminates. This can reduce the number of passes needed to find all the errors in an input deck.

The third output section presents a temporal snapshot of the state of the core-concrete interaction. This is generated at the start of the problem, TIMEO, and at subsequent times as specified in the input. The information is presented in several sections, each starting on a new page of output, with a running header to identify the version of the code in use, the problem title, the problem time, and the timestep number. The sections are a general summary, and summaries of gas generation, cavity geometry, heat transfer, chemical reactions, melt pool geometry, melt pool composition, melt layer properties for the melt pool, aerosol generation and radionuclide release, and aerosol removal in an overlying water pool. The latter two sections are printed only if the user has chosen to perform the VANESA calculation. These sections are described in greater detail below.

Various informational messages, such as those describing changes in melt layer orientation or warnings concerning the number of iterations required in various routines, are printed between the snapshot edits. A fourth section of

output may be generated by use of the TPRIN variable on Card 3. This section contains extensive diagnostic information, and is intended primarily for debugging the code; it is labeled in terms of FORTRAN variable names and assumes that the user has detailed knowledge of the code. Under ordinary circumstances, this output should be suppressed by specifying TPRIN greater than the problem end time, TIMEND.

General Summary

The general summary section of the snapshot edit contains the pool configuration, the maximum depth and radius of the cavity, an approximate energy budget, and quantities needed to check the accuracy of the numerics of the code.

The pool configuration is given as the number of layers in the pool, the configuration of the layers, and the presence of coolant.

The maximum depth and radius of the cavity are given in meters, with the locations of the points of maximum depth and maximum radius, and the remaining axial and radial concrete thicknesses.

The energy budget is a summary of the rates of gain or loss of energy (in watts) from the pool through various mechanisms. The budget is not exact: some rates are current and some are averages over the preceding timestep. In some cases, approximations have been made in the calculation of the rates given in the energy budget which are not used in the internal CORCON calculations. For these reasons, the printed energy budget may not balance exactly, although the error is usually small (on the order of a few percent). However, large discrepancies may appear following a major discontinuity in the physical phenomena, such as problem initiation, depletion of the coolant, or layer flip. The energy budget is for debris-containing layers only; it does not include the coolant or the concrete.

Detailed checks on conservation of mass and energy in the entire pool (including coolant, if present) are made and printed in this section. The printed values are the discrepancies between the sums of layer contents and the values required by conservation within the pool boundaries, and are presented as relative errors in mass and enthalpy. Normally each value should be near machine round-off for single-precision arithmetic.

Gas Generation Summary

The gas generation summary section of the snapshot edit contains generation rates and cumulative releases for all the condensible and noncondensible gas species in the problem. These are presented as masses and moles, and include the gases in bubbles, the gas film, and vaporized coolant.

Cavity Geometry Summary

The cavity geometry summary section of the snapshot edit presents the locations of the body points defining the cavity shape, the distance of each body point from the bottom center along the concrete surface, the local slope of the wall, and the angle of the ray which defines the point. Also, the cumulative volume and surface area below each point, the average void fraction at the elevation of the point are presented for each point. The locations of interfaces between pool layers are also given.

Heat Transfer Summary

The heat transfer summary section of the snapshot edit presents, for each body point, the local normal concrete ablation rate, the film conditions, the temperature of the pool/film interface or of the pool/concrete interface, the film thickness, film-wise mass flow rate, the average velocity of the gas in the film (if a gas film is present), the Reynolds number, the film flow regime, the contributions of radiation and convection to the heat flux, and the heat transfer coefficient. If no gas film is present, the film thickness, film-wise mass flow rate, the average velocity of the gas in the film, and the Reynolds number will all be zero or very small numbers.

Chemical Reactions Summary

The chemical reactions summary section of the snapshot edit presents the results of the chemical reactions in each layer during the timestep. For a metal layer, the results of the metal/gas or metal/gas/concrete oxide reactions are printed. For a heterogeneous layer, the results of the bulk metal/oxide/gas reactions, are printed. For the film, the results of the film metal/gas reactions during the timestep are printed. The quantities of the reactants and products are printed in moles for each of the oxide, metal, and gas species involved in the reactions.

Melt Pool Composition Summary

The melt pool composition summary section of the snapshot edit presents the mass of each species present in each occupied layer of the pool and the total mass of each species present in the pool.

Melt Pool Geometry Summary

The melt pool geometry summary section of the snapshot edit presents the radius and thickness of the melt pool. This section is printed only if the time-dependent melt radius option is used.

Melt Layer Properties Summary

The melt layer properties summary section of the snapshot edit presents the values of thermophysical and transport properties for each layer in the melt pool. Also, quantities related to gas bubbles, such as the bubble radius and velocity, are presented, and heat transfer coefficients, crust model quantities, and axial interface temperatures and layer edge temperatures are presented. Important terms in the layer energy equation are given.

All quantities are evaluated at the current time, with the exception of the heat of reaction entry, which is an average over the preceding timestep.

Interlayer Mixing Summary

The interlayer mixing summary is provided if a mixture layer exists; it is not necessary for the mixing option to be active. The summary lists properties for each phase in a mixture layer. This information supplements the layer property information provided in the preceding edit summary. Also included in this summary are the masses of oxide or metal entrained and de-entrained during the timestep.

Aerosol and Radionuclide Release Summary

The aerosol and radionuclide release summary is provided if the user has chosen to perform the VANESA calculation. This output summary provides the aerosol release rate, aerosol concentration in the gas stream, aerosol composition, aerosol material density, aerosol particle size, and the temperatures and gas composition used in the VANESA calculation.

Aerosol Removal in an Overlying Water Pool Summary

This section is provided only if the user has chosen to perform the VANESA analysis and an overlying water pool is present. The output in this section includes particle size-dependent decontamination factors and mass distribution. Also printed are the overall decontamination factor and total mass of aerosol emerging from the water pool.

4.3.2 Graphical Output

Output files for generating graphical depictions of the data are obtained by setting IPG to a non-zero value to obtain a set of files for plotting such things as gas generation rates and melt temperatures as functions of time, or setting IMOV to a non-zero value to obtain a file of cavity shape data for making movies of the evolution of the cavity shape.

The quantities written to the various output files for plotting are described below. Except as noted, each quantity is written at each edit time.

Unit 30 (movie.dat)

The quantities written to Unit 30 are the number of rays, the outer radius of the concrete crucible [m], and the axial coordinate of the bottom of the crucible [m] (on the first line of the file). Then the time [s], the rz-coordinates of each body point, the radius of the top surface of the melt pool or coolant, and the axial location of this surface (all in meters) are written. This information can be used to generate plots of the temporal cavity shape, but doing so requires that the user develop his/her own post-processor.

Unit 31 (ccmod3.plt)

The quantities written to Unit 31 include the time [s] and then, for each layer, the layer temperature [K], the layer mass [kg], the layer density [kg/m], the layer void faction [-], the temperature of the lower layer surface [K], and the heat transfer from the lower surface [W]. Also written are the coordinates [m] of the locations of maximum radius and maximum axial depth of the melt pool, the maximum axial and radial erosion distances, the axial erosion rate at the first body point (i.e., at the cavity centerline), the cumulative gas generated [g-mole] by species, and the rate of gas generation [g-moles/s] by species.

If a VANESA calculation is performed, Unit 31 is also used to store time-dependent information on radionuclide release and aerosol generation. The quantities written to Unit 31 are the aerosol generation rate [g/s], and the aerosol concentration at ambient conditions [g/m^3].

The quantities written to this file may be read by any FORTRAN program that includes the appropriate unformatted read statements. An example of the required read statements for each time point follows:

```
real time(npts),tlay(npts,6),amlay(npts,6)
real sdot(npts),dz(npts),dr(npts)
```

```
      real outgas(npts,4),doutgs(npts,4),q(npts,6),asum(6).aer(npts,3)
      double precision xmas
c
      read(ntp2) times(jpt)
      do 10 i=1,6
        read(ntp2) tlay(jpt,i),amlay(jpt,i),x1,x2,x3,x4
 10   continue
      read(ntp2) z1,r1,r2,z2
      read(ntp2) sdot(jpt)
      read(ntp2) dz(jpt,dr(jpt)
      read(ntp2) (outgas(jpt,i),i=1,4)
      read(ntp2) (doutgs(jpt,i),i=1,4)
      read(ntp2) (q(jpt,i),i=1,5)
      read(ntp2) aer(jpt,1),aer(jpt,2),xmas
      aer(jpt,3)=xmas
```

4.4 Description of the Warning and Error Messages

CORCON-Mod3 performs a number of error checks during execution. First the input data are examined for obvious errors or inconsistences. Then various intermediate results of the transient calculation are tested to determine if they are physically realistic within the limits of the models in CORCON-Mod3 and if they have converged numerically.

When an error condition is detected, an appropriate message is issued. Subsequent action depends on the severity of the error: execution may

- continue with a warning, or
- terminate at the end of the timestep, or
- terminate immediately.

The messages that the user may encounter are listed in Table 4.2, together with the action taken by the code.

Most of the error messages are self-explanatory. In a few cases, additional comments have been added to clarify the meaning of the message.

Examination of the code listing will reveal several other locations where an error or warning message could be printed and execution terminated by a call to FAIL. In general they correspond to errors which, short of machine error, cannot exist in CORCON- Mod3. These messages might appear if incorrect modifications were made to the code, and are included for that reason.

4.5 General Programming Information

CORCON-Mod3 is coded in FORTRAN which conforms to ANSI Standard X3.9-1978 ("FORTRAN 77").[5] The only changes in language from CORCON-Mod1 are the use of type CHARACTER for alpha-numeric data, and the use of BLOCK IF structures in the newer routines. The code contains approximately 23600 source lines, including 6200 lines of COMMENTS.

In cases where constants are required to have full machine accuracy, they are evaluated by execution of a short routine called SETUP.

The code reads data from a file named "ccmod3.in," which must exist at the start of the run. (On UNIX systems, the file name should be in lower case.) ASCII output is written to a file named "ccmod3.out," which will be created with "unknown" FORTRAN status. On some systems, this will cause an existing file with the name "ccmod3.out" to be overwritten. Additional binary files, "movie.dat" and "ccmod3.plt," may be created and written for post-execution printing and plotting.

Table 4.2 CORCON-generated warning and error messages for each subroutine

ABLATE

"* * * ABLATE * * * INTERPOLATION FOR MASS ADDITION
() AT () OFF LOW END OF TABLE ()"
[Warning only]

"* * * ABLATE * * * INTERPOLATION FOR MASS ADDITION
() AT ( ) OFF HIGH END OF TABLE ()"
[Warning only]

ADDLYR

"* * * ADDLYR * * * CONVERGENCE FAILURE.
L,HTOT(L),TLAY(L) = (), (), ()"
[Warning only]
Convergence failure for layer temperature in call to TMPFND.

ATMPRO

"* * * ATMPRO * * * INTERPOLATION FOR ATMOSPHERIC
PRESSURE AT () OFF LOW END OF TABLE ()"
[Warning only]

"* * * ATMPRO * * * INTERPOLATION FOR ATMOSPHERIC
PRESSURE AT () OFF HIGH END OF TABLE ()"
[Warning only]

ATMSUR

"* * * ATMSUR * * * INTERPOLATION FOR SURROUNDINGS
TEMPERATURE AT () LOW END OF TABLE ()"
[Warning only]

"* * * ATMSUR * * * INTERPOLATION FOR SURROUNDINGS
TEMPERATURE AT () OFF HIGH END OF TABLE ()"
[Warning only]

"* * * ATMSUR * * * CONVERGENCE FAILURE"
[Immediate termination]
Failure to match the above-pool heat transfer to the pool surface.

Table 4.2 CORCON-generated warning and error messages for each subroutine (continued)

CHEKCV

"* * * CHEKCV * * * NO MORE COOLANT."
[Immediate termination]

"* * * LEVSWL\CHEKCV * * * NOT ENOUGH COOLANT
TO COVER THE MELT AT () SECONDS."
[Immediate termination]

"* * * ENRCN1\CHEKCV * * * NOT ENOUGH COOLANT
TO COVER THE MELT AT () SECONDS."
[Immediate termination]

CONFND

"* * * CONFND * * * INSERT = () EXCEEDS DIMENSIONS"
[Immediate termination]
Can only occur if data tables have been changed.

"* * * CONFND * * * IOPT = () OR IN = () NOT IN MASTER LIST"
[Immediate termination]
Can only occur if data tables have been changed.

CONPRP

"* * * CONPRP * * * CONCRETE INPUT SPECIES () NOT IN MASTER LIST"
[Deferred termination]

"* * * CONPRP * * * REBAR INPUT SPECIES () NOT IN MASTER LIST"
[Deferred termination]

CPENTH

"* * * CPENTH * * * IOPT = () IS IN ERROR"
[Immediate termination]

CREATE

"* * * PLLAYR * * * CONVERGENCE FAILURE.
L,HTOT(L),TLAY(L) = () () ()"
[Immediate termination]

Table 4.2 CORCON-generated warning and error messages for each subroutine (continued)

CYLIND

"* * * CYLIND * * * NRAYS = () LESS THAN NBOT+NCORN+3"
[Deferred termination]
Too few rays or two many bottom and corner points in cavity definition.

D1MACH

"D1MACH -- I OUT OF BOUNDS"
[Immediate termination]
Incorrect index in calling statement: 1 .LE. I .LE. 5. Can only occur if the code has been modified incorrectly.

DATAIN

"* * * DATAIN * * * NO DATA ON UNIT 5"
[Immediate termination]

"* * * DATAIN * * * TOO MANY TIMESTEP INTERVALS"
[Deferred termination]

"* * * DATATIN * * * NO TIMESTEP INPUT"
[Deferred termination]

"* * * DATAIN * * * TOO MANY EDIT INTERVALS"
[Deferred termination]

"* * * DATAIN * * * INVALID IFP = ()"
[Immediate termination]

"* * * DATAIN * * * IREO = () IREM = () IRES = ()"
[Immediate termination]
Improper type for emissivity tables. Should be "TIME" or "TEMP".

DCSEVL

"DCSEVL NUMBER OF TERMS LE 0"
[Immediate termination]

"DCSEVL NUMBER OF TERMS GT 1000"
[Immediate termination]

"DCSEVL X OUTSIDE (-1,+1)"
[Immediate termination]

Table 4.2 CORCON-generated warning and error messages for each subroutine (continued)

DCYINT

"* * * DCYINT * * *, PROBABLE ERROR. POOL CONTAINS () PERCENT OF CORE"
[Warning only]
Input has specified a mass of UO2 greater than the entire core.

DHGEN

"* * * DHGEN * * * INTERPOLATION FOR SOURCE POWER IN OXIDE AT () OFF LOW END OF TABLE ()"
[Warning only]

"* * * DHGEN * * * INTERPOLATION FOR SOURCE POWER IN OXIDE AT () OFF HIGH END OF TABLE ()"
[Warning only]

"* * * DHGEN * * * INTERPOLATION FOR SOURCE POWER IN METAL AT () OFF LOW END OF TABLE ()"
[Warning only]

"* * * DHGEN * * * INTERPOLATION FOR SOURCE POWER IN METAL AT () OFF HIGH END OF TABLE ()"
[Warning only]

EDIT

EMISIV

"* * * EMISIV * * *, INTERPOLATION FOR SURROUNDINGS EMISSIVITY AT () OFF LOW END OF TABLE ()"
[Warning only]

"* * * EMISIV * * * INTERPOLATION FOR SURROUNDINGS EMISSIVITY AT () OFF HIGH END OF TABLE ()"
[Warning only]

"* * * EMISIV * * * INTERPOLATION FOR OXIDE EMISSIVITY AT () OFF LOW END OF TABLE ()"
[Warning only]

"* * * EMISIV * * * INTERPOLATION FOR OXIDE EMISSIVITY AT () OFF HIGH END OF TABLE ()"
[Warning only]

Table 4.2 CORCON-generated warning and error messages for each subroutine (continued)

"* * * EMISIV * * * INTERPOLATION FOR METAL
EMISSIVITY AT () OFF LOW END OF TABLE ()"
[Warning only]

"* * * EMISIV * * * INTERPOLATION FOR METAL
EMISSIVITY AT () OFF HIGH END OF TABLE ()"
[Warning only]

"* * * EMISIV * * * NSPL,NSPU = () ()"
[Immediate termination]
Invalid species range.

ENRCN1

"* * * ENRCN1 * * * MASS IN LAYER ()"
[Immediate termination]
Improper layer. Can only occur if the code has been modified incorrectly.

"* * * ENRCN1 * * * BAD DQDT, LLO, DQTDTT(LLO), LUP, DQBDTB(LUP) =
() () () () ()"
[Immediate termination]
Some heat flux vs temperature relation has a negative slope.

"* * * ENRCN1 * * * MATRIX AMTRX IS SINGULAR AS DETECTED BY SAXB"
[Immediate termination]
The equations for the solution of the implicit energy equations are singular.

ENRCN2

"* * * ENRCN2 * * * CONVERGENCE FAILURE. L,HTOT(L),TLAY(L) = () () ()"
[Immediate termination]
Failure to determine new layer temperature after energy update.

FILM

"* * * FILM * * * CONVERGENCE FAILURE. JBODY,LYR,EMDO,EMD = () () () ()"
[Immediate termination]
Failure to determine consistent film properties (heat transfer coefficient and gas generation).

Table 4.2 CORCON-generated warning and error messages for each subroutine (continued)

HTRCLN

"* * * HTRCLN * * * CONVERGENCE FAILURE"
[Immediate termination]
Failure to determine radiative contribution to the boiling heat transfer.

"* * * HTRCLN * * * NCL = ()"
[Immediate termination]
Invalid coolant. Can only occur if the code has been modified incorrectly.

HTRLAY

"* * * HTRLAY * * * MATRIX AMTRX IS SINGULAR AS DETECTED BY SAXB"
[Immediate termination]

"* * * HTRLAY * * * AXIAL CONVERGENCE FAILURE. L,KOUNT,LOOPL,LOOPT = () () () ()"
[Warning only]
Failure to determine state of layer consistent with boundary conditions. Has only been observed for vanishingly thin liquid sublayers, and usually in early iterations of INTEMP (so that the result does not affect the end-of-timestep results). Code continues, using conductive heat transfer for layer.

"* * * HTRLAY * * * AXIAL SOLID CORE/LIQUID SURFACE
WITH L,TS,TB,TL,TT = () () () () ()"
[Warning only]
Solid layer is being melted from the top and bottom. Has only been observed in early iterations of INTEMP (so that the result does not affect the end-of-timestep results). Code continues, using convective heat transfer to the solidus temperature.

"* * * HTRLAY * * * RADIAL CONVERGENCE FAILURE. L,KOUNT,LOOPL,LOOPT = () () () ()"
[Warning only]
Failure to determine state of layer consistent with boundary conditions.

"* * * HTRLAY * * *, RADIAL SOLID CORE/LIQUID SURFACE
WITH L,TS,TLTR = () () () ()"
[Immediate termination]
Solid layer being melted from outside.

INCOOL

"* * * INCOOL * * * COOLANT () NOT IN MASTER LIST"
[Deferred termination]

Table 4.2 CORCON-generated warning and error messages for each subroutine (continued)

INGEOM

"* * * INGEOM * * * NRAYS = (), GREATER THAN LIMIT OF 100"
[Immediate termination]

"* * * INGEOM * * * RO = (). MUST BE 0.0"
[Immediate termination]

INITL

"* * * INITL * * * INVALID ILYR = ()"
[Deferred termination]

INPCON

"* * * INPCON * * * OXIDE () NOT IN MASTER LIST"
[Deferred termination]

"* * * INPCON * * * METAL () NOT IN MASTER LIST"
[Deferred termination]

INPGAS

"* * * INPGAS * * * GAS () NOT IN MASTER LIST"
[Deferred termination]

"* * * INPGAS * * * INTERPOLATION FOR ATMOSPHERIC
PRESSURE AT () OFF LOW END OF TABLE ()"
[Warning only]

"* * * INPGAS * * * INTERPOLATION FOR ATMOSPHERIC
PRESSURE AT () OFF HIGH END OF TABLE ()"
[Warning only]

INTEMP

"* * * INTEMP * * * MATRIX AMTRX IS SINGULAR AS DETECTED BY SAXB"
[Immediate termination]
The equations for determining interface temperatures are singular.

Table 4.2 CORCON-generated warning and error messages for each subroutine (continued)

"* * * INTEMP * * * CONVERGENCE FAILURE"
[Warning only]
Newton iteration to determine interface temperatures failed to converge in 20 iterations.

LEVSWL

"* * * LEVSWL * * * FIRST OCCUPIED LAYER .GT. ()"
[Immediate termination]
Can only occur if the code has been modified incorrectly.

"* * * LEVSWL * * * CAVITY TOO SMALL FOR MELT"
[Immediate termination]
Need to specify a larger cavity (remember level swell).

MASRAT

"* * * MASRAT * * * FIRST OCCUPIED LAYER .GT. ()"
[Immediate termination]

"* * * MASRAT * * * CONVERGENCE FAILURE"
[Immediate termination]
Failure to match film heat transfer results to pool heat transfer at the bottom of the pool.

MASSEX

"* * * MASSEX * * * ICALL = ()"
[Immediate termination]
Invalid call to MASSEX. Can only occur if the code has been modified incorrectly.

MELTRD

"* * * MELTRD * * * NORAD = ()"
[Immediate termination]
The number of entries in the time-radius table is greater than the maximum allowed number (MAXRAD).

"* * * MELTRD * * * RADTIM() = () IS NEGATIVE."
[Immediate termination]

"* * * MELTRD * * * TIMRAD() = () IS NEGATIVE."
[Immediate termination]

Table 4.2 CORCON-generated warning and error messages for each subroutine (continued)

"* * * MELTRD * * * TIMRAD() > TIMRAD()"
[Immediate termination]
The entries in the time table must be increasing with time.

"* * * MELTRD * * * RADTIM() > RADTIM()"
[Immediate termination]
The entries in the radius table must be increasing with time.

"* * * MELTRD * * * TOO FEW ENTRIES IN TIME-RADIUS
TABLE. EXECUTION TERMINATED."
[Immediate termination]

MHTRAN

"* * * MHTRAN * * * MASS IN LAYER ()"
[Immediate termination]
Can only occur if the code has been modified incorrectly.

MLTPRP

"* * * MLTPRP * * * MASS IN LAYER ()"
[Immediate termination]
Can only occur if the code has been modified incorrectly.

MLTREA

"* * * MLTREA * * * REDOING SOLUTION FROM NEW STARTING GUESS"
The equations for determining the next correction to the equilibrium composition are singular or failed to converge. A new starting guess will usually avoid the problem region.

"* * * MLTREA * * * MATRIX AK IS SINGULAR IN FIRST CALL TO SAXB"
[Immediate termination]
The equations for determining the next correction to the equilibrium composition are singular despite a new starting guess.

"* * * MLTREA * * * APPARENT CONVERGENCE FAILURE
RELATIVE ERROR IN TOTAL MASS = ()"
[Warning only]
Failure of the chemical equilibrium routine. "Apparent" because error is often insignificant, although the code fails to recognize this. Check to verify that no serious violation of mass conservation has occurred.

Table 4.2 CORCON-generated warning and error messages for each subroutine (continued)

PLLAYR

"* * * PLLAYR * * * MASS IN LAYER ()"
[Immediate termination]
Can only occur if the code has been modified incorrectly.

PRTGAS

"INVALID IRE = () IN PRTGAS"
[Immediate termination]
Can only occur if the code has been modified incorrectly.

REACT

"* * * REACT * * * IMPROPER REACTION NUMBER = ()"
[Immediate termination]
Can only occur if the code has been modified incorrectly.

SOLLIQ

"* * * SOLLIQ * * * NSPL, NSPU = () ()"
[Immediate termination]
Invalid value for NSPL or NSPU. Can only occur if the code has been modified incorrectly.

SPHCYL

"* * * SPHCYL * * * IGEOM = 3 NOT OPERATIONAL"
[Immediate termination]

SURFEB

"* * * SURFEB * * * CONVERGENCE FAILURE.
ICOUNT,TTA,QP,DQPDTA,QW,DQWDTA = () () () () () ()"
[Immediate termination]
Failure to match film heat transfer results to the pool heat transfer.

Table 4.2 CORCON-generated warning and error messages for each subroutine (continued)

SVLAAR

"* * * SVLAAR * * * CONVERGENCE FAILURE"
[Immediate termination]
Failure to determine liquidus and solidus temperatures for oxidic mixture.

TMPFND

"* * * TMPFND * * * MASS IN LAYER ()"
[Immediate termination]
Can only occur if the code has been modified incorrectly.

VISCTY

"* * * VISCTY * * * NSPL,NSPU = () ()"
[Immediate termination]
Invalid value for NSPL or NSPU. Can only occur if the code has been modified incorrectly.

5.0 Coding Information

5.1 Descriptions of Subroutines

Subroutines developed specifically for CORCON are listed in Table 5.1 with brief descriptions of the functions they perform. Also included are routines such as SAXB which are used by CORCON but were not developed specifically for CORCON.

Also provided is a variety of coding information that may assist the user in understanding the function of the various subroutines in the code and the overall program flow. Table 5.2 is a list of subroutines called by each routine. Table 5.3 is a list of program routines which call each subroutine.

5.2 Use of Common

Most of the internal data in CORCON-Mod3 are contained in and communicated through named COMMON blocks. To assist the user in understanding the flow of information between subroutines, we provide Tables 5.4, 5.5, and 5.6. Table 5.4 lists the COMMON blocks contained in each program segment. Table 5.5 lists the program segments containing each COMMON block. A list of the program variables in each COMMON block is given in Table 5.6; the variables are defined in the next section.

5.3 Descriptions of Principal Variables

Table 5.7 provides a dictionary of the principal FORTRAN variables used in CORCON-Mod3. For arrays shown in the table, the different array elements may correspond to different layers, to different chemical species, etc. This is indicated by the index used, as follows:

- I - species
- J - body point
- K - element
- L - layer or layer interface
- M - temperature
- N - time

Interface L is the interface between layer L and layer L-1.

Table 5.1 List of CORCON subroutines

ABLATE	-	Computes mass flow rate of each species in surroundings material as it ablates and falls into pool
ACTMET	-	Computes the activity coefficients for metal phase constituents
ACTOXD	-	Computes the activity coefficients for oxide phase constituents
ADDLYR	-	Combines two layers into a third layer
AERPTL	-	Determines aerosol particle size, mass concentration, and evolution rate.
ANGAVL	-	Finds body angle at each ray (body) point
ARBINP	-	Initializes an arbitrary cavity shape
ATMPRO	-	Determines bulk properties of the gas mixture (atmosphere) above the molten pool
ATMSUR	-	Updates atmosphere and surroundings, or serves as an interface to a containment response code
BARRAY	-	Contains parametric values for fits to the free-energy functions
BCLTOV	-	Groups fission product elements and converts masses from g-mol to kg
BLKDTA	-	Contains data tables, including master species list, master molecular weight list, stoichiometric coefficients and phase table for MLTREA, and various pointers and global constants
BUBBLE	-	Determines bubble sizes and velocities where gas enters the pool and within pool layers
CHEKCV	-	Computes the critical volume of coolant needed to cover the melt when the time-dependent melt radius option is used
CHEKHT	-	Checks for valid melt thickness when the time-dependent melt radius option is used
CHEMPO	-	Computes enthalpy, entropy, and Gibbs free energy of each species required for the melt/gas chemical reaction calculation in MLTREA
COMBIN	-	Adds one mixture to another to produce a single mixture mass, composition, and enthalpy
COMBN2	-	Combines the mass and enthalpy of two layers to form a new layer.
CONFND	-	Initializes data tables and finds coefficients for specific heat, enthalpy, and entropy for a species as necessary for calculations in CHEMPO or CPENTH
CONPRP	-	Initializes concrete composition and properties
CORCON	-	Controls program flow
CPENTH	-	Computes specific heat and enthalpy of condensed melt phases for both single- and two-phase (liquid-solid) mixtures
CREATE	-	Creates separated layers if a mixture layer has lost a phase due to deentrainment
CVFAC	-	Translates CORCON variables into VANESA variables

Table 5.1 List of CORCON subroutines (continued)

CYLIND	-	Initializes a flat-base cylindrical cavity shape
DATAIN	-	Handles the input of data for the program
DCOEFF	-	Calculates drag coefficients for stable droplets in the melt
DCYINT	-	Sets up the initial intact core inventory of radioactive species and associated retention factors, and initializes decay product pseudo-species
DCYPOW	-	Evaluates the decay power of each radioactive element as a function of time
DENSTY	-	Computes the density of the condensed phases in the pool (the metallic and oxidic melt mixtures and coolant
DENTRN	-	Calculates the deentrainment (settling) of suspended liquid droplets
DF	-	Calculates the aerosol mass gradient in the pool
DHGEN	-	Computes the decay heat generated within each pool layer
EDIT	-	Manages the printed output of the code
EMISIV	-	Determines the emissivities of the condensed phases of the condensed phases of the pool from input tables of emissivity vs time or temperature
ENRCN1	-	Performs the explicit update of the layer energy equations, including boiling of the coolant, and sets up the implicit terms
ENRCN2	-	Finishes the update of the layer energy equations by adding the implicit terms, and calculates new layer temperatures
ENTRN	-	Calculates bubble-drive entrainment of a heavy fluid by a less dense fluid
EXPRNT	-	Controls the generation of extra debug printed output
FAIL	-	Performs error handling when called by a subroutine which detects abnormal data or an invalid computation
FDZ	-	Calculates exp(z) for SRPP
FIIRAD	-	Finds the index of the body point closest to the edge of the melt
FILM	-	Advances the state of the gas film from one point to another and integrates results
FPUPD	-	Updates the fission product composition of each group given the initial composition and changes in composition due to mass addition or fission product release
GEOM	-	Determines the volume, surface area, and stream length of the concrete cavity as a function of body point
GFLMPR	-	Computes the average gas mixture properties in the gas film at each body point

Table 5.1 List of CORCON subroutines (continued)

HCBBOT	-	Calculates the bubble-enhanced liquid-liquid heat transfer coefficient at the bottom of a layer
HCBINJ	-	Calculates the heat transfer coefficient for bubble injection at the bottom of the pool
HCBSID	-	Calculates the bubble-enhanced heat transfer coefficient at the side of the pool
HCBTOP	-	Calculates the bubble-enhanced liquid-liquid heat transfer coefficient at the top of a layer
HSPCYL	-	Initializes a cylindrical cavity with a hemispherical bottom
HTRCLN	-	Evaluates heat transfer in the coolant layer, including boiling
HTRLAY	-	Evaluates heat transfer in a layer, including conduction in solid regions
HTRLIQ	-	Computes heat transfer coefficients in a liquid layer or sub-layer, including bubble-enhanced convection, natural convection, and conduction
HTRN	-	Computes gas film heat transfer coefficients in all regimes
INCOOL	-	Inputs the initial mass, temperature, and identity of the coolant
INGEOM	-	Inputs and defines the initial geometry of the concrete crucible
INITL	-	Initializes necessary variables before entering the main computational loop
INPCON	-	Inputs initial masses of core constituents and their temperatures
INPGAS	-	Inputs and defines the initial composition and state of the atmosphere
INTEMP	-	Computes temperatures and heat flows at layer interfaces
INVERF	-	Computes the inverse of the error function
LEVSWL	-	Calculates pool level swell, layer interface locations, and layer average void fractions
LININT	-	Performs linear interpolation or extrapolation from tables
LOSSES	-	Calculates aerosol losses by vaporization
MASLOS	-	Computes mass loss from the melt due to volatilization of fission products
MASRAT	-	Determines concrete ablation rates (mass loss rates) at body points
MASSEX	-	Serves as an interface for mass exchange with atmosphere and surroundings
MECLOS	-	Computes aerosol losses by mechanical processes
MELTRD	-	Input data for the time-dependent melt radius
MHTRAN	-	Updates layer species masses and evaluates effects of mass transport and chemical reactions on layer enthalpies

Table 5.1 List of CORCON subroutines (continued)

MLTPRP	-	Determines transport properties of metallic and oxide phases of the melt
MLTREA	-	Solves the problem of chemical equilibrium iteratively by a constrained first-order steepest descent technique, to minimize the free energy
ORIENT	-	Changes the layer configuration if density differences warrant a change
PAGEHD	-	Prints a page header with code version identification and the problem title
PHSPRP	-	Determines layer phase properties for aerosol calculations
PLLAYR	-	Calculates layer densities and determines need for reorientation of layers
PLOTS	-	Writes data files for a post-processor plotting program
POOLV	-	Integrates aerosol losses in the pool and determines aerosol size distribution
PRTGAS	-	Prints results from the metal/gas/oxide reactions
QMELT	-	Evaluates the local heat flux on the pool side of the gas film
REACT	-	Sets up necessary reactants for MLTREA and distributes the products returned
RECEDE	-	Computes the concrete normal recession and relocation of body points during a timestep
RFBS	-	Module of the equation solver SAXB
RLUD	-	Module of the equation solver SAXB
SATP	-	Evaluates saturation pressure as a function of temperature
SATT	-	Evaluates saturation temperature as a function of pressure (an ENTRY in SATP)
SAXB	-	Solves a system of real linear algebraic equations AX = B (a Sandia Mathematical Library routine)
SETTL	-	Calculates the drag coefficients for stable and unstable drops in deentrainment
SETUP	-	Performs code set up requiring execution (as opposed to DATA statements) including the evaluation of machine round off
SIGMY	-	Computes surface tensions of the condensed phases of the pool
SOLLIQ	-	Sets up the components of pseudo-mixtures of oxides or metals and calls either SSMELT or SVLAAR to calculate the mixture solidus and liquidus temperatures
SOURCE	-	Evaluates the decay heat source in the pool
SPHCYL	-	Initializes a cylindrical cavity with a spherical-segment bottom
SRPP	-	Calculates the equilibrium partial pressures of vapor species

Table 5.1 List of CORCON subroutines (continued)

SSMELT	-	Calculates the liquidus and solidus temperatures of a metallic phase based on stainless steel (Cr-Fe-Ni ternary)
SUBSIZ	-	Sections the aerosol size distribution and calculates the size range and characteristic size
SURFEB	-	Performs a surface energy balance at a point on the cavity surface to determine mass flux of ablated concrete at a point
SVLAAR	-	Performs a Schroeder-von Laar pseudo-binary construction of the liquidus and solidus temperatures of an oxidic phase
THKOND	-	Determines the thermal conductivity of the condensed phases in the pool
TIMSTP	-	Determines the new timestep
TMPFND	-	Determines the mixture temperature, given the composition and enthalpy
TMPSET	-	Initializes temperatures for newly-created layers
TRADII	-	Determines the time-dependent melt radius from a linear interpolation within the input table
UCOEFF	-	Calculates the droplet drag coefficient for an unstable drop
UDU	-	Module of equation solver SAXB
UNDEFN	-	Sets layer temperatures and property values to zero when a layer disappears following an orientation change
VANESA	-	Controls the aerosol calculations
VANFP	-	Calculates the fission product content of the melt for use in aerosol calculations
VBUBL	-	Calculates bubble properties for use in aerosol calculations
VCFAC	-	Prepares the VANESA aerosol calculations for use in CORCON
VIS2PH	-	Computes the Kunitz two-phase viscosity multiplier for suspended solids in the melt
VISCTY	-	Computes the viscosity of the metallic and oxidic phases of the melt
VOUTP	-	Prints VANESA aerosol calculation output to the output file
VSCRIT	-	Computes the critical superficial gas velocities into the pool for use in determining bubble sizes
XNDAR	-	Initializes species molecular weights, and densities for condensed species

Table 5.2 Subroutines called by each program routine

ABLATE	calls	LININT	FAIL					
ACTMET	calls							
ACTOXD	calls							
ADDLYR	calls	COMBIN	COMBN2	DENSTY	FAIL	SOLLIQ	TMPFND	UNDEFN
AERPTL	calls							
AERPTL	calls	AERSOL	LOSSES					
ANGAVL	calls							
ARBINP	calls							
ATMPRO	calls	LININT	FAIL					
ATMSUR	calls	ATMPRO	EMISIV	EXPRNT	FAIL	LININT		
BARRAY	calls							
BCLTOV	calls							
BLKDTA	calls							
BUBBLE	calls	VSCRIT						
CHEKCV	calls	FAIL						
CHEKHT	calls							
CHEMPO	calls	CONFND						
COMBIN	calls							
COMBN2	calls							
CONFND	calls	FAIL						
CONPRP	calls	CPENTH	DENSTY	FAIL	SOLLIQ			
CORCON	calls	ATMSUR	DATAIN	EDIT	ENRCN1	ENRCN2	GFLMPR	INTEMP
		INITL	LEVSWL	MASRAT	MHTRAN	MLTPRP	PLLAYR	PLOTEX
		PLOTIN	PLOTS	RECEDE	SETUP	SOURCE	TIMSTP	
CPENTH	calls	CONFND	FAIL					
CREATE	calls	ADDLYR	CPENTH	FAIL	SOLLIQ	TMPSET	UNDEFN	
CVFAC	calls							

Table 5.2 Subroutines called by each program routine (continued)

CYLIND	calls	FAIL						
D1MACH	calls							
DATAIN	calls	BCLTOV MELTRD	CONPRP	FAIL	INCOOL	INGEOM	INPCON	INPGAS
DCOEFF	calls							
DCSEVL	calls							
DCYINT	calls	DCYPOW	FAIL	VANFP				
DCYPOW	calls							
DENSTY	calls							
DENTRN	calls	SETTL						
DERF	calls	D1MACH	DCSEVL	DERFC	INITDS			
DERFC	calls	D1MACH	DCSEVL	INITDS				
DF	calls							
DFDZ	calls							
DHGEN	calls	DCYPOW	FAIL	LININT				
EDIT	calls	PAGEHD	PRTGAS	VOUTP				
EMISIV	calls	FAIL	LININT					
ENRCN1	calls	CHEKCV SOLLIQ	CPENTH	EXPRNT	FAIL	MASSEX	SATT	SAXB
ENRCN2	calls	EXPRNT	FAIL	TMPFND				
ENTRN	calls							
EXPRNT	calls							
FAIL	calls							
FDZ	calls							
FIIRAD	calls	EDIT						
FILM	calls	FAIL	HTRN	SURFEB				
FPUPD	calls							

Table 5.2 Subroutines called by each program routine (continued)

GEOM	calls	ANGAVL					
GFLMPR	calls						
HCBBOT	calls						
HCBINJ	calls						
HCBSID	calls						
HCBTOP	calls						
HSPCYL	calls						
HTRCLN	calls	EXPRNT	FAIL	HTRLIQ			
HTRLAY	calls	EXPRNT	FAIL	HTRLIQ	SAXB		
HTRLIQ	calls	HCBBOT	HCBINJ	HCBTOP			
HTRN	calls						
INCOOL	calls	FAIL					
INGEOM	calls	ARBINP	CYLIND	FAIL	GEOM	HSPCYL	SPHCYL
INITDS	calls						
INITL	calls	ATMSUR	CPENTH	DENSTY	FAIL	SOLLIQ	
INPCON	calls	DCYINT	FAIL				
INPGAS	calls	FAIL	LININT				
INTEMP	calls	EXPRNT	FAIL	FILM	HTRCLN	HTRLAY	SAXB
INVERF	calls	DERF					
LEVSWL	calls	BUBBLE	CHEKCV	EXPRNT	FAIL	TRADII	
LININT	calls						
LOSSES	calls	MECLOS					
MASLOS	calls	CPENTH					
MASRAT	calls	CPENTH	EXPRNT	FAIL	FILM		
MASSEX	calls	CPENTH	FAIL	FPUPD	LININT	SOLLIQ	

Table 5.2 Subroutines called by each program routine (continued)

MECLOS	calls							
MELTRD	calls	FAIL						
MHTRAN	calls	BUBBLE FAIL	COMBIN MASLOS	CPENTH MASSEX	CVFAC POOLV	DENTRN REACT	ENTRN SOLLIQ	EXPRNT VANESA
MLTPRP	calls	CPENTH VISCTY	EMISIV VIS2PH	EXPRNT	FAIL	SATT	SIGMY	THKOND
MLTREA	calls	CHEMPO	EXPRNT	FAIL	PRTGAS	SAXB		
ORIENT	calls	ADDLYR						
PAGEHD	calls							
PHSPRP	calls							
PLLAYR	calls	CREATE	DENSTY	EXPRNT	FAIL	ORIENT		
PLOTS	calls							
POOLV	calls	DF	INVERF	SUBSIZ				
PRTGAS	calls	FAIL	PAGEHD					
QMELT	calls							
REACT	calls	CPENTH	EXPRNT	FAIL	MLTREA	SOLLIQ		
RECEDE	calls	GEOM						
RFBS	calls	FAIL						
RLUD	calls	FAIL						
SATP	calls							
SATT	calls							
SAXB	calls	FAIL	RFBS	RLUD	UDU			
SETTL	calls	DCOEFF	UCOEFF					
SETUP	calls	CONFND						
SIGMY	calls							
SOLLIQ	calls	FAIL	SSMELT	SVLAAR				

Table 5.2 Subroutines called by each program routine (continued)

SOURCE	calls	DHGEN				
SPHCYL	calls	FAIL				
SRPP	calls	FDZ				
SSMELT	calls					
SUBSIZ	calls	DERF				
SURFEB	calls	FAIL	QMELT			
SVLAAR	calls	FAIL				
THKOND	calls					
TIMSTP	calls	EXPRNT				
TMPFND	calls	CPENTH	FAIL	SOLLIQ		
TMPSET	calls					
TRADII	calls	CHEKCV	CHEKHT	FIIRAD		
UCOEFF	calls					
UDU	calls					
UNDEFN	calls					
VANESA	calls	AERSOL	PHSPRP	SRPP	VBUBL	VCFAC
VANFP	calls					
VBUBL	calls					
VCFAC	calls	FPUPD				
VIS2PH	calls					
VISCTY	calls	FAIL				
VOUTP	calls	PAGEHD				
VSCRIT	calls					
XNDAR	calls					

Table 5.3 Program routines which call each routine

ABLATE	is called by	
ACTMET	is called by	VANESA
ACTOXD	is called by	VANESA
ADDLYR	is called by	CREATE ORIENT
AERPTL	is called by	AERSOL
AERSOL	is called by	VANESA
ANGAVL	is called by	GEOM
ARBINP	is called by	INGEOM
ATMPRO	is called by	ATMSUR
ATMSUR	is called by	CORCON INITL
BARRAY	is called by	
BCLTOV	is called by	DATAIN
BLKDTA	is called by	
BUBBLE	is called by	LEVSWL MHTRAN
CHEKCV	is called by	ENRCN1 LEVSWL TRADII
CHEKHT	is called by	TRADII
CHEMPO	is called by	MLTREA
COMBIN	is called by	ADDLYR MHTRAN
COMBN2	is called by	ADDLYR
CONFND	is called by	CHEMPO CPENTH SETUP
CONPRP	is called by	DATAIN
CORCON	is called by	
CPENTH	is called by	CONPRP CREATE ENRCN1 INITL MASLOS MASRAT MASSEX MHTRAN MLTPRP REACT TMPFND
CREATE	is called by	PLLAYR
CVFAC	is called by	MHTRAN
CYLIND	is called by	INGEOM

Table 5.3 Program routines which call each routine (continued)

D1MACH	is called by	DERF	DERFC				
DATAIN	is called by	CORCON					
DCOEFF	is called by	SETTL					
DCSEVL	is called by	DERF	DERFC				
DCYINT	is called by	INPCON					
DCYPOW	is called by	DCYINT	DHGEN				
DENSTY	is called by	ADDLYR	CONPRP	INITL	PLLAYR		
DENTRN	is called by	MHTRAN					
DERF	is called by	INVERF	SUBSIZ				
DERFC	is called by	DERF					
DF	is called by	POOLV					
DFDZ	is called by						
DHGEN	is called by	SOURCE					
EDIT	is called by	CORCON	FIIRAD				
EMISIV	is called by	ATMSUR	MLTPRP				
ENRCN1	is called by	CORCON					
ENRCN2	is called by	CORCON					
ENTRN	is called by	MHTRAN					
EXPRNT	is called by	ATMSUR	ENRCN1	ENRCN2	HTRCLN	HTRLAY	INTEMP	LEVSWL
		MASRAT	MHTRAN	MLTPRP	PLLAYR	REACT	TIMSTP	
FAIL	is called by	ABLATE	ADDLYR	ATMPRO	ATMSUR	CHEKCV	CONFND	CONPRP
		CPENTH	CREATE	CYLIND	DATAIN	DCYINT	DHGEN	EMISIV
		ENRCN1	ENRCN2	FILM	HTRCLN	HTRLAY	INCOOL	INGEOM
		INITL	INPCON	INPGAS	INTEMP	LEVSWL	MASRAT	MASSEX
		MELTRD	MHTRAN	MLTPRP	MLTREA	PLLAYR	PRTGAS	REACT
		RFBS	RLUD	SAXB	SOLLIQ	SPHCYL	SURFEB	SVLAAR
		TMPFND	VISCTY					
FDZ	is called by	SRPP						
FIIRAD	is called by	TRADII						
FILM	is called by	INTEMP	MASRAT					

Table 5.3 Program routines which call each routine (continued)

FPUPD	is called by	MASSEX	VCFAC					
GEOM	is called by	INGEOM	RECEDE					
GFLMPR	is called by	CORCON						
HCBBOT	is called by	HTRLIQ						
HCBINJ	is called by	HTRLIQ						
HCBSID	is called by							
HCBTOP	is called by	HTRLIQ						
HSPCYL	is called by	INGEOM						
HTRCLN	is called by	INTEMP						
HTRLAY	is called by	INTEMP						
HTRLIQ	is called by	HTRCLN	HTRLAY					
HTRN	is called by	FILM						
INCOOL	is called by	DATAIN						
INGEOM	is called by	DATAIN						
INITDS	is called by	DERF	DERFC					
INITL	is called by	CORCON						
INPCON	is called by	DATAIN						
INPGAS	is called by	DATAIN						
INTEMP	is called by	CORCON						
INVERF	is called by	POOLV						
LEVSWL	is called by	CORCON						
LININT	is called by	ABLATE	ATMPRO	ATMSUR	DHGEN	EMISIV	INPGAS	MASSEX
LOSSES	is called by	AERSOL						
MASLOS	is called by	MHTRAN						
MASRAT	is called by	CORCON						

Table 5.3 Program routines which call each routine (continued)

MASSEX	is called by	ENRCN1	MHTRAN					
MECLOS	is called by	LOSSES						
MELTRD	is called by	DATAIN						
MHTRAN	is called by	CORCON						
MLTPRP	is called by	CORCON						
MLTREA	is called by	REACT						
ORIENT	is called by	PLLAYR						
PAGEHD	is called by	EDIT	PRTGAS	VOUTP				
PHSPRP	is called by	VANESA						
PLLAYR	is called by	CORCON						
PLOTS	is called by	CORCON						
POOLV	is called by	MHTRAN						
PRTGAS	is called by	EDIT	MLTREA					
QMELT	is called by	SURFEB						
REACT	is called by	MHTRAN						
RECEDE	is called by	CORCON						
RFBS	is called by	SAXB						
RLUD	is called by	SAXB						
SATP	is called by							
SATT	is called by	ENRCN1	MLTPRP					
SAXB	is called by	ENRCN1	HTRLAY	INTEMP	MLTREA			
SETTL	is called by	DENTRN						
SETUP	is called by	CORCON						
SIGMY	is called by	MLTPRP						
SOLLIQ	is called by	ADDLYR	CONPRP	CREATE	ENRCN1	INITL	MASSEX	MHTRAN
		REACT	TMPFND					

Table 5.3 Program routines which call each routine (continued)

SOURCE	is called by	CORCON		
SPHCYL	is called by	INGEOM		
SRPP	is called by	VANESA		
SSMELT	is called by	SOLLIQ		
SUBSIZ	is called by	POOLV		
SURFEB	is called by	FILM		
SVLAAR	is called by	SOLLIQ		
THKOND	is called by	MLTPRP		
TIMSTP	is called by	CORCON		
TMPFND	is called by	ADDLYR	CREATE	ENRCN2
TMPSET	is called by	ADDLYR	CREATE	
TRADII	is called by	LEVSWL		
UCOEFF	is called by	SETTL		
UDU	is called by	SAXB		
UNDEFN	is called by	ADDLYR	CREATE	
VANESA	is called by	MHTRAN		
VANFP	is called by	DCYINT		
VBUBL	is called by	VANESA		
VCFAC	is called by	VANESA		
VIS2PH	is called by	MLTPRP		
VISCTY	is called by	MLTPRP		
VOUTP	is called by	EDIT		
VSCRIT	is called by	BUBBLE		
XNDAR	is called by			

Table 5.4 COMMON blocks contained by each program routine

ABLATE	contains	A42	TWO	MASTER				
ACTMET	contains	ACTIV						
ACTOXD	contains	ACTIV						
ADDLYR	contains	A45 TWO	B0	B1	B2	B8	MASTER	MX
AERPTL	contains	BCL	CNDCON	CTOV	VAN	VANPRP	VPL	XND
AERSOL	contains	BCL	CTOV	VAN	VANPRP	XND		
ANGAVL	contains	A3	ONE	TWNEIT	CNSTNT			
ARBINP	contains	A3	ONE	TWNEIT				
ATMPRO	contains	A21	TWO	ATMDAT				
ATMSUR	contains	HEATEX A20	ATMDAT A23	B0 VAN	B1 CTOV	TWO	CNSTNT	A4
BCLTOV	contains	COMP	XND	BCL	A31			
BUBBLE	contains	A32	B0	B1	B3	TWNTWO	CNSTNT	
CHEKCV	contains	A3 MRCI	B0	B1	CNSTNT	ONE	TWO	MRCR
CHEKHT	contains	B1	CNSTNT	MRCR	MRCI			
CHEMPO	contains	PFDAT						
COMBIN	contains							
COMBN2	contains							
CONFND	contains	MASTER						
CONPRP	contains	CNDCON	A32	B3	MASTER	SPECNM		
CORCON	contains	B4	ONE	TWO				
CPENTH	contains	MASTER						
CREATE	contains	A45	B0	B1	B2	MASTER	MX	TWO
CVFAC	contains	ARGLST MASTER MX	TWO BCL VAN	B0 CTOV VANPRP	B1 CTOP	B2 VTOC	B6 CNDCON	B6A
CYLIND	contains	A3	ONE	FORTN	TWNEIT	CNSTNT		

Table 5.4 COMMON blocks contained by each program routine (continued)

D1MACH	contains							
DATAIN	contains	A43	B6	A4	A9	A17	A19	A20
		A23	A42	B1	ONE	TWO	THREE	
		SPECNM	TITLE	CNDCON	CTOV	CTOP	COMP	XND
		VAN	BCL	CDF	VPL	MRCR	MRCI	
DCOEFF	contains							
DCSEVL	contains							
DCYINT	contains	B6A	B6B	A31	B6	TWO	MASTER	SPECNM
DCYPOW	contains	B6						
DENSTY	contains	MASTER						
DENTRN	contains	B0	B1	CNSTNT	MX	TWO		
DERF	contains							
DERFC	contains							
DF	contains	CDF						
DFDZ	contains							
DHGEN	contains	A4	A17	B0	B1	B2	B6	MASTER
EDIT	contains	A3	A4	A32	A39	A44	A45	B0
		B1	B2	B5	B8	B9	ONE	
		TWO	THREE	FOUR	TWNTWO	GASEDT	MASTER	CNSTNT
		CONSRV	SPECNM	MRCR	MRCI	MX		
EMISIV	contains	TWO	A19	A20	B9	MASTER		
ENRCN1	contains	HEATEX	A4	B0	B1	B2	B5	B7
		B9	TWO	MASTER	IMP	CONSRV	MX	
		MRCR	MRCI					
ENRCN2	contains	HEATEX	B0	B1	IMP	CONSRV		
ENTRN	contains	B0	B1	CNSTNT	MX			
EXPRNT	contains	ONE	TWO					
FAIL	contains	ONE	TWO	B4				
FDZ	contains							
FIIRAD	contains	A3	ONE	TWNEIT	MRCR	MRCI		

Table 5.4 COMMON blocks contained by each program routine (continued)

FILM	contains	ARGLST	A4	A32	B1	CNSTNT		
FPUPD	contains	MASTER	B6	B6A	B6B			
GEOM	contains	A3	ONE	FOUR	FORTN	TWNEIT	CNSTNT	
GFLMPR	contains	A32	A39	ONE				
HCBBOT	contains	B1	CNSTNT					
HCBINJ	contains	B1	CNSTNT					
HCBSID	contains	B1	CNSTNT					
HCBTOP	contains	B0	B1	CNSTNT				
HSPCYL	contains	A3	ONE	FOUR	FORTN	TWNEIT	CNSTNT	
HTRCLN	contains	B0 MRCI	B1	B5	B8	B9	CNSTNT	MRCR
HTRLAY	contains	B1	B5	B8	TWO	CNSTNT	MRCR	MRCI
HTRLIQ	contains	B0	B1	CNSTNT				
HTRN	contains	MX B1	A4 CNSTNT	A32	B0	B5	B8	A39
INCOOL	contains	B9						
INGEOM	contains	ONE	FORTN	CNSTNT				
INITDS	contains							
INITL	contains	HEATEX B0 B9 MX	A3 B1 ONE MRCR	A4 B2 TWNTWO MRCI	A10 B3 GASEDT	A31 B5 CNSTNT	A32 B8 CONSRV	A45 MASTER
INPCON	contains	A4	A10	A31	B6	MASTER	SPECNM	
INPGAS	contains	A10	A21	A31	MASTER	SPECNM	TWO	
INTEMP	contains	HEATEX B8	ARGLST TWO	A3 CNSTNT	A32 A4	B0 MRCR	B1 MRCI	B5
INVERF	contains							

Table 5.4 COMMON blocks contained by each program routine (continued)

LEVSWL	contains	A3	A32	A44	B0	B1	B3	ONE
		TWNTWO		TWNEIT	CNSTNT	A4	TWO	MRCR
		MRCI						
LININT	contains							
LOSSES	contains	BCL	CTOV					
MASLOS	contains	B0	B1	B2	B6	TWO	CONSRV	MASTER
		CTOV	VTOC					
MASRAT	contains	ARGLST	A3	A32	CNSTNT	MASTER	B0	B1
		B3	B5	TWO	TWNTWO	TWNEIT	ONE	
		MRCR	MRCI					
MASSEX	contains	B6A	B0	B1	B2	B7	B9	MASTER
		CONSRV	A31	B6	A42	A43	TWO	
		A4						
MECLOS	contains	BCL	CTOV	VAN	VANPRP	XND		
MELTRD	contains	A3	A4	B0	B1	CNSTNT	ONE	TWNEIT
		TWO	MRCR	MRCI				
MHTRAN	contains	A4	A32	B0	B1	B2	B3	B7
		B8	MASTER	CONSRV	TWO	MX	CTOV	
		VAN						
MLTPRP	contains	B0	B1	B2	B8	MASTER	B9	MX
MLTREA	contains	A4	PFDAT	RNDOFF				
ORIENT	contains	A4	B0	B1	MX	MASTER		
PAGEHD	contains	ONE	TWO	TITLE				
PHSPRP	contains	BCL	VANPRP	XND				
PLLAYR	contains	A45	B0	B1	B2	B8	B9	TWO
		MASTER	MX	A4				
PLOTS	contains	A32	B8	A3	A4	B0	B1	B2
		ONE	TWO	CNSTNT	MASTER	MRCR	MRCI	
POOLV	contains	CDF	POOL	CTOP	VPL			
PRTGAS	contains	A4	A45	PFDAT	MASTER	SPECNM		
QMELT	contains	B1	B5	B8				

Table 5.4 COMMON blocks contained by each program routine (continued)

REACT	contains	A4 GASEDT	A45 ONE	TWO PFDAT	B0 MASTER	B1 CONSRV	B2 MX	B7
RECEDE	contains	A3	ONE	TWO	FOUR	TWNEIT		
RFBS	contains							
RLUD	contains							
SATP	contains							
SAXB	contains							
SETTL	contains	CNSTNT						
SETUP	contains	CNSTNT	RNDOFF					
SIGMY	contains							
SOLLIQ	contains	A32	B9	MASTER				
SOURCE	contains	B0	B1	TWO				
SPHCYL	contains							
SRPP	contains	B						
SSMELT	contains							
SUBSIZ	contains							
SURFEB	contains	A32						
SVLAAR	contains							
THKOND	contains							
TIMSTP	contains	ONE	TWO	THREE	FOUR	TWNEIT	A3	
TMPFND	contains	B0	B1	B2	B9	TWO	MASTER	MX
TMPSET	contains	B1	B8					
TRADII	contains	A3 MRCR	A4 MRCI	B0	B1	B8	CNSTNT	ONE
UCOEFF	contains							
UDU	contains	RNDOFF						

Table 5.4 COMMON blocks contained by each program routine (continued)

UNDEFN	contains	B0	B1	MX				
VANESA	contains	A4 XND	VAN B	BCL VANPRP	CNDCON	CTOV	CTOP	VPL
VANFP	contains	B6	COMP	B6B				
VBUBL	contains	BCL	CTOV	VAN	VANPRP	XND		
VCFAC	contains	BCL	XND	VTOC	MASTER	CNDCON	B6	B6A
VIS2PH	contains							
VISCTY	contains	MASTER	B9					
VOUTP	contains	A4 CNDCON	XND CTOV	VAN CTOP	BCL TITLE	VPL	CDF	POOL
VSCRIT	contains	CNSTNT						

Table 5.5 Program routines containing each COMMON block

A10	is contained in	INITL	INPCON	INPGAS			
A17	is contained in	DATAIN	DHGEN				
A19	is contained in	DATAIN	EMISIV				
A20	is contained in	ATMSUR	DATAIN	EMISIV			
A21	is contained in	ATMPRO	INPGAS				
A23	is contained in	ATMSUR	DATAIN				
A3	is contained in	ANGAVL GEOM MELTRD	ARBINP HSPCYL PLOTS	CHEKCV INITL RECEDE	CYLIND INTEMP TIMSTP	EDIT LEVSWL TRADII	FIIRAD MASRAT
A31	is contained in	BCLTOV	DCYINT	INITL	INPCON	INPGAS	MASSEX
A32	is contained in	BUBBLE INITL SOLLIQ	CONPRP INTEMP SURFEB	EDIT LEVSWL	FILM MASRAT	GFLMPR MHTRAN	HTRN PLOTS
A39	is contained in	EDIT	GFLMPR	HTRN			
A4	is contained in	ATMSUR HTRN MELTRD PRTGAS	DATAIN INIL MHTRAN REACT	DHGEN INPCON MLTREA TRADII	EDIT INTEMP ORIENT VANESA	ENRCN1 LEVSWL PLLAYR VOUTP	FILM MASSEX PLOTS
A42	is contained in	ABLATE	DATAIN	MASSEX			
A43	is contained in	DATAIN	MASSEX				
A44	is contained in	EDIT	LEVSWL				
A45	is contained in	ADDLYR REACT	CREATE	EDIT	INITL	PLLAYR	PRTGAS
A9	is contained in	DATAIN					
ACTIV	is contained in	ACTMET	ACTOXD	INTCOF	VANESA		
ARGLST	is contained in	CVFAC	FILM	INTEMP	MASRAT		
ATMDAT	is contained in	ATMPRO	ATMSUR				
B	is contained in	BARRAY	SRPP	VANESA			

Table 5.5 Program routines containing each COMMON block (continued)

B0	is contained in	ADDLYR	ATMSUR	BLKDTA	BUBBLE	CHEKCV	CREATE
		CVFAC	DENTRN	DHGEN	EDIT	ENRCN1	ENRCN2
		ENTRN	HCBTOP	HTRCLN	HTRLIQ	HTRN	INITL
		INTEMP	LEVSWL	MASLOS	MASRAT	MASSEX	MELTRD
		MHTRAN	MLTPRP	ORIENT	PLLAYR	PLOTS	REACT
		SOURCE	TMPFND	TRADII	UNDEFN		
B1	is contained in	ADDLYR	ATMSUR	BUBBLE	CHEKCV	CHEKHT	CREATE
		CVFAC	DATAIN	DENTRN	DHGEN	EDIT	ENRCN1
		ENRCN2	ENTRN	FILM	HCBROT	HCBINJ	HCBSID
		HCBTOP	HTRCLN	HTRLAY	HTRLIQ	HTRN	INITL
		INTEMP	LEVSWL	MASLOS	MASRAT	MASSEX	MELTRD
		MHTRAN	MLTPRP	ORIENT	PLLAYR	PLOTS	QMELT
		REACT	SOURCE	TMPFND	TMPSET	TRADII	UNDEFN
B2	is contained in	ADDLYR	CREATE	CVFAC	DHGEN	EDIT	ENRCN1
		INITL	MASLOS	MASSEX	MHTRAN	MLTPRP	PLLAYR
		PLOTS	REACT	TMPFND			
B3	is contained in	BUBBLE	CONPRP	INITL	LEVSWL	MASRAT	MHTRAN
B4	is contained in	BLKDTA	CORCON	FAIL			
B5	is contained in	EDIT	ENRCN1	HTRCLN	HTRLAY	HTRN	INITL
		INTEMP	MASRAT	QMELT			
B6	is contained in	BLKDTA	CVFAC	DATAIN	DCYINT	DCYPOW	DHGEN
		FPUPD	INPCON	MASLOS	MASSEX	VANFP	VCFAC
B6A	is contained in	CVFAC	DCYINT	FPUPD	MASSEX	VCFAC	
B6B	is contained in	DCYINT	FPUPD	VANFP			
B7	is contained in	ENRCN1	MASSEX	MHTRAN	REACT		
B8	is contained in	ADDLYR	EDIT	HTRCLN	HTRLAY	HTRN	INITL
		INTEMP	MHTRAN	MLTPRP	PLLAYR	PLOTS	QMELT
		TMPSET	TRADII				
B9	is contained in	BLKDTA	EDIT	EMISIV	ENRCN1	HTRCLN	INCOOL
		INITL	MASSEX	MLTPRP	PLLAYR	SOLLIQ	TMPFND
		VISCTY					
BCL	is contained in	AERPTL	BCLTOV	CVFAC	DATAIN	LOSSES	MECLOS
		PHSPRP	VANESA	VBUBL	VCFAC	VOUTP	
CDF	is contained in	DATAIN	DF	POOLV	VOUTP		
COMP	is contained in	BCLTOV	DATAIN	VANFP			

Table 5.5 Program routines containing each COMMON block (continued)

CONSRV	is contained in	EDIT	ENRCN1	ENRCN2	INITL	MASLOS	MASSEX
		MHTRAN	REACT				
CNDCON	is contained in	AERPTL	CONPRP	CVFAC	DATAIN	VANESA	VCFAC
		VOUTP					
CNSTNT	is contained in	ANGAVL	ATMSUR	BLKDTA	BUBBLE	CHEKCV	CHEKHT
		CYLIND	DENTRN	EDIT	ENTRN	FILM	GEOM
		HCBBOT	HCBINJ	HCBSID	HCBTOP	HSPCYL	HTRCLN
		HTRLAY	HTRLIQ	HTRN	INGEOM	INITL	INTEMP
		LEVSWL	MASRAT	MELTRD	PLOTS	SETTL	SETUP
		TRADII	VSCRIT				
CTOP	is contained in	DATAIN	POOLV	VANESA	VOUTP		
CTOV	is contained in	AERPTL	AEROSOL	ATMSUR	CVFAC	DATAIN	LOSSES
		MASLOS	MECLOS	MHTRAN	VANESA	VBUBL	VOUTP
FORTN	is contained in	CYLIND	GEOM	HSPCYL	INGEOM		
FOUR	is contained in	EDIT	GEOM	HSPCYL	RECEDE	TIMSTP	
GASEDT	is contained in	EDIT	INITL	REACT			
HEATEX	is contained in	ATMSUR	ENRCN1	ENRCN2	INITL	INTEMP	
IMP	is contained in	ENRCN1	ENRCN2				
MASTER	is contained in	ABLATE	ADDLYR	BLKDTA	CONFND	CONPRP	CPENTH
		CREATE	CVFAC	DCYINT	DENSTY	DHGEN	EDIT
		EMISIV	ENRCN1	FPUPD	INITL	INPCON	INPGAS
		MASLOS	MASRAT	MASSEX	MHTRAN	MLTPRP	ORIENT
		PLLAYR	PLOTS	PRTGAS	REACT	SOLLIQ	TMPFND
		VCFAC	VISCTY				
MRCI	is contained in	CHEKCV	CHEKHT	DATAIN	EDIT	ENRCN1	FIIRAD
		HTRCLN	HTRLAY	INITL	INTEMP	LEVSWL	MASRAT
		MELTRD	PLOTS	TRADII			
MRCR	is contained in	CHEKCV	CHEKHT	DATAIN	EDIT	ENRCN1	FIIRAD
		HTRCLN	HTRLAY	INITL	INTEMP	LEVSWL	MASRAT
		MELTRD	PLOTS	TRADII			
MX	is contained in	ADDLYR	CREATE	CVFAC	DENTRN	EDIT	ENRCN1
		ENTRN	HTRN	INITL	MHTRAN	MLTPRP	ORIENT
		PLLAYR	REACT	TMPFND	UNDEFN		
PFDAT	is contained in	BLKDTA	CHEMPO	MLTREA	PRTGAS	REACT	

Table 5.5 Program routines containing each COMMON block (continued)

ONE	is contained in	ANGAVL	ARBINP	CHEKCV	CORCON	CYLIND	DATAIN
		EDIT	EXPRNT	FAIL	FIIRAD	GEOM	GFLMPR
		HSPCYL	INGEOM	INITL	LEVSWL	MASRAT	MELTRD
		PAGEHD	PLOTS	REACT	RECEDE	TIMSTP	TRADII
POOL	is contained in	POOLV	VOUTP				
RNDOFF	is contained in	MLTREA	SETUP	UDU			
SPECNM	is contained in	BLKDTA	CONPRP	DATAIN	DCYINT	EDIT	INPCON
		INPGAS	PRTGAS				
THREE	is contained in	DATAIN	EDIT	TIMSTP			
TITLE	is contained in	DATAIN	PAGEHD	VOUTP			
TWNEIT	is contained in	ANGAVL	ARBINP	CYLIND	FIIRAD	GEOM	HSPCYL
		LEVSWL	MASRAT	MELTRD	RECEDE	TIMSTP	
TWNTWO	is contained in	BUBBLE	EDIT	INITL	LEVSWL	MASRAT	
TWO	is contained in	ADDLYR	ATMPRO	ATMSUR	CHEKCV	CORCON	CREATE
		CVFAC	DATAIN	DCYINT	DENTRN	EDIT	EMISIV
		ENRCN1	EXPRNT	FAIL	HTRLAY	INPGAS	INTEMP
		LEVSWL	MASLOS	MASRAT	MASSEX	MELTRD	MHTRAN
		PAGEHD	PLLAYR	PLOTS	REACT	RECEDE	SOURCE
		TIMSTP	TMPFND				
VAN	is contained in	AERPTL	AERSOL	ATMSUR	CVFAC	DATAIN	MECLOS
		MHTRAN	VANESA	VBUBL	VOUTP		
VANPRP	is contained in	AERPTL	AERSOL	CVFAC	MECLOS	PHSPRP	VANESA
		VBUBL					
VPL	is contained in	AERPRL	DATAIN	POOLV	VANESA	VOUTP	
VTOC	is contained in	CVFAC	MASLOS	VCFAC			
XND	is contained in	AERPTL	AERSOL	BCLTOV	DATAIN	MECLOS	PHSPRP
		VANESA	VBUBL	VCFAC	VOUTP	XNDAR	

Table 5.6 Variables contained in each COMMON block

A10	contains variables	VA, PA, TA, TMI, TOI
A17	contains variables	NDECM, PIM(30), TIM(30), PIO(30), TIO(30), NDECO
A19	contains variables	TEMPM, TEMPO, TEMPS
A20	contains variables	EMM(5), EO(5), ES(5), NEM, NS, NEO, TORT1(5), TORT2(5), TORT6(5), RADLEN
A21	contains variables	NATMPR, TPA(10), PAT(10)
A23	contains variables	NTP, TMPS(10), TTS(10)
A3	contains variables	DDODS, R(100) , Z(100) , RMAX , ZB, IMAXR, VOL(100), X(100) , ZMAX , ZT, IMAXZ, RW , HANGL(100), FLMANG(100), SDOT(100)
A31	contains variables	CONINP(109)
A32	contains variables	DELH , OMSI , RHOC , SI , EW , RHOPCT, GDPMWT, TSOLCT, TLIQCT, HFCT, TW , TIC
A39	contains variables	GFCP(100), GFKOND(100), GFMWT(100), GFPR(100), GFRHO(100), GFVISC(100)
A4	contains variables	ICOOL , IGAS, IMOV, IREAC, ISRABL, IMIX , ICHEM , ICOK, IFP , ILYR, IPG , IAOPAC, IFILM, IFILMB, IFILMS
A42	contains variables	NSPG, NMP(20), NSR(20), FMS(10,20), TMS(10,20), IFPOPT
A43	contains variables	NMTS, NOTS, NCTS, TIMTS(10), TIOTS(10), TICTS(10), TMTS(10), TOTS(10), TCTS(10)
A44	contains variables	ALPHZB(100)
A45	contains variables	IRE, IBALF1, IBALF2, IBALF3
A9	contains variables	FMM(10), TMM(10), NSP1, FMO(10), TMO(10), NSP2
ACTIV	contains variables	ACMET(26), ACOXD(26), AIJ(26,26), H0(26,26), H1(26,26), H2(26,26), W0(26,26), W1(26,26), W2(26,26)
ARGLST	contains variables	JBODY, LYR , IM , HCN, DEL, RYNLD, TTA, EMD, FF, WFILM, WGIN, WCNDIN

Table 5.6 Variables contained in each COMMON block (continued)

ATMDAT	contains variables	PATM
B	contains variables	B(25,10,8)
B0	contains variables	NLAY, IHOX, IHMX, IMET, ILMX, ILOX, ICLN, IATM, NLAYER, LAYER(6)
B1	contains variables	ALPLAY(7), THKLAY(7) , ARINT(8) , TINT(8) , AMLAY(7) , PLAY(7) , GFLINT(8) , ZINT(8) , BETLAY(7), RHOLAY(7) , VISLAY(7) , GMWINT(8), AMSTRT(7), CPLAY(7) , SIGLAY(7) , QABL(7) , PINT(8) , HTOT(7) , EMLAY(7) , TLAY(7) , UBUB(7) , QINT(8) , QPOOL(7) , QDCY(7) , TSOLLA(7) , TLIQLA(7) , QREAC(7) , VISLIQ(7) , TSIDE(7) , TSOLID(7) , TSTART(7) , VSGINT(7) , BUBRAD(6)
B2	contains variables	SMOXY(40,5), SMMET(15,5), SMGATM(30), SMGGEN(30), DELSMG(3)
B3	contains variables	BAR , FCDP(7) , FG(7) , FMMRBR(15), HTG(7), HMIN , HCDPIN , FMGDCY(30), FMDOCY(40), FGFL(7), HTGFL(7)
B4	contains variables	KSTP
B5	contains variables	DQBDTB(7), DQBDTL(7) , DBQDTT(7) , DQTDTB(7) , DQTDTL(7), DQTDTT(7), QZEROZ(7), DQZDTA(7), QZEROR(7), DQRDTA(7), HCBOTT(7), HCSIDE(7) , HCINTB(7) , HCINTT(7) , DQRDTL(7)
B6	contains variables	IUO2, IZRO2, IZR, NFPEL, NGRP, CNCTRN(25), ILAST(4), NMASTR, IMASTR(8), IGROUP(8), FRACTO(8), VOLRAT(8), IU, IAL
B6A	contains variables	CNTRNO(25), XMOLG(4), XMOLP(4)
B6B	contains variables	FPATWT(25), IGRP(4)
B7	contains variables	FOTRN , SMOTRN(40) , TOTR , HTOTRN , FMTRN, SMMTRN(15), TMTR, HTMTRN, FMSAV , SMMSAV(15) , TMSV , HTMSAV , FGTRN , SMGTRN(30) , TGFL , HTGTRN , FGFLM , SMGFLM(30) , TGTR , HTGFLM , FGSAV , SMGSAV(30) , TGSV , HTGSAV , FCTRN , SMCTRN , TCTR , HTCTRN
B8	contains variables	CRUSTB(7), CRUSTT(7), CRUSTR(7), TLCNTZ(7), TLCNTR(7)
B9	contains variables	IH2OL , IH2OG, NCL , NCG , TCI , FMCI , TSAT, HSCLIQ, HSCGAS

Table 5.6 Variables contained in each COMMON block (continued)

BCL	contains variables	XM(25,10), XL(25,3), P(25,10), IRST, SXMP(25,2), YKG(25,2)
CDF	contains variables	GSD, BSIZI, VROVR, IDMF, IMPF, NOSC
COMP	contains variables	CES, IOD, XEN, KRY, TE, BA, SN, RU, MO, SR , RB , Y , TC , RH , PD, LA, CE, PR , ND , SM, PU , AG , SB , NB , NBO
CONSRV	contains variables	TOTALM, TOTALH, RELERM, RELERH
CNDCON	contains variables	WF(6), CH2OG, CCO2G, WFRBR, CAOMGO
CNSTNT	contains variables	PI , PIO2 , PIO3 , GRAV, RNOT, SIGMA
CTOP	contains variables	DEPTH, PRESS, TEMP
CTOV	contains variables	TMET, TOXD, ST2, FLAR, COART, GMOL, HYSPR, OXMOL, CMOL, RVM , RVO, IFVAN, IVANFP
FORTN	contains variables	RO, ZO
FOUR	contains variables	THET(100)
GASEDT	contains variables	AMOLD1(56,5), FMOL1(56,5), IR31(5), ITGAS1(5), AMOLD2(56) , FMOL2(56) , IR32 , ITGAS2 , AMOLD3(56) , FMOL3(56) , IR33 , ITGAS3
HEATEX	contains variables	OMEGA, DTIME, ASRF, EMSRF, TSN, QSN, TSNP1, QSNP1, DQSDTS
IMP	contains variables	HTHAT(6), DHTLDT(6), BORX(6,3)
MASTER	contains variables	NO3, NM1 , NM2, NG1, NG2, SPEMW(109)
MRCI	contains variables	IRAD, ITIMR, ITOPR, NORAD
MRCR	contains variables	AFLUX, CAVHIT, CAVRAD, CVCOOL, HTMIN, HTMELT, HTMAX, RADT , TIMECR, TIMESD, RADTIM,TIMRAD, EJAREA,QSIDE , RINT

Table 5.6 Variables contained in each COMMON block (continued)

MX	contains variables	FOENT , FMENT , FODNT , FMDNT , ENTO(5) , ENTOMX(5), ENTM(5) , ENTMMX(5), DENTO(5), ENTM(5) , RHOM(5) , RHOO(5) , VOLM(5) , VOLO(5) , AMM(5) , AMO(5) , RDROP(5), TSOLM(5) , TSOLO(5) , TLIQM(5), TLIQO(5) , SIGM(5) , SIGO(5) , VISM(5) , VISO(5) , THKM(5) , THKO(5) , HTM(5) , HTO(5) , CPM(5) , CPO(5)
PFDAT	contains variables	NOP1 , NMP1 , NMP2 , NGP1 , NUMSPE , IPNT(56), SG(56), NUMELE, ANE(56,15)
ONE	contains variables	IFLOR, IGEOM, IRSTRT, IT, NRAYS
POOL	contains variables	DSSG(MNOSC), APM(MNOSC), RSIZ(MNOSC), DLCC, DNMS, DNGSD , ENM , EGSD
RNDOFF	contains variables	URO
SPECNM	contains variables	ISPNAM(109)
THREE	contains variables	IDELT, NDELT, TIMDT(10) , DTMIN(10), DTMAX(10), IEDIT , NEDIT , TIMED(10), DEDIT(10)
TITLE	contains variables	ITITL
TWNEIT	contains variables	ITANG, NBOT, RTANG
TWNTWO	contains variables	BUBMLI(100), DELL(100) , GFLMFL(100), HCON(100) , IMOD(100), REYNLD(100), TEMPA(100)
TWO	contains variables	DELTIM, IPINC , TIME, TIMEO, TPRIN, DPRIN , TEDIT, TIMEND
VAN	contains variables	VAPOR, BURST, AER1 , AER2, GOXD, IBUB, BUBDM, BUBDO, KATIS , DC , BUBD, PTBB, PTDIA, INOPL
VANPRP	contains variables	BUBNM, BUBNO, DMETP , DOXP , G(25,10), GMET , PMETP , POXP , PVAR , QMETP , QOXP , SMETP, SOXP, BNM , BNO , RTM , RTO , STM , STO , VISMET, VISOXD, VMET , VOXD
VPL	contains variables	SIZ, XMAS, DEN
VTOC	contains variables	XMLS(14), XOLS(33), ICVSPE(49), ICVFP(25)
XND	contains variables	XN(25,10), DARR(25,2)

Table 5.7 Dictionary of principal variables in CORCON

FORTRAN Symbol	Algebraic Symbol	Description	Units
ACMET(I)	γ_i	The activity coefficient for metal phase constituents	--
ACOXD(I)	γ_i	The activity coefficient for oxide phase constituents	
AER1	--	The concentration of aerosol particles created by vaporization and bubble bursting	g/cc
AER2	--	The concentration of aerosol particles created by vaporization and bubble bursting, for gas at standard conditions	g/cc
AFLUX	--	The fraction of the top melt surface heat flux used in setting the melt edge temperatures for a time-dependent melt radius	--
AG	Ag	Quantity of silver (Ag) in the fission product inventory	g-mol
ALPHZB (J)	$\alpha(Z)$	Local axial void fraction at Z(J)	--
ALPLAY (L)	α_L	Average void fraction	--
AM (I)	--	Amount of species	g-mol
AMLAY (L)	m_L	Mass	kg
AMM (L)	--	Mass of metal phase in new layer produced by the combination of two old layers	kg
AMO (L)	--	Mass of oxide phase in new layer produced by the combination of two old layers	kg
AMOLD1 (I,L)	--	Amount of species in layer at start of timestep	g-mol
AMOLD2 (I)	--	Amount of species in atmosphere at start of timestep	g-mol
AMOLD3 (I)	--	Amount of species in gas film at start of timestep	g-mol
AMSTRT (L)	m_L^o	Mass at start of timestep	kg
ANE (I,K)	--	Stoichiometric coefficients	--
APM (N)	--	Aerosol mass in distribution range N to N+1	g
ARINT (L)	A	Interface area	m^2
ASRF	A_s	Melt surface area exposed to atmosphere or coolant	m^2
B (I,N,K)	--	Array containing parametric values for fits to the free-energy functions	--
BA	Ba	Quantity of barium (Ba) in the fission product inventory	g-mol
BAR	--	Weight fraction of rebar in the concrete	--
BETLAY (L)	β_L	Volumetric coefficient of expansion	K^{-1}

Table 5.7 Dictionary of principal variables in CORCON (continued)

FORTRAN Symbol	Algebraic Symbol	Description	Units
BNM	--	Morton number for the metal phase in aerosol calculations	--
BNO	--	Morton number for the oxide phase in aerosol calculations	--
BSIZI	--	Initial bubble size in aerosol calculations	cm
BUBD	--	Fixed input bubble diameter, used in aerosol calculations	cm
BUBDM	--	Bubble diameter for the metal phase, used in aerosol calculations	cm
BUBDO	--	Bubble diameter for the oxide phase, used in aerosol calculations	cm
BUBMLI (J)	--	Molar flux of gas entering bubbles	g-mol/m^2-s
BUBNM	--	Number of bubbles passing through the metal phase, in aerosol calculations	--
BUBNO	--	Number of bubbles passing through the oxide phase, in aerosol calculations	--
BUBRAD (L)	r_b	Average bubble radius	m
BURST	--	The concentration of aerosol particles generated by bubble bursting	--
CAOMGO	--	Mass fraction of CaO in CaO and MgO	--
CAVHIT	--	Axial location of the original cavity floor (time-dependent melt radius)	m
CAVRAD	--	Radius of the cavity, until the melt reaches the cavity wall (time-dependent melt radius)	m
CCO2G	--	Mass fraction of original concrete CO	--
CE	Ce	Quantity of cerium (Ce) in the fission product inventory	g-mol
CES	Cs	Quantity of cesium (Cs) in the fission product inventory	g-mol
CH2OG	--	Mass fraction of chemically bound and evaporable water in the concrete	--
CMOL	--	Total quantity of carbon, used in aerosol calculations	g-mol
CNCTRN (I)	--	Fission product quantity	g-mol
CNTRNO (I)	--	Original fission product quantity	g-mol
COART	--	Mass rate of addition of concrete to the melt	g/s

Table 5.7 Dictionary of principal variables in CORCON (continued)

FORTRAN Symbol	Algebraic Symbol	Description	Units
CHPOT (I)	μ_i°	Standard state chemical potential	cal/g-mol
CONINP (I)	m	Initial mass of condensed species	kg
CPLAY (L)	c_{P_L}	Specific heat	J/kg-K
CRUSTx (L)	δ_{x_L}	Crust thickness of face x (= B, bottom; = T, top; = R, radial)	m
CVCOOL	--	Critical volume of coolant required to cover the melt (time-dependent melt radius)	m^3
DARR (I,K)	--	Array containing the densities for the condensed species	kg/m^3
DDODS	--	Ratio of normal recision to normal distance to adjacent ray	--
DEDIT (N)	--	Time between printed edits	s
DELH		Heat of ablation of concrete	J/kg
DELL (J)	δ	Gas film thickness	m
DELSMG (I)	--	Mass of gaseous species generated during timestep	kg
DELTIM	Δt	Timestep	s
DEN	--	Aerosol density	g/cc
DEPTH	--	Depth of coolant, used in aerosol calculations	cm
DHPOW	--	Decay heat power	W
DHTLDT (L)	--	Total heat capacity of new mass at old temperature	J/kg-K
DLCC	--	Linear correlation coefficient in the aerosol model	--
DMETP	--	Mass density of the metallic phase in aerosol calculations	g/cc
DNGSD	--	Geometric standard deviation of the aerosol particle size distribution	--
DNMS	--	Mean particle size for the aerosol particle size distribution	μm
DOXP	--	Mass density of the metallic phase in aerosol calculations	g/cc
DPRIN	--	Time interval for diagnostic prints	s
DQBDTx (L)	dq_B/dT_x	Rate of change of upward heat flux at the bottom surface with respect to temperature x (= B, bottom; = L, layer; = T, top)	W/m^2-K
DQRDTA (L)	dq_R/dT_A	Rate of change of outward heat flux to the radial surface with respect to the surface temperature	W/m^2-K

Table 5.7 Dictionary of principal variables in CORCON (continued)

FORTRAN Symbol	Algebraic Symbol	Description	Units
DQRDTL (L)	dq_R/dT_L	Rate of change of outward heat flux to the radial surface with respect to the layer temperature	W/m²-K
DQSDTS	dq_s/dT_s	Rate of change of the heat flux to/from the pool surface with respect to the surface temperature	W/m²-K
DQTDTx (L)	dq_T/dT_x	Rate of change of upward heat flux at the bottom surface with respect to temperature x (= B, bottom; = L, layer; = T, top)	W/m²-K
DQZDTA (L)	--	Rate of change of heat flux to the axial surface with respect to surface temperature	W/m²-K
DSSG (N)	--	Aerosol particle size ranges	μm
DTIME	--	Timestep	s
DTMAX (N)	--	Maximum timestep	s
DTMIN (N)	--	Minimum timestep	s
GSD	--	Error in geometric standard deviation for aerosol particle size distribution	--
EJAREA	A_R	Area of the edge of each layer exposed to atmosphere or coolant	m²
EMD	--	Energy loss to the concrete ablation products	W
EMLAY (L)	ϵ_L	Emissivity	--
EMM (M or N)	ϵ_M	Emissivity of metallic phase	--
EMSRF	ϵ_{sur}	Emissivity of melt surface exposed to atmosphere	--
EMSUR	ϵ_{sur}	Emissivity of the above-pool surroundings	--
ENM	--	Error in the natural logarithm of the aerosol particle size distribution	--
EO (M or N)	ϵ_o	Emissivity of oxidic phase	--
ES (M or N)	ϵ_{sur}	Emissivity of atmosphere surroundings	--
EW	ϵ_w	Emissivity of ablating concrete surface	--
FCTRN	--	Mass of coolant added during timestep	kg
FG (L)	--	Gas flow rate	kg/s
FGFLM	--	Mass of gas transported in film during timestep	kg
FGSAV	--	Mass of gas transformed by oxide/atmosphere reaction during timestep	kg
FGTRN	--	Mass of gas transported as bubbles during timestep	kg
FLAR	--	Surface area of the top melt layer, used in aerosol calculations	cm²

Table 5.7 Dictionary of principal variables in CORCON (continued)

FORTRAN Symbol	Algebraic Symbol	Description	Units
FLMANG (J)	--	Average slope of the gas film over a Taylor cell radius	rad
FMCI	--	Initial mass of coolant	kg
FMM (N)	--	Metallic phase splashout rate	kg/s
FMMRBR (I)	--	Mass fraction composition of rebar	--
FMO (N)	--	Oxidic phase splashout rate	kg/s
FMS (N,I)	--	Specified rate of additions to pool	kg/s
FMSAV	--	Mass of reinforcing steel ablated by the light oxide layer during timestep	kg
FMTRN	--	Mass of metal rising or sinking in the pool during the timestep	kg
FOTRN	--	Mass of oxide rising or sinking in the pool during the timestep	kg
FPATWT (I)	--	Fission product atomic weights	g/g-mol
G (I,K)	--	Free energy of species I involving element K	cal/mol
GDPMWT	--	Molecular weight of gaseous products of concrete ablation	g/g-mol
GFCP (J)	--	Gas film specific heat	J/kg-K
GFKOND (J)	--	Gas film thermal conductivity	W/m-K
GFLINT (L)	--	Mass of flow of gas at interface	kg/s
GFLMFL (J)	--	Mass flow of gas in the film	kg/s
GFMWT (J)	--	Gas film molecular weight	g/g-mol
GFPR (J)	--	Gas film Prandtl number	--
GFRHO (J)	--	Gas film density	kg/m
GFVISC (J)	--	Gas film dynamic viscosity	kg/m-s
GMET	--	Quantity of gas sparging the through the metal, used in aerosol calculations	g-mol/s
GMOL	--	Total quantity of gas sparging through the metal during the timestep, used in aerosol calculations	g-mol/s
GMWINT (L)	--	Molecular weight of gas at interface	g/g-mol
GOXD	--	Quantity of gas sparging through the oxide, used in aerosol calculations	g-mol/s
GRAV	g	Gravitational acceleration	m/s
GSD	--	Geometric standard deviation of aerosol particle size distribution	--

Table 5.7 Dictionary of principal variables in CORCON (continued)

FORTRAN Symbol	Algebraic Symbol	Description	Units
HANGL (J)	--	Negative of cavity surface inclination angle	rad
HBB	--	Concrete crucible base thickness, Figure 4.3	m
HBC	--	Concrete crucible dimension, top to center of hemisphere, Figure 4.2	m
HC	--	Concrete crucible dimension, top to start of hemisphere, Figure 4.2	m
HCINTB (L)	h_L	Heat transfer coefficient, bulk to bottom	W/m²-K
HCINTT (L)	h_U	Heat transfer coefficient, bulk to top	W/m²-K
HCN	--	Heat transfer coefficient across gas film	W/m²-K
HCON (J)	h	Gas film heat transfer coefficient	W/m²-K
HCSIDE (L)	h	Heat transfer coefficient, bubble agitation	W/m²-K
HEATUP	--	Heat to concrete decomposition products during timestep; converted to rate [W] in EDIT	J
HFCT	--	Latent heat of fusion for concrete	J/kg
HIT	--	Concrete crucible depth, Figure 4.3	m
HTCTRN	--	Total enthalpy of coolant added during timestep	J
HTGFLM	--	Total enthalpy of gas transported in film during timestep	J
HTGSAV	--	Total enthalpy of gas transformed by oxide/atmosphere reaction during timestep	J
HTGTRN	--	Total enthalpy of gas transported as bubbles during the timestep	J
HTHAT (L)	--	Total enthalpy of new layer mass at old temperature	J
HTM (L)	--	Enthalpy of the metal in the layer	J
HTMAX	--	Maximum allowed melt thickness for the time-dependent melt radius (entered in cm; used internally in m)	m
HTMELT	--	Thickness of the melt layer (time-dependent melt radius)	m
HTMIN	--	Minimum allowed melt thickness for the time-dependent melt radius (entered in cm; used internally in m)	m
HTMSAV	--	Total enthalpy of reinforcing steel ablated by the light oxide layer during the timestep	J
HTMTRN	--	Total enthalpy of metal rising or sinking in pool during timestep	J
HTO (L)	--	Enthalpy of the oxide in the layer	J

Table 5.7 Dictionary of principal variables in CORCON (continued)

FORTRAN Symbol	Algebraic Symbol	Description	Units
HTOT (L)	--	Total enthalpy	J
HTOTRN	--	Total enthalpy of oxide rising or sinking in pool during timestep	J
HYSPR	--	Hydrogen/steam pressure ratio	--
IABL	--	Surroundings ablation index	--
IAOPAC	--	Aerosol opacity index	--
IATM	--	Index of top surface of the pool, including coolant	--
ICHEM	--	Flag for condensed phase chemistry and coking options	--
ICLN	--	Index of the coolant layer	--
ICOK	--	Switch for coking reaction	--
ICON	--	Concrete composition index	--
ICOOL	--	Coolant layer flag	--
IDMF	--	Diffusion mechanism flag for aerosol calculations	--
IFILMB	--	Flag for gas film on pool bottom	--
IFILMS	--	Flag for gas film on pool side	--
IFLOR	--	Index for cavity top ray	--
IFP	--	Decay heat power index	--
IFVAN	--	Switch for using the VANESA aerosol model	--
IGAS	--	Gas phase index	--
IGEOM	--	Cavity geometry index	--
IHMX	--	Index for heavy mixed layer	--
IHOX	--	Index for heavy oxide layer	--
ILMX	--	Index for light mixed layer	--
ILOX	--	Index for light oxide layer	--
ILYR	--	Melt layer configuration index	--
IMASTR (N)	--	Master list of fission product groups	--
IMAXR	--	Body point at maximum cavity radius	--
IMAXZ	--	Body point at maximum cavity depth	--
IMET	--	Index for metal layer	--
IMIX	--	Flag for calculating entrainment and deentrainment	--
IMOD (J)	--	Heat transfer model number	--
IMOV	--	Cavity shape plot index	--

Table 5.7 Dictionary of principal variables in CORCON (continued)

FORTRAN Symbol	Algebraic Symbol	Description	Units
IMPF	--	Impaction mechanism flag for aerosol calculations	--
IOD	I	Quantity of iodine (I) in the fission product inventory	g-mol
IPG	--	Time plot index	--
IPINC	--	Print increment, number of timesteps	--
IPNT (I)	--	Position of Ith species in the CORCON master list	--
IR31 (L)	--	Number of iterations required in MLTREA for convergence	--
IRAD	--	Flag for calls to TRADII (time-dependent melt radius)	--
IRE	--	Identifying number of chemical reaction	--
IRSTRT	--	Restart option index	--
ISPNAM	--	CHARACTER*8 name of master-list species	--
ISRABL	--	Atmosphere surroundings ablation index	--
IT	--	Iteration (timestep) number	--
ITANG	--	Number of the body point constrained to move vertically at the limit of a flat bottom	--
ITIMR	--	Flag for time-dependent melt radius option	--
ITITL	--	CHARACTER*80 run identification	--
ITOPR	--	Index of the top interface of the melt	--
IUSER	--	Flag enabling user flexibility options	--
JBODY	--	Index of body point	--
KATIS	--	Flag to signal use of Kataoka and Ishii, and Azbel models for mechanical release of aerosols	--
KRY	--	Quantity of lanthanum (La), ytterbium (Y), praseodymium (Pr), samarium (Sm) and neodymium (Nd) in the fission product inventory	g-mol
LA	La	Quantity of lanthanum (La) in the fission product inventory	g-mol
LAYER (L)	--	Numbers (1-7) of occupied layers	--
LYR	--	Index of current melt layer	--
MO	Mo	Quantity of molybdenum (Mo) in the fission product inventory	g-mol
NAMSP	--	CHARACTER*8 name of input species	--
NB	Nb	Quantity of niobium (Nb) in the fission product inventory	g-mol

Table 5.7 Dictionary of principal variables in CORCON (continued)

FORTRAN Symbol	Algebraic Symbol	Description	Units
NBO	NbO	Quantity of niobium oxide (NbO) in the fission product inventory	g-mol
NBOT	--	Number of body points on the flat bottom of cavity, including the center line and tangency point	--
NCL	--	Master list number of coolant species	--
NCORN	--	Number of body points defining a cavity corner, not including tangency points	--
ND	Nd	Quantity of neodymium (Nd) in the fission product inventory	g-mol
NDECM	--	Number of points in metallic phase power input table	--
NDECO	--	Number of points in oxidic phase power input table	--
NEM	--	Number of points in metallic phase emissivity table	--
NEO	--	Number of points in metallic phase emissivity table	--
NFPEL	--	Number of fission product elements	--
NG1	--	Location of first gas in master species list	--
NG2	--	Location of last gas in master species list	--
NGRP	--	Number of groups of fission product elements	--
NINP	--	Number of concrete species input	--
NLAY	--	Total number of layers allowed (includes coolant and atmosphere)	--
NLAYER	--	Total number of occupied layers	--
NMASTR	--	Maximum number of species containing a fission product element	--
NMP (I)	--	Number of points in the input mass addition tables	--
NMSI	--	Number of metallic species input	--
NM1	--	Location of the first metal in the master species list	--
NM2	--	Location of the last metal in the master species list	--
NO3	--	Location of the last oxide in the master species list	--
NORAD	--	Maximum number of entries in the table of times and melt radii	--
NOSC	--	Number of sections in the aerosol particle size distribution	--
NRAYS	--	Number of rays	--
NS	--	Number of points in surroundings emissivity table	--

Table 5.7 Dictionary of principal variables in CORCON (continued)

FORTRAN Symbol	Algebraic Symbol	Description	Units
NSIDE	--	Number of body points defining the side of the cylindrical cavity	--
NSP1	--	Number of metallic species in the splashout tables	--
NSP2	--	Number of oxidic species in the splashout tables	--
NSPG	--	Number of species in surroundings	--
NSR (N)	--	Species number of species in fission product inventory	--
NTP	--	Number of points in surroundings temperature table	--
NUMELE	--	Maximum number of elements	--
NUMSPE	--	Maximum number of chemical species	--
OMEGA	--	Implicitness fraction (= 1)	--
OXMOL	--	Total quantity of oxides	g-mol
P (I,K)	--	Partial pressure of species K involving element I	Pa
PA	--	Initial gas pressure	Pa
PAT (N)	--	Gas (atmosphere) pressure	Pa
PATM	--	Atmospheric pressure	Pa
PD	Pd	Quantity of palladium (Pd) in the fission product inventory	g-mol
PI	π	Pi	--
PIM (N)	P_m	Metallic phase input power	W
PINT (L)	--	Interface pressure	Pa
PIO (N)	P	Oxidic phase input power	W
PIO2	$\pi/2$	Pi/2	--
PIO3	$\pi/3$	Pi/3	--
PLAY (L)	P	Average pressure	Pa
PMETP	--	Volume of metallic phase	cm^3
POXP	--	Volume of oxidic phase	cm^3
PR	Pr	Quantity of praseodymium (Pr) in the fission product inventory	g-mol
PRESS	--	Ambient (atmospheric) pressure for aerosol calculations	atm
PTBB	--	Number of particles per bubble, for aerosol calculations	--
PTDIA	--	Mean particle size for aerosol produced by mechanical processes	m

Table 5.7 Dictionary of principal variables in CORCON (continued)

FORTRAN Symbol	Algebraic Symbol	Description	Units
PU	Pu	Quantity of plutonium (Pu) in the fission product inventory	g-mol
PVAR	--	Average pressure in the coolant pool for aerosol calculations	atm
QABL (L)	--	Rate of change in enthalpy due to heat loss to concrete	W
QCONV	q_{conv}	Convective heat flux across gas film	W/m^2
QDCY (L)	--	Internal heat source rate	W
QINT (L)	--	Interface heat flow rate (positive up)	W
QMETP	--	Molar density of metallic phase for aerosol calculations	g-mol/cm^3
QOXP	--	Molar density of oxidic phase for aerosol calculations	g-mol/cm^3
QPOOL (L)	--	Rate of change in enthalpy due to heat from adjacent layers	W
QRAD	$q_{rad_{net}}$	Net radiative heat flux across the gas film	W/m^2
QREAC (L)	--	Heat source rate from chemical reactions	W
QSIDE (L)	q_R	Radial heat flux	W/m^2
QSN	Q_s^n	Surface heat flux at the start of the timestep	W/m^2
QSNP1	Q_s^{n+1}	Surface heat flux at the end of the timestep	W/m^2
QZEROR (L)	--	Radial heat flux to the gas film, extrapolated to a surface temperature equal to the layer temperature	W
QZEROZ (L)	--	Axial heat flux to the gas film, extrapolated to a surface temperature equal to the layer temperature	W
R (J)	r	Radial coordinate	m
RAD	--	Concrete crucible radius, Figure 4.3	m
RADC	--	Concrete crucible corner radius, Figure 4.3	m
RADLEN	L	Characteristic path length for aerosol opacity	m
RADT	--	Current melt radius (time-dependent melt radius)	m
RADTIM (N)	--	Melt radius at time TIMRAD (N) in the table of times and radii (time-dependent melt radius)	m
RB	Rb	Quantity of rubidium (Rb) in the fission product inventory	g-mol
RBR	--	Mass fraction of reinforcing steel in concrete	--

Table 5.7 Dictionary of principal variables in CORCON (continued)

FORTRAN Symbol	Algebraic Symbol	Description	Units
RDROP (L)	--	Radius of entrained or deentrained drops	m
RELERH	--	Relative numerical error in energy conservation	--
RELERM	--	Relative numerical error in mass conservation	--
REYNLD (J)	Re	Gas film Reynolds number	--
RH	Rh	Quantity of rhodium (Rh) in the fission product inventory	g-mol
RHOC	ρ_c	Concrete density	kg/m^3
RHOLAY (L)	ρ_L	Average density	kg/m^3
RHOM (L)	--	Density of metal phase	kg/m^3
RHOO (L)	--	Density of oxide phase	kg/m3
RHOPCT	--	Partial density of concrete in reinforced concrete	kg/m^3
RI	--	Interface radius in EDIT; also used as R (J) elsewhere	m
RINT (I)	--	Interface radius	m
RMAX	--	Maximum radius of concrete cavity	m
RNOT	R_o	Universal gas constant	J/g-mol K
RO	--	Radial location of ray origin (= 0)	m
RS	--	Concrete crucible radius, Figure 4.2	m
RSIZ (N)	--	Characteristic aerosol particle size in range N	μm
RTANG	--	Radius of flat bottom of concrete crucible	m
RTM	--	Bubble rise time in the metal phase for aerosol calculations	s
RTO	--	Bubble rise time in the oxide phase for aerosol calculations	s
RU	Ru	Quantity of ruthenium (Ru) in the fission product inventory	g-mol
RVM	--	Bubble rise velocity in the metal phase for aerosol calculations	cm/s
RVO	--	Bubble rise velocity in the oxide phase for aerosol calculations	cm/s
RW	--	Outer radius of concrete crucible, Figures 4.2-4.4	m
SAREA	--	Surface area of the cavity	m^3
SB	Sb	Quantity of antimony (Sb) in the fission product inventory	g-mol

Table 5.7 Dictionary of principal variables in CORCON (continued)

FORTRAN Symbol	Algebraic Symbol	Description	Units
SCALRG	--	Free energy divided by R_oT for chemical system	--
SCALRM	--	Total moles in gas phase of chemical system	g-mol
SDOT (J)	$\dot{s}$	Concrete recession rate	m/s
SI	--	Mass fraction of concrete decomposing into gas; silicon	--
SIGEFF	$\sigma_B F$	Stefan-Boltzmann constant times shape factor	$W/m^2\text{-}K^4$
SIGLAY (L)	σ_L	Surface tension	N/m
SIGM (L)	--	Surface tension for metal phase	N/m
SIGMA	σ_B	Stefan-Boltzmann constant	$W/m^2\text{-}K^4$
SIGO (L)	--	Surface tension for oxide phase	N/m
SIZ	--	Aerosol particle size	μm
SM	-- -- Sm	Mass fraction of concrete species; mole fraction of gaseous species; quantity of samarium (Sm) in the fission product inventory	-- -- g-mol
SMCTRN	--	Mass of coolant species added during timestep	kg
SMETP	--	Total quantity of metal phase in aerosol calculations	g-mol
SMGATM (I)	--	Mass of gas in atmosphere	kg
SMGFLM (I)	--	Mass of gas transported in the gas film during the timestep	kg
SMGGEN (I)	--	Cumulative mass of gases species generated	kg
SMGSAV (I)	--	Mass of gas transformed by oxide/atmosphere reaction during timestep	kg
SMGTRN (I)	--	Mass of gas transported as bubbles during timestep	kg
SMMET (I,L)	--	Mass of metallic species	kg
SUMMHO	--	Total enthalpy of new pool mass for old temperatures and melting ranges	J
SMMSAV (I)	--	Mass of metallic products of oxide/atmosphere reaction during timestep	kg
SMMTRN (I)	--	Mass of metal rising or sinking in the pool during timestep	kg
SMOTRN (I)	--	Mass of oxide rising or sinking in the pool during the timestep	kg
SMOXY (I,L)	--	Mass of oxidic species	kg

Table 5.7 Dictionary of principal variables in CORCON (continued)

FORTRAN Symbol	Algebraic Symbol	Description	Units
SN	Sn	Quantity of tin (Sn) in the fission product inventory	g-mol
SOXP	--	Total quantity of oxide phase in aerosol calculations	g-mol
SPEMW (I)	--	Molecular weight	g/g-mol
SR	Sr	Quantity of strontium (Sr) in the fission product inventory	g-mol
ST2	--	Timestep in aerosol calculations	s
STM	--	Surface tension of the metal phase in aerosol calculations	dyne/cm
STO	--	Surface tension of the oxide phase in aerosol calculations	dyne/cm
SXMP (I,K)	--	Cumulative quantity of chemical species	g-mol
TA	T_a	Initial gas (atmosphere) temperature	K
TC	Tc	Quantity of technetium (Tc) in the fission product inventory	g-mol
TCI	--	Initial coolant temperature	K
TCTR	--	Temperature of coolant added	K
TE	Te	Quantity of tellurium (Te) in the fission product inventory	g-mol
TEDIT	--	Time when next edit will be generated	s
TEMP	--	Average coolant pool temperature used in aerosol calculations	K
TEMPA (J)	--	Temperature of pool/film interface at Z(J)	K
TEMPx	--	Flag for emissivity table for x (= M, metal; = O, oxide; = S, surroundings); true if independent variable is temperature rater than time	K
TGFL	--	Temperature of gas transported through the film	K
TGSV	--	Temperature of gas transformed by the oxide/atmosphere reaction	K
TGTR	--	Temperature of gas transported as bubbles	K
THET (J)	--	Ray angle	rad
THKLAY (L)	k_L	Thermal conductivity	W/m-K
THKM (L)	k_{LM}	Thermal conductivity of metal phase	W/m-K
THKO (L)	k_{LO}	Thermal conductivity of oxide phase	W/m-K
TIC	--	Initial concrete temperature	K

Table 5.7 Dictionary of principal variables in CORCON (continued)

FORTRAN Symbol	Algebraic Symbol	Description	Units
TIM (N)	--	Times in metal phase input power table	s
TIME	t	Current time	s
TIMECR	--	Time at which the layer crusts are thick enough to stop melt spreading (time-dependent melt radius)	s
TIMEND	--	End time for calculation	s
TIMEO	--	Start time for calculation	s
TIMESD	--	Time at which the spreading melt layer contacts the side of the concrete cavity	s
TIMRAD (N)	--	Time at which the melt has radius RADTIM (N) in the table of times and radii (time-dependent melt radius)	s
TINT (L)	T_I	Interface temperature	K
TIO (N)	--	Times in oxide phase input power table	s
TLAY (L)	T_L	Average (bulk) temperature	K
TLCNTR (L)	$\bar{T}_{\ell r}$	Average liquid temperature, radial	K
TLCNTZ (L)	$\bar{T}_{\ell z}$	Average liquid temperature, axial	K
TLIQCT	T_c'	Concrete liquidus temperature	K
TLIQLA (L)	T_L'	Liquidus temperature	K
TLIQM (L)	--	Metal phase liquidus	K
TLIQO (L)	--	Oxide phase liquidus	K
TMET	--	Mass -averaged metal phase temperature used in aerosol calculations	K
TMI	--	Initial temperature of metallic phase	K
TMM (N)	--	Times for metallic phase splashout table	s
TMO (N)	--	Times for metallic phase splashout table	s
TMPS (N)	--	Temperature of surroundings	K
TMS (N,I)	--	Time in mass addition table	s
TMSV	--	Temperature of metallic products of oxide/atmosphere reaction	K
TMTR	--	Temperature of metal rising of sinking in the pool	K
TOI	--	Initial temperature of the oxidic phase	K
TORT1 (M or N)	--	Time or temperature for oxidic phase emissivity table	s or K

Table 5.7 Dictionary of principal variables in CORCON (continued)

FORTRAN Symbol	Algebraic Symbol	Description	Units
TORT2 (M or N)	--	Time or temperature for metallic phase emissivity table	s or K
TORT6 (M or N)	--	Time or temperature for surroundings emissivity table	s or K
TOTALH	--	Total pool enthalpy required by energy conservation	J
TOTALM	--	Total pool mass required by mass conservation	kg
TOTR	--	Temperature of oxide rising or sinking in the pool	K
TOXD	--	Mass-averaged oxide phase temperature used in aerosol calculations	K
TPA (N)	--	Time in gas (atmosphere) pressure table	s
TPRIN	--	Time for start of diagnostic print	s
TSAT			
TSIDE (L)	--	Side (radial) boundary temperature	K
TSN	T	Surface temperature at the start of the timestep	K
TSNP1	T	Surface temperature at the end of the timestep	K
TSOLCT	T_c^s	Concrete solidus temperature	K
TSOLID (L)	--	Solidification temperature	K
TSOLLA (L)	T_L^S	Solidus temperature	K
TSOLM (L)	--	Metal phase solidus	K
TSOLO (L)	--	Oxide phase solidus	K
TSTART (L)	--	Temperature at the start of a timestep	K
TTA	--	Current layer temperature	K
TTS (N)	--	Time in surroundings temperature table	s
TW	T_W	Concrete ablation temperature	K
UBUB (L)	U_g	Bubble rise velocity	m/s
URO	--	Unit round off error	--
VA	--	Initial gas volume	m^3
VAPOR	--	The concentration of aerosol particles generated by vaporization	--
VISLAY (L)	--	Dynamic viscosity	kg/m-s
VISLIQ (L)	μ_ℓ	Dynamic viscosity of liquid	kg/m-s
VISM (L)	--	Dynamic viscosity of the metal phase	kg/m-s
VISMET	--	Mass-averaged dynamic viscosity of the metal phase, used in aerosol calculations	g/cm-s

Table 5.7 Dictionary of principal variables in CORCON (continued)

FORTRAN Symbol	Algebraic Symbol	Description	Units
VISO (L)	--	Dynamic viscosity of the oxide phase	kg/m-s
VISOXD	--	Mass-averaged dynamic viscosity of the oxide phase, used in aerosol calculations	g/cm-s
VMET	--	Superficial gas velocity through the metal, used in aerosol calculations	cm/s
VOL (J)	--	Cumulative cavity volume	m^3
VOLM (L)	--	Volume of the metal phase in entrainment calculations	m^3
VOLO (L)	--	Volume of the oxide phase in entrainment calculations	m^3
VOLRAT (I)	--	Exponential volatization rate of fission products	s^{-1}
VOXD	--	Superficial gas velocity through the oxide, used in aerosol calculations	cm/s
VROVR	--	Velocity ratio for aerosol calculations	--
VSGINT (L)	V_s	Superficial gas velocity	m/s
WF (I)	--	Weight fraction of concrete constituents	--
WFRBR	--	Weight fraction of rebar in concrete	--
X (J)	--	Path length in the film	m
XEN	--	Quantity of ruthenium (Ru), technetium (Tc), rhodium (Rh), and palladium (Pd) in the fission product inventory	g-mol
XL (I, K)	--	Quantity of fission product inventory species	kg
XM (I, K)	--	Quantity of fission product inventory species	g-mol
XMAS	--	Aerosol generation rate	g/s
XMTU	--	Core size, metric tonnes of uranium	Mg
XMWTH	--	Core operating power (thermal)	MW
XN (I,K)	--	Array containing the molecular weights for species K of element I	g/g-mol
Y	Y	Quantity of ytterbium (Y) in the fission product inventory	g-mol
YKG (I,N)	--	Array containing the quantities of fission product in kg	kg
Z (j)	z	Axial coordinate (positive down)	m
ZB	--	Axial coordinate of the bottom of the concrete crucible	m
ZINT (L)	--	Interface location	m

Table 5.7 Dictionary of principal variables in CORCON (continued)

FORTRAN Symbol	Algebraic Symbol	Description	Units
ZMAX	--	Axial coordinate of deepest point in the cavity	m
ZO	--	Axial coordinate of ray origin	m
ZT	--	Axial coordinate of the top of the concrete crucible, Figure 4.3	m

6.0 Sample Problems

To illustrate the use of CORCON-Mod3, and to verify the correct functioning of the code following its installation, we have provided a set of sample problems. The input decks for these samples should provide valuable help to the new user in assembling correct input decks. The sample problems also demonstrate the capabilities of the code.

No one problem utilizes all the capabilities of CORCON-Mod3. The CORCON standard problem exercises the more commonly used capabilities of CORCON; the additional sample problem exercises some of the newer features in the code.

6.1 The CORCON Standard Problem

The CORCON standard problem describes deposition of essentially the entire core of a typical large (3400 MWt) PWR into a reactor cavity formed of limestone aggregate/common sand concrete. Deposition takes place three hours after reactor SCRAM, at which time the zirconium cladding is assumed to be approximately 50 percent oxidized. The melt also includes a significant amount of steel, from the upper internals and the breached lower head; the steel is assumed to be 5 percent oxidized. The initial water inventory of 60 metric tonnes represents the contents of the accumulators of a typical PWR. The cavity radius is taken as 3.0 meters, and does not include the area of the keyway in a plant such as Zion or Indian Point. Containment pressure is assumed to rise linearly from 1.5 bars at deposition time to 3.0 bars 3 hours later. The effects of aerosol opacity are included with the characteristic path length taken as a nominal 1.0 m.

This problem does not model any particular plant or accident sequence. It is intended merely to provide a typical problem to exercise the basic capabilities of CORCON.

The calculation assumes that the core melt is initially stratified. It remains stratified because the interlayer mixing models are not activated (ILYR < 10). Condensed phase chemistry is not calculated and the coking reaction is disabled (ICHEM = 0). Slag heat transfer is assumed at the bottom surface, while gas film heat transfer is assumed at the side surface (IFILM = 1). A full VANESA calculation is performed (IFVAN = 1), and the VANESA fission product composition is determined from the CORCON composition (IVANFP = 0). The effects of aerosol in the cavity atmosphere is included in the calculation of radiative heat transfer (IAOPAC = 1).

The release calculation is performed assuming ideal chemistry (IDEAL = 1).

The data cards used for this problem are shown in Table 6.1. This input follows the input description of Section 4.1.

A partial output listing for time 16200 seconds (270 min) for this calculation is shown in Table 6.2. Plots of the output are shown in Figures 6.1 through 6.9.

In the Standard Problem calculation, the melt remains stratified in a three layer configuration with the heavy oxide layer on the bottom, a metal layer in the middle, and a light oxide on the top. Unlike the calculations with earlier versions of CORCON, no layer flip is calculated during the three hours of the interaction.

Because the heavy oxide layer remains on the bottom of the melt, axial (downward) ablation is rather slow. This is true because an oxide crust exists at the interface with the concrete. The crust remains throughout the calculation and grows to a quasi-steady thickness of approximately 4 centimeters. As the crust grows, the ablation rate decreases to a nearly constant value of 2 cm/hr.

Figure 6.2 shows the maximum axial and radial ablation distances calculated by the code. Note that the hot metallic layer ablates concrete at a fairly rapid rate during the first hour of the calculation. After about one hour, the lower oxide layer has grown such that the maximum radial ablation location is adjacent to the oxide layer rather than the metal layer. This is true until 80 minutes later. At this time, the maximum radial ablation location is adjacent to the metal phase, and the maximum radial ablation distance again increases rapidly.

The calculated layer temperatures are shown in Figure 6.3. The three layer temperatures decrease during the first 100 minutes of the interaction. At approximately, 110 minutes after the start of the interaction, the overlying coolant pool boils off, and the layers begin to increase in temperature. By the end of the calculation, the layers have reached a new quasi-steady temperature levels of between 2100 and 2200 K.

Figures 6.4 and 6.5 show the cumulative amount of gas entering the cavity atmosphere, and the rate of gas generation. As expected, the early gas generation is dominated by the steam from coolant boiling. (Note that the steam production is initially low because the coolant pool is subcooled. When the coolant is subcooled, steam is assumed to condense before reaching the pool surface.) Boiloff of the coolant is shown clearly in Figure 6.5 at

about 295 minutes, where the steam generation rate abruptly decreases.

Figure 6.6 shows the calculated rates of energy generation and energy loss. Energy generation occurs by radionuclide decay and by chemical reactions. Energy losses include heat losses to the concrete and to the overlying water pool, atmosphere, and structures. In addition, energy lost from the melt in heating the incoming ablation products is included. This term is usually small, as is the case here. In cases where the ablation rate is extremely rapid, this term is larger.

Heat transfer to the coolant is initially quite high. During the first 15 minutes of the interaction, the coolant heat flux is greater than 1 MW/m^2 over the approximately 32 m^2 surface area. After 110 minutes, however, the coolant heat flux has decreased to 0.5 MW/m^2. Boiloff of the coolant occurs at this time, and the surface heat flux drops rapidly. Late in the calculation, the heat flux due to thermal radiation is approximately 0.3 MW/m^2.

In this sample calculation, energy generation from chemical reactions is much smaller than that from radionuclide decay. This is true because the ablation rate and consequently gas generation rates are relatively low. In calculations with higher ablation rates, the energy generation from chemical reactions can greatly exceed the contribution from radionuclide decay.

Figures 6.7 through 6.9 show the calculated aerosol concentration and aerosol generation rate for the CORCON Standard Problem. The general trend of the aerosol concentration and aerosol generation curves follows that of the gas generation and melt temperature curves. The aerosol concentration is greatest early in the calculation, with a maximum value of approximately 200 g/m^3 at STP, but declines rapidly to a quasi-steady level of approximately 30 to 40 g/m^3. Similarly, the aerosol generation rate is highest at the onset of the interaction (at > 150 g/s), but quickly reaches a nearly constant value of 20 g/s.

Another important safety consideration is the magnitude of radionuclide release from the core debris. The calculated release fractions for several of the important refractory radionuclides are shown below:

Radionuclide	Release Fraction
Tellurium	0.399
Molybdenum	1.30×10^{-6}
Uranium	5.24×10^{-5}
Barium	3.49×10^{-3}
Strontium	4.34×10^{-3}
Cerium	1.13×10^{-3}
Lanthanum	8.53×10^{-5}

It should be noted that these releases are for only the first three hours of the interaction. Though the bulk of the release occurs during this period, radionuclides will continue to be released for several hours. It should also be noted that these are releases from the melt surface rather than into the cavity atmosphere. A significant fraction of the released radionuclides is trapped within the overlying water pool. Currently, this material is effectively lost from the problem once it becomes trapped. It is not returned to the core debris if the water pool evaporates completely. Also, the code does not treat decay power generation in the water pool from the trapped radionuclides.

6.2 Additional Sample Problem

A second sample problem is provided to illustrate some of the new features of CORCON-Mod3. This problem simulates an accident at a typical BWR plant. The core-concrete interaction is assumed to begin three hours after reactor shutdown. Initially, approximately one-third of the core is deposited into the reactor cavity. The zirconium included in the initial pour is assumed to be 20 percent oxidized. During the next 3 hours of the calculation, the second third of the core is assumed to enter the cavity. The reactor cavity is assumed to be constructed from basaltic concrete and is assumed to have a diameter of 3.2 meters. Water is added after one hour of the interaction. The water addition rate of 20 kg/s (approximately 300 gal/min) is sufficient to fill the 5 meter deep cavity in approximately 2 hours. The pressure in the cavity atmosphere is assumed to rise from 1.5 bars to 2.5 bars during the 3 hours of the calculation.

The core melt is assumed to be well-mixed initially, and the interlayer mixing models are enabled (ILYR = 13). Condensed phase chemistry is

calculated and coking is disabled (ICHEM = 1). Slag film heat transfer is assumed at both the bottom and side surfaces (IFILM = 0). A complete VANESA calculation is performed (IFVAN = 1), and the VANESA fission product composition is determined from the CORCON composition (IVANFP = 0). The release calculation is performed assuming ideal chemistry (IDEAL = 1). The effects of aerosols on thermal radiation is included (IAOPAC = 1), and a mean path length of 3.0 meters is assumed. The optional user flexibility input is provided (IUSER = 1), with the following user modifications specified:

1) the thermal conductivity for the metal phase is multiplied by 0.5,

2) the viscosity of the oxide phase is multiplied by 5.0,

3) the oxide phase solidus temperature is assumed to decrease to the concrete solidus at 20 mole percent concrete oxides.

The input for this sample problem is shown in Table 6.3. A partial listing of the output for time = 16200 s (270 min) from the calculation is provided in Table 6.4. of the calculated results are provided in Figures 6.10 through 6.18.

The melt is assumed to be well-mixed at the start of the interaction. After 10 minutes, the melt is calculated to be a dense oxide layer and a mixture of dense oxides and metal. In this sample calculation, a mixture of dense oxides and metals is calculated to form (i.e., an HMX layer). (The oxides are denser than the metals because fuel oxides are being continuously added to the melt.) Immediately, this layer begins to stratify, with the dense oxides settling out of the mixture. The evolution of the layering configuration is shown clearly in the layer temperature plot of Figure 6.12.

Figures 6.10 and 6.11 show the calculated axial ablation rate, and axial and radial ablation distances for the BWR sample problem. Because the heavy oxide layer is on the bottom of the melt during most of the calculation, the ablation rate is slow due to the existence of a oxide crust at the interface with the concrete. The spike in ablation rate seen at 9 minutes arises from the changes in layer configuration occurring at this time. The crust reaches a quasi-steady thickness of 2.5 cm prior to water addition. After water addition, the crust is calculated to shrink as concrete oxides mix with the fuel oxides lowering the mixture solidus temperature. By the end of the calculation the crust thickness is 0.2 cm. Thinning of the crust is not accompanied by an increase in the ablation rate because the oxide temperature has fallen to 1865 K.

Figure 6.12 shows the rapid decline in the melt temperature during the first hour of the calculation. At this point, water is added onto the melt. After water addition, the melt temperature decreases at a slightly faster rate. Approximately 100 minutes after water addition, energy generation from radionuclide decay and chemical reactions exceeds losses to the coolant and the concrete, and the temperature of the melt begins to increase slightly.

Figures 6.13 and 6.14 show the cumulative gas generation and the gas generation rate calculated for the BWR sample problem. Production of H_2O and CO_2 is suppressed. The code predicts that gas reactions with the HMX mixture produce methane (CH_4) and other hydrocarbons at the expense of steam and carbon dioxide production. The steam release seen at 270 minutes is, of course, the steam produced by boiling of the coolant.

The calculated energy generation and energy loss terms are shown in Figure 6.15. The decay power is calculated to increase from 7 MW to 11 MW as core debris enters the cavity. Energy generation from chemical reactions is comparable to the decay power during the first hour of the calculation. The spike in chemical energy generation at 8 to 10 minutes occurs when the core debris becomes fully mixed and all of the oxides, metals, and gases are suddenly assumed to react chemically. When water is added at 240 minutes, heat loss through the melt surface quickly increases to 20 MW (0.65 MW/m^2), and then declines to a level that almost exactly balances the decay power.

Figures 6.16 through 6.18 show the calculated aerosol concentration and aerosol generation rate for the BWR sample problem. The high concentration and generation rates seen during the first 10 minutes of interaction arise from the relatively high melt temperatures and the gas generation rate spikes seen in Figures 6.12 and 6.14 respectively. The gas generation spike occurred during the rapid melt layer configuration changes. This could also influence the chemistry driving release. After the first 10 minutes the high hydrogen to steam ratio (i.e., low oxygen potential) in the gas stream promotes the reduction of refractory oxides to more volatile species. This enhances the release of both oxides from the concrete such as silica and fission product oxides such as BaO and La_2O_3. The aerosol generation rate and concentration increase to about 200 g/s and 250 g/m^3 (STP). At water addition at 240 minutes, the aerosol release shows a distinct drop corresponding to the melt temperature decrease. The increasing generation rate and

concentration during the last 1 1/2 hours of the concentration can be attributed to the slight increase in melt temperature and to the release of concrete oxides such as NaO_2 and KO_2, which comprise nearly 3/4 of the aerosol mass at the end of the calculation.

The following are the release fractions calculated for some of the more important radionuclides:

Radionuclide	Release Fraction	New Results (2.28)
Tellurium	0.155	0.13
Molybdenum	6.28×10^{-9}	5.8×10^{-9}
Uranium	6.23×10^{-5}	5.65×10^{-5}
Barium	0.110	9.92×10^{-2}
Strontium	0.187	1.89×10^{-1}
Cerium	0.0513	4.48×10^{-2}
Lanthanum	2.26×10^{-3}	1.83×10^{-3}

Note that these releases are relative to the total mass of core debris in the reactor cavity (i.e., two-thirds of the total core mass). To determine release fractions relative to the total core inventory, multiply the above values by 2/3.

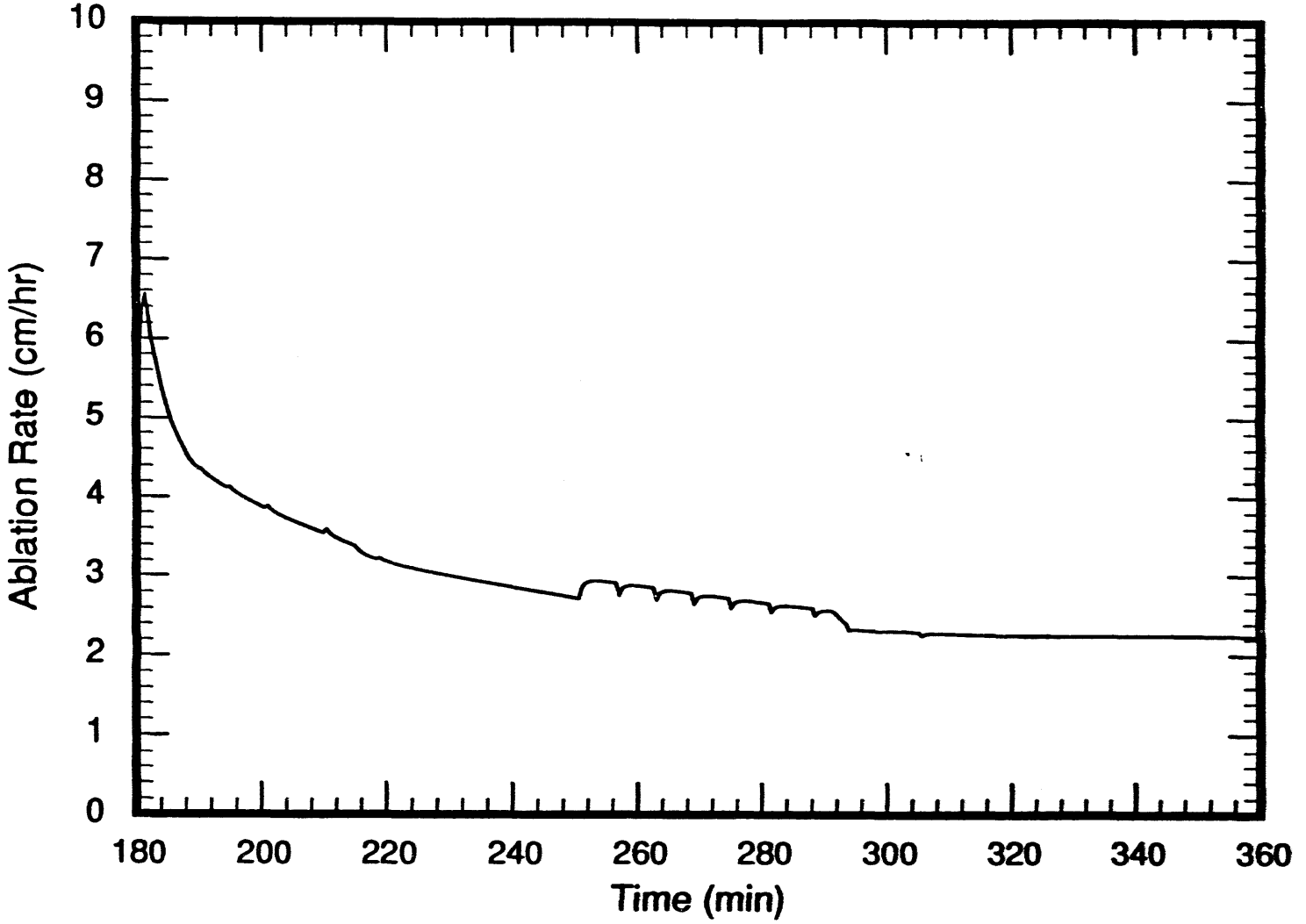

Figure 6.1 Axial ablation rate calculated for the CORCON standard problem

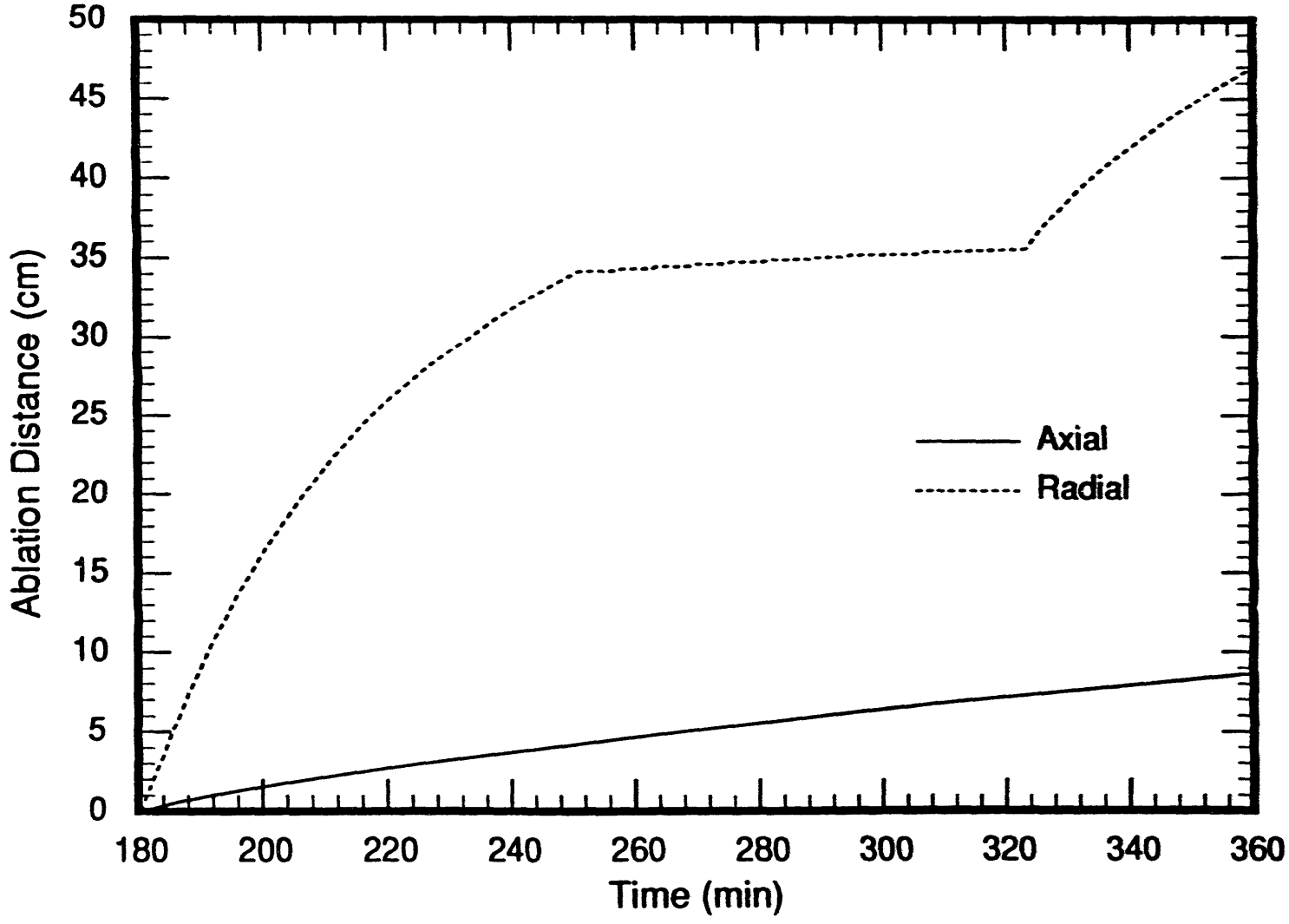

Figure 6.2 Axial and radial ablation distance calculated for the CORCON standard problem

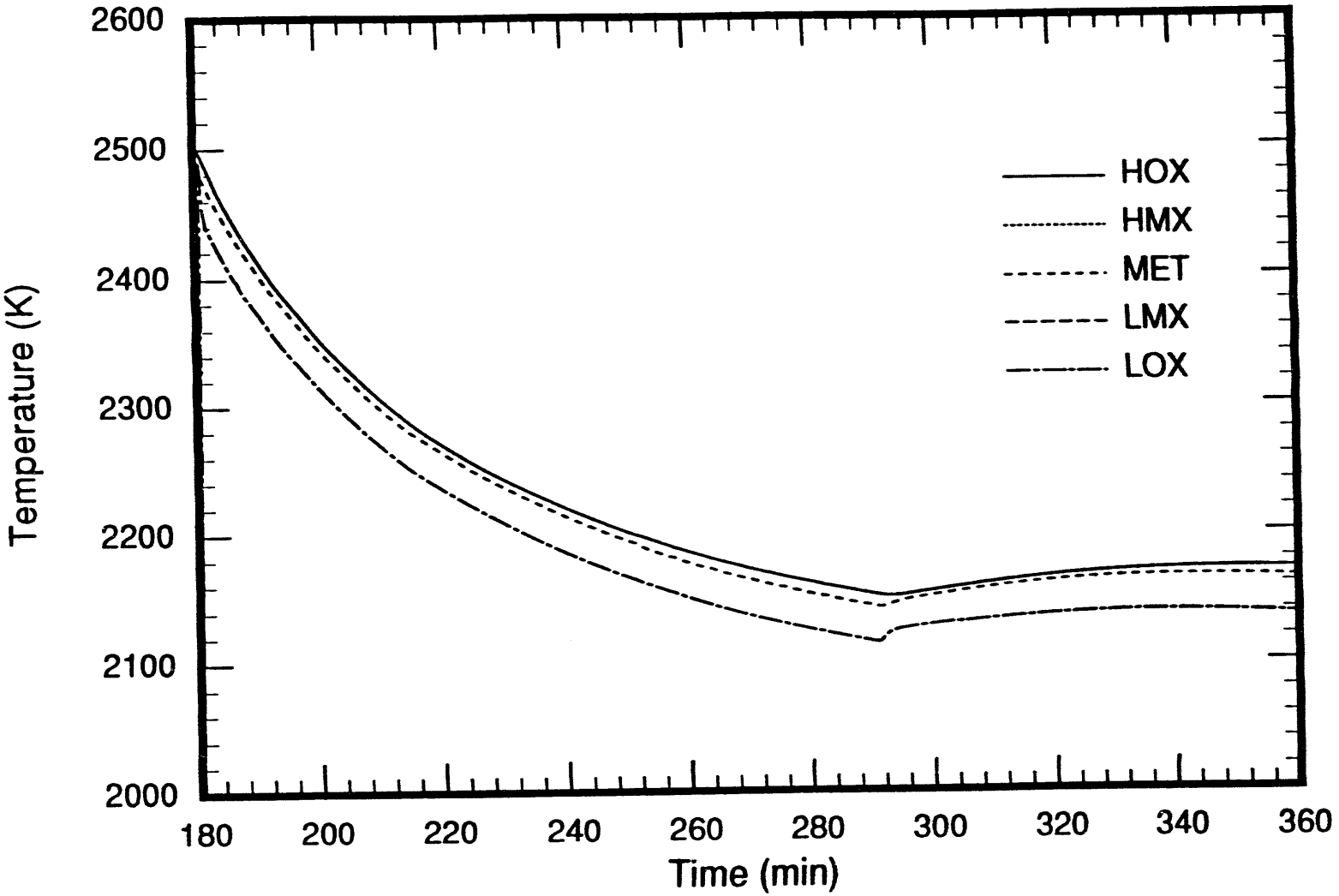

Figure 6.3 Layer temperatures calculated for the CORCON standard problem

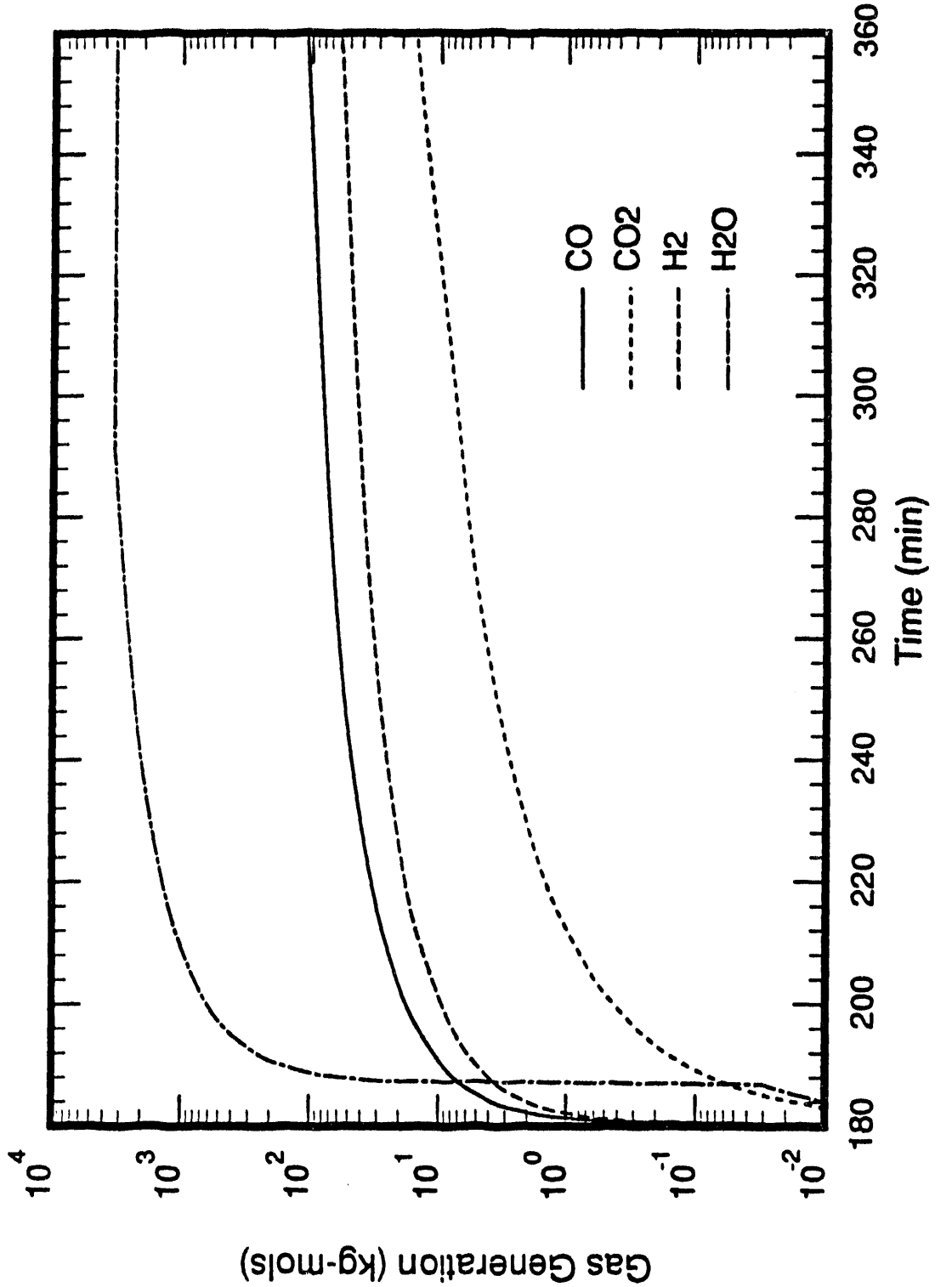

Figure 6.4 Cumulative gas generation calculated for the CORCON standard problem

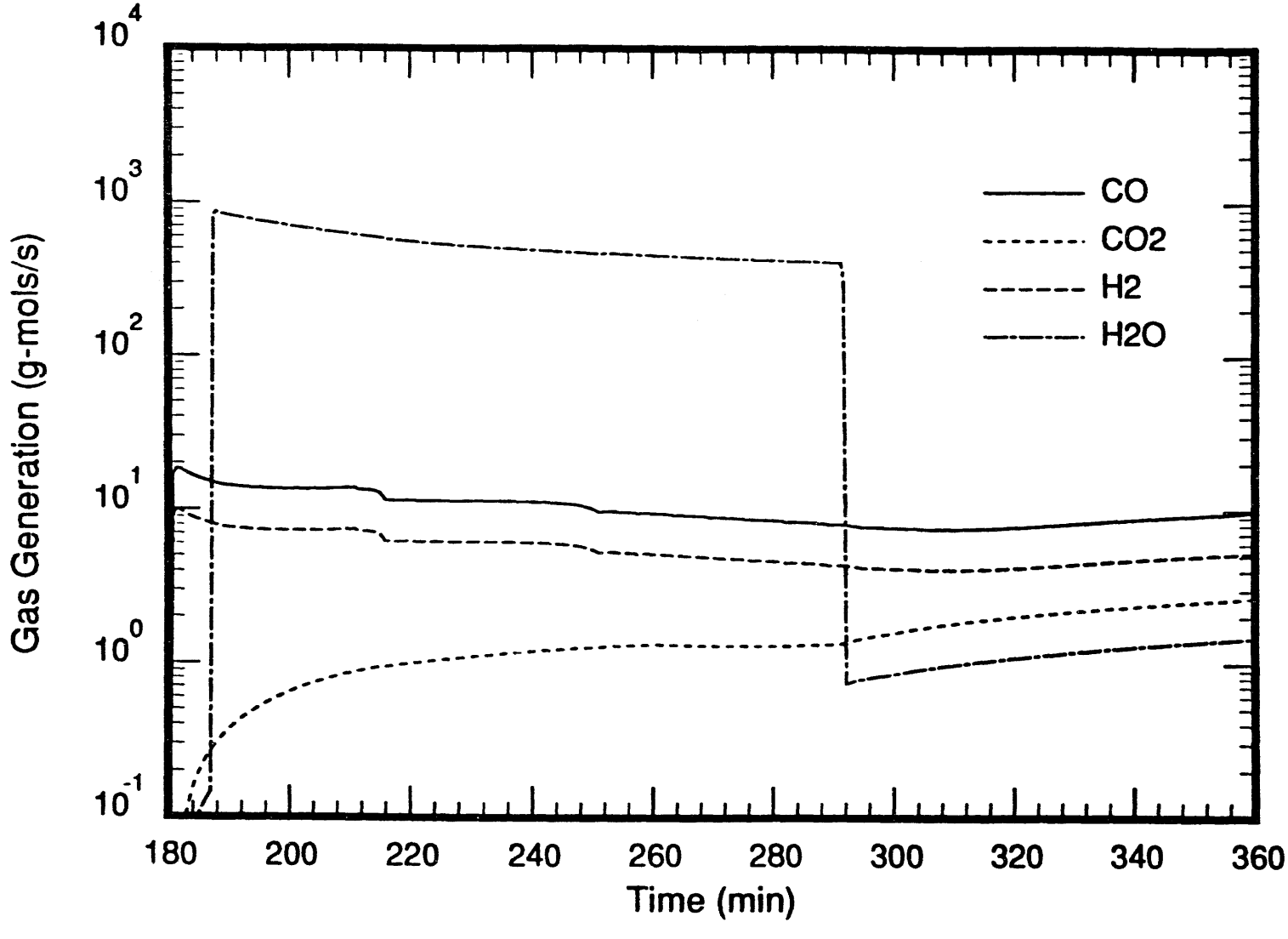

Figure 6.5 Gas generation rate calculated for the CORCON standard problem

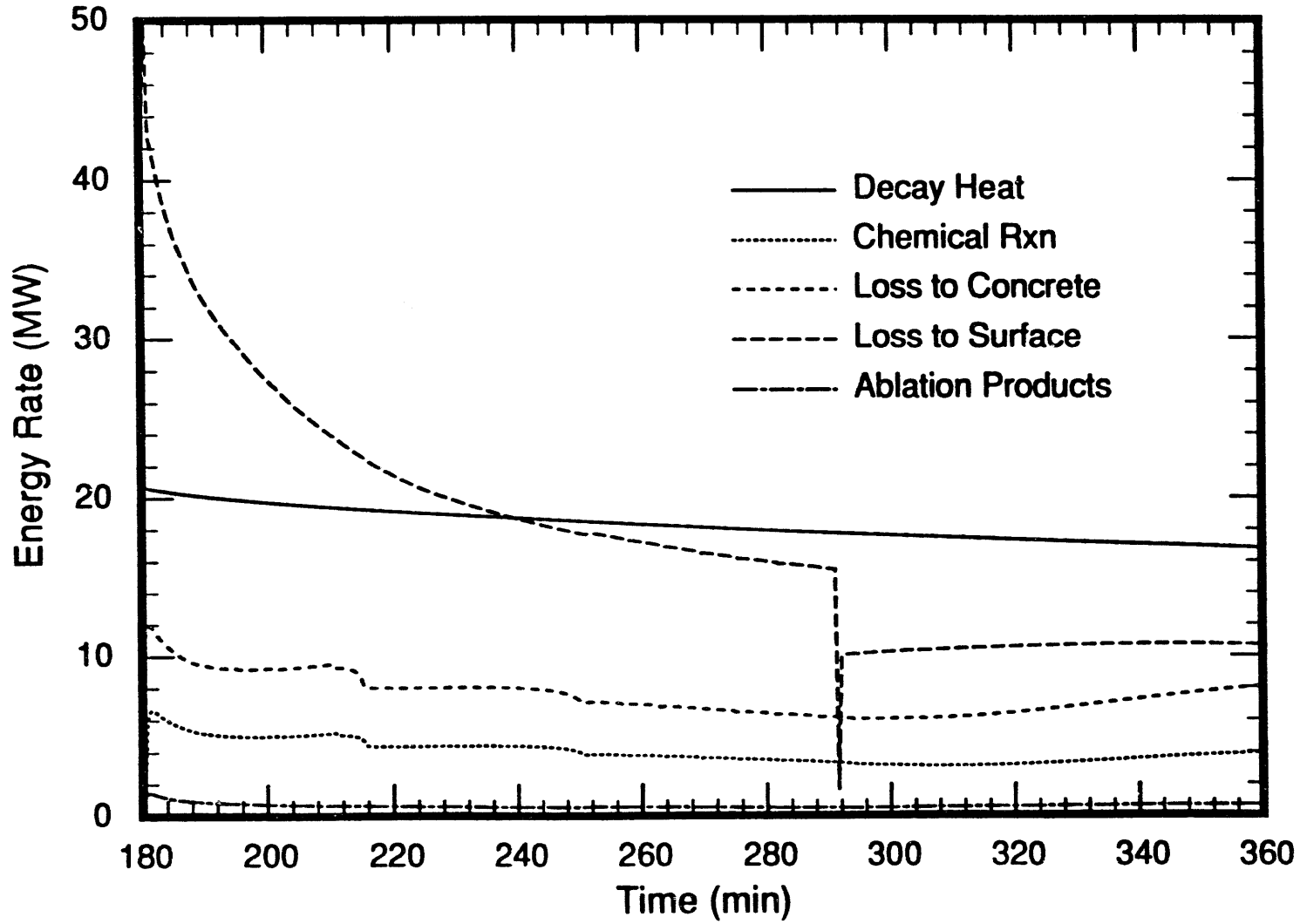

Figure 6.6 Energy terms calculated for the CORCON standard problem

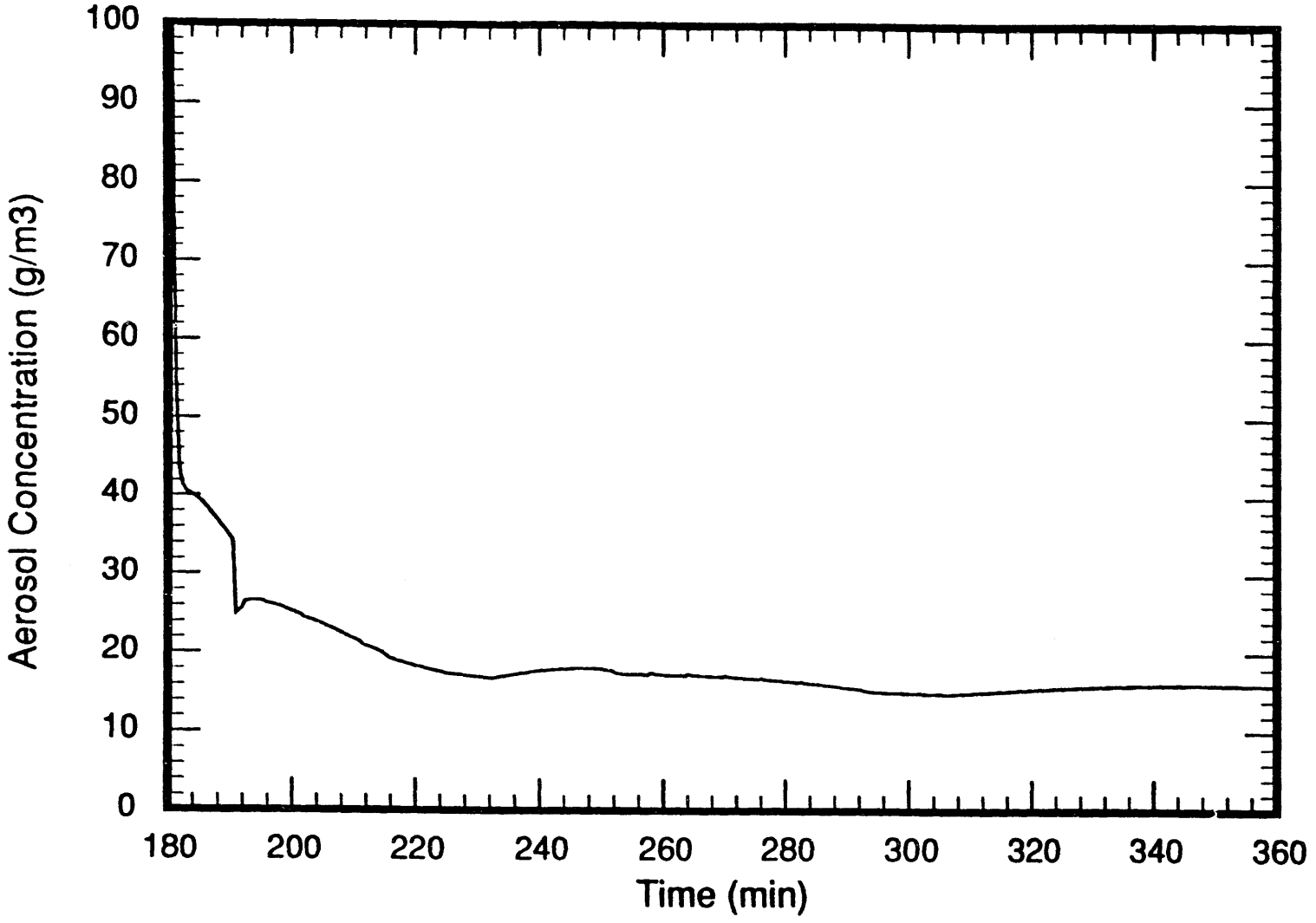

Figure 6.7 Aerosol concentration (ambient conditions) calculated for the CORCON standard problem

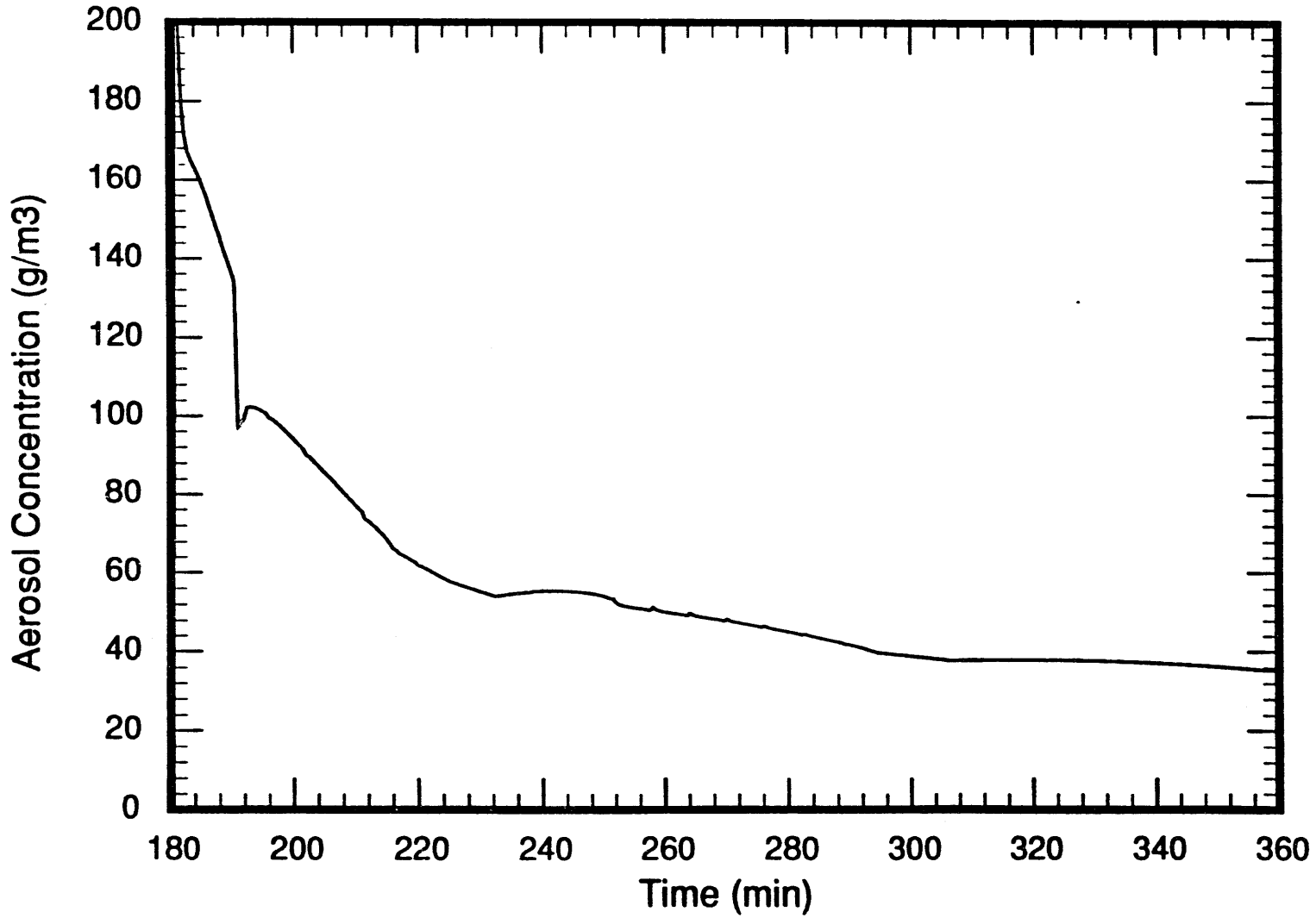

Figure 6.8 Aerosol concentration (STP) calculated for the CORCON standard problem

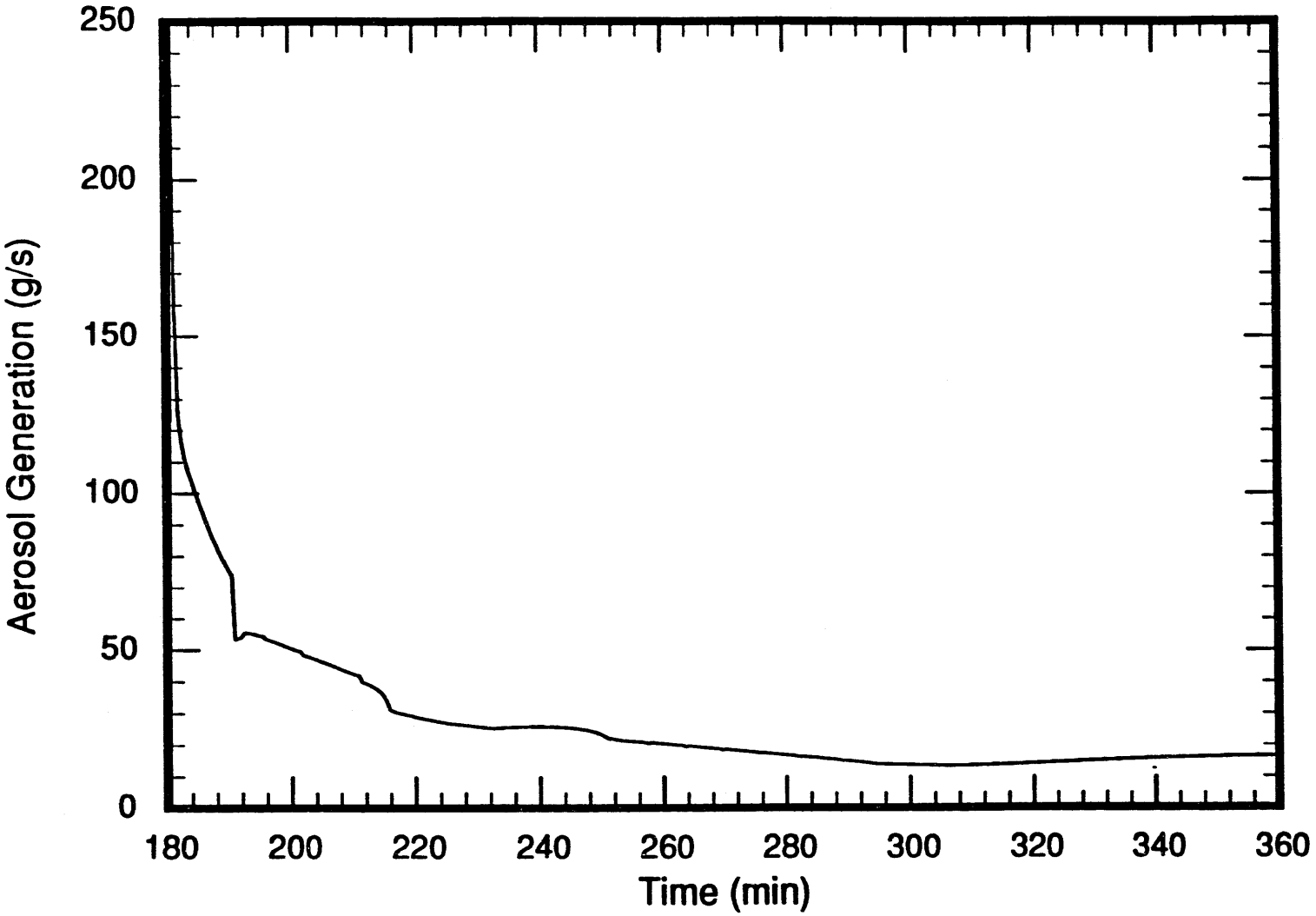

Figure 6.9 Aerosol generation rate calculated for the CORCON standard problem

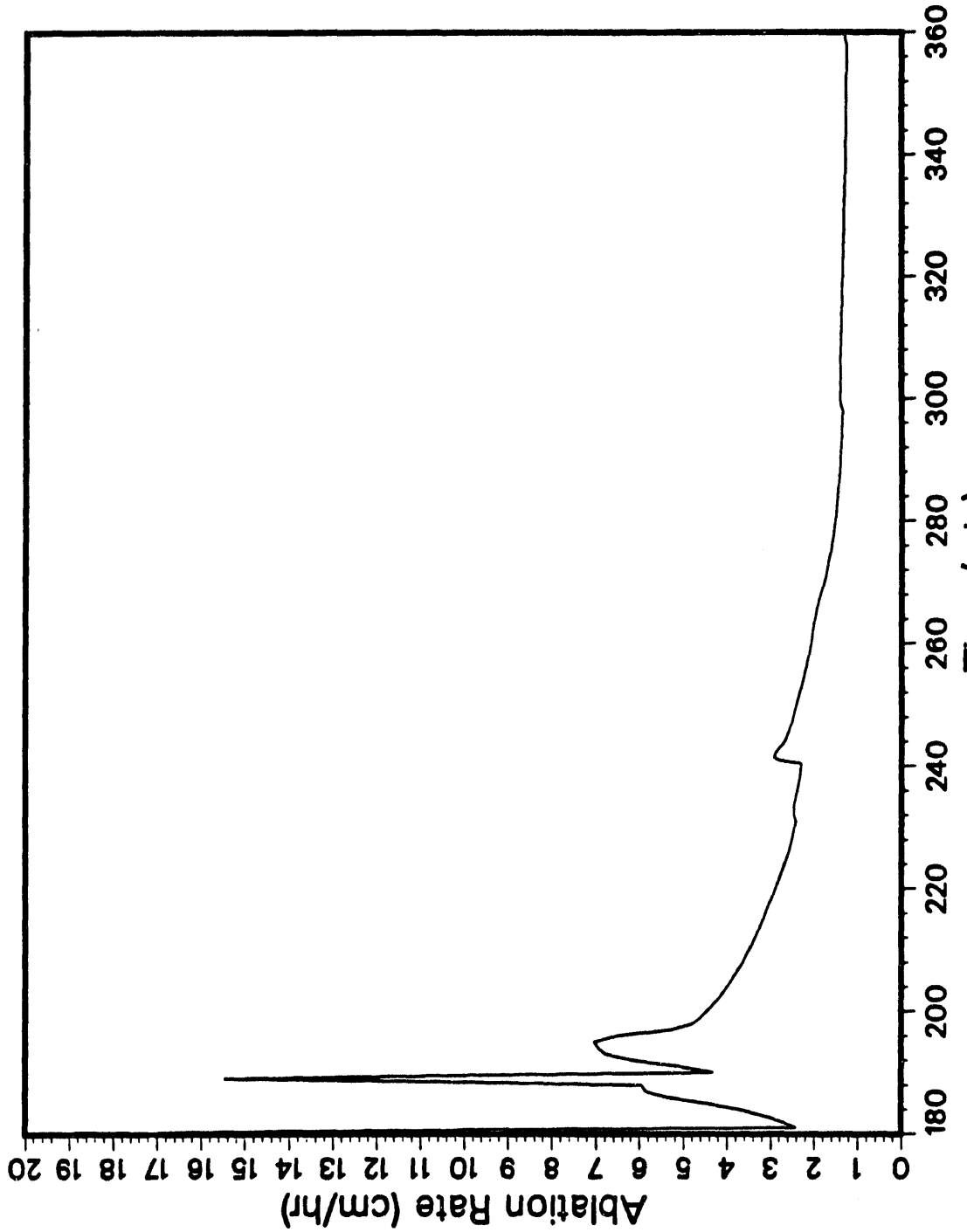

Figure 6.10 Axial ablation rate calculated for the BWR sample problem

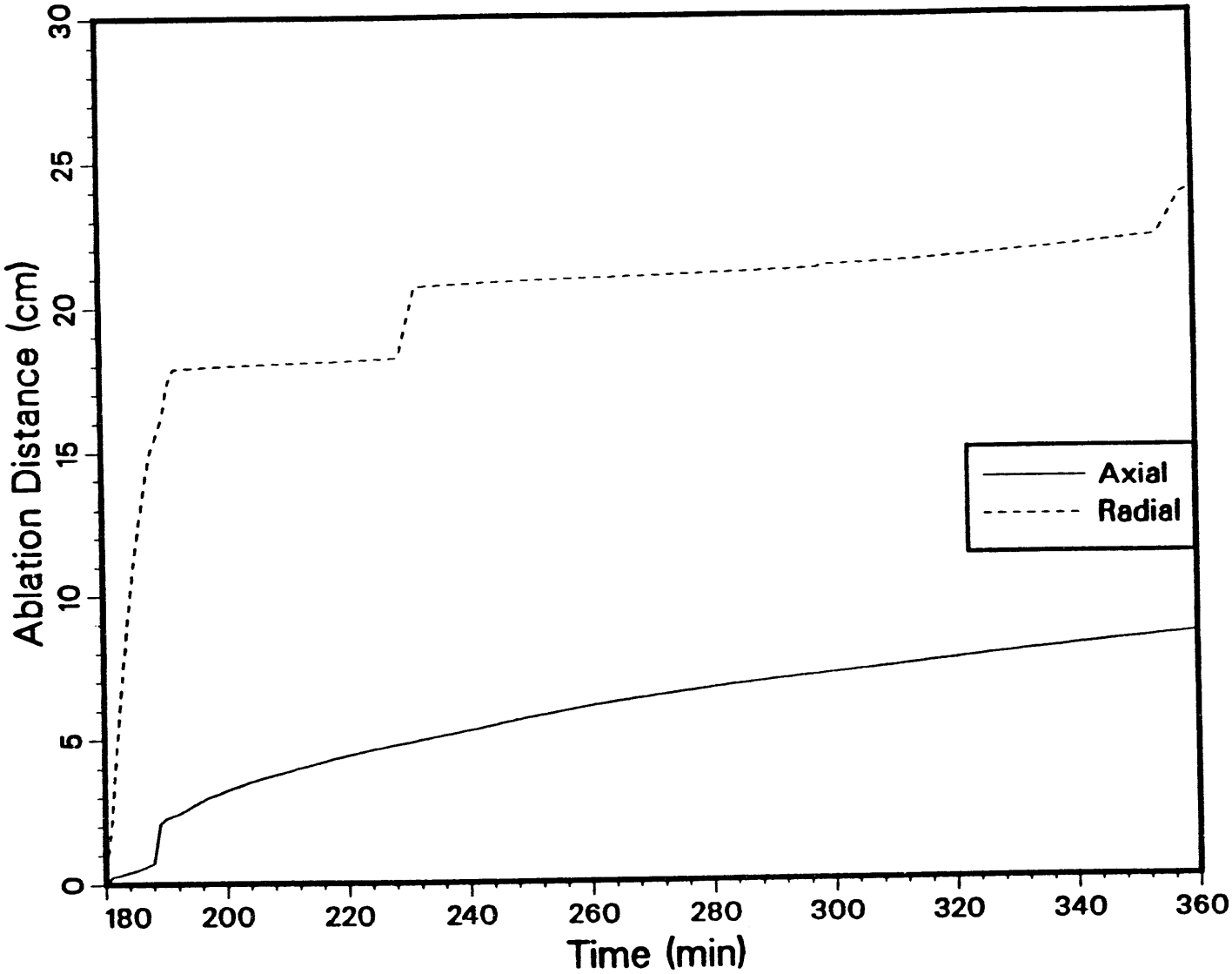

Figure 6.11 Axial and radial ablation distances calculated for the BWR sample problem

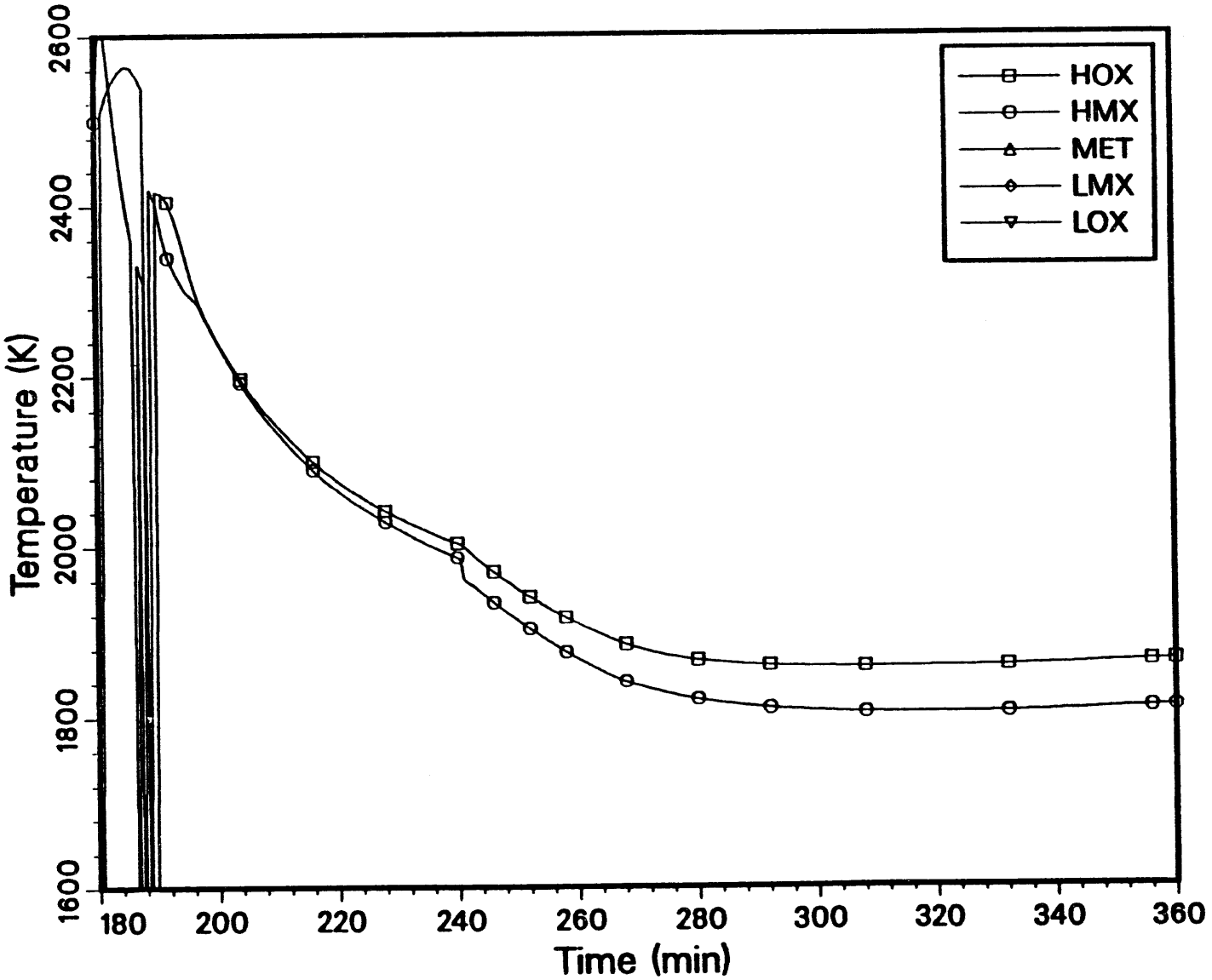

Figure 6.12 Layer temperatures calculated for the BWR sample problem

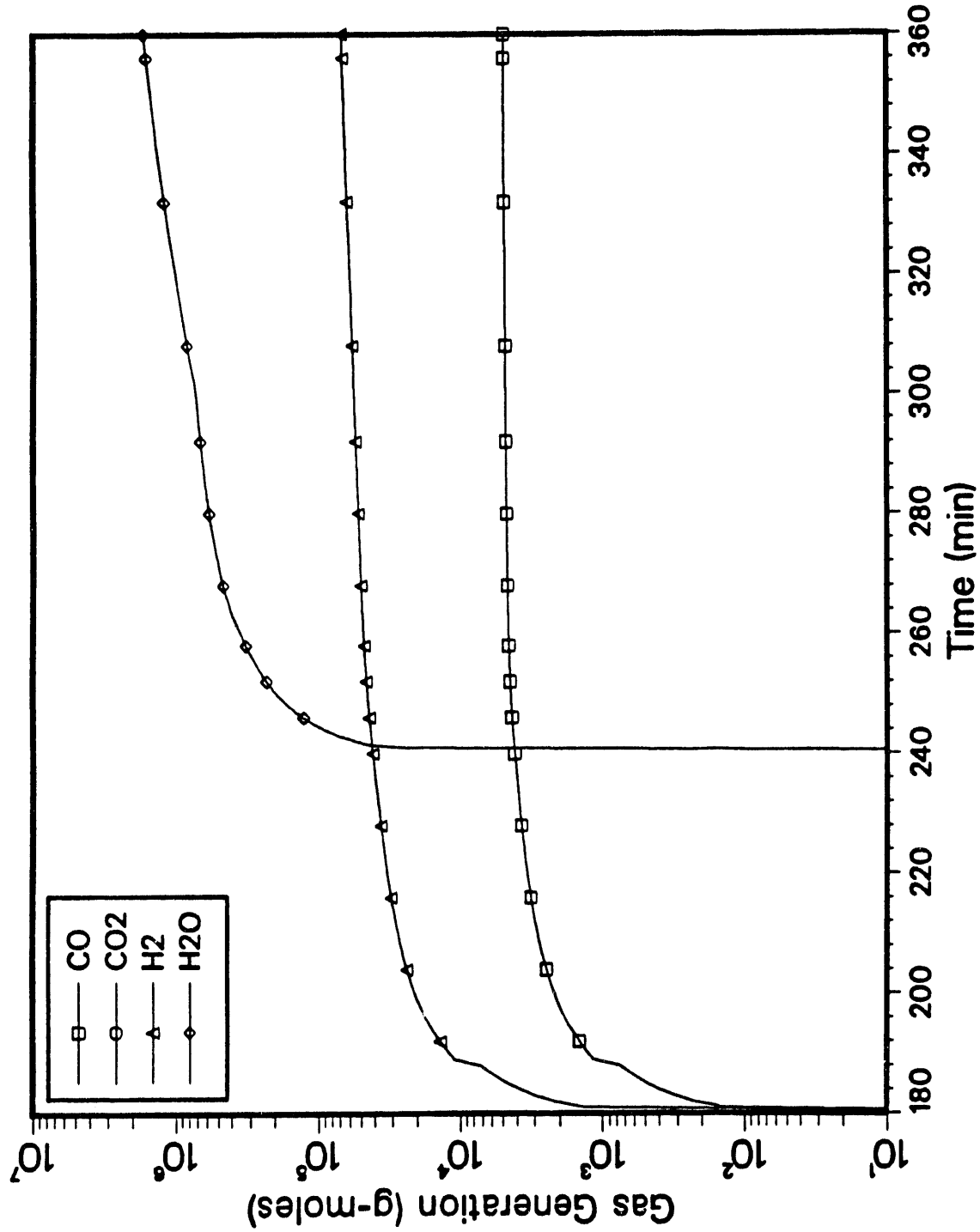

Figure 6.13 Cumulative gas generation calculated for the BWR sample problem

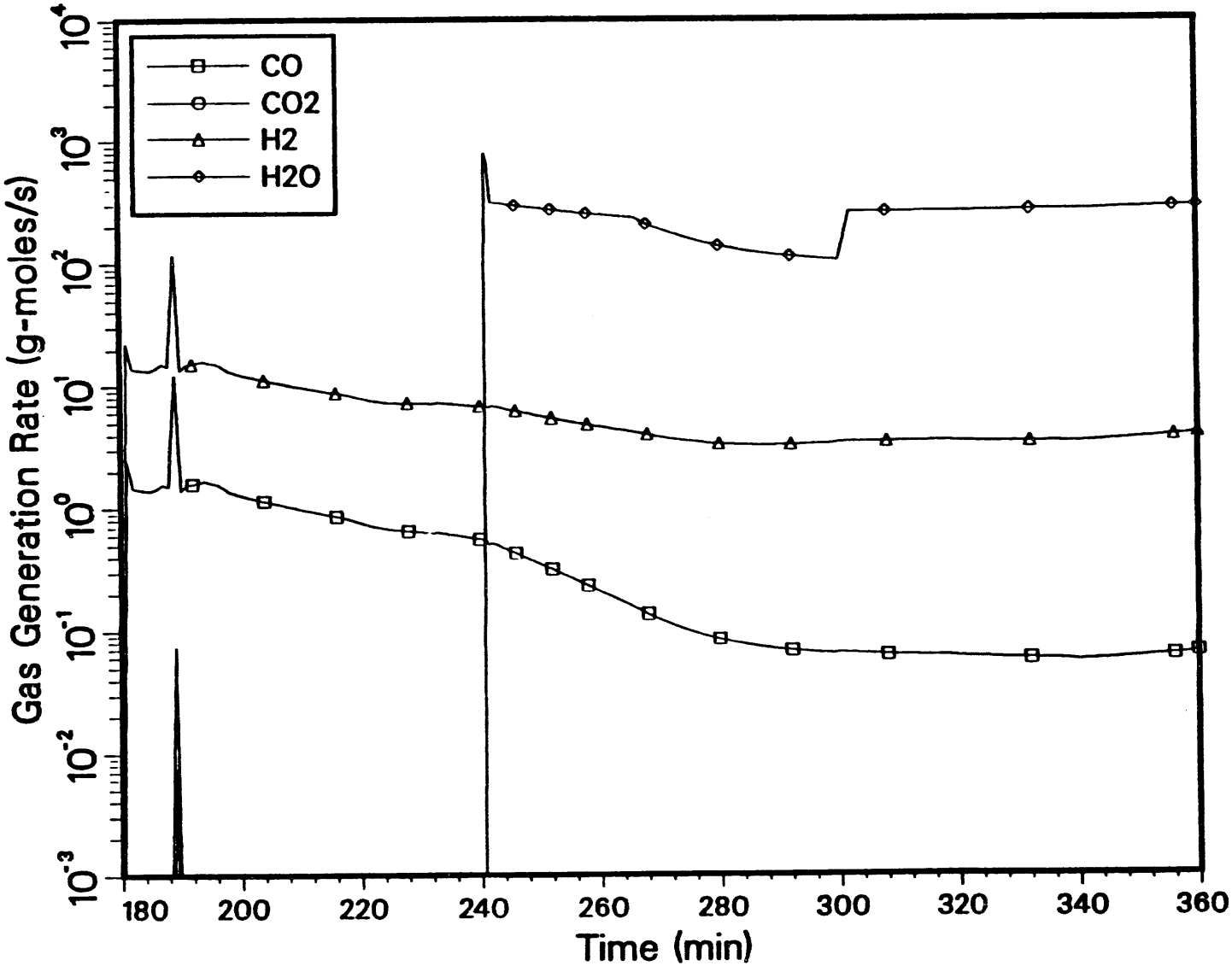

Figure 6.14 Gas generation rate calculated for the BWR sample problem

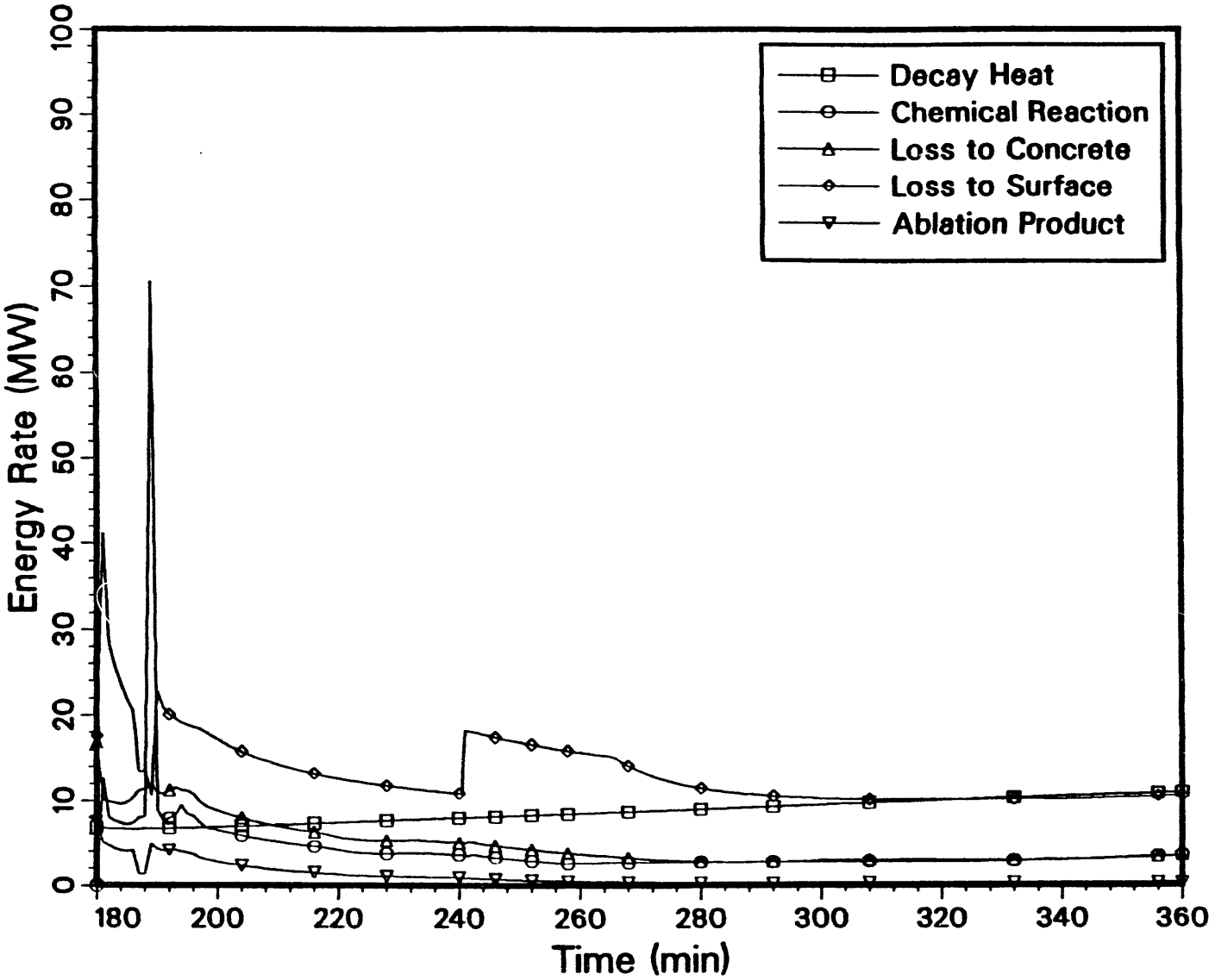

Figure 6.15 Energy terms calculated for the BWR sample problem

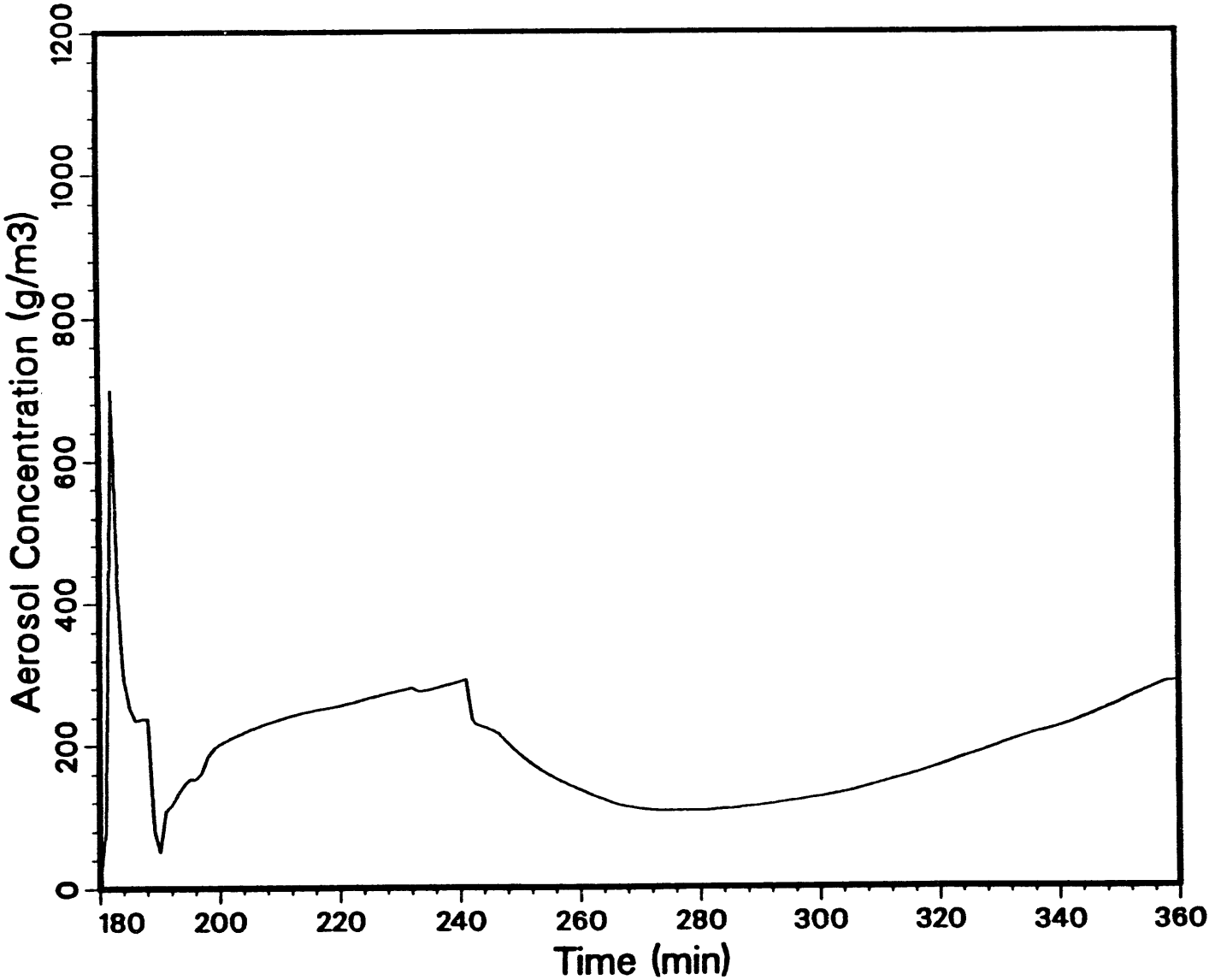

Figure 6.16 Aerosol concentration (ambient conditions) calculated for the BWR sample problem

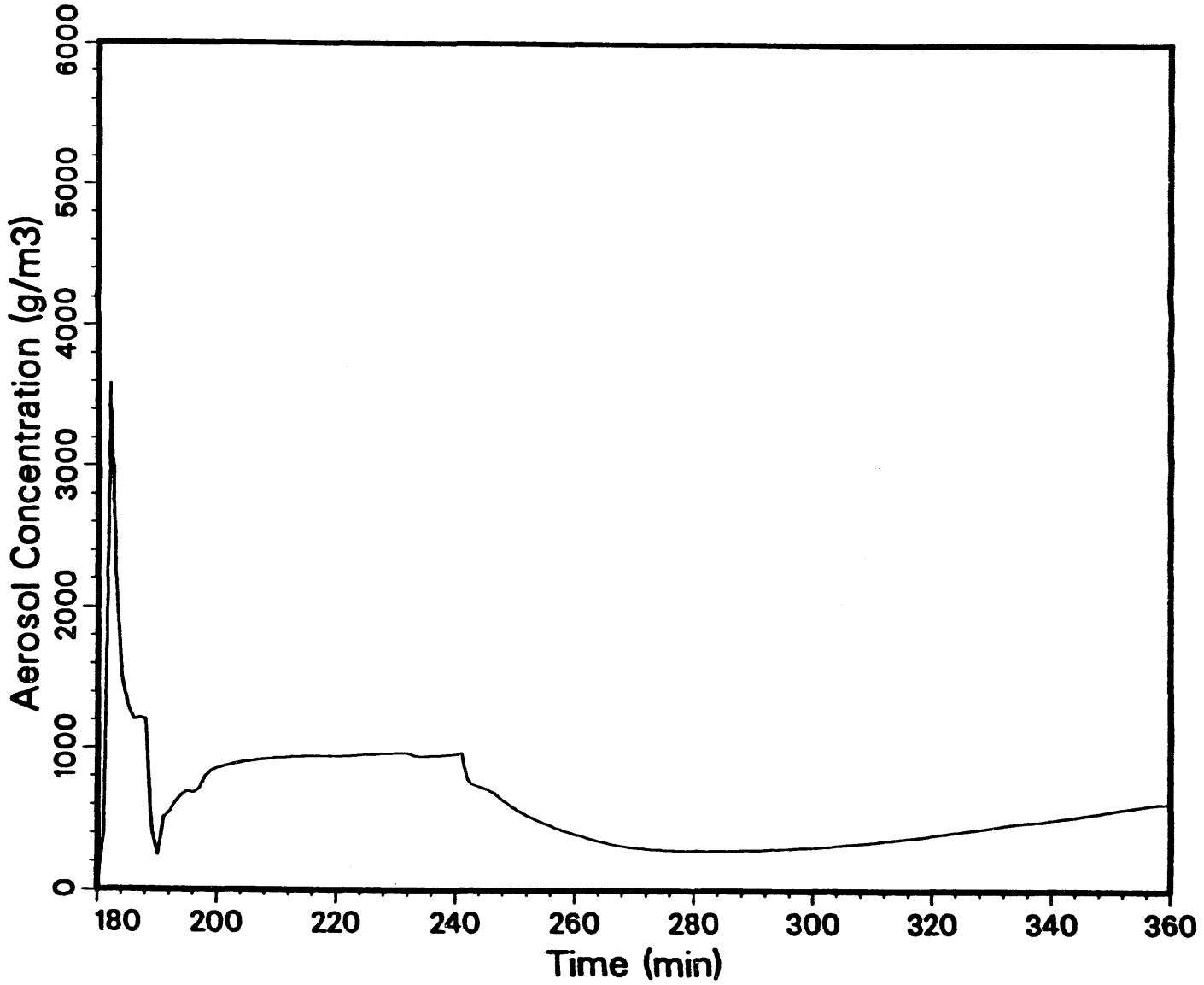

Figure 6.17 Aerosol concentration (STP) calculated for the BWR sample problem

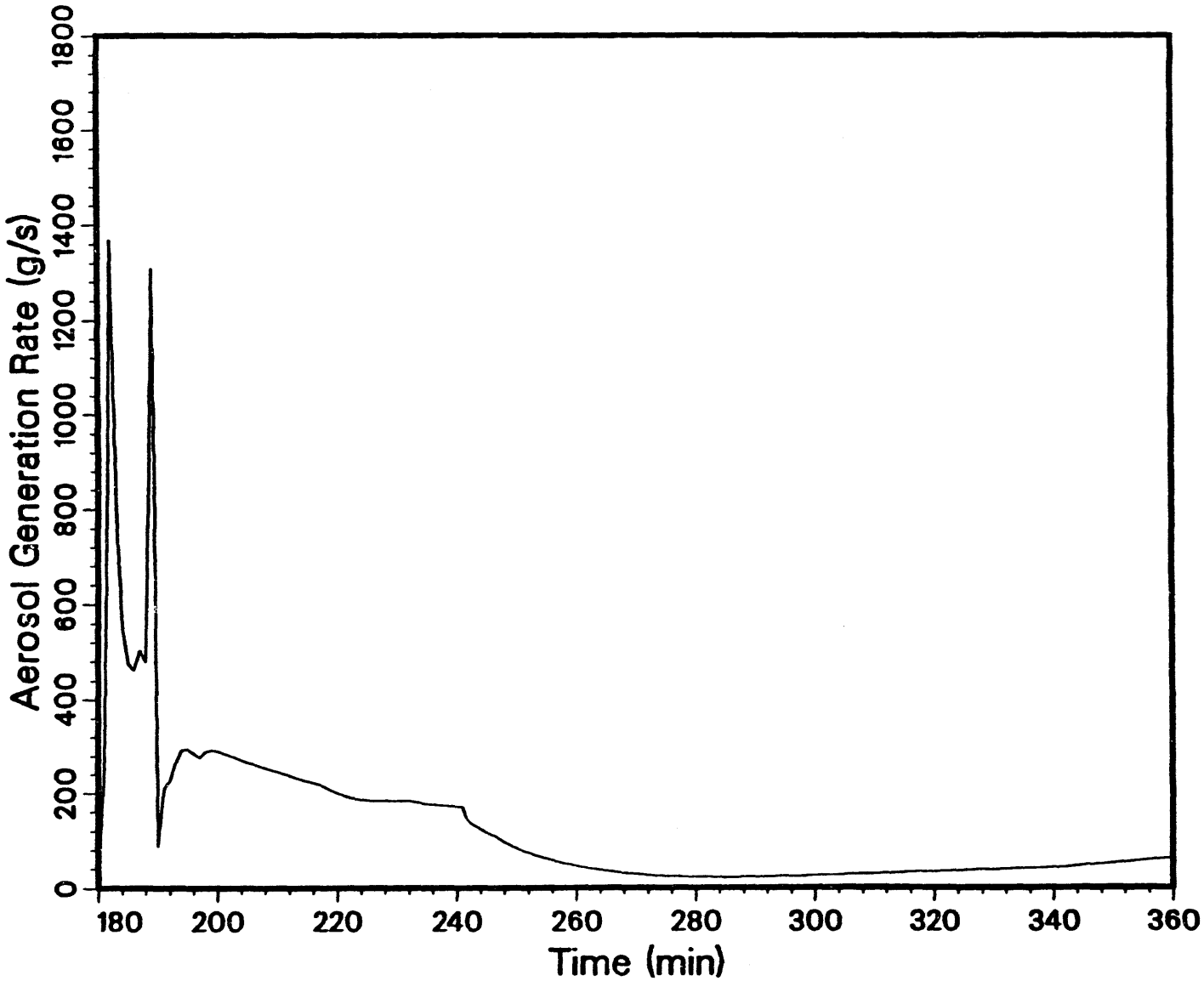

Figure 6.18 Aerosol generation rate calculated for the BWR sample problem

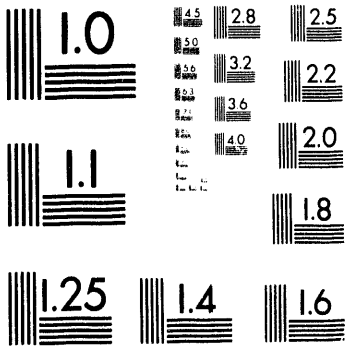
1.0
1.1
1.25
1.4
1.6
1.8
2.0
2.2
2.5
2.8
3.2
3.6
4.0
4.5
5.0
5.6
6.3
7.1

3 of 3

Table 6.1 Input listing for the CORCON standard problem

```
CORCON STANDARD PROBLEM (slightly different from Mod1/Mod2 problem)
$
$ user flags
$   *ILYR (stratified, mixing off)
$   ^                  *ICHEM (condensed phase chemistry off, coking off)
$   ^                  ^                                  *IFILM (slag/film)
$                                                         ^          *IMOV (movies)
    0    1    2    2    0    0    1    0    0  180    1    0    1    1    0    1
$ additional user flags
$        *IFVAN (do VANESA calculation)
&   0    1    0    0
$
$ time information
      30.0    10800.    21600.              70000.
$
$ ray system information
   60        0.0       1.5
$
$ geometry information - rt. circular cylinder 3.2 m radius
       0.0       3.0       5.00       0.1       4.0       2.0   10    6
$
$ concrete specifications - abl temp = 1650 K
     300.0     1650.        .6      .135
$
$ initial debris composition and temperature (T = 2500 K)
    3    4     2500.     2500.
UO2            1.0E5
ZRO2           1.4E4
FEO            6.0E3
ZR             1.0E4
FE             4.0E4
CR             1.0E4
NI             6.0E3
$
$ core MTU and operating power
       90.     3400.    0
$
$ initial water inventory and temperature - 60000 kg. subcooled
      322.
H2O            6.0E4
$
$ cavity atmosphere conditions and composition
     5.0E4       0.0       380.    2
H2             0.5
H2O            0.5
$
$ pressure in cavity vs. time (Pa)
    2
   10800.0     1.5E5   21600.0     3.0E5
```

Table 6.1 Input listing for the CORCON standard problem (continued)

```
$
$ temperature of surfaces above melt
    2
   10800.0      400.0   21600.0      800.0
$
$ emissivities vs. time - oxides, metals, surroundings
TIMETIMETIME
    1    1    1
       0.0        0.8
       0.0        0.6
       0.0        0.6
$
$ mean beam length for atmospheric opacity calculation (m)
       3.0
$
$ VANESA input
$ user options
$                    * IDEAL=1, run with ideal chemistry turned on
    1    1    1    1
$
$ pool scrubbing parameters
        20       2.3         1         1       1.0       1.0
```

Table 6.2 Output listing for the CORCON standard problem

```
CARD IMAGES IN INPUT FILE (TAPE5)
1.   CORCON STANDARD PROBLEM (slightly different from Mod1/Mod2 problem)
     $
     $ user flags
     $   *ILYR (stratified, mixing off)
     $   ^                  *ICHEM (condensed phase chemistry off, coking off)
     $   ^                  ^                                *IFILM (slag/film)
2.       0    1    2    2    0    0    1    0    0  180    1    0    0    1    0    1
     $ additional user flags
     $         *IFVAN (do VANESA calculation)
3.   &   0    1    0    0
     $
     $ time information
4.         30.0    10800.    21600.              70000.
     $
     $ ray system information
5.      60       0.0       1.5
     $
     $ geometry information - rt. citcular cylinder 3.2 m radius
6.         0.0       3.0       5.00       0.1       4.0       2.0   10    6
     $
     $ concrete specifications - abl temp = 1650 K
7.       300.0     1650.        .6      .135
     $
     $ initial debris composition and temperature (T = 2500 K)
8.       3    4     2500.     2500.
9.   UO2             1.0E5
10.  ZRO2            1.4E4
11.  FEO             6.0E3
12.  ZR              1.0E4
13.  FE              4.0E4
14.  CR              1.0E4
15.  NI              6.0E3
     $
     $ core MTU and operating power
16.        90.     3400.    0
     $
     $ initial water inventory and temperature - 60000 kg. subcooled
17.        322.
18.  H2O             6.0E4
     $
     $ cavity atmosphere conditions and composition
19.       5.0E4       0.0      380.    2
20.  H2              0.5
21.  H2O             0.5
     $
     $ pressure in cavity vs. time (Pa)
22.      2
```

Table 6.2 Output listing for the CORCON standard problem (continued)

```
23.      10800.0     1.5E5   21600.0     3.0E5
         $
         $ temperature of surfaces above melt
24.        2
25.      10800.0     400.0   21600.0     800.0
         $
         $ emissivities vs. time - oxides, metals, surroundings
26.      TIMETIMETIME
27.        1    1    1
28.           0.0       0.8
29.           0.0       0.6
30.           0.0       0.6
         $
         $ mean beam length for atmospheric opacity calculation (m)
31.           3.0
         $
         $ VANESA input
         $ user options
32.        1    1    1
         $
         $ pool scrubbing parameters
33.            20       2.3         1         1       1.0       1.0
```

Table 6.2 Output listing for the CORCON standard problem (continued)

```
                CORCON STANDARD PROBLEM (slightly different from Mod1/Mod2 problem)

                                        * * *  I N P U T  * * *


                          ***  FLAGS  ***                          ***  CONTROL PARAMETERS  ***
     ILYR  = 0    ICOOL  = 1    IGEOM  = 2    ICON   = 2     TIMEO  = 10800.00 (SEC)    DELTIM =  30.0000 (SEC)
     ICHEM = 0    IFP    = 0    ISUR   = 1    IABL   = 0     TIMEND = 21600.00 (SEC)
     ISPLSH= 0    IPINC  =**    IFILM  = 1    IRSTRT = 0     DPRIN  =     0.00 (SEC)    TPRIN  = 70000.00 (SEC)
     IMOV  = 0    IPG    = 1    ISRABL = 0    IAOPAC = 1
     ITIMR = 0    IFVAN  = 1    IVANFP = 0    IUSER  = 0

 TIMESTEP CONTROL.  DTMIN(I)  DTMAX(I)      TIMDT(I)
                      30.000    30.000     1.000E+10

 EDIT CONTROL.  DEDIT(I)      TEDIT(I)
                5400.000     1.000E+10
                                    RAY CENTER COORDINATES

                               R0 =  0.000000E+00          Z0 =   1.50000

                                        CONCRETE CAVITY GEOMETRY

                                            RIGHT CYLINDER

                                   NRAYS - NUMBER OF RAYS =   60

                                   ZT - Z-COORDINATE OF TOP =   0.000000E+00

                                   RAD - CYLINDER RADIUS (M) =    3.00000

                                   HIT - CYLINDER HEIGHT (M) =    5.00000

                                   RADC - CORNER RADIUS (M) =   0.100000

                                   NBOT - NUMBER OF BOTTOM POINTS =   10

                                   NCORN = NUMBER OF CORNER POINTS =    6
```

* * * CONCRETE SPECIFICATIONS * * *

LIMESTONE AGGREGATE - COMMON SAND CONCRETE

RHOC (KG/M3)	RBR (KG/KG C)	SI (-)	TSOL (K)	TLIQ (K)	TIC (K)	TW (K)	DELH (J/KG)	EW (-)
2.340000E+03	1.350000E-01	2.585400E-01	1.420000E+03	1.670000E+03	3.000000E+02	1.650000E+03	3.118502E+06	6.000000E-01

SPECIES NAME	MASS FR.(KG/KG C)	MOLECULAR WT.
SIO2	0.3580	60.0843
TIO2	0.0018	79.8988
MNO	0.0003	70.9374
MGO	0.0048	40.3044
CAO	0.3130	56.0794
NA2O	0.0008	61.9790
K2O	0.0122	94.1960
FE2O3	0.0144	159.6922
AL2O3	0.0360	101.9613
CR2O3	0.0001	151.9902
CO2	0.2115	44.0098
H2OEVAP	0.0270	18.0152
H2OCHEM	0.0200	18.0152

MELT FISSION PRODUCT INVENTORY
BASED ON 9.00000E+01 METRIC TON URANIUM CORE OPERATED AT 3.40000E+03 MW(THERMAL)
MELT CONTAINS 8.81390E+01 METRIC TONS URANIUM, CORRESPONDING TO 97.93 PERCENT OF CORE

ELEMENTS, RETAINED FRACTIONS (**DENOTES USER INPUT, OTHERS FROM WASH 1400), AND GRAM-ATOMS IN MELT

MO	(0.970)	1.8885E+03	TC	(0.970)	4.8318E+02	RU	(0.970)	1.1976E+03	RH	(0.970)	2.1821E+02
SB	(0.850)	6.5124E+00	TE	(0.850)	1.6880E+02	SR	(0.900)	6.3021E+02	BA	(0.900)	5.5260E+02
ZR	(0.990)	2.3563E+03	CE	(0.990)	1.2329E+03	NP	(0.990)	1.2203E+02	CM	(0.990)	5.0995E+00
NB	(0.990)	3.6129E+01	PU	(0.990)	2.2541E+03	AM	(0.990)	1.6241E+01	Y	(0.990)	3.5403E+02
LA	(0.990)	5.3006E+02	PR	(0.990)	4.6084E+02	ND	(0.990)	1.4801E+03	SM	(0.990)	1.7342E+02
EU	(0.990)	5.1556E+01	RB	(0.190)	5.0434E+01	CS	(0.190)	2.2933E+02	BR	(0.100)	1.7078E+00
I	(0.100)	1.0109E+01									

FISSION PRODUCTS GROUPED AS 4 PSEUDO-SPECIES

3.96277E+03 GRAM-ATOMS OF FPM WITH ATOMIC FRACTIONS

MO	4.76552E-01	TC	1.21930E-01	RU	3.02216E-01	RH	5.50639E-02	SB	1.64339E-03		
TE	4.25953E-02										

Table 6.2 Output listing for the CORCON standard problem (continued)

```
1.02555E+04 GRAM-ATOMS OF FPOX     WITH ATOMIC FRACTIONS
      SR  6.14511E-02          BA  5.38829E-02          ZR  2.29756E-01          CE  1.20214E-01          NP  1.18992E-02
      CM  4.97248E-04          NB  3.52284E-03          PU  2.19792E-01          AM  1.58367E-03          Y   3.45213E-02
      LA  5.16855E-02          PR  4.49355E-02          ND  1.44321E-01          SM  1.69103E-02          EU  5.02712E-03

2.79767E+02 GRAM-ATOMS OF FPALKMET WITH ATOMIC FRACTIONS
      RB  1.80272E-01          CS  8.19728E-01

1.18168E+01 GRAM-ATOMS OF FPHALOGN WITH ATOMIC FRACTIONS
      BR  1.44524E-01          I   8.55476E-01

                  INITIAL POWER AT START OF CORCON, 1.08000E+04 SEC AFTER SCRAM IS 2.06797E+07 WATTS
                      REPRESENTING   0.62 PERCENT OF OPERATING POWER OF FRACTION OF CORE IN MELT

                                  INITIAL CORE MASSES (KG) OF CONSTITUENTS AND TEMPERATURES

               OXIDES            SPEMW          CONINP          METALS            SPEMW          CONINP

                FEO          7.1846397E+01  6.0000000E+03        FE          5.5847000E+01  4.0000000E+04
                UO2          2.7002780E+02  1.0000000E+05        CR          5.1995998E+01  1.0000000E+04
                ZRO2         1.2321880E+02  1.4000000E+04        NI          5.8709999E+01  6.0000000E+03
                FPOX         1.4748473E+02  1.5125297E+03        ZR          9.1220001E+01  1.0000000E+04
                FPALKMET     1.2435149E+02  3.4789448E+01        FPM         9.9529678E+01  3.9441333E+02
                FPHALOGN     1.2011028E+02  1.4193141E+00

INITIAL TEMPERATURE (TO) IN DEGREES K =     2.5000000E+03

INITIAL TEMPERATURE (TM) IN DEGREES K =     2.5000000E+03

INITIAL MASS OF OXIDES =     1.2154874E+05

INITIAL MASS OF METALS =     6.6394414E+04
                                                                  COOLANT IS H2O
INITIAL MASS OF COOLANT =     6.0000000E+04

INITIAL TEMPERATURE OF COOLANT =     3.2200000E+02

                                                * * * REACTING GAS MIXTURE * * *

      ***  ATMOSPHERIC PRESSURE SPECIFIED AS OF TIME  ***
      TIME  1.0800E+04  2.1600E+04
  PRESSURE  1.5000E+05  3.0000E+05

                                                VA                PA                TA
                                               (M3)            (N/M2)          (DEG K)

                                          5.0000000E+04     1.5000000E+05     3.8000000E+02
```

Table 6.2 Output listing for the CORCON standard problem (continued)

```
                                        GAS INPUT

                                SPECIES NAME     MOLE FR. (-)    MOLECULAR WT.

                                     H2              0.5000          2.0158
                                     H2O             0.5000         18.0152

***  MELT INTERNAL CONDITIONS  ***

***  BOUNDARY CONDITIONS - SURROUNDINGS ABOVE MELT  ***

     ***  SURFACE TEMPERATURE VARIATION WITH TIME  ***

          ***  TS(DEG K) INPUT AS TABLES .VS. TIME  ***

               TIME(SEC)      TS(DEG K)
                1.0800E+04     4.0000E+02
                2.1600E+04     8.0000E+02

     ***  SURROUNDINGS MATERIAL MELTING OR ABLATION DURING INTERACTION  ***

          ***  ABLATION OF SURROUNDINGS IS COMPUTED IN PROGRAM  ***

***  BOUNDARY CONDITIONS - RADIATIVE HEAT TRANSFER  ***

                                    ***  SURFACE EMISSIVITIES .VS. TIME OR TEMP.  ***

    TIME  0.0000E+00
      EO  8.0000E-01

    TIME  0.0000E+00
      EM  6.0000E-01

    TIME  0.0000E+00
      ES  6.0000E-01

     ***  AEROSOL OPACITY INCLUDED IN ATMOSPHERE  ***
            CHARACTERISTIC PATH LENGTH (M) =  3.0000E+00

     ***  NO MELT/COOLANT SPLASHOUT  ***

     ***  NO TIME-DEPENDENT MELT RADIUS USED  ***

*** PLOTS WERE NOT SPECIFIED, IMOV = 0

                                *** ADDITIONAL USER SUPPLIED MODEL INPUTS ***

                    *** THIS CALCULATION IS BEING PERFORMED USING THE DEFAULT CORCON MODELS
```

Table 6.2 Output listing for the CORCON standard problem (continued)

```
                    * * * VANESA INPUT * * *


      BUBBLE DIAMETER IS CALCULATED
    PARTICLE DIAMETER =     1.00 MICROMETERS
     PARTICLES/BUBBLE IS CALCULATED

            INITIAL MELT COMPOSITION
            G-MOLES              KG
FE          716242.6        40000.000
CR          192322.5        10000.000
FEO          83511.5         6000.000
CR203            0.0            0.000
NI          102197.2         6000.000
MO           1888.7          181.198
RU           1899.3          191.966
SN              0.0            0.000
SB              6.5            0.793
TE            168.8           21.538
AG              0.0            0.000
MN              0.0            0.000
CAO             0.0            0.000
AL203           0.0            0.000
SIO2            0.0            0.000
UO2        370372.0       100000.000
ZRO2       113619.0        14000.000
CS2O          134.0           37.755
BAO           552.8           84.772
SRO           630.3           65.310
LA203        1524.8          496.813
CEO2         5976.6         1028.693
NBO            36.1            3.935
CSI            11.8            3.070
ZR         109625.1        10000.000

***  WATER POOL DECONTAMINATION  ***
INITIAL BUBBLE SIZE(CM)=     1.00
SIZE SEGMENTS IN DISTRIBUTION =   20
ALL SCAVENGING MECHANISMS ARE OPERATING
IMPACTION BASE ON V(REL)/V(RISE)=     1.00

GEOMETRIC STANDARD DEVIATION OF INPUT SIZE DISTRIBUION=  2.30


                    * * *   END OF INPUT  * * *
```

Table 6.2 Output listing for the CORCON standard problem (continued)

```
  TIME =  16200.00        CORCON STANDARD PROBLEM (slightly different from Mod1/Mod2 problem)                IT. NO. = 180
                                  ****GENERAL  SUMMARY****

MELT AND COOLANT LAYERS

  NUMBER OF LAYERS,    NLYR  = 4
  CONFIGURATION,       ILYR  = 4
  COOLANT PRESENT,     ICOOL = 1

EXTREME CAVITY DIMENSIONS, WITH LOCATIONS

      RADIAL                                              AXIAL
  MAXIMUM CAVITY RADIUS        (M) =   3.34555     DEEPEST POINT IN CAVITY      (M) =   5.05129
  OUTSIDE RADIUS OF CONCRETE   (M) =   4.00000     MAXIMUM DEPTH OF CONCRETE    (M) =   7.00000
  REMAINING THICKNESS          (M) =   0.65445     REMAINING THICKNESS          (M) =   1.94871
  CORRESPONDING BODY POINT          =        24     CORRESPONDING BODY POINT          =         1  APPROXIMATE OVERALL ENERGY BUDGET FOR DEBRIS
(SEE MANUAL FOR EXPLANATION AND CAVEATS)

  INTERNAL (DECAY) SOURCE      (W) =  1.813E+07
  CHEMICAL REACTION SOURCE     (W) =  3.591E+06

  HEAT LOSS TO CONCRETE        (W) =  6.680E+06
  HEATUP OF ABLATION PRODUCTS  (W) =  1.243E+06
  HEAT LOSS FROM SURFACE       (W) =  1.592E+07
    (TO COOLANT)

  CHANGE IN POOL ENTHALPY      (W) = -2.126E+06
   (SUMMATION OF M*DH/DT)

NUMERICAL CHECKS ON MASS AND ENERGY CONSERVATION

  RELATIVE ERROR IN MASS     =    9.41753E-06     RELATIVE ERROR IN ENTHALPY =    9.41753E-06

CHECK ON RECESSION CALCULATION (DD/DS SHOULD BE .LE. 1)

  MAXIMUM DD/DS =   0.01143
```

Table 6.2 Output listing for the CORCON standard problem (continued)

CORCON VERSION 2.26

TIME = 16200.00 CORCON STANDARD PROBLEM (slightly different from Mod1/Mod2 problem) IT. NO. = 180

* * * * G A S G E N E R A T I O N * * * *

GAS EXITING POOL (INCLUDES FILM AND COOLANT)

	GENERATION RATE		CUMULATIVE RELEASE		
SPECIES	MASS (KG/S)	MOLES (1/S)	MASS (KG)	MOLES (-)	SPECIES
C(G)	2.50932E-10	2.08918E-08	5.72707E-06	4.76819E-04	C(G)
CH4	1.59294E-04	9.92945E-03	4.06591E-01	2.53444E+01	CH4
CO	2.48936E-01	8.88729E+00	1.80765E+03	6.45349E+04	CO
CO2	5.87681E-02	1.33534E+00	2.26163E+02	5.13892E+03	CO2
C2H2	0.00000E+00	0.00000E+00	0.00000E+00	0.00000E+00	C2H2
C2H4	4.94777E-05	1.76372E-03	9.37977E-02	3.34359E+00	C2H4
C2H6	1.69260E-08	5.62896E-07	2.69389E-05	8.95890E-04	C2H6
H	2.04044E-05	2.02445E-02	3.34079E-01	3.31460E+02	H
H2	9.67077E-03	4.79748E+00	7.01920E+01	3.48209E+04	H2
H2O	7.62427E+00	4.23213E+02	5.01489E+04	2.78370E+06	H2O
N	0.00000E+00	0.00000E+00	0.00000E+00	0.00000E+00	N
NH3	0.00000E+00	0.00000E+00	0.00000E+00	0.00000E+00	NH3
N2	0.00000E+00	0.00000E+00	0.00000E+00	0.00000E+00	N2
O	1.91931E-12	1.19961E-10	4.64784E-07	2.90501E-05	O
O2	2.71057E-17	8.47086E-16	2.96563E-11	9.26793E-10	O2
OH	6.57951E-10	3.86864E-08	4.25586E-05	2.50237E-03	OH
CHO	2.46702E-07	8.50161E-06	2.58788E-03	8.91811E-02	CHO
CH2O	1.56753E-07	5.22054E-06	9.59070E-04	3.19411E-02	CH2O
CRO3(G)	4.38491E-22	4.38516E-21	1.39577E-15	1.39586E-14	CRO3(G)
FPMO2(G)	7.18199E-17	5.51032E-16	7.19931E-11	5.52361E-10	FPMO2(G)
FPMO3(G)	3.59882E-21	2.45928E-20	1.07032E-14	7.31408E-14	FPMO3(G)
AL2O2(G)	0.00000E+00	0.00000E+00	0.00000E+00	0.00000E+00	AL2O2(G)
AL2O(G)	0.00000E+00	0.00000E+00	0.00000E+00	0.00000E+00	AL2O(G)
ALO(G)	0.00000E+00	0.00000E+00	0.00000E+00	0.00000E+00	ALO(G)
OALH(G)	0.00000E+00	0.00000E+00	0.00000E+00	0.00000E+00	OALH(G)
ALOH(G)	0.00000E+00	0.00000E+00	0.00000E+00	0.00000E+00	ALOH(G)
OALOH(G)	0.00000E+00	0.00000E+00	0.00000E+00	0.00000E+00	OALOH(G)
ALO2(G)	0.00000E+00	0.00000E+00	0.00000E+00	0.00000E+00	ALO2(G)

Table 6.2 Output listing for the CORCON standard problem (continued)

CORCON VERSION 2.26

TIME = 16200.00 CORCON STANDARD PROBLEM (slightly different from Mod1/Mod2 problem) IT. NO. = 180

* * * * G E O M E T R Y * * * *

BODY POINT	R COORDINATE (M)	Z COORDINATE (M)	STREAM LENGTH (M)	BODY ANGLE (DEG)	RAY ANGLE (DEG)	VOLUME (M3)	SURFACE AREA (M2)	VOID FRACTION (-)
1	0.000000	5.051285	0.000000	0.000	0.000	0.00000	0.00000	0.01628
2	0.326944	5.051285	0.326944	0.000	5.260	0.00000	0.33581	0.01628
3	0.653888	5.051285	0.653888	0.000	10.433	0.00000	1.34325	0.01628
4	0.980832	5.051285	0.980832	0.000	15.440	0.00000	3.02231	0.01628
5	1.307775	5.051285	1.307775	0.000	20.216	0.00000	5.37299	0.01628
6	1.634720	5.051285	1.634720	0.000	24.717	0.00000	8.39531	0.01628
7	1.961663	5.051285	1.961663	0.000	28.915	0.00000	12.08923	0.01628
8	2.288607	5.051285	2.288607	0.000	32.800	0.00000	16.45480	0.01628
9	2.615551	5.051285	2.615551	0.000	36.372	0.00000	21.49197	0.01628
10	2.900000	5.051285	2.900000	0.000	0.000	0.00000	26.42080	0.01628
11	2.936159	5.043640	2.936958	20.508	39.644	0.20453	27.09842	0.01627
12	2.952988	5.034281	2.956215	35.813	39.880	0.45945	27.45469	0.01622
13	2.968581	5.019969	2.977380	47.606	40.143	0.85361	27.84843	0.01612
14	2.982452	5.001785	3.000250	56.445	40.421	1.35938	28.27601	0.01604
15	2.994296	4.981081	3.024102	64.466	40.701	1.94024	28.72387	0.01596
16	3.003136	4.958404	3.048442	72.560	40.970	2.58090	29.18247	0.01591
17	3.008763	4.935117	3.072399	80.453	41.215	3.24192	29.63494	0.01587
18	3.010952	4.912412	3.095209	86.997	41.424	3.88811	30.06631	0.01586
19	3.011958	4.796422	3.211204	89.746	42.418	7.19277	32.26112	0.01585
20	3.011981	4.679314	3.328312	89.258	43.452	10.53039	34.47736	0.01585
21	3.014917	4.565163	3.442500	61.456	44.527	13.78692	36.63940	0.01584
22	3.085455	4.516893	3.527973	16.527	45.644	15.19784	38.27748	0.01541
23	3.216498	4.519936	3.659051	1.315	46.805	15.10290	40.87259	0.01468
24	3.345553	4.511001	3.788416	66.009	48.013	15.40512	43.53947	0.01402
	3.345036	4.510341	OXIDE / METAL INTERFACE					
	3.113224	4.214241	METAL / OXIDE INTERFACE					
25	3.032957	4.111713	4.295512	115.429	49.268	28.17427	53.70102	0.01573
	3.024810	4.075857	OXIDE / COOLANT INTERFACE					
26	3.000000	3.966667	4.444256	96.401	50.572	32.32059	56.52018	0.01744
27	3.000000	3.850000	4.560923	90.000	51.927	35.61926	58.71929	0.00659
28	3.000000	3.733334	4.677589	90.000	53.334	38.91792	60.91840	0.00659
	3.000000	3.698615	COOLANT / ATMSPHRE INTERFACE					
29	3.000000	3.616667	4.794256	90.000	54.795	42.21660	63.11752	1.00000
30	3.000000	3.500000	4.910923	90.000	56.310	45.51527	65.31664	1.00000
31	3.000000	3.383333	5.027590	90.000	57.880	48.81394	67.51575	1.00000
32	3.000000	3.266667	5.144257	90.000	59.507	52.11261	69.71487	1.00000
33	3.000000	3.150000	5.260923	90.000	61.189	55.41129	71.91399	1.00000
34	3.000000	3.033334	5.377590	90.000	62.928	58.70995	74.11310	1.00000
35	3.000000	2.916667	5.494257	90.000	64.722	62.00863	76.31222	1.00000
36	3.000000	2.800000	5.610924	90.000	66.571	65.30730	78.51133	1.00000
37	3.000000	2.683333	5.727591	90.000	68.474	68.60597	80.71045	1.00000
38	3.000000	2.566667	5.844257	90.000	70.427	71.90464	82.90956	1.00000

Table 6.2 Output listing for the CORCON standard problem (continued)

39	3.000000	2.450000	5.960924	90.000	72.429	75.20332	85.10868	1.00000
40	3.000000	2.333333	6.077591	90.000	74.476	78.50198	87.30779	1.00000
41	3.000000	2.216667	6.194258	90.000	76.564	81.80066	89.50691	1.00000
42	3.000000	2.100000	6.310925	90.000	78.690	85.09933	91.70602	1.00000
43	3.000000	1.983333	6.427591	90.000	80.848	88.39800	93.90514	1.00000
44	3.000000	1.866667	6.544258	90.000	83.032	91.69667	96.10426	1.00000
45	3.000000	1.750000	6.660925	90.000	85.236	94.99535	98.30338	1.00000
46	3.000000	1.633333	6.777592	90.000	87.455	98.29401	100.50249	1.00000
47	3.000000	1.516667	6.894258	90.000	89.682	101.59269	102.70161	1.00000
48	3.000000	1.400000	7.010925	90.000	91.909	104.89136	104.90072	1.00000
49	3.000000	1.283333	7.127592	90.000	94.131	108.19003	107.09984	1.00000
50	3.000000	1.166667	7.244259	90.000	96.340	111.48870	109.29895	1.00000
51	3.000000	1.050000	7.360926	90.000	98.531	114.78737	111.49806	1.00000
52	3.000000	0.933333	7.477592	90.000	100.697	118.08604	113.69718	1.00000
53	3.000000	0.816667	7.594259	90.000	102.832	121.38472	115.89630	1.00000
54	3.000000	0.700000	7.710926	90.000	104.931	124.68338	118.09541	1.00000
55	3.000000	0.583333	7.827592	90.000	106.991	127.98206	120.29453	1.00000
56	3.000000	0.466667	7.944259	90.000	109.006	131.28073	122.49365	1.00000
57	3.000000	0.350000	8.060926	90.000	110.973	134.57941	124.69277	1.00000
58	3.000000	0.233334	8.177593	90.000	112.891	137.87807	126.89188	1.00000
59	3.000000	0.116667	8.294260	90.000	114.755	141.17674	129.09100	1.00000
60	3.000000	0.000000	8.410927	90.000	116.565	144.47542	131.29012	1.00000

CORCON VERSION 2.26

TIME = 16200.00 CORCON STANDARD PROBLEM (slightly different from Mod1/Mod2 problem) IT. NO. = 180

* * * * HEAT TRANSFER RESULTS * * * *

BODY POINT	ABLATION RATE (M/S)	FILM THICKNESS (M)	FILM FLOW (KG/S)	FILM VELOCITY (M/S)	REYNOLDS NUMBER (-)	REGIME	HT TRANS COEFF (W/M2-K)	INTERFACE TEMPERATURE (K)	CONVECTIVE FLUX (W/M2)	RADIATIVE FLUX (W/M2)
1	7.512E-06	1.000E-10	0.000E+00	0.000E+00	0.181	SLG.BUB.	1.000E+03	1702.6	5.262E+04	0.000E+00
2	7.512E-06	1.000E-10	0.000E+00	0.000E+00	0.181	SLG.BUB.	1.000E+03	1702.6	5.262E+04	0.000E+00
3	7.512E-06	1.000E-10	0.000E+00	0.000E+00	0.181	SLG.BUB.	1.000E+03	1702.6	5.262E+04	0.000E+00
4	7.512E-06	1.000E-10	0.000E+00	0.000E+00	0.181	SLG.BUB.	1.000E+03	1702.6	5.262E+04	0.000E+00
5	7.512E-06	1.000E-10	0.000E+00	0.000E+00	0.181	SLG.BUB.	1.000E+03	1702.6	5.262E+04	0.000E+00
6	7.512E-06	1.000E-10	0.000E+00	0.000E+00	0.181	SLG.BUB.	1.000E+03	1702.6	5.262E+04	0.000E+00
7	7.512E-06	1.000E-10	0.000E+00	0.000E+00	0.181	SLG.BUB.	1.000E+03	1702.6	5.262E+04	0.000E+00
8	7.512E-06	1.000E-10	0.000E+00	0.000E+00	0.181	SLG.BUB.	1.000E+03	1702.6	5.262E+04	0.000E+00
9	7.512E-06	1.000E-10	0.000E+00	0.000E+00	0.181	SLG.BUB.	1.000E+03	1702.6	5.262E+04	0.000E+00
10	7.512E-06	1.000E-10	0.000E+00	0.000E+00	0.181	SLG.BUB.	1.000E+03	1702.6	5.262E+04	0.000E+00
11	6.742E-06	1.000E-10	0.000E+00	0.000E+00	0.162	SLG.BUB.	1.000E+03	1697.2	4.723E+04	0.000E+00
12	5.502E-06	1.237E-04	4.573E-04	1.752E+00	0.427	TRN.BUB.	1.537E+03	1669.0	2.925E+04	9.285E+03
13	4.048E-06	1.647E-04	1.542E-03	4.414E+00	1.390	LAM.FLM.	1.198E+03	1666.3	1.955E+04	8.806E+03
14	2.979E-06	1.810E-04	2.414E-03	6.262E+00	2.166	LAM.FLM.	1.090E+03	1662.8	1.398E+04	6.894E+03
15	2.114E-06	1.903E-04	3.077E-03	7.559E+00	2.750	LAM.FLM.	1.037E+03	1659.4	9.761E+03	5.047E+03
16	1.413E-06	1.947E-04	3.547E-03	8.492E+00	3.160	LAM.FLM.	1.013E+03	1656.4	6.481E+03	3.419E+03
17	9.544E-07	1.973E-04	3.858E-03	9.098E+00	3.431	LAM.FLM.	1.000E+03	1654.4	4.359E+03	2.326E+03
18	7.712E-07	1.993E-04	4.074E-03	9.505E+00	3.620	LAM.FLM.	9.901E+02	1653.5	3.511E+03	1.891E+03
19	7.508E-07	2.136E-04	5.044E-03	1.097E+01	4.481	LAM.FLM.	9.236E+02	1653.6	3.334E+03	1.795E+03
20	7.517E-07	2.265E-04	6.011E-03	1.233E+01	5.340	LAM.FLM.	8.712E+02	1653.7	3.266E+03	2.000E+03
21	2.414E-06	2.491E-04	8.004E-03	1.492E+01	7.103	LAM.FLM.	7.920E+02	1662.7	1.007E+04	6.837E+03
22	7.070E-06	3.476E-04	1.258E-02	1.641E+01	10.906	LAM.FLM.	5.676E+02	1694.2	2.508E+04	2.445E+04
23	7.217E-06	1.619E-03	2.344E-02	6.301E+00	19.498	LAM.FLM.	1.219E+02	1723.3	8.932E+03	4.163E+04
24	1.933E-06	9.172E-04	3.063E-02	1.397E+01	24.497	LAM.FLM.	2.151E+02	1667.9	3.857E+03	9.686E+03
			OXIDE / METAL		INTERFACE					
			METAL / OXIDE		INTERFACE					
25	3.815E-05	1.363E-03	4.194E-01	1.420E+02	369.984	TRN.FLM.	4.278E+02	1895.2	1.049E+05	1.624E+05
			OXIDE / COOLANT		INTERFACE					
26	0.000E+00	1.964E-03	4.349E-01	1.033E+02	387.920	TRN.FLM.	3.039E+02	397.1	0.000E+00	0.000E+00
27	0.000E+00	1.948E-03	4.349E-01	1.042E+02	387.920	TRN.FLM.	3.065E+02	397.1	-0.000E+00	0.000E+00
28	0.000E+00	1.948E-03	4.349E-01	1.042E+02	387.920	TRN.FLM.	3.065E+02	397.1	0.000E+00	0.000E+00
			COOLANT / ATMSPHRE		INTERFACE					

Table 6.2 Output listing for the CORCON standard problem (continued)

```
                                CORCON VERSION 2.26
TIME =  16200.00        CORCON STANDARD PROBLEM (slightly different from Mod1/Mod2 problem)        IT. NO. = 180
                        * * * * BULK METAL/GAS REACTION DURING TIMESTEP * * * *
```

OXIDES			METALS			GASES		
SPECIES NAMES	REACTANTS (MOLS)	PRODUCTS (MOLS)	SPECIES NAMES	REACTANTS (MOLS)	PRODUCTS (MOLS)	SPECIES NAMES	REACTANTS (MOLS)	PRODUCTS (MOLS)
FEO	0.0000E+00	1.4685E-03	FE	7.5115E+05	7.5115E+05	C(G)	0.0000E+00	1.9405E-07
MNO	0.0000E+00	0.0000E+00	CR	1.9232E+05	1.9232E+05	CH4	0.0000E+00	4.3962E-02
AL2O3	0.0000E+00	0.0000E+00	NI	1.0219E+05	1.0219E+05	CO	0.0000E+00	6.4663E+01
UO2	0.0000E+00	0.0000E+00	ZR	6.0012E+04	5.9962E+04	CO2	6.4719E+01	2.5253E-04
ZRO2	0.0000E+00	4.9949E+01	FPM	3.9344E+03	3.9344E+03	C2H2	0.0000E+00	0.0000E+00
CR2O3	0.0000E+00	5.2261E-10	MN	0.0000E+00	0.0000E+00	C2H4	0.0000E+00	5.7203E-03
NIO	0.0000E+00	1.6783E-06	C(C)	0.0000E+00	0.0000E+00	C2H6	0.0000E+00	1.5751E-06
FPMO2	0.0000E+00	0.0000E+00	AL	0.0000E+00	0.0000E+00	H	0.0000E+00	1.7938E-01
FPMO3	0.0000E+00	9.6365E-18	U	0.0000E+00	0.0000E+00	H2	0.0000E+00	3.4937E+01
FE3O4	0.0000E+00	1.6218E-19	SI	0.0000E+00	0.0000E+00	H2O	3.5127E+01	6.8712E-04
MN3O4	0.0000E+00	0.0000E+00	UAL3	0.0000E+00	0.0000E+00	N	0.0000E+00	0.0000E+00
SIO2	0.0000E+00	0.0000E+00	UAL2	0.0000E+00	0.0000E+00	NH3	0.0000E+00	0.0000E+00
U3O8	0.0000E+00	0.0000E+00	CA	0.0000E+00	0.0000E+00	N2	0.0000E+00	0.0000E+00
CAO	0.0000E+00	0.0000E+00	X	0.0000E+00	0.0000E+00	O	0.0000E+00	1.6306E-09
						O2	0.0000E+00	1.3711E-14
						OH	0.0000E+00	4.5300E-07
						CHO	0.0000E+00	7.0703E-05
						CH2O	0.0000E+00	3.7694E-05
						CRO3(G)	0.0000E+00	7.9216E-20
						FPMO2(G)	0.0000E+00	8.8495E-15
						FPMO3(G)	0.0000E+00	4.4033E-19
						AL2O2(G)	0.0000E+00	0.0000E+00
						AL2O(G)	0.0000E+00	0.0000E+00
						ALO(G)	0.0000E+00	0.0000E+00
						OALH(G)	0.0000E+00	0.0000E+00
						ALOH(G)	0.0000E+00	0.0000E+00
						OALOH(G)	0.0000E+00	0.0000E+00
						ALO2(G)	0.0000E+00	0.0000E+00

```
NO. OF ITERATIONS =  36
```

Table 6.2 Output listing for the CORCON standard problem (continued)

CORCON VERSION 2.26

TIME = 16200.00 CORCON STANDARD PROBLEM (slightly different from Mod1/Mod2 problem) IT. NO. = 180

* * * * FILM METAL/GAS REACTION DURING TIMESTEP * * * *

OXIDES			METALS			GASES		
SPECIES NAMES	REACTANTS (MOLS)	PRODUCTS (MOLS)	SPECIES NAMES	REACTANTS (MOLS)	PRODUCTS (MOLS)	SPECIES NAMES	REACTANTS (MOLS)	PRODUCTS (MOLS)
FEO	0.0000E+00	3.2491E-03	FE	7.5115E+05	7.5115E+05	C(G)	0.0000E+00	4.3271E-07
MNO	0.0000E+00	0.0000E+00	CR	1.9232E+05	1.9232E+05	CH4	0.0000E+00	2.5392E-01
AL2O3	0.0000E+00	0.0000E+00	NI	1.0219E+05	1.0219E+05	CO	0.0000E+00	2.0196E+02
UO2	0.0000E+00	0.0000E+00	ZR	5.9962E+04	5.9806E+04	CO2	2.0230E+02	5.7203E-04
ZRO2	0.0000E+00	1.5623E+02	FPM	3.9344E+03	3.9344E+03	C2H2	0.0000E+00	0.0000E+00
CR2O3	0.0000E+00	9.1865E-10	MN	0.0000E+00	0.0000E+00	C2H4	0.0000E+00	4.7191E-02
NIO	0.0000E+00	3.6791E-06	C(C)	0.0000E+00	0.0000E+00	C2H6	0.0000E+00	1.5312E-05
FPMO2	0.0000E+00	0.0000E+00	AL	0.0000E+00	0.0000E+00	H	0.0000E+00	4.2796E-01
FPMO3	0.0000E+00	8.9785E-18	U	0.0000E+00	0.0000E+00	H2	0.0000E+00	1.0899E+02
FE3O4	0.0000E+00	1.2365E-19	SI	0.0000E+00	0.0000E+00	H2O	1.0981E+02	1.5092E-03
MN3O4	0.0000E+00	0.0000E+00	UAL3	0.0000E+00	0.0000E+00	N	0.0000E+00	0.0000E+00
SIO2	0.0000E+00	0.0000E+00	UAL2	0.0000E+00	0.0000E+00	NH3	0.0000E+00	0.0000E+00
U3O8	0.0000E+00	0.0000E+00	CA	0.0000E+00	0.0000E+00	N2	0.0000E+00	0.0000E+00
CAO	0.0000E+00	0.0000E+00	X	0.0000E+00	0.0000E+00	O	0.0000E+00	1.9682E-09
						O2	0.0000E+00	1.1701E-14
						OH	0.0000E+00	7.0759E-07
						CHO	0.0000E+00	1.8434E-04
						CH2O	0.0000E+00	1.1892E-04
						CRO3(G)	0.0000E+00	5.2339E-20
						FPMO2(G)	0.0000E+00	7.6814E-15
						FPMO3(G)	0.0000E+00	2.9745E-19
						AL2O2(G)	0.0000E+00	0.0000E+00
						AL2O(G)	0.0000E+00	0.0000E+00
						ALO(G)	0.0000E+00	0.0000E+00
						OALH(G)	0.0000E+00	0.0000E+00
						ALOH(G)	0.0000E+00	0.0000E+00
						OALOH(G)	0.0000E+00	0.0000E+00
						ALO2(G)	0.0000E+00	0.0000E+00

NO. OF ITERATIONS = 36

Table 6.2 Output listing for the CORCON standard problem (continued)

CORCON VERSION 2.26

TIME = 16200.00 CORCON STANDARD PROBLEM (slightly different from Mod1/Mod2 problem) IT. NO. = 180

* * * * POOL COMPOSITION * * * *

	OXIDE	METAL	OXIDE	COOLANT	
MASS OF LAYER	1.2424E+05	6.3804E+04	1.3990E+04	9.9014E+03	
MASS OF SPECIES					
SIO2	1.3383E+03		3.8309E+03		SIO2
TIO2	6.7653E+00		1.9338E+01		TIO2
FEO	5.9750E+03		1.6931E-01		FEO
MNO	1.1275E+00		3.2230E+00		MNO
MGO	1.8040E+01		5.1567E+01		MGO
CAO	1.1764E+03		3.3626E+03		CAO
NA2O	4.4579E-01		1.2506E+00		NA2O
K2O	1.3185E+01		3.8901E+01		K2O
FE2O3	5.4122E+01		1.5471E+02		FE2O3
AL2O3	1.3528E+02		3.8672E+02		AL2O3
UO2	9.9997E+04		0.0000E+00		UO2
ZRO2	1.4000E+04		6.1388E+03		ZRO2
CR2O3	5.2406E-01		1.4996E+00		CR2O3
NIO	0.0000E+00		2.3492E-04		NIO
FPMO2	0.0000E+00		4.0894E-34		FPMO2
FPMO3	0.0000E+00		3.8946E-14		FPMO3
FPOX	1.5109E+03		0.0000E+00		FPOX
FPALKMET	1.1119E+01		0.0000E+00		FPALKMET
FPHALOGN	4.3336E-01		0.0000E+00		FPHALOGN
FE3O4	0.0000E+00		1.6749E-15		FE3O4
FE		4.1958E+04			FE
CR		1.0000E+04			CR
NI		5.9995E+03			NI
ZR		5.4555E+03			ZR
FPM		3.9049E+02			FPM
H2OCLN				9.9014E+03	H2OCLN

Table 6.2 Output listing for the CORCON standard problem (continued)

CORCON VERSION 2.26

TIME = 16200.00 CORCON STANDARD PROBLEM (slightly different from Mod1/Mod2 problem) IT. NO. = 180

* * * * L A Y E R P R O P E R T I E S * * * *

		OXIDE	METAL	OXIDE	COOLANT	
MASS	(KG)	1.2424E+05	6.3804E+04	1.3990E+04	9.9014E+03	
DENSITY	(KG/M3)	8.1834E+03	6.8386E+03	3.3051E+03	9.3454E+02	
THERMAL EXPANSIVITY	(1/K)	3.5134E-05	2.7389E-05	6.5698E-05	3.6279E-04	
AVERAGE TEMPERATURE	(K)	2.1751E+03	2.1677E+03	2.1408E+03	3.9714E+02	
INTERFACE TEMPERATURE	(K)	1.7026E+03	2.1745E+03	2.1603E+03	1.7061E+03	3.9726E+02
EDGE TEMPERATURE	(K)	1.6678E+03	2.1228E+03	1.8937E+03	3.9714E+02	
SOLIDUS TEMPERATURE	(K)	2.1663E+03	1.7357E+03	1.5616E+03	2.6821E+02	
LIQUIDUS TEMPERATURE	(K)	2.7594E+03	1.7481E+03	2.3464E+03	2.7821E+02	
SPECIFIC ENTHALPY	(J/KG)	-4.1876E+06	1.5372E+06	-9.2276E+06	-1.5462E+07	
TOTAL ENTHALPY	(J)	-5.2026E+11	9.8082E+10	-1.2909E+11	-1.5309E+11	
SPECIFIC HEAT	(J/KG K)	5.6732E+02	7.3921E+02	1.0475E+03	4.2723E+03	
VISCOSITY	(KG/M S)	1.7888E+02	4.9610E-03	9.6411E-02	2.2203E-04	
THERMAL CONDUCTIVITY	(W/M K)	2.8134E+00	4.9019E+01	4.1632E+00	6.0000E-01	
THERMAL DIFFUSIVITY	(M2/S)	6.0599E-07	9.6969E-06	1.2026E-06	1.5028E-07	
SURFACE TENSION	(N/M)	4.8896E-01	1.7679E+00	5.0125E-01	7.3000E-02	
EMISSIVITY	(-)	8.0000E-01	6.0000E-01	8.0000E-01	1.0000E+00	
SUPERFICIAL GAS VEL	(M/S)	6.0021E-03	8.2516E-03	8.9130E-03	9.1706E-03	1.7271E-03
BUBBLE RADIUS	(M)	1.7714E-03	1.8421E-03	1.8657E-03	1.0702E-03	
BUBBLE VELOCITY	(M/S)	4.6921E-04	4.1037E-01	3.2474E-01	2.9782E-01	
VOID FRACTION	(-)	1.5844E-02	1.4711E-02	1.6500E-02	9.8439E-03	
BOT CRUST THICKNESS	(M)	4.0531E-02	0.0000E+00	0.0000E+00	0.0000E+00	
HT COEFF, LIQ TO BOT	(W/M2 K)	4.8306E+02	7.1721E+04	2.8838E+04	1.0386E+03	
Z-AVE LIQ TEMPERATURE	(K)	2.1906E+03	2.1677E+03	2.1408E+03	3.9714E+02	
HT COEFF, LIQ TO TOP	(W/M2 K)	3.0639E+04	7.5815E+04	1.2956E+03	2.7328E+04	
TOP CRUST THICKNESS	(M)	0.0000E+00	0.0000E+00	0.0000E+00	0.0000E+00	
R-AVE LIQ TEMPERATURE	(K)	2.2325E+03	2.1677E+03	2.1408E+03	3.9714E+02	
HT COEFF, LIQ TO SID	(W/M2 K)	7.0102E+01	1.3018E+04	1.0882E+03	1.0000E-10	
SIDE CRUST THICKNESS	(M)	2.8749E-01	0.0000E+00	0.0000E+00	0.0000E+00	
DECAY HEAT	(W)	1.6045E+07	2.0809E+06	1.4077E-10	0.0000E+00	
HEAT TO CONCRETE	(W)	1.8039E+06	4.0124E+06	8.6398E+05	0.0000E+00	
HEAT OF REACTION	(W)	0.0000E+00	3.5914E+06	0.0000E+00	0.0000E+00	
INTERLAYER HEAT FLOW	(W)	1.4246E+07	1.6236E+07	1.5925E+07	-9.5822E+04	

Table 6.2 Output listing for the CORCON standard problem (continued)

```
                                        CORCON VERSION 2.26
TIME =  16200.00        CORCON STANDARD PROBLEM (slightly different from Mod1/Mod2 problem)        IT. NO. = 180
                                    * * * * *  V A N E S A  O U T P U T  * * * * *

 TEMPERATURE OF METAL (K)                              2.1677E+03
 TEMPERATURE OF OXIDE (K)                              2.1724E+03
 AEROSOL - AMBIENT CONDITIONS (G/CC)                   1.6011E-05
 AEROSOL - STANDARD STATE CONDITIONS (G/CC)            4.5203E-05
           ( 298.15 (K) AND 1 ATM. )
 GAS (G-MOLES/S)                                       1.5768E+01
 AEROSOL RATE (GRAMS/S)                                1.7439E+01
 AEROSOL DENSITY (G/CM3)                               2.1587E+00
 PARTICLE SIZE (MICROMETERS)                           5.1680E-01
 BUBBLE DIAMETER FOR THE METAL PHASE (CM)              3.7568E-01
 BUBBLE DIAMETER FOR THE OXIDE PHASE (CM)              3.6322E-01
 MECHANICAL RELEASES FROM THE AZBEL AND THE ISHII AND KATAOKA CORRELATIONS ARE CALCULATED.

  I            AEROSOL COMPOSITION   MELT COMPOSITION   LOSS(MOLES)     RELEASE FRACTION
                   (WEIGHT %)             (KG)
  2     FE                           4.1957E+04
  3     CR                           1.0000E+04
  4     NI          1.3288E-01       5.9995E+03       1.1841E-02      1.1475E-04
  5     MO          4.2230E-05       1.8118E+02       2.3028E-06      1.5092E-07
  6     RU          1.3939E-07       1.9193E+02       7.2155E-09      4.6916E-09
  7     SN          0.0000E+00       0.0000E+00       0.0000E+00      0.0000E+00
  8     SB          5.1569E-02       3.5001E-01       2.2160E-03      5.5855E-01
  9     TE          2.1472E+00       1.6951E+01       8.8038E-02      2.1298E-01
 10     AG          0.0000E+00       0.0000E+00       0.0000E+00      0.0000E+00
 11     MN          0.0000E+00       0.0000E+00       0.0000E+00      0.0000E+00
 12     CAO         7.1594E-02       4.5390E+03       6.6791E-03      3.1164E-05
 13     AL2O3       6.9456E-03       5.2200E+02       3.5638E-04      1.3888E-04
 14     NA2O        8.4035E+00       1.6966E+00       7.0935E-01      8.5309E-01
 15     K2O         8.0945E+01       5.2091E+01       4.4954E+00      7.0141E-01
 16     SIO2        1.2329E+00       5.1692E+03       1.0735E-01      4.2576E-03
 17     UO2         1.4891E+00       9.9986E+04       2.8854E-02      3.2393E-05
 18     ZRO2        4.9667E-02       2.0139E+04       2.1088E-03      7.2723E-07
 19     CS2O        3.2348E+00       1.1987E+01       6.0052E-02      6.8164E-01
 20     BAO         4.0843E-02       8.4491E+01       1.3935E-03      2.8717E-03
 21     SRO         4.3326E-03       6.5023E+01       2.1875E-04      4.2697E-03
 22     LA2O3       1.8584E-03       4.9684E+02       2.9841E-05      6.4637E-05
 23     CEO2        2.7688E-02       1.0293E+03       8.4160E-04      1.0986E-03
 24     NBO         8.1685E-05       3.9345E+00       3.9241E-06      3.6349E-05
 25     CSI         4.8073E-01       9.3738E-01       9.6804E-03      6.9467E-01
202     FEO         1.6795E+00       5.9752E+03       1.2230E-01      4.1655E-04
302     CR2O3       8.7870E-05       2.0237E+00       3.0246E-06      2.1690E-07
CARBON IN MELT                       0.0000E+00
ZIRCONIUM IN MELT                    5.4555E+03
```

Table 6.2 Output listing for the CORCON standard problem (continued)

I		GAS COMPOSITION (WEIGHT %)	RELEASE RATE (GRAMS/SECOND)
1	H2O	4.6914E+00	1.3327E+01
2	H2	3.0311E+01	9.6350E+00
3	H	1.6385E-01	2.6042E-02
4	OH	3.4767E-03	9.3238E-03
5	O	1.2898E-05	3.2529E-05
6	O2	8.5013E-07	4.2894E-06
7	CO2	1.9020E+00	1.3199E+01
8	CO	6.2928E+01	2.7794E+02

Table 6.2 Output listing for the CORCON standard problem (concluded)

```
                                    CORCON VERSION 2.26
TIME =  16200.00        CORCON STANDARD PROBLEM (slightly different from Mod1/Mod2 problem)        IT. NO. = 180
                              ****** POOL SCRUBBING ******

 INFORMATION SUPPLIED BY VANESA

 MEAN PARTICLE SIZE (UM)                          5.1680E-01
 AEROSOL RATE (GRAMS/S)                           1.7439E+01
 AEROSOL DENSITY (G/CM3)                          2.1587E+00
 POOL DEPTH (CM)                                  3.8610E+01
 POOL TEMPERATURE (K)                             3.9708E+02
 AMBIENT PRESSURE (ATM)                           2.2516E+00

   SIZE          CHARACTERISTIC      MASS       DECONTAMINATION
   RANGE             SIZE          IN RANGE        FACTOR
0.000- 0.131        0.101         7.7098E-01      1.1310E+00
0.131- 0.178        0.156         7.9560E-01      1.0960E+00
0.178- 0.218        0.198         8.0501E-01      1.0831E+00
0.218- 0.256        0.237         8.1029E-01      1.0761E+00
0.256- 0.295        0.275         8.1357E-01      1.0718E+00
0.295- 0.334        0.314         8.1557E-01      1.0691E+00
0.334- 0.375        0.354         8.1663E-01      1.0677E+00
0.375- 0.418        0.396         8.1689E-01      1.0674E+00
0.418- 0.465        0.441         8.1637E-01      1.0681E+00
0.465- 0.517        0.491         8.1503E-01      1.0698E+00
0.517- 0.574        0.545         8.1278E-01      1.0728E+00
0.574- 0.638        0.605         8.0942E-01      1.0773E+00
0.638- 0.712        0.674         8.0463E-01      1.0837E+00
0.712- 0.800        0.754         7.9792E-01      1.0928E+00
0.800- 0.906        0.850         7.8844E-01      1.1059E+00
0.906- 1.042        0.970         7.7472E-01      1.1255E+00
1.042- 1.225        1.126         7.5389E-01      1.1566E+00
1.225- 1.503        1.347         7.1949E-01      1.2119E+00
1.503- 2.034        1.714         6.5287E-01      1.3356E+00
2.034-******        2.644         4.5833E-01      1.9024E+00

 ---------------------------------------------------------
 OVERALL DECONTAMINATION FACTOR                     1.1289
 MASS OUT                                           1.5448E+01

 FIT OF DECONTAMINATED AEROSOL TO LOG NORMAL
 NEW MEAN PARTICLE SIZE (UM)                          0.488
 RANGE (UM)                              0.485 -      0.491
 NEW GEOMETRIC STANDARD DEVIATION                     2.183
 RANGE (UM)                              2.208 -      2.158

 LINEAR CORRELATION COEFFICIENT                   0.999763

*****************************************
* COOLANT DEPLETED AT TIME = 1.75200E+04 *
*****************************************
```

Table 6.3 Input listing for the BWR sample problem

```
BWR ACCIDENT - WATER ADDED AFTER 1 HOUR
$
$ user flags
$   *ILYR(mixed, mixing on)
$   ^                   *ICHEM (condensed phase chem on, coking off)
$   ^                   ^                                *IFILM (slag/film)
   13    0    2    1    1    0    1    0    0  180    0    0    0    1    1
1
$
$ additional user flags
$        *IFVAN (do VANESA calculation)
$        ^          *IUSER (include user flexibility input)
&   0    1    0    1
$
$ time information
      30.0    10800.    21600.              70000.
$
$ ray system information
   60        0.0       1.5
$
$ geometry information - rt. circular cylinder 3.2 m radius
       0.0       3.2       5.00       0.1      4.438      3.05   10    6
$
$ concrete specifications - abl temp = 1630 K
     300.0     1630.        .6       .135
$
$ initial debris composition and temperature (T = 2500 K)
    3    4     2500.     2500.
UO2           53133.
ZRO2          10997.
FEO            1000.
ZR            13690.
FE            23387.
CR             3700.
NI             2055.
$
$ core MTU and operating power
     140.1     3293.    0
$
$ cavity atmosphere conditions and composition
     4505.      0.        380.    3
CO2             0.17
H2              0.13
N2              0.70
$
$ pressure in cavity atmosphere vs. time
    2
   10800.0     1.5E5   21600.0     2.5E5
```

Table 6.3 Input listing for the BWR sample problem (continued)

```
$
$ temperature of surfaces above the melt
    2
   10800.0      500.0   21600.0     1000.0
$
$ time-dependent mass addition
$ species added
    8    0
UO2
ZRO2
FEO
FE
CR
NI
ZR
H2OCLN
$
$ time and flow rate information
    2    2    2    2    2    2    2    6
    10800.      4.920    21600.      4.920
    10800.      1.018    21600.      1.018
    10800.      .0926    21600.     0.0926
    10800.      0.926    21600.      0.926
    10800.      .3426    21600.     0.3426
    10800.      .1902    21600.     0.1902
    10800.      1.267    21600.      1.267
    10800.         0.    14400.         0.    14430.     20.00    18030.     20.00
    18060.         0.    21600.         0.
$
$ temperature of added material - oxides, metals, coolant
    2    2    2
    10800.      2300.    80000.      2300.
    10800.      2300.    80000.      2300.
    10800.       320.    80000.       320.
$
$ emissivities vs. time - oxides, metals, surroundings
TIMETIMETIME
    1    1    1
       0.0       0.8
       0.0       0.6
       0.0       0.6
$
$ mean beam length
      3.0
$
$ user flexibility input
    0    0    0    0    0    0    0    0    0    0    0    0    0    1    0
    0    1    0    0    0    0    0    1    1
```

Table 6.3 Input listing for the BWR sample problem (continued)

```
$
$ temperature dependent metal phase thermal conductivity multiplier
    1
        0.        0.5
$
$ temperature dependent oxide phase viscosity multiplier
    1
        0.        5.0
$
$ mole fraction concrete oxides at which oxide solidus = concrete solidus
       0.2
$
$ cutoff for inclusion in chemistry solution - ZILCH
      0.01
$
$ VANESA input
$ user options
$                   * IDEAL=1, run with ideal chemistry on
    1    1    1    1
$
$ pool scrubbing parameters
        20        2.3          1          1        1.0        1.0
```

Table 6.4 Output listing for the BWR sample problem

```
CARD IMAGES IN INPUT FILE (TAPE5)
1.   BWR ACCIDENT - WATER ADDED AFTER 1 HOUR
     $
     $ user flags
     $   *ILYR(mixed, mixing on)
     $   ^                  *ICHEM (condensed phase chem on, coking off)
     $   ^                  ^                                  *IFILM (slag/film)
2.     13    0    2    1    1    0    1    0    0  180    0    0    0    1    1    1
     $
     $ additional user flags
     $        *IFVAN (do VANESA calculation)
     $        ^         *IUSER (include user flexibility input)
3.   &   0    1    0    1
     $
     $ time information
4.         30.0    10800.    21600.              70000.
     $
     $ ray system information
5.     60       0.0       1.5
     $
     $ geometry information - rt. circular cylinder 3.2 m radius
6.         0.0       3.2      5.00       0.1     4.438      3.05   10    6
     $
     $ concrete specifications - abl temp = 1630 K
7.        300.0     1630.        .6      .135
     $
     $ initial debris composition and temperature (T = 2500 K)
8.       3    4     2500.     2500.
9.   UO2            53133.
10.  ZRO2           10997.
11.  FEO             1000.
12.  ZR             13690.
13.  FE             23387.
14.  CR              3700.
15.  NI              2055.
     $
     $ core MTU and operating power
16.       140.1     3293.    0
     $
     $ cavity atmosphere conditions and composition
17.       4505.      0.        380.    3
18.  CO2             0.17
19.  H2              0.13
20.  N2              0.70
     $
     $ pressure in cavity atmosphere vs. time
21.      2
```

```
22.      10800.0      1.5E5    21600.0      2.5E5
         $
         $ temperature of surfaces above the melt
23.         2
24.      10800.0      500.0    21600.0     1000.0
         $
         $ time-dependent mass addition
         $ species added
25.         8    0
26.      UO2
27.      ZRO2
28.      FEO
29.      FE
30.      CR
31.      NI
32.      ZR
33.      H2OCLN
         $
         $ time and flow rate information
34.         2    2    2    2    2    2    2    6
35.         10800.      4.920    21600.      4.920
36.         10800.      1.018    21600.      1.018
37.         10800.      .0926    21600.     0.0926
38.         10800.      0.926    21600.      0.926
39.         10800.      .3426    21600.     0.3426
40.         10800.      .1902    21600.     0.1902
41.         10800.      1.267    21600.      1.267
42.         10800.         0.    14400.         0.    14430.     20.00    18030.     20.00
43.         18060.         0.    21600.         0.
         $
         $ temperature of added material - oxides, metals, coolant
44.         2    2    2
45.         10800.      2300.    80000.      2300.
46.         10800.      2300.    80000.      2300.
47.         10800.       320.    80000.       320.
         $
         $ emissivities vs. time - oxides, metals, surroundings
48.      TIMETIMETIME
49.         1    1    1
50.            0.0       0.8
51.            0.0       0.6
52.            0.0       0.6
         $
         $ mean beam length
53.            3.0
         $
```

Table 6.4 Output listing for the BWR sample problem (continued)

```
      $ user flexibility input
54.     0   0   0   0   0   0   0   0   0   0   0   0   0   1   0
55.     0   1   0   0   0   0   0   1   1
      $ temperature dependent metal phase thermal conductivity multiplier
56.     1
57.         0.      0.5
      $
      $ temperature dependent oxide phase viscosity multiplier
58.     1
59.         0.      5.0
      $
      $ mole fraction concrete oxides at which oxide solidus = concrete solidus
60.       0.2
      $
      $ cutoff for inclusion in chemistry solution - ZILCH
61.       0.01
      $
      $ VANESA input
      $ user options
      $                 * IDEAL=1, run with ideal chemistry on
62.     1   1   1   1
      $
      $ pool scrubbing parameters
63.       20      2.3       1       1      1.0      1.0
```

```
                BWR ACCIDENT - WATER ADDED AFTER 1 HOUR

                                        * * *  I N P U T  * * *


                        ***  FLAGS  ***

   ILYR  = 3    ICOOL  = 0    IGEOM  = 2    ICON   = 1
   ICHEM = 1    IFP    = 0    ISUR   = 1    IABL   = 0
   ISPLSH= 0    IPINC  =**    IFILM  = 0    IRSTRT = 0
   IMOV  = 0    IPG    = 1    ISRABL = 1    IAOPAC = 1
   ITIMR = 0    IFVAN  = 1    IVANFP = 0    IUSER  = 1

TIMESTEP CONTROL.  DTMIN(I)  DTMAX(I)      TIMDT(I)
                     30.000    30.000     1.000E+10

EDIT CONTROL.  DEDIT(I)      TEDIT(I)
              5400.000     1.000E+10

                                    RAY CENTER COORDINATES

                              RO =        0.              ZO =   1.50000

                                 CONCRETE CAVITY GEOMETRY

                                      RIGHT CYLINDER

                             NRAYS - NUMBER OF RAYS =    60

                             ZT - Z-COORDINATE OF TOP =          0.

                             RAD - CYLINDER RADIUS (M) =     3.20000

                             HIT - CYLINDER HEIGHT (M) =     5.00000

                             RADC - CORNER RADIUS (M) =    0.100000

                             NBOT - NUMBER OF BOTTOM POINTS =    10

                             NCORN = NUMBER OF CORNER POINTS =     6


                        ***  CONTROL PARAMETERS  ***

   TIMEO  = 10800.00 (SEC)     DELTIM =  30.0000 (SEC)
   TIMEND = 21600.00 (SEC)
   DPRIN  =     0.00 (SEC)     TPRIN  = 70000.00 (SEC)
```

Table 6.4 Output listing for the BWR sample problem (continued)

* * * CONCRETE SPECIFICATIONS * * *

BASALTIC AGGREGATE CONCRETE

RHOC (KG/M3)	RBR (KG/KG C)	SI (-)	TSOL (K)	TLIQ (K)	TIC (K)	TW (K)	DELH (J/KG)	EW (-)
2.340000E+03	1.350000E-01	7.360000E-02	1.350000E+03	1.650000E+03	3.000000E+02	1.630000E+03	2.339836E+06	6.000000E-01

SPECIES NAME	MASS FR.(KG/KG C)	MOLECULAR WT.
SIO2	0.5484	60.0843
TIO2	0.0105	79.8988
MGO	0.0616	40.3044
CAO	0.0882	56.0794
NA2O	0.0180	61.9790
K2O	0.0539	94.1960
FE2O3	0.0626	159.6922
AL2O3	0.0832	101.9613
CO2	0.0150	44.0098
H2OEVAP	0.0386	18.0152
H2OCHEM	0.0200	18.0152

MELT FISSION PRODUCT INVENTORY

BASED ON 1.40100E+02 METRIC TON URANIUM CORE OPERATED AT 3.29300E+03 MW(THERMAL)

MELT CONTAINS 4.68309E+01 METRIC TONS URANIUM, CORRESPONDING TO 33.43 PERCENT OF CORE

ELEMENTS, RETAINED FRACTIONS (**DENOTES USER INPUT, OTHERS FROM WASH 1400), AND GRAM-ATOMS IN MELT

MO	(0.970)	6.2430E+02	TC	(0.970)	1.5973E+02	RU	(0.970)	3.9591E+02	RH	(0.970)	7.2135E+01
SB	(0.850)	2.1529E+00	TE	(0.850)	5.5801E+01	SR	(0.900)	2.0834E+02	BA	(0.900)	1.8268E+02
ZR	(0.990)	7.7894E+02	CE	(0.990)	4.0756E+02	NP	(0.990)	4.0342E+01	CM	(0.990)	1.6858E+00
NB	(0.990)	1.1944E+01	PU	(0.990)	7.4516E+02	AM	(0.990)	5.3691E+00	Y	(0.990)	1.1704E+02
LA	(0.990)	1.7523E+02	PR	(0.990)	1.5235E+02	ND	(0.990)	4.8929E+02	SM	(0.990)	5.7331E+01
EU	(0.990)	1.7043E+01	RB	(0.190)	1.6673E+01	CS	(0.190)	7.5814E+01	BR	(0.100)	5.6457E-01
I	(0.100)	3.3419E+00									

FISSION PRODUCTS GROUPED AS 4 PSEUDO-SPECIES

1.31003E+03 GRAM-ATOMS OF FPM WITH ATOMIC FRACTIONS

MO	4.76552E-01	TC	1.21930E-01	RU	3.02216E-01	RH	5.50639E-02
TE	4.25953E-02					SB	1.64339E-03

3.39030E+03 GRAM-ATOMS OF FPOX WITH ATOMIC FRACTIONS

SR	6.14511E-02	BA	5.38829E-02	ZR	2.29756E-01	CE	1.20214E-01	NP	1.18992E-02
CM	4.97248E-04	NB	3.52284E-03	PU	2.19792E-01	AM	1.58367E-03	Y	3.45213E-02
LA	5.16855E-02	PR	4.49356E-02	ND	1.44321E-01	SM	1.69103E-02	EU	5.02713E-03

```
9.24864E+01 GRAM-ATOMS OF FPALKMET WITH ATOMIC FRACTIONS
      RB  1.80272E-01          CS  8.19728E-01

3.90643E+00 GRAM-ATOMS OF FPHALOGN WITH ATOMIC FRACTIONS
      BR  1.44524E-01          I   8.55476E-01

                INITIAL POWER AT START OF CORCON, 1.08000E+04 SEC AFTER SCRAM IS 6.86111E+06 WATTS
                    REPRESENTING   0.62 PERCENT OF OPERATING POWER OF FRACTION OF CORE IN MELT

                                INITIAL CORE MASSES (KG) OF CONSTITUENTS AND TEMPERATURES

              OXIDES            SPEMW          CONINP          METALS          SPEMW          CONINP

              FEO          7.1846397E+01  1.0000000E+03    FE          5.5847000E+01  2.3387000E+04
              UO2          2.7002780E+02  5.3133000E+04    CR          5.1995998E+01  3.7000000E+03
              ZRO2         1.2321880E+02  1.0997000E+04    NI          5.8709999E+01  2.0550000E+03
              FPOX         1.4748474E+02  5.0001773E+02    ZR          9.1220001E+01  1.3690000E+04
              FPALKMET     1.2435149E+02  1.1500827E+01    FPM         9.9529694E+01  1.3038666E+02
              FPHALOGN     1.2011028E+02  4.0920219E-01

INITIAL TEMPERATURE (TO) IN DEGREES K =     2.5000000E+03

INITIAL TEMPERATURE (TM) IN DEGREES K =     2.5000000E+03

INITIAL MASS OF OXIDES =     6.5641984E+04

INITIAL MASS OF METALS =     4.2962387E+04

                                        * * * REACTING GAS MIXTURE * * *

     ***  ATMOSPHERIC PRESSURE SPECIFIED AS OF TIME  ***

    TIME  1.0800E+04  2.1600E+04
PRESSURE  1.5000E+05  2.5000E+05

                                    VA              PA              TA
                                   (M3)          (N/M2)         (DEG K)

                            4.5050000E+03   1.5000000E+05   3.8000000E+02

                                          GAS INPUT

                                SPECIES NAME    MOLE FR. (-)    MOLECULAR WT.

                                     CO2          0.1700          44.0098
                                     H2           0.1300           2.0158
                                     N2           0.7000          28.0134
```

Table 6.4 Output listing for the BWR sample problem (continued)

```
***  MELT INTERNAL CONDITIONS  ***

***  BOUNDARY CONDITIONS - SURROUNDINGS ABOVE MELT  ***

     ***  SURFACE TEMPERATURE VARIATION WITH TIME  ***

          ***  TS(DEG K) INPUT AS TABLES .VS. TIME  ***

               TIME(SEC)      TS(DEG K)
               1.0800E+04     5.0000E+02
               2.1600E+04     1.0000E+03

     ***  SURROUNDINGS MATERIAL MELTING OR ABLATION DURING INTERACTION  ***

          ***  ABLATION OF SURROUNDINGS IS COMPUTED IN PROGRAM  ***

          ***  MASS FLOW RATES OF METALS AND OXIDES INTO POOL SPECIFIED AS INPUT  ***

        SPECIES  TIME(SEC)  FLOW RATE(KG/S)

       UO2
               1.0800E+04     4.9200E+00
               2.1600E+04     4.9200E+00

       ZRO2
               1.0800E+04     1.0180E+00
               2.1600E+04     1.0180E+00

       FEO
               1.0800E+04     9.2600E-02
               2.1600E+04     9.2600E-02

       FE
               1.0800E+04     9.2600E-01
               2.1600E+04     9.2600E-01

       CR
               1.0800E+04     3.4260E-01
               2.1600E+04     3.4260E-01
```

```
      NI
                1.0800E+04      1.9020E-01
                2.1600E+04      1.9020E-01

      ZR
                1.0800E+04      1.2670E+00
                2.1600E+04      1.2670E+00

      H2OCLN
                1.0800E+04      0.0000E+00
                1.4400E+04      0.0000E+00
                1.4430E+04      2.0000E+01
                1.8030E+04      2.0000E+01
                1.8060E+04      0.0000E+00
                2.1600E+04      0.0000E+00
*** F. P. COMPOSITION NOT SPECIFIED. - WILL ASSUME SAME RELATIVE COMPOSITION AS INITIAL MELT. ***

         ***   T(DEG K) INPUT AS TABLES .VS. TIME  ***

              TIME(SEC)     TMET(DEG K)
              1.0800E+04      2.3000E+03
              8.0000E+04      2.3000E+03

              TIME(SEC)      TOX(DEG K)
              1.0800E+04      2.3000E+03
              8.0000E+04      2.3000E+03

              TIME(SEC)     TCLN(DEG K)
              1.0800E+04      3.2000E+02
              8.0000E+04      3.2000E+02

***  BOUNDARY CONDITIONS - RADIATIVE HEAT TRANSFER  ***
                                    ***  SURFACE EMISSIVITIES .VS. TIME OR TEMP.  ***

     TIME  0.0000E+00
       EO  8.0000E-01

     TIME  0.0000E+00
       EM  6.0000E-01

     TIME  0.0000E+00
       ES  6.0000E-01
```

Table 6.4 Output listing for the BWR sample problem (continued)

```
      ***  AEROSOL OPACITY INCLUDED IN ATMOSPHERE  ***
             CHARACTERISTIC PATH LENGTH (M) =  3.0000E+00

      ***  NO MELT/COOLANT SPLASHOUT  ***

      ***  NO TIME-DEPENDENT MELT RADIUS USED  ***

*** PLOTS WERE NOT SPECIFIED, IMOV = 0

                                *** ADDITIONAL USER SUPPLIED MODEL INPUTS ***

                  *** THE USER HAS CHOSEN TO MODIFY SOME CORCON MODELS AND PARAMETERS


   IKM =  1
   THE USER HAS CHOSEN TO SUPPLY TEMPERATURE-DEPENDENT MULTIPLIERS
   FOR THE CALCULATED METAL MIXTURE THERMAL CONDUCTIVITY

               TEMP(K)         MULTIPLIER

                0.0000E+00      5.0000E-01

   IVSO =  1
   THE USER HAS CHOSEN TO SUPPLY TEMPERATURE-DEPENDENT MULTIPLIERS
   FOR THE CALCULATED OXIDE MIXTURE VISCOSITY

               TEMP(K)         MULTIPLIER

                0.0000E+00      5.0000E+00

   IPHO =  1
   THE USER HAS CHOSEN TO MODIFY THE OXIDE PHASE DIAGRAM

   THE OXIDE SOLIDUS TEMPERATURE EQUALS THE CONCRETE SOLIDUS AT X(CONCRETE) = 2.0000E-01

   IZIP =  1
   THE USER HAS CHOSEN TO SUPPLY THE VALUE FOR ZILCH USED IN MLTREA

   ZILCH =  1.0000E-02
```

```
                    * * * VANESA INPUT * * *


      BUBBLE DIAMETER IS CALCULATED
    PARTICLE DIAMETER =     1.00 MICROMETERS
     PARTICLES/BUBBLE IS CALCULATED
     IDEAL CHEMISTRY IS ASSUMED

              INITIAL MELT COMPOSITION
              G-MOLES                KG
FE          418769.1          23387.000
CR           71159.3           3700.000
FEO          13918.6           1000.000
CR203            0.0              0.000
NI           35002.6           2055.000
MO             624.4             59.901
RU             627.9             63.461
SN               0.0              0.000
SB               2.2              0.262
TE              55.8              7.120
AG               0.0              0.000
MN               0.0              0.000
CAO              0.0              0.000
AL203            0.0              0.000
SI02             0.0              0.000
U02         196789.8          53133.000
ZR02         89247.7          10997.000
CS20            44.3             12.481
BAO            182.8             28.024
SRO            208.4             21.590
LA203          504.1            164.238
CE02          1975.8            340.069
MBO             11.9              1.301
CSI              3.9              1.015
ZR          150076.7          13690.000

 ***  WATER POOL DECONTAMINATION  ***

INITIAL BUBBLE SIZE(CM)=      1.00
SIZE SEGMENTS IN DISTRIBUTION =   20
ALL SCAVENGING MECHANISMS ARE OPERATING
IMPACTION BASE ON V(REL)/V(RISE)=      1.00

GEOMETRIC STANDARD DEVIATION OF INPUT SIZE DISTRIBUION=  2.30


                    * * *   END OF INPUT  * * *
```

Table 6.4 Output listing for the BWR sample problem (continued)

```
                                    CORCON VERSION 2.28
  TIME =  10800.00        BWR ACCIDENT - WATER ADDED AFTER 1 HOUR                    IT. NO. =   0
                          ****GENERAL  SUMMARY****

MELT AND COOLANT LAYERS

  NUMBER OF LAYERS,   NLYR  = 1
  CONFIGURATION,      ILYR  = 2
  NO COOLANT PRESENT, ICOOL = 0

EXTREME CAVITY DIMENSIONS, WITH LOCATIONS

      RADIAL                                          AXIAL
  MAXIMUM CAVITY RADIUS       (M) =   3.20000   DEEPEST POINT IN CAVITY     (M) =   5.00000
  OUTSIDE RADIUS OF CONCRETE  (M) =   4.43800   MAXIMUM DEPTH OF CONCRETE   (M) =   8.05000
  REMAINING THICKNESS         (M) =   1.23800   REMAINING THICKNESS         (M) =   3.05000
  CORRESPONDING BODY POINT        =        18   CORRESPONDING BODY POINT        =         1

APPROXIMATE OVERALL ENERGY BUDGET FOR DEBRIS
(SEE MANUAL FOR EXPLANATION AND CAVEATS)

  INTERNAL (DECAY) SOURCE      (W) =  6.848E+06
  CHEMICAL REACTION SOURCE     (W) =  0.000E+00

  HEAT LOSS TO CONCRETE        (W) =  1.686E+07
  HEATUP OF ABLATION PRODUCTS  (W) =  0.000E+00
  HEAT LOSS FROM SURFACE       (W) =  1.756E+07
    (TO SURROUNDINGS)

  CHANGE IN POOL ENTHALPY      (W) =  0.000E+00
   (SUMMATION OF M*DH/DT)

NUMERICAL CHECKS ON MASS AND ENERGY CONSERVATION

  RELATIVE ERROR IN MASS     =    0.00000E+00     RELATIVE ERROR IN ENTHALPY =    0.00000E+00

CHECK ON RECESSION CALCULATION (DD/DS SHOULD BE .LE. 1)

  MAXIMUM DD/DS =   0.00000
```

Table 6.4 Output listing for the BWR sample problem (continued)

```
                                    CORCON VERSION 2.28
TIME =  10800.00        BWR ACCIDENT - WATER ADDED AFTER 1 HOUR                    IT. NO. =   0
                                  * * * * G A S   G E N E R A T I O N * * * *

GAS EXITING POOL (INCLUDES FILM AND COOLANT)

                        GENERATION RATE                CUMULATIVE RELEASE
      SPECIES     MASS (KG/S)     MOLES (1/S)      MASS (KG)       MOLES (-)      SPECIES
      C(G)      0.00000E+00     0.00000E+00     0.00000E+00     0.00000E+00     C(G)
      CH4       0.00000E+00     0.00000E+00     0.00000E+00     0.00000E+00     CH4
      CO        0.00000E+00     0.00000E+00     0.00000E+00     0.00000E+00     CO
      CO2       0.00000E+00     0.00000E+00     0.00000E+00     0.00000E+00     CO2
      C2H2      0.00000E+00     0.00000E+00     0.00000E+00     0.00000E+00     C2H2
      C2H4      0.00000E+00     0.00000E+00     0.00000E+00     0.00000E+00     C2H4
      C2H6      0.00000E+00     0.00000E+00     0.00000E+00     0.00000E+00     C2H6
      H         0.00000E+00     0.00000E+00     0.00000E+00     0.00000E+00     H
      H2        0.00000E+00     0.00000E+00     0.00000E+00     0.00000E+00     H2
      H2O       0.00000E+00     0.00000E+00     0.00000E+00     0.00000E+00     H2O
      N         0.00000E+00     0.00000E+00     0.00000E+00     0.00000E+00     N
      NH3       0.00000E+00     0.00000E+00     0.00000E+00     0.00000E+00     NH3
      N2        0.00000E+00     0.00000E+00     0.00000E+00     0.00000E+00     N2
      O         0.00000E+00     0.00000E+00     0.00000E+00     0.00000E+00     O
      O2        0.00000E+00     0.00000E+00     0.00000E+00     0.00000E+00     O2
      OH        0.00000E+00     0.00000E+00     0.00000E+00     0.00000E+00     OH
      CHO       0.00000E+00     0.00000E+00     0.00000E+00     0.00000E+00     CHO
      CH2O      0.00000E+00     0.00000E+00     0.00000E+00     0.00000E+00     CH2O
      CRO3(G)   0.00000E+00     0.00000E+00     0.00000E+00     0.00000E+00     CRO3(G)
      FPMO2(G)  0.00000E+00     0.00000E+00     0.00000E+00     0.00000E+00     FPMO2(G)
      FPMO3(G)  0.00000E+00     0.00000E+00     0.00000E+00     0.00000E+00     FPMO3(G)
      AL2O2(G)  0.00000E+00     0.00000E+00     0.00000E+00     0.00000E+00     AL2O2(G)
      AL2O(G)   0.00000E+00     0.00000E+00     0.00000E+00     0.00000E+00     AL2O(G)
      ALO(G)    0.00000E+00     0.00000E+00     0.00000E+00     0.00000E+00     ALO(G)
      OALH(G)   0.00000E+00     0.00000E+00     0.00000E+00     0.00000E+00     OALH(G)
      ALOH(G)   0.00000E+00     0.00000E+00     0.00000E+00     0.00000E+00     ALOH(G)
      OALOH(G)  0.00000E+00     0.00000E+00     0.00000E+00     0.00000E+00     OALOH(G)
      ALO2(G)   0.00000E+00     0.00000E+00     0.00000E+00     0.00000E+00     ALO2(G)
```

Table 6.4 Output listing for the BWR sample problem (continued)

CORCON VERSION 2.28

TIME = 10800.00 BWR ACCIDENT - WATER ADDED AFTER 1 HOUR IT. NO. = 0

* * * * G E O M E T R Y * * * *

BODY POINT	R COORDINATE (M)	Z COORDINATE (M)	STREAM LENGTH (M)	BODY ANGLE (DEG)	RAY ANGLE (DEG)	VOLUME (M3)	SURFACE AREA (M2)	VOID FRACTION (-)
1	0.000000	5.000000	0.000000	0.000	0.000	0.00000	0.00000	0.00000
2	0.344444	5.000000	0.344444	0.000	5.621	0.00000	0.37272	0.00000
3	0.688889	5.000000	0.688889	0.000	11.135	0.00000	1.49090	0.00000
4	1.033333	5.000000	1.033333	0.000	16.449	0.00000	3.35452	0.00000
5	1.377778	5.000000	1.377778	0.000	21.487	0.00000	5.96360	0.00000
6	1.722222	5.000000	1.722222	0.000	26.200	0.00000	9.31812	0.00000
7	2.066667	5.000000	2.066667	0.000	30.561	0.00000	13.41809	0.00000
8	2.411111	5.000000	2.411111	0.000	34.563	0.00000	18.26351	0.00000
9	2.755556	5.000000	2.755556	0.000	38.213	0.00000	23.85439	0.00000
10	3.100000	5.000000	3.100000	0.000	41.532	0.00000	30.19071	0.00000
11	3.100000	5.000000	3.100000	0.000	0.000	0.00000	30.19071	0.00000
12	3.122252	4.997493	3.122393	12.857	41.756	0.07624	30.62844	0.00000
13	3.143389	4.990097	3.144786	25.714	42.008	0.30428	31.06922	0.00000
14	3.162349	4.978183	3.167179	38.572	42.277	0.67634	31.51283	0.00000
15	3.178183	4.962349	3.189572	51.429	42.550	1.17630	31.95889	0.00000
16	3.190097	4.943388	3.211965	64.286	42.813	1.78023	32.40689	0.00000
17	3.197493	4.922252	3.234357	77.143	43.055	2.45755	32.85625	0.00000
18	3.200000	4.900000	3.256750	86.786	43.264	3.17283	33.30631	0.00000
19	3.200000	4.783333	3.373417	90.000	44.264	6.92599	35.65203	0.00000
20	3.200000	4.666667	3.490083	90.000	45.300	10.67914	37.99775	0.00000
	3.200000	4.550531	MIXTURE / ATMSPHRE INTERFACE					
21	3.200000	4.550000	3.606750	90.000	46.375	14.43230	40.34348	1.00000
22	3.200000	4.433333	3.723417	90.000	47.490	18.18546	42.68920	1.00000
23	3.200000	4.316667	3.840084	90.000	48.645	21.93862	45.03493	1.00000
24	3.200000	4.200000	3.956750	90.000	49.844	25.69177	47.38064	1.00000
25	3.200000	4.083333	4.073417	90.000	51.086	29.44493	49.72637	1.00000
26	3.200000	3.966667	4.190084	90.000	52.374	33.19809	52.07209	1.00000
27	3.200000	3.850000	4.306750	90.000	53.707	36.95124	54.41782	1.00000
28	3.200000	3.733334	4.423417	90.000	55.088	40.70439	56.76353	1.00000
29	3.200000	3.616667	4.540084	90.000	56.517	44.45755	59.10926	1.00000
30	3.200000	3.500000	4.656751	90.000	57.995	48.21071	61.45499	1.00000
31	3.200000	3.383333	4.773417	90.000	59.521	51.96386	63.80070	1.00000
32	3.200000	3.266667	4.890084	90.000	61.098	55.71701	66.14642	1.00000
33	3.200000	3.150000	5.006751	90.000	62.723	59.47017	68.49215	1.00000
34	3.200000	3.033333	5.123418	90.000	64.398	63.22333	70.83788	1.00000
35	3.200000	2.916667	5.240085	90.000	66.121	66.97648	73.18359	1.00000
36	3.200000	2.800000	5.356751	90.000	67.891	70.72963	75.52931	1.00000
37	3.200000	2.683333	5.473418	90.000	69.706	74.48279	77.87504	1.00000
38	3.200000	2.566667	5.590085	90.000	71.565	78.23594	80.22076	1.00000

Table 6.4 Output listing for the BWR sample problem (continued)

39	3.200000	2.450000	5.706752	90.000	73.465	81.98910	82.56648	1.00000
40	3.200000	2.333333	5.823419	90.000	75.403	85.74225	84.91220	1.00000
41	3.200000	2.216667	5.940085	90.000	77.376	89.49541	87.25793	1.00000
42	3.200000	2.100000	6.056752	90.000	79.380	93.24856	89.60365	1.00000
43	3.200000	1.983333	6.173419	90.000	81.411	97.00172	91.94937	1.00000
44	3.200000	1.866667	6.290086	90.000	83.463	100.75487	94.29509	1.00000
45	3.200000	1.750000	6.406753	90.000	85.533	104.50803	96.64082	1.00000
46	3.200000	1.633333	6.523419	90.000	87.614	108.26118	98.98653	1.00000
47	3.200000	1.516667	6.640086	90.000	89.702	112.01434	101.33226	1.00000
48	3.200000	1.400000	6.756753	90.000	91.790	115.76749	103.67798	1.00000
49	3.200000	1.283333	6.873420	90.000	93.873	119.52065	106.02370	1.00000
50	3.200000	1.166667	6.990087	90.000	95.947	123.27380	108.36942	1.00000
51	3.200000	1.050000	7.106753	90.000	98.005	127.02695	110.71514	1.00000
52	3.200000	0.933333	7.223420	90.000	100.042	130.78011	113.06087	1.00000
53	3.200000	0.816667	7.340087	90.000	102.054	134.53326	115.40659	1.00000
54	3.200000	0.700000	7.456753	90.000	104.036	138.28641	117.75231	1.00000
55	3.200000	0.583333	7.573420	90.000	105.985	142.03957	120.09804	1.00000
56	3.200000	0.466667	7.690087	90.000	107.896	145.79272	122.44376	1.00000
57	3.200000	0.350000	7.806754	90.000	109.767	149.54588	124.78949	1.00000
58	3.200000	0.233334	7.923420	90.000	111.595	153.29903	127.13521	1.00000
59	3.200000	0.116667	8.040087	90.000	113.378	157.05219	129.48093	1.00000
60	3.200000	0.000000	8.156754	90.000	115.115	160.80534	131.82664	1.00000

Table 6.4 Output listing for the BWR sample problem (continued)

CORCON VERSION 2.28

TIME = 10800.00 BWR ACCIDENT - WATER ADDED AFTER 1 HOUR IT. NO. = 0

* * * * H E A T T R A N S F E R R E S U L T S * * * *

BODY POINT	ABLATION RATE (M/S)	FILM THICKNESS (M)	FILM FLOW (KG/S)	FILM VELOCITY (M/S)	REYNOLDS NUMBER (-)	REGIME	HT TRANS COEFF (W/M2-K)	INTERFACE TEMPERATURE (K)	CONVECTIVE FLUX (W/M2)	RADIATIVE FLUX (W/M2)
1	7.389E-05	1.000E-10	0.000E+00	0.000E+00	0.748	SLG.BUB.	1.000E+03	2018.4	3.884E+05	0.000E+00
2	7.389E-05	1.000E-10	0.000E+00	0.000E+00	0.748	SLG.BUB.	1.000E+03	2018.4	3.884E+05	0.000E+00
3	7.389E-05	1.000E-10	0.000E+00	0.000E+00	0.748	SLG.BUB.	1.000E+03	2018.4	3.884E+05	0.000E+00
4	7.389E-05	1.000E-10	0.000E+00	0.000E+00	0.748	SLG.BUB.	1.000E+03	2018.4	3.884E+05	0.000E+00
5	7.389E-05	1.000E-10	0.000E+00	0.000E+00	0.748	SLG.BUB.	1.000E+03	2018.4	3.884E+05	0.000E+00
6	7.389E-05	1.000E-10	0.000E+00	0.000E+00	0.748	SLG.BUB.	1.000E+03	2018.4	3.884E+05	0.000E+00
7	7.389E-05	1.000E-10	0.000E+00	0.000E+00	0.748	SLG.BUB.	1.000E+03	2018.4	3.884E+05	0.000E+00
8	7.389E-05	1.000E-10	0.000E+00	0.000E+00	0.748	SLG.BUB.	1.000E+03	2018.4	3.884E+05	0.000E+00
9	7.389E-05	1.000E-10	0.000E+00	0.000E+00	0.748	SLG.BUB.	1.000E+03	2018.4	3.884E+05	0.000E+00
10	7.389E-05	1.000E-10	0.000E+00	0.000E+00	0.748	SLG.BUB.	1.000E+03	2018.4	3.884E+05	0.000E+00
11	7.389E-05	1.000E-10	0.000E+00	0.000E+00	0.748	SLG.BUB.	1.000E+03	2018.4	3.884E+05	0.000E+00
12	7.565E-05	1.000E-10	0.000E+00	0.000E+00	0.766	SLG.BUB.	1.000E+03	2027.6	3.976E+05	0.000E+00
13	8.024E-05	1.000E-10	2.941E-04	0.000E+00	0.822	TRN.BUB.	1.000E+03	2051.7	4.217E+05	0.000E+00
14	8.610E-05	1.000E-10	4.664E-03	0.000E+00	3.946	SLG.FLM.	1.000E+03	2082.5	4.525E+05	0.000E+00
15	9.173E-05	1.000E-10	1.123E-02	0.000E+00	9.452	SLG.FLM.	1.000E+03	2112.1	4.821E+05	0.000E+00
16	9.616E-05	1.000E-10	1.819E-02	0.000E+00	15.256	SLG.FLM.	1.000E+03	2135.4	5.054E+05	0.000E+00
17	9.893E-05	1.000E-10	2.544E-02	0.000E+00	21.286	SLG.FLM.	1.000E+03	2150.0	5.200E+05	0.000E+00
18	9.981E-05	1.000E-10	3.283E-02	0.000E+00	27.452	SLG.FLM.	1.000E+03	2154.6	5.246E+05	0.000E+00
19	9.987E-05	1.000E-10	7.155E-02	0.000E+00	59.827	SLG.FLM.	1.000E+03	2154.9	5.249E+05	0.000E+00
20	9.987E-05	1.000E-10	1.103E-01	0.000E+00	92.212	SLG.FLM.	1.000E+03	2154.9	5.249E+05	0.000E+00

MIXTURE / ATMSPHRE INTERFACE

```
                                        CORCON VERSION 2.28
TIME =  10800.00        BWR ACCIDENT - WATER ADDED AFTER 1 HOUR                IT. NO. =   0
                                  * * * * POOL  COMPOSITION * * * *

                        MIXTURE

MASS OF LAYER           1.0860E+05

MASS OF SPECIES
        FEO             1.0000E+03      FEO
        UO2             5.3133E+04      UO2
        ZRO2            1.0997E+04      ZRO2
        FPOX            5.0002E+02      FPOX
        FPALKMET        1.1501E+01      FPALKMET
        FPHALOGN        4.6920E-01      FPHALOGN
        FE              2.3387E+04      FE
        CR              3.7000E+03      CR
        NI              2.0550E+03      NI
        ZR              1.3690E+04      ZR
        FPM             1.3039E+02      FPM
```

Table 6.4 Output listing for the BWR sample problem (continued)

```
                                    CORCON VERSION 2.28                          IT. NO. =   0
TIME =  10800.00        BWR ACCIDENT - WATER ADDED AFTER 1 HOUR
                              ****LAYER  PROPERTIES*****

                                      MIXTURE
MASS                      (KG)        1.0860E+05
DENSITY                  (KG/M3)      7.5340E+03
THERMAL EXPANSIVITY      (1/K)        2.6364E-05

AVERAGE TEMPERATURE       (K)         2.5000E+03
INTERFACE TEMPERATURE     (K)  2.0184E+03     2.1392E+03
EDGE TEMPERATURE          (K)         2.1549E+03
SOLIDUS TEMPERATURE       (K)         1.7575E+03
LIQUIDUS TEMPERATURE      (K)         2.8522E+03
SPECIFIC ENTHALPY        (J/KG)      -1.8419E+06
TOTAL ENTHALPY            (J)        -2.0004E+11
SPECIFIC HEAT           (J/KG K)      5.8900E+02

VISCOSITY               (KG/M S)      4.8300E-01
THERMAL CONDUCTIVITY    (W/M K)       1.1414E+01
THERMAL DIFFUSIVITY     (M2/S)        2.5722E-06
SURFACE TENSION           (N/M)       9.7989E-01
EMISSIVITY                (-)         7.0832E-01

SUPERFICIAL GAS VEL       (M/S) 5.4636E-02     5.4636E-02
BUBBLE RADIUS             (M)         2.6460E-03
BUBBLE VELOCITY           (M/S)       2.8072E-01
VOID FRACTION             (-)         0.0000E+00

BOT CRUST THICKNESS       (M)         0.0000E+00
HT COEFF, LIQ TO BOT   (W/M2 K)       8.0640E+02
Z-AVE LIQ TEMPERATURE     (K)         2.5000E+03
HT COEFF, LIQ TO TOP   (W/M2 K)       1.5127E+03
TOP CRUST THICKNESS       (M)         0.0000E+00

R-AVE LIQ TEMPERATURE     (K)         2.5007E+03
HT COEFF, LIQ TO SID   (W/M2 K)       1.5195E+03
SIDE CRUST THICKNESS      (M)         1.2881E-03

DECAY HEAT                (W)         6.8481E+06
HEAT TO CONCRETE          (W)         1.6855E+07
HEAT OF REACTION          (W)         0.0000E+00
INTERLAYER HEAT FLOW      (W)                     1.7557E+07
```

```
                                        CORCON VERSION 2.28
  TIME =  10800.00        BWR ACCIDENT - WATER ADDED AFTER 1 HOUR                    IT. NO. =   0
                                  * * * * I N T E R L A Y E R  M I X I N G * * * *


      LOWER MIXTURE LAYER

                                        OXIDE          METAL

  PHASE MASSES              (KG)      6.5642E+04     4.2962E+04
  PHASE DENSITIES         (KG/M3)     8.4080E+03     6.5014E+03
  LIQUIDUS TEMPERATURE      (K)       2.4432E+03     1.7575E+03
  SOLIDUS TEMPERATURE       (K)       2.8522E+03     1.7675E+03
  PHASE ENTHALPIES          (J)      -2.6854E+11     6.8492E+10
  MASS ENTRAINED            (KG)      0.0000E+00     0.0000E+00
  MASS DE-ENTRAINED         (KG)      0.0000E+00     0.0000E+00

 MLTREA REQUIRED 111 ITERATIONS
 MLTREA REQUIRED  51 ITERATIONS

 ********************************************************
 * LAYER ORIENTATION CHANGE AT TIME = 1.08300E+04       *
 * LAYER HMX BECOMES A NEW MET LAYER                    *
 ********************************************************

 MLTREA REQUIRED 111 ITERATIONS
 MLTREA REQUIRED  51 ITERATIONS

 ********************************************************
 * LAYER ORIENTATION CHANGE AT TIME = 1.08600E+04       *
 * LAYERS LOX AND MET COMBINED TO FORM A NEW HMX LAYER *
 ********************************************************

 MLTREA REQUIRED 194 ITERATIONS
```

Table 6.4 Output listing for the BWR sample problem (continued)

```
**********************************************************
* LAYER ORIENTATION CHANGE AT TIME = 1.11900E+04       *
* LAYER HMX BECOMES A NEW LMX LAYER                    *
**********************************************************

 MLTREA REQUIRED  94 ITERATIONS
 MLTREA REQUIRED  53 ITERATIONS

**********************************************************
* LAYER ORIENTATION CHANGE AT TIME = 1.12200E+04       *
* LAYER LMX BECOMES A NEW LOX LAYER                    *
**********************************************************

*******************************************
* LMX LAYER CREATED AT TIME = 1.12500E+04 *
*******************************************

 MLTREA REQUIRED 114 ITERATIONS
 MLTREA REQUIRED  51 ITERATIONS

**********************************************************
* LAYER ORIENTATION CHANGE AT TIME = 1.13100E+04       *
* LAYER HOX BECOMES A NEW LOX LAYER                    *
**********************************************************

 MLTREA REQUIRED  51 ITERATIONS

**********************************************************
* LAYER ORIENTATION CHANGE AT TIME = 1.13400E+04       *
* LAYERS LMX AND LOX COMBINED TO FORM A NEW LOX LAYER  *
**********************************************************
```

Table 6.4 Output listing for the BWR sample problem (continued)

```
*********************************************************
* LAYER ORIENTATION CHANGE AT TIME = 1.13400E+04        *
* LAYERS LOX AND MET COMBINED TO FORM A NEW HMX LAYER *
*********************************************************


MLTREA REQUIRED  94 ITERATIONS
MLTREA REQUIRED  51 ITERATIONS
INITDS  ETA MAY BE TOO SMALL
INITDS  ETA MAY BE TOO SMALL
INITDS  ETA MAY BE TOO SMALL
INITDS  ETA MAY BE TOO SMALL
MLTREA REQUIRED  52 ITERATIONS
MLTREA REQUIRED  51 ITERATIONS
```

Table 6.4 Output listing for the BWR sample problem (continued)

```
                                                    CORCON VERSION 2.28
 TIME =  16200.00          BWR ACCIDENT - WATER ADDED AFTER 1 HOUR                    IT. NO. = 180
                          ****GENERAL  SUMMARY****

MELT AND COOLANT LAYERS

  NUMBER OF LAYERS,    NLYR  = 3
  CONFIGURATION,       ILYR  = 0
  NO COOLANT PRESENT,  ICOOL = 0


EXTREME CAVITY DIMENSIONS, WITH LOCATIONS

      RADIAL                                          AXIAL
  MAXIMUM CAVITY RADIUS          (M) =   3.40992   DEEPEST POINT IN CAVITY     (M) =   5.06399
  OUTSIDE RADIUS OF CONCRETE     (M) =   4.43800   MAXIMUM DEPTH OF CONCRETE   (M) =   8.05000
  REMAINING THICKNESS            (M) =   1.02808   REMAINING THICKNESS         (M) =   2.98601
  CORRESPONDING BODY POINT           =        22   CORRESPONDING BODY POINT       =         1


APPROXIMATE OVERALL ENERGY BUDGET FOR DEBRIS
(SEE MANUAL FOR EXPLANATION AND CAVEATS)

  INTERNAL (DECAY) SOURCE        (W) =  8.780E+06
  CHEMICAL REACTION SOURCE       (W) =  2.674E+06

  HEAT LOSS TO CONCRETE          (W) =  3.107E+06
  HEATUP OF ABLATION PRODUCTS    (W) = -1.212E+06
  HEAT LOSS FROM SURFACE         (W) =  1.344E+07
    (TO SURROUNDINGS)

  CHANGE IN POOL ENTHALPY        (W) = -1.372E+10
   (SUMMATION OF M*DH/DT)


NUMERICAL CHECKS ON MASS AND ENERGY CONSERVATION

  RELATIVE ERROR IN MASS     =   -2.26498E-06      RELATIVE ERROR IN ENTHALPY =   -1.07288E-06


CHECK ON RECESSION CALCULATION (DD/DS SHOULD BE .LE. 1)

  MAXIMUM DD/DS =   0.02083
```

CORCON VERSION 2.28

TIME = 16200.00 BWR ACCIDENT - WATER ADDED AFTER 1 HOUR IT. NO. = 180

****GAS GENERATION****

GAS EXITING POOL (INCLUDES FILM AND COOLANT)

	GENERATION RATE		CUMULATIVE RELEASE		
SPECIES	MASS (KG/S)	MOLES (1/S)	MASS (KG)	MOLES (-)	SPECIES
C(G)	2.45079E-13	2.04045E-11	4.61357E-07	3.84112E-05	C(G)
CH4	3.76314E-03	2.34572E-01	9.11339E+00	5.68074E+02	CH4
CO	3.43946E-03	1.22792E-01	1.30867E+02	4.67209E+03	CO
CO2	8.02764E-10	1.82406E-08	1.75248E-02	3.98202E-01	CO2
C2H2	0.00000E+00	0.00000E+00	0.00000E+00	0.00000E+00	C2H2
C2H4	1.38922E-03	4.95214E-02	3.04785E+00	1.08646E+02	C2H4
C2H6	4.94181E-06	1.64347E-04	7.74307E-03	2.57507E-01	C2H6
H	9.58165E-07	9.50654E-04	1.71173E-01	1.69832E+02	H
H2	7.63946E-03	3.78979E+00	1.02100E+02	5.06498E+04	H2
H2O	3.42554E+00	1.90147E+02	8.81155E+03	4.89117E+05	H2O
N	0.00000E+00	0.00000E+00	0.00000E+00	0.00000E+00	N
NH3	0.00000E+00	0.00000E+00	0.00000E+00	0.00000E+00	NH3
N2	0.00000E+00	0.00000E+00	0.00000E+00	0.00000E+00	N2
O	1.20597E-16	7.53760E-15	1.68767E-07	1.05483E-05	O
O2	6.92543E-23	2.16428E-21	1.29229E-11	4.03857E-10	O2
OH	5.71401E-13	3.35974E-11	1.33089E-05	7.82540E-04	OH
CHO	1.07627E-09	3.70892E-08	1.73820E-04	5.99001E-03	CHO
CH2O	5.51553E-09	1.83691E-07	1.55793E-04	5.18856E-03	CH2O
CRO3(G)	5.50218E-29	5.50250E-28	3.56293E-16	3.56314E-15	CRO3(G)
FPMO2(G)	1.28187E-22	9.83506E-22	1.63963E-11	1.25799E-10	FPMO2(G)
FPMO3(G)	6.04694E-28	4.13222E-27	2.40653E-15	1.64452E-14	FPMO3(G)
AL2O2(G)	2.90604E-15	2.07575E-14	5.23587E-09	3.73991E-08	AL2O2(G)
AL2O(G)	1.39218E-07	1.98989E-06	1.33456E-02	1.90754E-01	AL2O(G)
ALO(G)	7.87894E-13	1.83312E-11	4.93128E-06	1.14732E-04	ALO(G)
OALH(G)	1.07344E-14	2.44025E-13	2.73683E-08	6.22164E-07	OALH(G)
ALOH(G)	1.51476E-08	3.44351E-07	1.85552E-03	4.21815E-02	ALOH(G)
OALOH(G)	4.21733E-14	7.03026E-13	1.33582E-07	2.22681E-06	OALOH(G)
ALO2(G)	1.11161E-21	1.88471E-20	1.93918E-12	3.28783E-11	ALO2(G)

Table 6.4 Output listing for the BWR sample problem (continued)

TIME = 16200.00 BWR ACCIDENT - WATER CORCON VERSION 2.28 ADDED AFTER 1 HOUR IT. NO. = 180

**** G E O M E T R Y ****

BODY POINT	R COORDINATE (M)	Z COORDINATE (M)	STREAM LENGTH (M)	BODY ANGLE (DEG)	RAY ANGLE (DEG)	VOLUME (M3)	SURFACE AREA (M2)	VOID FRACTION (-)
1	0.000000	5.063988	0.000000	0.000	0.000	0.00000	0.00000	0.00732
2	0.350742	5.063988	0.350742	0.000	5.621	0.00000	0.38648	0.00732
3	0.701483	5.063988	0.701483	0.000	11.135	0.00000	1.54591	0.00732
4	1.052226	5.063988	1.052226	0.000	16.449	0.00000	3.47830	0.00732
5	1.402967	5.063988	1.402967	0.000	21.487	0.00000	6.18365	0.00732
6	1.753709	5.063988	1.753709	0.000	26.200	0.00000	9.66195	0.00732
7	2.104451	5.063988	2.104451	0.000	30.561	0.00000	13.91322	0.00732
8	2.455193	5.063988	2.455193	0.000	34.563	0.00000	18.93744	0.00732
9	2.805934	5.063988	2.805934	0.000	38.213	0.00000	24.73459	0.00732
10	3.100000	5.063988	3.100000	0.000	0.000	0.00000	30.19071	0.00732
11	3.146289	5.052261	3.147751	25.465	41.532	0.35935	31.12774	0.00732
12	3.161209	5.041134	3.166363	39.886	41.756	0.70702	31.49655	0.00728
13	3.176493	5.026852	3.187282	46.857	42.008	1.15758	31.91305	0.00724
14	3.190768	5.009441	3.209797	54.686	42.277	1.71198	32.36342	0.00720
15	3.202973	4.989352	3.233302	62.992	42.550	2.35697	32.83557	0.00717
16	3.212225	4.967273	3.257242	70.875	42.813	3.07064	33.31804	0.00714
17	3.218485	4.944720	3.280647	78.561	43.055	3.80313	33.79089	0.00713
18	3.221335	4.922668	3.302882	84.182	43.264	4.52139	34.24074	0.00712
19	3.229483	4.813581	3.412274	54.390	44.264	8.08670	36.45766	0.00710
20	3.312683	4.778177	3.502693	28.102	45.300	9.27686	38.31603	0.00689
21	3.387869	4.729066	3.592498	55.551	46.375	11.00869	40.20645	0.00671
22	3.409921	4.625760	3.698131	100.226	47.490	14.75801	42.46235	0.00666
	3.359040	4.545898	OXIDE / MIXTURE INTERFACE					
23	3.229580	4.342703	4.033756	112.106	48.646	24.56062	49.46302	0.00710
	3.221595	4.304179	MIXTURE / COOLANT INTERFACE					
24	3.200000	4.200000	4.179492	95.855	49.844	29.19392	52.40676	0.00363
25	3.200000	4.083333	4.296159	90.000	51.086	32.94707	54.75248	0.00298
26	3.200000	3.966667	4.412826	90.000	52.374	36.70023	57.09821	0.00298
27	3.200000	3.850000	4.529492	90.000	53.707	40.45338	59.44393	0.00298
28	3.200000	3.733334	4.646159	90.000	55.088	44.20654	61.78965	0.00298
29	3.200000	3.616667	4.762826	90.000	56.517	47.95969	64.13538	0.00298
30	3.200000	3.500000	4.879493	90.000	57.995	51.71285	66.48110	0.00298
	3.200000	3.419232	COOLANT / ATMSPHRE INTERFACE					
31	3.200000	3.383333	4.996160	90.000	59.521	55.46600	68.82682	1.00000
32	3.200000	3.266667	5.112826	90.000	61.098	59.21915	71.17254	1.00000
33	3.200000	3.150000	5.229493	90.000	62.723	62.97231	73.51826	1.00000
34	3.200000	3.033333	5.346160	90.000	64.398	66.72547	75.86399	1.00000
35	3.200000	2.916667	5.462827	90.000	66.121	70.47862	78.20971	1.00000
36	3.200000	2.800000	5.579494	90.000	67.891	74.23177	80.55543	1.00000

37	3.200000	2.683333	5.696160	90.000	69.706	77.98493	82.90115	1.00000
38	3.200000	2.566667	5.812827	90.000	71.565	81.73808	85.24687	1.00000
39	3.200000	2.450000	5.929494	90.000	73.465	85.49124	87.59260	1.00000
40	3.200000	2.333333	6.046161	90.000	75.403	89.24439	89.93832	1.00000
41	3.200000	2.216667	6.162827	90.000	77.376	92.99755	92.28404	1.00000
42	3.200000	2.100000	6.279494	90.000	79.380	96.75070	94.62976	1.00000
43	3.200000	1.983333	6.396161	90.000	81.411	100.50386	96.97549	1.00000
44	3.200000	1.866667	6.512828	90.000	83.463	104.25701	99.32121	1.00000
45	3.200000	1.750000	6.629495	90.000	85.533	108.01017	101.66693	1.00000
46	3.200000	1.633333	6.746161	90.000	87.614	111.76332	104.01265	1.00000
47	3.200000	1.516667	6.862828	90.000	89.702	115.51648	106.35838	1.00000
48	3.200000	1.400000	6.979495	90.000	91.790	119.26963	108.70409	1.00000
49	3.200000	1.283333	7.096162	90.000	93.873	123.02279	111.04982	1.00000
50	3.200000	1.166667	7.212829	90.000	95.947	126.77594	113.39554	1.00000
51	3.200000	1.050000	7.329495	90.000	98.005	130.52910	115.74126	1.00000
52	3.200000	0.933333	7.446162	90.000	100.042	134.28226	118.08698	1.00000
53	3.200000	0.816667	7.562829	90.000	102.054	138.03542	120.43271	1.00000
54	3.200000	0.700000	7.679495	90.000	104.036	141.78856	122.77843	1.00000
55	3.200000	0.583333	7.796162	90.000	105.985	145.54172	125.12415	1.00000
56	3.200000	0.466667	7.912829	90.000	107.896	149.29488	127.46988	1.00000
57	3.200000	0.350000	8.029495	90.000	109.767	153.04803	129.81560	1.00000
58	3.200000	0.233334	8.146162	90.000	111.595	156.80118	132.16132	1.00000
59	3.200000	0.116667	8.262829	90.000	113.378	160.55434	134.50703	1.00000
60	3.200000	0.000000	8.379496	90.000	115.115	164.30750	136.85275	1.00000

Table 6.4 Output listing for the BWR sample problem (continued)

CORCON VERSION 2.28

TIME = 16200.00 BWR ACCIDENT - WATER ADDED AFTER 1 HOUR IT. NO. = 180

****HEAT TRANSFER RESULTS****

BODY POINT	ABLATION RATE (M/S)	FILM THICKNESS (M)	FILM FLOW (KG/S)	FILM VELOCITY (M/S)	REYNOLDS NUMBER (-)	REGIME	HT TRANS COEFF (W/M2-K)	INTERFACE TEMPERATURE (K)	CONVECTIVE FLUX (W/M2)	RADIATIVE FLUX (W/M2)
1	4.970E-06	1.000E-10	0.000E+00	0.000E+00	0.038	SLG.BUB.	1.000E+03	1656.1	2.612E+04	0.000E+00
2	4.970E-06	1.000E-10	0.000E+00	0.000E+00	0.038	SLG.BUB.	1.000E+03	1656.1	2.612E+04	0.000E+00
3	4.970E-06	1.000E-10	0.000E+00	0.000E+00	0.038	SLG.BUB.	1.000E+03	1656.1	2.612E+04	0.000E+00
4	4.970E-06	1.000E-10	0.000E+00	0.000E+00	0.038	SLG.BUB.	1.000E+03	1656.1	2.612E+04	0.000E+00
5	4.970E-06	1.000E-10	0.000E+00	0.000E+00	0.038	SLG.BUB.	1.000E+03	1656.1	2.612E+04	0.000E+00
6	4.970E-06	1.000E-10	0.000E+00	0.000E+00	0.038	SLG.BUB.	1.000E+03	1656.1	2.612E+04	0.000E+00
7	4.970E-06	1.000E-10	0.000E+00	0.000E+00	0.038	SLG.BUB.	1.000E+03	1656.1	2.612E+04	0.000E+00
8	4.970E-06	1.000E-10	0.000E+00	0.000E+00	0.038	SLG.BUB.	1.000E+03	1656.1	2.612E+04	0.000E+00
9	4.970E-06	1.000E-10	0.000E+00	0.000E+00	0.038	SLG.BUB.	1.000E+03	1656.1	2.612E+04	0.000E+00
10	4.970E-06	1.000E-10	0.000E+00	0.000E+00	0.038	SLG.BUB.	1.000E+03	1656.1	2.612E+04	0.000E+00
11	4.299E-06	1.000E-10	0.000E+00	0.000E+00	0.033	SLG.BUB.	1.000E+03	1652.6	2.260E+04	0.000E+00
12	3.456E-06	1.000E-10	1.398E-04	0.000E+00	0.118	SLG.FLM.	1.000E+03	1648.2	1.816E+04	0.000E+00
13	2.994E-06	1.000E-10	3.619E-04	0.000E+00	0.305	SLG.FLM.	1.000E+03	1645.7	1.574E+04	0.000E+00
14	2.478E-06	1.000E-10	5.657E-04	0.000E+00	0.474	SLG.FLM.	1.000E+03	1643.0	1.302E+04	0.000E+00
15	1.974E-06	1.000E-10	7.395E-04	0.000E+00	0.618	SLG.FLM.	1.000E+03	1640.4	1.038E+04	0.000E+00
16	1.579E-06	1.000E-10	8.813E-04	0.000E+00	0.734	SLG.FLM.	1.000E+03	1638.3	8.301E+03	0.000E+00
17	1.305E-06	1.000E-10	9.940E-04	0.000E+00	0.826	SLG.FLM.	1.000E+03	1636.9	6.858E+03	0.000E+00
18	1.187E-06	1.000E-10	1.087E-03	0.000E+00	0.903	SLG.FLM.	1.000E+03	1636.2	6.237E+03	0.000E+00
19	2.497E-06	1.000E-10	1.764E-03	0.000E+00	1.461	SLG.FLM.	1.000E+03	1643.1	1.312E+04	0.000E+00
20	4.163E-06	1.000E-10	2.790E-03	0.000E+00	2.254	SLG.FLM.	1.000E+03	1651.9	2.188E+04	0.000E+00
21	2.423E-06	1.000E-10	3.821E-03	0.000E+00	3.018	SLG.FLM.	1.000E+03	1642.7	1.273E+04	0.000E+00
22	1.145E-06	1.000E-10	4.487E-03	0.000E+00	3.521	SLG.FLM.	1.000E+03	1636.0	6.017E+03	0.000E+00
			OXIDE / MIXTURE INTERFACE							
23	7.031E-05	1.000E-10	6.284E-02	0.000E+00	52.079	SLG.FLM.	2.532E+03	1776.0	3.695E+05	0.000E+00
			MIXTURE / COOLANT INTERFACE							
24	0.000E+00	1.000E-10	7.210E-02	0.000E+00	60.292	SLG.FLM.	1.000E+03	393.4	0.000E+00	0.000E+00
25	0.000E+00	1.000E-10	7.210E-02	0.000E+00	60.292	SLG.FLM.	1.000E+03	393.4	0.000E+00	0.000E+00
26	0.000E+00	1.000E-10	7.210E-02	0.000E+00	60.292	SLG.FLM.	1.000E+03	393.4	0.000E+00	0.000E+00
27	0.000E+00	1.000E-10	7.210E-02	0.000E+00	60.292	SLG.FLM.	1.000E+03	393.4	0.000E+00	0.000E+00
28	0.000E+00	1.000E-10	7.210E-02	0.000E+00	60.292	SLG.FLM.	1.000E+03	393.4	0.000E+00	0.000E+00
29	0.000E+00	1.000E-10	7.210E-02	0.000E+00	60.292	SLG.FLM.	1.000E+03	393.4	0.000E+00	0.000E+00
30	0.000E+00	1.000E-10	7.210E-02	0.000E+00	60.292	SLG.FLM.	1.000E+03	393.4	0.000E+00	0.000E+00
			COOLANT / ATMSPHRE INTERFACE							

```
                                    CORCON VERSION 2.28
TIME =  16200.00        BWR ACCIDENT - WATER ADDED AFTER 1 HOUR                    IT. NO. = 180
                  * * * * BULK METAL/OXIDE/GAS REACTION IN  MRK LAYER DURING TIMESTEP * * * *
```

OXIDES			METALS			GASES		
SPECIES NAMES	REACTANTS (MOLS)	PRODUCTS (MOLS)	SPECIES NAMES	REACTANTS (MOLS)	PRODUCTS (MOLS)	SPECIES NAMES	REACTANTS (MOLS)	PRODUCTS (MOLS)
FEO	1.9766E+01	2.1284E-03	FE	5.6412E+05	5.6414E+05	C(G)	0.0000E+00	3.6536E-10
MNO	0.0000E+00	0.0000E+00	CR	1.0654E+05	1.0654E+05	CH4	0.0000E+00	1.3934E+00
AL203	2.3525E+01	1.0559E+00	NI	5.2389E+04	5.2389E+04	CO	0.0000E+00	1.5769E+00
UO2	6.3566E+02	6.1182E+02	ZR	5.5457E+04	5.5113E+04	CO2	3.5968E+00	3.0861E-07
ZRO2	7.2761E+02	1.0718E+03	FPM	1.9496E+03	1.9496E+03	C2H2	0.0000E+00	0.0000E+00
CR203	1.8154E-10	2.1527E-11	MN	0.0000E+00	0.0000E+00	C2H4	0.0000E+00	3.1241E-01
NIO	3.7869E-06	1.5396E-06	C(C)	0.0000E+00	0.0000E+00	C2H6	0.0000E+00	8.0338E-04
FPM02	2.2580E-36	0.0000E+00	AL	2.0658E+04	2.0722E+04	H	0.0000E+00	1.0871E-02
FPM03	1.2690E-16	3.7533E-21	U	6.6506E+02	6.9854E+02	H2	0.0000E+00	3.0907E+01
FE304	3.2003E-18	1.1578E-23	SI	1.1482E+05	1.1508E+05	H2O	3.4327E+01	2.3463E-05
MN304	0.0000E+00	0.0000E+00	UAL3	3.6726E-01	2.8939E-01	N	0.0000E+00	0.0000E+00
SIO2	2.5571E+02	2.7372E-02	UAL2	7.0164E+01	6.0602E+01	NH3	0.0000E+00	0.0000E+00
U308	4.8613E-16	3.5876E-21	CA	2.3012E+02	2.3225E+02	N2	0.0000E+00	0.0000E+00
CAO	9.7071E+01	9.4967E+01	X	1.8691E+02	1.8691E+02	O	0.0000E+00	1.5328E-13
						O2	0.0000E+00	5.1498E-20
						OH	0.0000E+00	5.6969E-10
						CHO	0.0000E+00	5.6969E-07
						CH2O	0.0000E+00	2.3278E-06
						CRO3(G)	0.0000E+00	1.4224E-26
						FPM02(G)	0.0000E+00	2.3224E-20
						FPM03(G)	0.0000E+00	1.0517E-25
						AL202(G)	0.0000E+00	3.6254E-13
						AL2O(G)	0.0000E+00	2.6484E-05
						ALO(G)	0.0000E+00	3.1823E-10
						OALH(G)	0.0000E+00	4.0254E-12
						ALOH(G)	0.0000E+00	4.3880E-06
						OALOH(G)	0.0000E+00	1.1952E-11
						ALO2(G)	0.0000E+00	4.2534E-19

```
                    NO. OF ITERATIONS =  41
```

Table 6.4 Output listing for the BWR sample problem (continued)

```
                                    CORCON VERSION 2.2B
TIME =  16200.00        BWR ACCIDENT - WATER ADDED AFTER 1 HOUR                    IT. NO. = 180
                    * * * * FILM METAL/GAS REACTION DURING TIMESTEP * * * *
```

OXIDES			METALS			GASES		
SPECIES NAMES	REACTANTS (MOLS)	PRODUCTS (MOLS)	SPECIES NAMES	REACTANTS (MOLS)	PRODUCTS (MOLS)	SPECIES NAMES	REACTANTS (MOLS)	PRODUCTS (MOLS)
FEO	0.0000E+00	3.4646E-05	FE	5.6414E+05	5.6414E+05	C(G)	0.0000E+00	2.4678E-10
MNO	0.0000E+00	0.0000E+00	CR	1.0654E+05	1.0654E+05	CH4	0.0000E+00	5.6438E+00
AL2O3	0.0000E+00	4.0162E-02	NI	5.2389E+04	5.2389E+04	CO	0.0000E+00	2.1068E+00
UO2	0.0000E+00	2.0957E+01	ZR	5.5113E+04	5.5078E+04	CO2	1.0105E+01	2.3861E-07
ZRO2	0.0000E+00	3.4457E+01	FPM	1.9496E+03	1.9496E+03	C2H2	0.0000E+00	0.0000E+00
CR2O3	0.0000E+00	2.3390E-13	MN	0.0000E+00	0.0000E+00	C2H4	0.0000E+00	1.1732E+00
NIO	0.0000E+00	2.5112E-08	C(C)	0.0000E+00	0.0000E+00	C2H6	0.0000E+00	4.1270E-03
FPMO2	0.0000E+00	0.0000E+00	AL	2.0722E+04	2.0702E+04	H	0.0000E+00	1.7649E-02
FPMO3	0.0000E+00	1.4156E-23	U	6.9854E+02	6.6740E+02	H2	0.0000E+00	8.2787E+01
FE3O4	0.0000E+00	3.8678E-26	SI	1.1508E+05	1.1508E+05	H2O	9.6442E+01	3.4182E-05
MN3O4	0.0000E+00	0.0000E+00	UAL3	2.8939E-01	3.7086E-01	N	0.0000E+00	0.0000E+00
SIO2	0.0000E+00	6.4176E-04	UAL2	6.0602E+01	7.0708E+01	NH3	0.0000E+00	0.0000E+00
U3O8	0.0000E+00	2.1627E-23	CA	2.3225E+02	2.2865E+02	N2	0.0000E+00	0.0000E+00
CAO	0.0000E+00	3.5951E+00	X	0.0000E+00	0.0000E+00	O	0.0000E+00	7.2847E-14
						O2	0.0000E+00	1.3430E-20
						OH	0.0000E+00	4.3823E-10
						CNO	0.0000E+00	5.4299E-07
						CN2O	0.0000E+00	3.1829E-06
						CRO3(G)	0.0000E+00	2.2830E-27
						FPMO2(G)	0.0000E+00	6.2813E-21
						FPMO3(G)	0.0000E+00	1.8797E-26
						AL2O2(G)	0.0000E+00	2.6019E-13
						AL2O(G)	0.0000E+00	3.3213E-05
						ALO(G)	0.0000E+00	2.3170E-10
						OALH(G)	0.0000E+00	3.2954E-12
						ALOH(G)	0.0000E+00	5.9426E-06
						OALOH(G)	0.0000E+00	9.1383E-12
						ALO2(G)	0.0000E+00	1.4007E-19

```
                    NO. OF ITERATIONS =  45
```

```
                                    CORCON VERSION 2.28
TIME =  16200.00        BWR ACCIDENT - WATER ADDED AFTER 1 HOUR                    IT. NO. = 180
                              ****POOL  COMPOSITION****

                        OXIDE          MIXTURE        COOLANT

MASS OF LAYER       1.2343E+05     4.9660E+04     2.6589E+04

MASS OF SPECIES
        SIO2        1.2749E+03     8.3979E-04                    SIO2
        TIO2        1.6784E+02     3.1878E-01                    TIO2
        FEO         2.1650E+02     1.3866E+00                    FEO
        MGO         9.7082E+02     1.8680E+00                    MGO
        CAO         1.3778E+03     2.7581E+00                    CAO
        NA2O        1.8187E+02     5.2867E-01                    NA2O
        K2O         6.0860E+02     1.5946E+00                    K2O
        FE2O3       1.0006E+03     1.9006E+00                    FE2O3
        AL2O3       2.6908E+02     5.5779E-02                    AL2O3
        UO2         7.9336E+04     1.5895E+02                    UO2
        ZRO2        3.7307E+04     8.3274E+01                    ZRO2
        CR2O3       1.6546E-07     1.6502E-12                    CR2O3
        NIO         1.4285E-03     5.8346E-08                    NIO
        FPMO2       1.8810E-33     0.0000E+00                    FPMO2
        FPMO3       1.1868E-13     2.7516E-22                    FPMO3
        FPOX        7.0081E+02     1.4956E+00                    FPOX
        FPALKMET    1.6124E+01     3.4400E-02                    FPALKMET
        FPHALOGN    4.1236E-01     1.3637E-03                    FPHALOGN
        FE3O4       4.7360E-15     1.3425E-24                    FE3O4
        U3O8        2.6164E-12     1.5169E-21                    U3O8
        FE                         3.1539E+04                    FE
        CR                         5.5501E+03                    CR
        NI                         3.0815E+03                    NI
        ZR                         5.0623E+03                    ZR
        FPM                        1.9393E+02                    FPM
        AL                         5.5857E+02                    AL
        U                          1.5886E+02                    U
        SI                         3.2321E+03                    SI
        UAL3                       1.1830E-01                    UAL3
        UAL2                       2.0646E+01                    UAL2
        CA                         9.1644E+00                    CA
        H2OCLN                                    2.6589E+04     H2OCLN
```

Table 6.4 Output listing for the BWR sample problem (continued)

```
                                    CORCON VERSION 2.28
 TIME =  16200.00        BWR ACCIDENT - WATER ADDED AFTER 1 HOUR                    IT. NO. = 180
                              * * * *  L A Y E R   P R O P E R T I E S  * * * *

                                        OXIDE          MIXTURE        COOLANT
 MASS                      (KG)       1.2343E+05     4.9660E+04     2.6589E+04
 DENSITY                   (KG/M3)    7.0929E+03     6.0277E+03     9.3580E+02
 THERMAL EXPANSIVITY       (1/K)      4.6053E-05     2.2891E-05     3.6328E-04

 AVERAGE TEMPERATURE       (K)        1.8798E+03     1.8358E+03     3.9341E+02
 INTERFACE TEMPERATURE     (K)   1.6561E+03     1.8544E+03     1.6763E+03     4.0314E+02
 EDGE TEMPERATURE          (K)        1.6360E+03     1.7760E+03     3.9341E+02
 SOLIDUS TEMPERATURE       (K)        1.7838E+03     1.7534E+03     2.6821E+02
 LIQUIDUS TEMPERATURE      (K)        2.7553E+03     2.7664E+03     2.7821E+02
 SPECIFIC ENTHALPY         (J/KG)    -5.2045E+06     1.3785E+06    -1.5478E+07
 TOTAL ENTHALPY            (J)       -6.4239E+11     6.8454E+10    -4.1153E+11
 SPECIFIC HEAT             (J/KG K)   6.0514E+02     7.4533E+02     4.2651E+03

 VISCOSITY                 (KG/M S)   7.4446E+02     6.9844E-03     2.2941E-04
 THERMAL CONDUCTIVITY      (W/M K)    2.8554E+00     2.4069E+01     6.0000E-01
 THERMAL DIFFUSIVITY       (M2/S)     6.6526E-07     5.3574E-06     1.5033E-07
 SURFACE TENSION           (N/M)      5.1718E-01     1.6444E+00     7.3000E-02
 EMISSIVITY                (-)        8.0000E-01     6.0086E-01     1.0000E+00

 SUPERFICIAL GAS VEL       (M/S)  2.1406E-03     2.7123E-03     2 5993E-03     5.7956E-04
 BUBBLE RADIUS             (M)        1.0211E-02     1.0331E-02     6.1839E-03
 BUBBLE VELOCITY           (M/S)      3.2471E-03     3.6135E-01     2.7339E-01
 VOID FRACTION             (-)        6.9650E-03     5.9156E-03     3.0615E-03

 BOT CRUST THICKNESS       (M)        1.6761E-02     0.0000E+00     0.0000E+00
 HT COEFF, LIQ TO BOT      (W/M2 K)   1.7162E+02     1.4951E+04     7.5858E+02
 Z-AVE LIQ TEMPERATURE     (K)        1.8850E+03     1.8381E+03     3.9341E+02
 HT COEFF, LIQ TO TOP      (W/M2 K)   7.9912E+03     4.8941E+03     9.8951E+02
 TOP CRUST THICKNESS       (M)        0.0000E+00     4.4561E-03     0.0000E+00

 R-AVE LIQ TEMPERATURE     (K)        1.8874E+03     1.8358E+03     3.9341E+02
 HT COEFF, LIQ TO SID      (W/M2 K)   5.6815E+01     6.1745E+03     1.0000E-10
 SIDE CRUST THICKNESS      (M)        7.0885E-02     0.0000E+00     0.0000E+00

 DECAY HEAT                (W)        7.6810E+06     1.0987E+06     0.0000E+00
 HEAT TO CONCRETE          (W)        9.6937E+05     2.1375E+06     0.0000E+00
 HEAT OF REACTION          (W)        0.0000E+00     2.6739E+06     0.0000E+00
 INTERLAYER HEAT FLOW      (W)                   8.0071E+06     1.3443E+07    -3.0993E+05
```

```
                                    CORCON VERSION 2.28
TIME =  16200.00        BWR ACCIDENT - WATER ADDED AFTER 1 HOUR          IT. NO. = 180
                        **** I N T E R L A Y E R  M I X I N G ****
```

LOWER MIXTURE LAYER

		OXIDE	METAL
PHASE MASSES	(KG)	2.5417E+02	4.9406E+04
PHASE DENSITIES	(KG/M3)	7.1571E+03	6.0228E+03
LIQUIDUS TEMPERATURE	(K)	1.9640E+03	1.7534E+03
SOLIDUS TEMPERATURE	(K)	2.7664E+03	1.7634E+03
PHASE ENTHALPIES	(J)	-1.3325E+09	6.9787E+10
MASS ENTRAINED	(KG)	0.0000E+00	0.0000E+00
MASS DE-ENTRAINED	(KG)	2.5508E+02	0.0000E+00

Table 6.4 Output listing for the BWR sample problem (continued)

```
                                                CORCON VERSION 2.28
TIME =  16200.00        BWR ACCIDENT - WATER ADDED AFTER 1 HOUR                    IT. NO. = 180
                                    * * * * *  V A N E S A  O U T P U T  * * * * *

 TEMPERATURE OF METAL (K)                                    1.8369E+03
 TEMPERATURE OF OXIDE (K)                                    1.8808E+03
 AEROSOL - AMBIENT CONDITIONS (G/CC)                         1.0962E-04
 AEROSOL - STANDARD STATE CONDITIONS (G/CC)                  3.0112E-04
          ( 298.15 (K) AND 1 ATM. )
 GAS (G-MOLES/S)                                             3.9139E+00
 AEROSOL RATE (GRAMS/S)                                      2.8835E+01
 AEROSOL DENSITY (G/CM3)                                     2.1824E+00
 PARTICLE SIZE (MICROMETERS)                                 9.8129E-01
 BUBBLE DIAMETER FOR THE METAL PHASE (CM)                    2.0706E+00
 BUBBLE DIAMETER FOR THE OXIDE PHASE (CM)                    2.0462E+00
 MECHANICAL RELEASES FROM THE AZBEL AND THE ISHII AND KATAOKA CORRELATIONS ARE CALCULATED.

  I            AEROSOL COMPOSITION   MELT COMPOSITION    LOSS(MOLES)     RELEASE FRACTION
                    (WEIGHT %)            (KG)
  2     FE                           3.1511E+04
  3     CR                           5.5398E+03
  4     NI          1.1610E-03       3.0757E+03          1.7107E-04      2.2240E-04
  5     MO          1.7980E-11       8.9914E+01          1.6212E-12      8.3773E-09
  6     RU          5.2327E-11       9.5250E+01          4.4787E-12      3.3728E-08
  7     SN          0.0000E+00       0.0000E+00          0.0000E+00      0.0000E+00
  8     SB          1.2069E-04       3.8510E-01          8.5752E-06      2.1320E-02
  9     TE          7.5508E-02       8.5732E+00          5.1191E-03      1.9793E-01
 10     AG          0.0000E+00       0.0000E+00          0.0000E+00      0.0000E+00
 11     MN          0.0000E+00       0.0000E+00          0.0000E+00      0.0000E+00
 12     CAO         6.7610E-01       1.3806E+03          1.0429E-01      2.3555E-02
 13     AL203       4.1087E-02       2.6913E+02          3.4859E-03      5.3254E-03
 14     NA2O        1.8041E+01       1.8240E+02          2.5181E+00      3.8645E-01
 15     K2O         2.9598E+01       6.1025E+02          2.7179E+00      2.9093E-01
 16     SIO2        5.1185E+01       1.2749E+03          7.3693E+00      6.7549E-02
 17     UO2         1.0945E-02       7.9339E+04          3.5068E-04      8.3010E-05
 18     ZRO2        3.9618E-03       3.7360E+04          2.7814E-04      3.1543E-06
 19     CS2O        7.2857E-02       1.7913E+01          2.2365E-03      5.8427E-02
 20     BAO         8.2746E-02       3.5917E+01          4.6681E-03      1.4437E-01
 21     SRO         1.1093E-01       2.4404E+01          9.2608E-03      2.4563E-01
 22     LA203       5.9528E-04       2.4540E+02          1.5805E-05      3.0109E-03
 23     CEO2        2.5337E-02       4.7559E+02          1.2734E-03      6.8293E-02
 24     NBO         2.0713E-07       1.9491E+00          1.6453E-08      4.2344E-06
 25     CSI         3.8499E-02       8.9518E-01          1.2819E-03      4.1200E-01
202     FEO         3.5513E-02       2.1511E+02          4.2759E-03      2.3861E-04
302     CR203       6.5855E-09       1.6546E-07          3.7482E-10      8.4718E-12
CARBON IN MELT                       0.0000E+00
ZIRCONIUM IN MELT                    5.0242E+03
```

Table 6.4 Output listing for the BWR sample problem (continued)

I		GAS COMPOSITION (WEIGHT %)	RELEASE RATE (GRAMS/SECOND)
1	H2O	1.8230E-04	1.2854E-04
2	H2	9.6818E+01	7.6390E+00
3	H	4.4239E-02	1.7453E-03
4	OH	6.7414E-09	4.4875E-09
5	O	2.2706E-12	1.4214E-12
6	O2	1.8782E-18	2.3523E-18
7	CO2	1.4430E-06	2.4856E-06
8	CO	3.1373E+00	3.4395E+00

Table 6.4 Output listing for the BWR sample problem (continued)

```
                                        CORCON VERSION 2.28
TIME =  16200.00        BWR ACCIDENT - WATER ADDED AFTER 1 HOUR                    IT. NO. = 180
                              ****** POOL  SCRUBBING ******

 INFORMATION SUPPLIED BY VANESA

 MEAN PARTICLE SIZE (UM)                          9.8129E-01
 AEROSOL RATE (GRAMS/S)                           2.8835E+01
 AEROSOL DENSITY (G/CM3)                          2.1824E+00
 POOL DEPTH (CM)                                  8.6848E+01
 POOL TEMPERATURE (K)                             3.9336E+02
 AMBIENT PRESSURE (ATM)                           2.0500E+00

   SIZE          CHARACTERISTIC      MASS        DECONTAMINATION
   RANGE             SIZE          IN RANGE        FACTOR
0.000- 0.249        0.192        1.1988E+00      1.2027E+00
0.249- 0.337        0.296        1.2362E+00      1.1663E+00
0.337- 0.414        0.376        1.2433E+00      1.1596E+00
0.414- 0.487        0.451        1.2407E+00      1.1621E+00
0.487- 0.560        0.523        1.2321E+00      1.1702E+00
0.560- 0.634        0.596        1.2187E+00      1.1830E+00
0.634- 0.712        0.672        1.2007E+00      1.2008E+00
0.712- 0.795        0.753        1.1778E+00      1.2241E+00
0.795- 0.884        0.838        1.1496E+00      1.2542E+00
0.884- 0.981        0.931        1.1151E+00      1.2929E+00
0.981- 1.090        1.034        1.0734E+00      1.3432E+00
1.090- 1.212        1.149        1.0227E+00      1.4097E+00
1.212- 1.353        1.280        9.6117E-01      1.5000E+00
1.353- 1.519        1.432        8.8595E-01      1.6274E+00
1.519- 1.721        1.614        7.9341E-01      1.8172E+00
1.721- 1.978        1.841        6.7877E-01      2.1241E+00
1.978- 2.327        2.137        5.3627E-01      2.6885E+00
2.327- 2.853        2.558        3.6109E-01      3.9928E+00
2.853- 3.862        3.255        1.6050E-01      8.9828E+00
3.862-******        5.021        8.6443E-03      1.6679E+02

 ---------------------------------------------------------
 OVERALL DECONTAMINATION FACTOR                   1.5591
 MASS OUT                                         1.8495E+01

 FIT OF DECONTAMINATED AEROSOL TO LOG NORMAL
 NEW MEAN PARTICLE SIZE (UM)                        0.726
 RANGE (UM)                              0.707 -    0.745
 NEW GEOMETRIC STANDARD DEVIATION                   1.829
 RANGE (UM)                              1.945 -    1.719

 LINEAR CORRELATION COEFFICIENT                  0.990469
```

Table 6.4 Output listing for the BWR sample problem (continued)

```
MLTREA REQUIRED  53 ITERATIONS
MLTREA REQUIRED  53 ITERATIONS
MLTREA REQUIRED  55 ITERATIONS
MLTREA REQUIRED  61 ITERATIONS
MLTREA REQUIRED  53 ITERATIONS
MLTREA REQUIRED  53 ITERATIONS
MLTREA REQUIRED  53 ITERATIONS
MLTREA REQUIRED  53 ITERATIONS
MLTREA REQUIRED  53 ITERATIONS
MLTREA REQUIRED  51 ITERATIONS
MLTREA REQUIRED  51 ITERATIONS
MLTREA REQUIRED  51 ITERATIONS
MLTREA REQUIRED  51 ITERATIONS
```

Table 6.4 Output listing for the BWR sample problem (continued)

```
                                    CORCON VERSION 2.28
  TIME =  21600.00        BWR ACCIDENT - WATER ADDED AFTER 1 HOUR                    IT. NO. = 360
                          * * * * G E N E R A L   S U M M A R Y * * * *

MELT AND COOLANT LAYERS

  NUMBER OF LAYERS,    NLYR  = 3
  CONFIGURATION,       ILYR  = 0
  NO COOLANT PRESENT,  ICOOL = 0


EXTREME CAVITY DIMENSIONS, WITH LOCATIONS

      RADIAL                                          AXIAL
  MAXIMUM CAVITY RADIUS        (M) =   3.43926   DEEPEST POINT IN CAVITY     (M) =   5.08486
  OUTSIDE RADIUS OF CONCRETE   (M) =   4.43800   MAXIMUM DEPTH OF CONCRETE   (M) =   8.05000
  REMAINING THICKNESS          (M) =   0.99874   REMAINING THICKNESS         (M) =   2.96514
  CORRESPONDING BODY POINT          =        24   CORRESPONDING BODY POINT         =         1


APPROXIMATE OVERALL ENERGY BUDGET FOR DEBRIS
(SEE MANUAL FOR EXPLANATION AND CAVEATS)

  INTERNAL (DECAY) SOURCE      (W) =  1.103E+07
  CHEMICAL REACTION SOURCE     (W) =  3.580E+06

  HEAT LOSS TO CONCRETE        (W) =  3.499E+06
  HEATUP OF ABLATION PRODUCTS  (W) = -1.487E+06
  HEAT LOSS FROM SURFACE       (W) =  1.058E+07
    (TO SURROUNDINGS)

  CHANGE IN POOL ENTHALPY      (W) = -2.164E+10
   (SUMMATION OF M*DH/DT)


NUMERICAL CHECKS ON MASS AND ENERGY CONSERVATION

  RELATIVE ERROR IN MASS     =   -4.05312E-06     RELATIVE ERROR IN ENTHALPY =   -1.78814E-07


CHECK ON RECESSION CALCULATION (DD/DS SHOULD BE .LE. 1)

  MAXIMUM DD/DS =   0.00402
```

CORCON VERSION 2.28

TIME = 21600.00 BWR ACCIDENT - WATER ADDED AFTER 1 HOUR IT. NO. = 360

* * * * G A S G E N E R A T I O N * * * *

GAS EXITING POOL (INCLUDES FILM AND COOLANT)

	GENERATION RATE		CUMULATIVE RELEASE		
SPECIES	MASS (KG/S)	MOLES (1/S)	MASS (KG)	MOLES (-)	SPECIES
C(G)	9.49796E-14	7.90771E-12	4.61905E-07	3.84568E-05	C(G)
CH4	5.24064E-03	3.26670E-01	3.20791E+01	1.99962E+03	CH4
CO	1.85434E-03	6.62017E-02	1.41000E+02	5.03383E+03	CO
CO2	3.28865E-10	7.47253E-09	1.75267E-02	3.98245E-01	CO2
C2H2	0.00000E+00	0.00000E+00	0.00000E+00	0.00000E+00	C2H2
C2H4	1.61999E-03	5.77475E-02	1.04995E+01	3.74275E+02	C2H4
C2H6	8.17197E-06	2.71770E-04	4.20700E-02	1.39910E+00	C2H6
H	7.31174E-07	7.25443E-04	1.74762E-01	1.73392E+02	H
H2	8.23833E-03	4.08688E+00	1.40011E+02	6.94568E+04	H2
H2O	5.25124E+00	2.91490E+02	3.05659E+04	1.69667E+06	H2O
N	0.00000E+00	0.00000E+00	0.00000E+00	0.00000E+00	N
NH3	0.00000E+00	0.00000E+00	0.00000E+00	0.00000E+00	NH3
N2	0.00000E+00	0.00000E+00	0.00000E+00	0.00000E+00	N2
O	4.28101E-17	2.67573E-15	1.68767E-07	1.05483E-05	O
O2	1.75147E-23	5.47356E-22	1.29229E-11	4.03857E-10	O2
OH	2.96114E-13	1.74110E-11	1.33104E-05	7.82628E-04	OH
CHO	5.53478E-10	1.90734E-08	1.76750E-04	6.09098E-03	CHO
CH2O	3.79128E-09	1.26266E-07	1.74482E-04	5.81101E-03	CH2O
CRO3(G)	1.13606E-29	1.13612E-28	3.56293E-16	3.56314E-15	CRO3(G)
FPMO2(G)	3.54648E-23	2.72101E-22	1.63963E-11	1.25799E-10	FPMO2(G)
FPMO3(G)	1.32464E-28	9.05205E-28	2.40653E-15	1.64452E-14	FPMO3(G)
AL2O2(G)	1.55346E-15	1.10962E-14	5.24340E-09	3.74528E-08	AL2O2(G)
AL2O(G)	1.00210E-07	1.43234E-06	1.38175E-02	1.97499E-01	AL2O(G)
ALO(G)	3.88366E-13	9.03576E-12	4.93327E-06	1.14778E-04	ALO(G)
OALH(G)	6.32648E-15	1.43820E-13	2.73988E-08	6.22858E-07	OALH(G)
ALOH(G)	1.15627E-08	2.62855E-07	1.90972E-03	4.34137E-02	ALOH(G)
OALOH(G)	2.38082E-14	3.96881E-13	1.33697E-07	2.22872E-06	OALOH(G)
ALO2(G)	3.51935E-22	5.96699E-21	1.93918E-12	3.28783E-11	ALO2(G)

Table 6.4 Output listing for the BWR sample problem (continued)

CORCON VERSION 2.28

TIME = 21600.00 BWR ACCIDENT - WATER ADDED AFTER 1 HOUR IT. NO. = 360

* * * * G E O M E T R Y * * * *

BODY POINT	R COORDINATE (M)	Z COORDINATE (M)	STREAM LENGTH (M)	BODY ANGLE (DEG)	RAY ANGLE (DEG)	VOLUME (M3)	SURFACE AREA (M2)	VOID FRACTION (-)
1	0.000000	5.084857	0.000000	0.000	0.000	0.00000	0.00000	0.00640
2	0.352796	5.084857	0.352796	0.000	5.621	0.00000	0.39102	0.00640
3	0.705591	5.084857	0.705591	0.000	11.135	0.00000	1.56407	0.00640
4	1.058387	5.084857	1.058387	0.000	16.449	0.00000	3.51916	0.00640
5	1.411182	5.084857	1.411182	0.000	21.487	0.00000	6.25628	0.00640
6	1.763978	5.084857	1.763978	0.000	26.200	0.00000	9.77543	0.00640
7	2.116774	5.084857	2.116774	0.000	30.561	0.00000	14.07663	0.00640
8	2.469569	5.084857	2.469569	0.000	34.563	0.00000	19.15986	0.00640
9	2.822365	5.084857	2.822365	0.000	38.213	0.00000	25.02512	0.00640
10	3.100000	5.084857	3.100000	0.000	0.000	0.00000	30.19071	0.00640
11	3.158984	5.066596	3.161746	29.973	41.532	0.56187	31.40483	0.00640
12	3.172656	5.053959	3.180363	43.983	41.756	0.95974	31.77515	0.00636
13	3.187466	5.039034	3.201390	48.886	42.008	1.43392	32.19528	0.00633
14	3.201279	5.021001	3.224105	56.149	42.277	2.01201	32.65119	0.00630
15	3.213223	5.000521	3.247813	63.518	42.550	2.67383	33.12896	0.00627
16	3.222498	4.978362	3.271836	70.326	42.813	3.39468	33.61465	0.00625
17	3.229142	4.956128	3.295041	77.392	43.055	4.12153	34.08499	0.00623
18	3.232414	4.934442	3.316972	83.118	43.264	4.83264	34.53018	0.00623
19	3.242194	4.826624	3.425232	53.493	44.264	8.38247	36.73225	0.00621
20	3.326801	4.792149	3.516594	29.131	45.300	9.55094	38.61769	0.00602
21	3.398903	4.739585	3.605822	56.923	46.375	11.41847	40.50303	0.00587
22	3.421339	4.636224	3.711591	83.221	47.490	15.19463	42.76927	0.00583
23	3.424139	4.513953	3.833894	85.502	48.646	19.69472	45.39948	0.00582
24	3.439260	4.401876	3.946985	104.613	49.844	23.84123	47.83797	0.00579
	3.436793	4.398592	OXIDE / MIXTURE INTERFACE					
	3.210626	4.097480	MIXTURE / COOLANT INTERFACE					
25	3.200000	4.083333	4.345376	108.455	51.086	34.87402	56.14754	0.00630
26	3.200000	3.966667	4.462043	90.000	52.374	38.62718	58.49326	0.00260
27	3.200000	3.850000	4.578710	90.000	53.707	42.38033	60.83898	0.00260
28	3.200000	3.733334	4.695376	90.000	55.088	46.13348	63.18470	0.00260
29	3.200000	3.616667	4.812043	90.000	56.517	49.88664	65.53043	0.00260
30	3.200000	3.500000	4.928710	90.000	57.995	53.63980	67.87615	0.00260
31	3.200000	3.383333	5.045377	90.000	59.521	57.39295	70.22187	0.00260
32	3.200000	3.266667	5.162044	90.000	61.098	61.14610	72.56759	0.00260
33	3.200000	3.150000	5.278710	90.000	62.723	64.89926	74.91331	0.00260
34	3.200000	3.033333	5.395377	90.000	64.398	68.65242	77.25904	0.00260
35	3.200000	2.916667	5.512044	90.000	66.121	72.40557	79.60476	0.00260
36	3.200000	2.800000	5.628711	90.000	67.891	76.15872	81.95048	0.00260
	3.200000	2.694737	COOLANT / ATMSPHRE INTERFACE					

37	3.200000	2.683333	5.745378	90.000	69.706	79.91188	84.29620	1.00000
38	3.200000	2.566667	5.862044	90.000	71.565	83.66503	86.64192	1.00000
39	3.200000	2.450000	5.978711	90.000	73.465	87.41819	88.98765	1.00000
40	3.200000	2.333333	6.095378	90.000	75.403	91.17134	91.33337	1.00000
41	3.200000	2.216667	6.212045	90.000	77.376	94.92450	93.67909	1.00000
42	3.200000	2.100000	6.328712	90.000	79.380	98.67765	96.02481	1.00000
43	3.200000	1.983333	6.445378	90.000	81.411	102.43081	98.37054	1.00000
44	3.200000	1.866667	6.562045	90.000	83.463	106.18396	100.71626	1.00000
45	3.200000	1.750000	6.678712	90.000	85.533	109.93712	103.06198	1.00000
46	3.200000	1.633333	6.795379	90.000	87.614	113.69027	105.40770	1.00000
47	3.200000	1.516667	6.912045	90.000	89.702	117.44343	107.75343	1.00000
48	3.200000	1.400000	7.028712	90.000	91.790	121.19658	110.09914	1.00000
49	3.200000	1.283333	7.145379	90.000	93.873	124.94974	112.44487	1.00000
50	3.200000	1.166667	7.262046	90.000	95.947	128.70290	114.79059	1.00000
51	3.200000	1.050000	7.378713	90.000	98.005	132.45605	117.13631	1.00000
52	3.200000	0.933333	7.495379	90.000	100.042	136.20921	119.48203	1.00000
53	3.200000	0.816667	7.612046	90.000	102.054	139.96237	121.82776	1.00000
54	3.200000	0.700000	7.728713	90.000	104.036	143.71552	124.17348	1.00000
55	3.200000	0.583333	7.845379	90.000	105.985	147.46867	126.51920	1.00000
56	3.200000	0.466667	7.962046	90.000	107.896	151.22183	128.86493	1.00000
57	3.200000	0.350000	8.078712	90.000	109.767	154.97499	131.21065	1.00000
58	3.200000	0.233334	8.195379	90.000	111.595	158.72813	133.55637	1.00000
59	3.200000	0.116667	8.312046	90.000	113.378	162.48129	135.90208	1.00000
60	3.200000	0.000000	8.428713	90.000	115.115	166.23445	138.24780	1.00000

CORCON VERSION 2.28

TIME = 21600.00 BWR ACCIDENT - WATER ADDED AFTER 1 HOUR IT. NO. = 360

****HEAT TRANSFER RESULTS****

BODY POINT	ABLATION RATE (M/S)	FILM THICKNESS (M)	FILM FLOW (KG/S)	FILM VELOCITY (M/S)	REYNOLDS NUMBER (-)	REGIME	HT TRANS COEFF (W/M2-K)	INTERFACE TEMPERATURE (K)	CONVECTIVE FLUX (W/M2)	RADIATIVE FLUX (W/M2)
1	3.735E-06	1.000E-10	0.000E+00	0.000E+00	0.028	SLG.BUB.	1.000E+03	1649.6	1.963E+04	0.000E+00
2	3.735E-06	1.000E-10	0.000E+00	0.000E+00	0.028	SLG.BUB.	1.000E+03	1649.6	1.963E+04	0.000E+00
3	3.735E-06	1.000E-10	0.000E+00	0.000E+00	0.028	SLG.BUB.	1.000E+03	1649.6	1.963E+04	0.000E+00
4	3.735E-06	1.000E-10	0.000E+00	0.000E+00	0.028	SLG.BUB.	1.000E+03	1649.6	1.963E+04	0.000E+00
5	3.735E-06	1.000E-10	0.000E+00	0.000E+00	0.028	SLG.BUB.	1.000E+03	1649.6	1.963E+04	0.000E+00
6	3.735E-06	1.000E-10	0.000E+00	0.000E+00	0.028	SLG.BUB.	1.000E+03	1649.6	1.963E+04	0.000E+00
7	3.735E-06	1.000E-10	0.000E+00	0.000E+00	0.028	SLG.BUB.	1.000E+03	1649.6	1.963E+04	0.000E+00
8	3.735E-06	1.000E-10	0.000E+00	0.000E+00	0.028	SLG.BUB.	1.000E+03	1649.6	1.963E+04	0.000E+00
9	3.735E-06	1.000E-10	0.000E+00	0.000E+00	0.028	SLG.BUB.	1.000E+03	1649.6	1.963E+04	0.000E+00
10	3.735E-06	1.000E-10	0.000E+00	0.000E+00	0.028	SLG.BUB.	1.000E+03	1649.6	1.963E+04	0.000E+00
11	3.838E-06	1.000E-10	7.797E-06	0.000E+00	0.031	TRN.BUB.	1.000E+03	1650.2	2.017E+04	0.000E+00
12	3.937E-06	1.000E-10	1.930E-04	0.000E+00	0.163	SLG.FLM.	1.000E+03	1650.7	2.069E+04	0.000E+00
13	3.973E-06	1.000E-10	4.678E-04	0.000E+00	0.393	SLG.FLM.	1.000E+03	1650.9	2.088E+04	0.000E+00
14	4.026E-06	1.000E-10	7.693E-04	0.000E+00	0.643	SLG.FLM.	1.000E+03	1651.2	2.116E+04	0.000E+00
15	4.075E-06	1.000E-10	1.089E-03	0.000E+00	0.907	SLG.FLM.	1.000E+03	1651.4	2.142E+04	0.000E+00
16	4.113E-06	1.000E-10	1.418E-03	0.000E+00	1.177	SLG.FLM.	1.000E+03	1651.6	2.162E+04	0.000E+00
17	4.143E-06	1.000E-10	1.739E-03	0.000E+00	1.441	SLG.FLM.	1.000E+03	1651.8	2.177E+04	0.000E+00
18	4.158E-06	1.000E-10	2.044E-03	0.000E+00	1.692	SLG.FLM.	1.000E+03	1651.9	2.185E+04	0.000E+00
19	4.007E-06	1.000E-10	3.531E-03	0.000E+00	2.914	SLG.FLM.	1.000E+03	1651.1	2.106E+04	0.000E+00
20	3.833E-06	1.000E-10	4.752E-03	0.000E+00	3.822	SLG.FLM.	1.000E+03	1650.1	2.015E+04	0.000E+00
21	4.032E-06	1.000E-10	5.978E-03	0.000E+00	4.706	SLG.FLM.	1.000E+03	1651.2	2.119E+04	0.000E+00
22	4.158E-06	1.000E-10	7.512E-03	0.000E+00	5.875	SLG.FLM.	1.000E+03	1651.9	2.185E+04	0.000E+00
23	4.161E-06	1.000E-10	9.321E-03	0.000E+00	7.284	SLG.FLM.	1.000E+03	1651.9	2.187E+04	0.000E+00
24	4.164E-06	1.000E-10	1.100E-02	0.000E+00	8.557	SLG.FLM.	1.000E+03	1651.9	2.188E+04	0.000E+00
			OXIDE / MIXTURE INTERFACE							
			MIXTURE / COOLANT INTERFACE							
25	0.000E+00	1.000E-10	9.061E-02	0.000E+00	75.766	SLG.FLM.	1.000E+03	400.6	0.000E+00	0.000E+00
26	0.000E+00	1.000E-10	9.061E-02	0.000E+00	75.766	SLG.FLM.	1.000E+03	400.6	0.000E+00	0.000E+00
27	0.000E+00	1.000E-10	9.061E-02	0.000E+00	75.766	SLG.FLM.	1.000E+03	400.6	0.000E+00	0.000E+00
28	0.000E+00	1.000E-10	9.061E-02	0.000E+00	75.766	SLG.FLM.	1.000E+03	400.6	0.000E+00	0.000E+00
29	0.000E+00	1.000E-10	9.061E-02	0.000E+00	75.766	SLG.FLM.	1.000E+03	400.6	0.000E+00	0.000E+00
30	0.000E+00	1.000E-10	9.061E-02	0.000E+00	75.766	SLG.FLM.	1.000E+03	400.6	0.000E+00	0.000E+00
31	0.000E+00	1.000E-10	9.061E-02	0.000E+00	75.766	SLG.FLM.	1.000E+03	400.6	0.000E+00	0.000E+00
32	0.000E+00	1.000E-10	9.061E-02	0.000E+00	75.766	SLG.FLM.	1.000E+03	400.6	0.000E+00	0.000E+00
33	0.000E+00	1.000E-10	9.061E-02	0.000E+00	75.766	SLG.FLM.	1.000E+03	400.6	0.000E+00	0.000E+00
34	0.000E+00	1.000E-10	9.061E-02	0.000E+00	75.766	SLG.FLM.	1.000E+03	400.6	0.000E+00	0.000E+00
35	0.000E+00	1.000E-10	9.061E-02	0.000E+00	75.766	SLG.FLM.	1.000E+03	400.6	0.000E+00	0.000E+00
36	0.000E+00	1.000E-10	9.061E-02	0.000E+00	75.766	SLG.FLM.	1.000E+03	400.6	0.000E+00	0.000E+00
			COOLANT / ATMSPHRE INTERFACE							

```
                                    CORCON VERSION 2.28
TIME =  21600.00        BWR ACCIDENT - WATER ADDED AFTER 1 HOUR                    IT. NO. = 360
                  * * * * BULK METAL/OXIDE/GAS REACTION IN  MIX LAYER DURING TIMESTEP * * * *
```

OXIDES			METALS			GASES		
SPECIES NAMES	REACTANTS (MOLS)	PRODUCTS (MOLS)	SPECIES NAMES	REACTANTS (MOLS)	PRODUCTS (MOLS)	SPECIES NAMES	REACTANTS (MOLS)	PRODUCTS (MOLS)
FEO	3.0591E+01	4.1609E-03	FE	6.7418E+05	6.7421E+05	C(G)	0.0000E+00	1.0986E-10
MNO	0.0000E+00	0.0000E+00	CR	1.4212E+05	1.4212E+05	CH4	0.0000E+00	1.4573E+00
AL203	2.9313E+01	3.6904E+00	NI	6.9884E+04	6.9884E+04	CO	0.0000E+00	6.3387E-01
UO2	1.8896E+03	1.8614E+03	ZR	6.4534E+04	6.4139E+04	CO2	2.7011E+00	9.7050E-08
ZRO2	2.3107E+03	2.7056E+03	FPM	2.6041E+03	2.6041E+03	C2H2	0.0000E+00	0.0000E+00
CR203	3.1817E-11	4.1287E-11	MN	0.0000E+00	0.0000E+00	C2H4	0.0000E+00	3.0384E-01
NIO	2.5855E-06	3.3371E-06	C(C)	0.0000E+00	0.0000E+00	C2H6	0.0000E+00	1.1306E-03
FPMO2	0.0000E+00	0.0000E+00	AL	2.8315E+04	2.8396E+04	H	0.0000E+00	5.5995E-03
FPMO3	3.2519E-21	4.2405E-21	U	8.9135E+02	9.3450E+02	H2	0.0000E+00	2.2250E+01
FE304	7.9595E-24	1.0386E-23	SI	1.5941E+05	1.5971E+05	H20	2.5779E+01	1.2858E-05
MN304	0.0000E+00	0.0000E+00	UAL3	7.2474E-01	5.8642E-01	N	0.0000E+00	0.0000E+00
SIO2	2.9571E+02	7.1775E-02	UAL2	1.2188E+02	1.0711E+02	NH3	0.0000E+00	0.0000E+00
U308	4.5309E-21	5.8839E-21	CA	2.1976E+02	2.2381E+02	N2	0.0000E+00	0.0000E+00
CAO	2.2009E+02	2.1604E+02	X	4.4415E+02	4.4415E+02	O	0.0000E+00	4.0856E-14
						O2	0.0000E+00	1.0494E-20
						OH	0.0000E+00	2.1046E-10
						CHO	0.0000E+00	2.2208E-07
						CH2O	0.0000E+00	1.1931E-06
						CRO3(G)	0.0000E+00	2.4953E-27
						FPMO2(G)	0.0000E+00	5.1549E-21
						FPMO3(G)	0.0000E+00	1.9350E-26
						AL202(G)	0.0000E+00	1.3909E-13
						AL2O(G)	0.0000E+00	1.3048E-05
						ALO(G)	0.0000E+00	1.1243E-10
						OALH(G)	0.0000E+00	1.6815E-12
						ALOH(G)	0.0000E+00	2.2826E-06
						OALOH(G)	0.0000E+00	4.8124E-12
						ALO2(G)	0.0000E+00	1.8560E-19

```
                    NO. OF ITERATIONS =  43
```

Table 6.4 Output listing for the BWR sample problem (continued)

```
                                    CORCON VERSION 2.28
TIME =  21600.00        BWR ACCIDENT - WATER ADDED AFTER 1 HOUR                    IT. NO. = 360
                    * * * * FILM METAL/GAS REACTION DURING TIMESTEP * * * *
```

OXIDES			METALS			GASES		
SPECIES NAMES	REACTANTS (MOLS)	PRODUCTS (MOLS)	SPECIES NAMES	REACTANTS (MOLS)	PRODUCTS (MOLS)	SPECIES NAMES	REACTANTS (MOLS)	PRODUCTS (MOLS)
FEO	0.0000E+00	3.3529E-05	FE	6.7421E+05	6.7421E+05	C(G)	0.0000E+00	1.2737E-10
MNO	0.0000E+00	0.0000E+00	CR	1.4212E+05	1.4212E+05	CH4	0.0000E+00	8.3428E+00
AL203	0.0000E+00	6.4360E-02	NI	6.9884E+04	6.9884E+04	CO	0.0000E+00	1.3522E+00
UO2	0.0000E+00	2.9314E+01	ZR	6.4139E+04	6.4098E+04	CO2	1.2566E+01	1.2713E-07
ZRO2	0.0000E+00	4.0574E+01	FPM	2.6041E+03	2.6041E+03	C2H2	0.0000E+00	0.0000E+00
CR203	0.0000E+00	2.3488E-13	MN	0.0000E+00	0.0000E+00	C2H4	0.0000E+00	1.4286E+00
NIO	0.0000E+00	2.7279E-08	C(C)	0.0000E+00	0.0000E+00	C2H6	0.0000E+00	7.0225E-03
FPMO2	0.0000E+00	0.0000E+00	AL	2.8396E+04	2.8366E+04	H	0.0000E+00	1.6164E-02
FPMO3	0.0000E+00	9.4048E-24	U	9.3450E+02	8.9029E+02	H2	0.0000E+00	1.0036E+02
FE304	0.0000E+00	1.9863E-26	SI	1.5971E+05	1.5971E+05	H20	1.1993E+02	3.3704E-05
MN304	0.0000E+00	0.0000E+00	UAL3	5.8642E-01	7.2514E-01	N	0.0000E+00	0.0000E+00
SIO2	0.0000E+00	8.1247E-04	UAL2	1.0711E+02	1.2188E+02	NH3	0.0000E+00	0.0000E+00
U308	0.0000E+00	1.9448E-23	CA	2.2381E+02	2.2007E+02	N2	0.0000E+00	0.0000E+00
CAO	0.0000E+00	3.7372E+00	X	0.0000E+00	0.0000E+00	O	0.0000E+00	3.9416E-14
						O2	0.0000E+00	5.9263E-21
						OH	0.0000E+00	3.1187E-10
						CHO	0.0000E+00	3.5013E-07
						CH2O	0.0000E+00	2.5948E-06
						CRO3(G)	0.0000E+00	9.1305E-28
						FPMO2(G)	0.0000E+00	3.0081E-21
						FPMO3(G)	0.0000E+00	7.8059E-27
						AL202(G)	0.0000E+00	1.9380E-13
						AL20(G)	0.0000E+00	2.9923E-05
						ALO(G)	0.0000E+00	1.5864E-10
						OALH(G)	0.0000E+00	2.6331E-12
						ALOH(G)	0.0000E+00	5.6030E-06
						OALOH(G)	0.0000E+00	7.0940E-12
						ALO2(G)	0.0000E+00	7.3414E-20

```
NO. OF ITERATIONS =  39
```

Table 6.4 Output listing for the BWR sample problem (continued)

```
                                    CORCON VERSION 2.28
TIME =  21600.00        BWR ACCIDENT - WATER ADDED AFTER 1 HOUR                    IT. NO. = 360
                              * * * * POOL  COMPOSITION * * * *

                        OXIDE          MIXTURE        COOLANT

MASS OF LAYER       1.6648E+05     6.1700E+04     4.2034E+04

MASS OF SPECIES
        SIO2        2.2839E+03     3.4521E-03                    SIO2
        TIO2        2.3866E+02     1.1734E+00                    TIO2
        FEO         4.2649E+02     2.1994E+00                    FEO
        MGO         1.3861E+03     6.8839E+00                    MGO
        CAO         1.9731E+03     9.7569E+00                    CAO
        NA2O        2.6081E+02     1.9972E+00                    NA2O
        K2O         8.8027E+02     5.9939E+00                    K2O
        FE2O3       1.4229E+03     6.9956E+00                    FE2O3
        AL2O3       4.4084E+02     3.0308E-01                    AL2O3
        UO2         1.0547E+05     5.2100E+02                    UO2
        ZRO2        5.0726E+04     2.9205E+02                    ZRO2
        CR2O3       1.5192E-07     4.9959E-12                    CR2O3
        NIO         1.4247E-03     1.9898E-07                    NIO
        FPMO2       1.8658E-33     0.0000E+00                    FPMO2
        FPMO3       1.1772E-13     4.9234E-22                    FPMO3
        FPOX        9.4722E+02     4.8849E+00                    FPOX
        FPALKMET    2.1681E+01     1.1234E-01                    FPALKMET
        FPHALOGN    6.1044E-01     4.5782E-03                    FPHALOGN
        FE3O4       4.6977E-15     1.9074E-24                    FE3O4
        U3O8        2.5952E-12     3.9353E-21                    U3O8
        FE                         3.7686E+04                    FE
        CR                         7.4002E+03                    CR
        NI                         4.1086E+03                    NI
        ZR                         5.8851E+03                    ZR
        FPM                        2.5907E+02                    FPM
        AL                         7.6536E+02                    AL
        U                          2.1191E+02                    U
        SI                         4.4855E+03                    SI
        UAL3                       2.3130E-01                    UAL3
        UAL2                       3.5588E+01                    UAL2
        CA                         8.8206E+00                    CA
        H2OCLN                                    4.2034E+04     H2OCLN
```

Table 6.4 Output listing for the BWR sample problem (continued)

```
                                    CORCON VERSION 2.28
TIME =  21600.00        BWR ACCIDENT - WATER ADDED AFTER 1 HOUR                    IT. NO. = 360
                              ****LAYER  PROPERTIES****

                                      OXIDE          MIXTURE        COOLANT
MASS                    (KG)        1.6648E+05     6.1700E+04     4.2034E+04
DENSITY                 (KG/M3)     6.9915E+03     5.9438E+03     9.3336E+02
THERMAL EXPANSIVITY     (1/K)       4.6773E-05     2.2572E-05     3.6233E-04

AVERAGE TEMPERATURE     (K)         1.8655E+03     1.8103E+03     4.0062E+02
INTERFACE TEMPERATURE   (K)   1.6496E+03     1.8373E+03     1.5077E+03     4.6163E+02
EDGE TEMPERATURE        (K)         1.6519E+03     1.7579E+03     4.0062E+02
SOLIDUS TEMPERATURE     (K)         1.6645E+03     1.7488E+03     2.6821E+02
LIQUIDUS TEMPERATURE    (K)         2.7459E+03     2.7658E+03     2.7821E+02
SPECIFIC ENTHALPY       (J/KG)     -5.2271E+06     1.3197E+06    -1.5447E+07
TOTAL ENTHALPY          (J)        -8.7018E+11     8.1424E+10    -6.4930E+11
SPECIFIC HEAT           (J/KG K)    6.1128E+02     7.4676E+02     4.2791E+03

VISCOSITY               (KG/M S)    8.1942E+01     7.9704E-03     2.1554E-04
THERMAL CONDUCTIVITY    (W/M K)     2.8648E+00     2.4104E+01     6.0000E-01
THERMAL DIFFUSIVITY     (M2/S)      6.7032E-07     5.4306E-06     1.5023E-07
SURFACE TENSION         (N/M)       5.1619E-01     1.6219E+00     7.3000E-02
EMISSIVITY              (-)         8.0000E-01     6.0233E-01     1.0000E+00

SUPERFICIAL GAS VEL     (M/S)  1.2638E-03     1.6330E-03     1.4629E-03     3.4032E-04
BUBBLE RADIUS           (M)         5.1573E-03     5.1753E-03     3.1141E-03
BUBBLE VELOCITY         (M/S)       7.4180E-03     3.2813E-01     2.4024E-01
VOID FRACTION           (-)         6.0040E-03     4.6563E-03     2.7775E-03

BOT CRUST THICKNESS     (M)         2.2077E-03     0.0000E+00     0.0000E+00
HT COEFF, LIQ TO BOT    (W/M2 K)    9.3934E+01     1.2488E+04     6.0676E+02
Z-AVE LIQ TEMPERATURE   (K)         1.8662E+03     1.8218E+03     4.0062E+02
HT COEFF, LIQ TO TOP    (W/M2 K)    6.7001E+03     4.4003E+03     5.1897E+02
TOP CRUST THICKNESS     (M)         0.0000E+00     1.7888E-02     0.0000E+00

R-AVE LIQ TEMPERATURE   (K)         1.8657E+03     1.8103E+03     4.0062E+02
HT COEFF, LIQ TO SID    (W/M2 K)    1.0872E+02     6.1330E+03     1.0000E-10
SIDE CRUST THICKNESS    (M)         1.6688E-03     0.0000E+00     0.0000E+00

DECAY HEAT              (W)         9.6270E+06     1.4042E+06     0.0000E+00
HEAT TO CONCRETE        (W)         9.6984E+05     2.5290E+06     0.0000E+00
HEAT OF REACTION        (W)         0.0000E+00     3.5801E+06     0.0000E+00
INTERLAYER HEAT FLOW    (W)                6.2253E+06     1.0584E+07    -1.0185E+06
```

```
                                CORCON VERSION 2.28
TIME =  21600.00        BWR ACCIDENT - WATER ADDED AFTER 1 HOUR          IT. NO. = 360
                        ****INTERLAYER MIXING****

     LOWER MIXTURE LAYER

                                    OXIDE           METAL

PHASE MASSES              (KG)      8.5336E+02      6.0847E+04
PHASE DENSITIES           (KG/M3)   7.0653E+03      5.9306E+03
LIQUIDUS TEMPERATURE      (K)       1.9657E+03      1.7488E+03
SOLIDUS TEMPERATURE       (K)       2.7658E+03      1.7589E+03
PHASE ENTHALPIES          (J)      -4.5495E+09      8.5968E+10
MASS ENTRAINED            (KG)      0.0000E+00      0.0000E+00
MASS DE-ENTRAINED         (KG)      2.2460E+02      0.0000E+00
```

Table 6.4 Output listing for the BWR sample problem (continued)

```
                                        CORCON VERSION 2.28
TIME =  21600.00        BWR ACCIDENT - WATER ADDED AFTER 1 HOUR                    IT. NO. = 360
                                  * * * * *  V A N E S A  O U T P U T  * * * * *

 TEMPERATURE OF METAL (K)                              1.8102E+03
 TEMPERATURE OF OXIDE (K)                              1.8651E+03
 AEROSOL - AMBIENT CONDITIONS (G/CC)                   2.8787E-04
 AEROSOL - STANDARD STATE CONDITIONS (G/CC)            6.1913E-04
         ( 298.15 (K) AND 1 ATM. )
 GAS (G-MOLES/S)                                       4.1542E+00
 AEROSOL RATE (GRAMS/S)                                6.2927E+01
 AEROSOL DENSITY (G/CM3)                               2.0860E+00
 PARTICLE SIZE (MICROMETERS)                           1.3745E+00
 BUBBLE DIAMETER FOR THE METAL PHASE (CM)              1.0374E+00
 BUBBLE DIAMETER FOR THE OXIDE PHASE (CM)              1.0339E+00
 MECHANICAL RELEASES FROM THE AZBEL AND THE ISHII AND KATAOKA CORRELATIONS ARE CALCULATED.


  I            AEROSOL COMPOSITION   MELT COMPOSITION   LOSS(MOLES)     RELEASE FRACTION
                    (WEIGHT %)            (KG)
  2     FE                           3.7659E+04
  3     CR                           7.3899E+03
  4     NI          3.7655E-04       4.1029E+03        1.2108E-04      1.6701E-04
  5     MO          4.2806E-12       1.1993E+02        8.4229E-13      6.2810E-09
  6     RU          1.2218E-11       1.2704E+02        2.2821E-12      2.5288E-08
  7     SN          0.0000E+00       0.0000E+00        0.0000E+00      0.0000E+00
  8     SB          4.1977E-05       5.1631E-01        6.5087E-06      1.6227E-02
  9     TE          2.9383E-02       1.2054E+01        4.3472E-03      1.5452E-01
 10     AG          0.0000E+00       0.0000E+00        0.0000E+00      0.0000E+00
 11     MN          0.0000E+00       0.0000E+00        0.0000E+00      0.0000E+00
 12     CAO         1.8433E-01       1.9828E+03        6.2050E-02      1.6844E-02
 13     AL2O3       9.3835E-03       4.4114E+02        1.7373E-03      3.8163E-03
 14     NA2O        2.4104E+01       2.6281E+02        7.3418E+00      3.7452E-01
 15     K2O         5.5831E+01       8.8634E+02        1.1188E+01      2.7860E-01
 16     SIO2        1.9549E+01       2.2839E+03        6.1420E+00      5.1632E-02
 17     UO2         3.0218E-03       1.0583E+05        2.1128E-04      6.2333E-05
 18     ZRO2        1.1493E-03       5.0987E+04        1.7608E-04      2.4342E-06
 19     CS2O        1.9079E-01       2.3895E+01        1.2781E-02      5.5371E-02
 20     BAO         2.2665E-02       4.9810E+01        2.7903E-03      1.0961E-01
 21     SRO         3.1240E-02       3.5069E+01        5.6915E-03      1.8657E-01
 22     LA2O3       1.4953E-04       3.2729E+02        8.6637E-06      2.2607E-03
 23     CEO2        6.0783E-03       6.4539E+02        6.6667E-04      5.1273E-02
 24     NBO         5.8690E-08       2.5976E+00        1.0173E-08      3.2588E-06
 25     CSI         2.7115E-02       1.3306E+00        1.9702E-03      3.4451E-01
202     FEO         1.1144E-02       4.2591E+02        2.9281E-03      1.9968E-04
302     CR2O3       3.4217E-15       1.5192E-07        4.2500E-16      6.9257E-12
CARBON IN MELT                       0.0000E+00
ZIRCONIUM IN MELT                    5.8470E+03
```

Table 6.4 Output listing for the BWR sample problem (continued)

I		GAS COMPOSITION (WEIGHT %)	RELEASE RATE (GRAMS/SECOND)
1	H2O	2.1330E-04	1.5963E-04
2	H2	9.8371E+01	8.2380E+00
3	H	3.5088E-02	1.4693E-03
4	OH	5.9564E-09	4.2083E-09
5	O	1.5731E-12	1.0452E-12
6	O2	1.5013E-18	1.9957E-18
7	CO2	8.5647E-07	1.5658E-06
8	CO	1.5936E+00	1.8543E+00

Table 6.4 Output listing for the BWR sample problem (continued)

```
                                        CORCON VERSION 2.28
TIME =  21600.00        BWR ACCIDENT - WATER ADDED AFTER 1 HOUR                    IT. NO. = 360
                              ****** POOL  SCRUBBING ******

 INFORMATION SUPPLIED BY VANESA

 MEAN PARTICLE SIZE (UM)                          1.3745E+00
 AEROSOL RATE (GRAMS/S)                           6.2927E+01
 AEROSOL DENSITY (G/CM3)                          2.0860E+00
 POOL DEPTH (CM)                                  1.4079E+02
 POOL TEMPERATURE (K)                             4.0059E+02
 AMBIENT PRESSURE (ATM)                           2.5920E+00


    SIZE          CHARACTERISTIC      MASS        DECONTAMINATION
    RANGE             SIZE          IN RANGE        FACTOR
 0.000- 0.349        0.269        2.4603E+00      1.2788E+00
 0.349- 0.473        0.414        2.5011E+00      1.2580E+00
 0.473- 0.580        0.527        2.4694E+00      1.2742E+00
 0.580- 0.682        0.631        2.4099E+00      1.3056E+00
 0.682- 0.784        0.733        2.3309E+00      1.3498E+00
 0.784- 0.888        0.835        2.2346E+00      1.4080E+00
 0.888- 0.997        0.942        2.1214E+00      1.4832E+00
 0.997- 1.113        1.054        1.9911E+00      1.5802E+00
 1.113- 1.238        1.174        1.8430E+00      1.7072E+00
 1.238- 1.375        1.305        1.6766E+00      1.8766E+00
 1.375- 1.526        1.448        1.4916E+00      2.1093E+00
 1.526- 1.697        1.609        1.2886E+00      2.4417E+00
 1.697- 1.895        1.792        1.0694E+00      2.9422E+00
 1.895- 2.127        2.006        8.3838E-01      3.7529E+00
 2.127- 2.411        2.261        6.0389E-01      5.2101E+00
 2.411- 2.771        2.579        3.8021E-01      8.2753E+00
 2.771- 3.259        2.994        1.8933E-01      1.6618E+01
 3.259- 3.997        3.583        5.8834E-02      5.3478E+01
 3.997- 5.409        4.559        5.3661E-03      5.8632E+02
 5.409-******        7.033        1.0000E-06      2.8603E+06

 ------------------------------------------------------
 OVERALL DECONTAMINATION FACTOR                   2.2503
 MASS OUT                                         2.7964E+01

 FIT OF DECONTAMINATED AEROSOL TO LOG NORMAL
 NEW MEAN PARTICLE SIZE (UM)                        0.846
 RANGE (UM)                          0.805 -        0.888
 NEW GEOMETRIC STANDARD DEVIATION                   1.581
 RANGE (UM)                          1.742 -        1.435

 LINEAR CORRELATION COEFFICIENT                  0.969414
```

7.0 References

1. USNRC, Reactor Safety Study, NUREG-75-014, WASH-1400, 1975.

2. Murfin, W. B., A Preliminary Model for Core-Concrete Interactions, SAND77-0370, Sandia National Laboratories, Albuquerque, NM, 1977.

3. Muir, J. F., et al., CORCON-Mod1: An Improved Model for Molten-Core/Concrete Interactions, SAND80-2415, Sandia National Laboratories, Albuquerque, NM, 1981.

4. Cole, R. K., D. P. Kelly, and M. A. Ellis, CORCON-Mod2: A Computer Program for Analysis of Molten-Core Concrete Interactions, NUREG/CR-3920, SAND84-1246, Sandia National Laboratories, Albuquerque, NM, 1984.

5. ANSI, American National Standard Programming Language FORTRAN, X3.9-1978, American National Standards Institute, New York, NY, 1978.

6. Copus, E. R., R. E. Blose, J. E. Brockmann, R. D. Gomez, and D. A. Lucero, Core-Concrete Interactions Using Molten Steel with Zirconium on a Basaltic Basemat: The SURC-4 Experiment, NUREG/CR-4994, SAND87-2008, Sandia National Laboratories, Albuquerque, NM, 1989.

7. Murata, K. K., D. E. Carroll, K. E. Washington, F. Gelbard, G. D. Valdez, D. C. Williams, and K. D. Bergeron, User's Manual for CONTAIN 1.1: A Computer Code for Severe Nuclear Reactor Accident Containment Analysis, NUREG/CR-5026, SAND87-2309, Sandia National Laboratories, Albuquerque, NM, 1989.

8. Summers, R. M., et al., MELCOR 1.8.0: A Computer Code for Nuclear Reactor Severe Accident Source Term and Risk Assessment Analyses, NUREG/CR-5531, SAND90-0364, Sandia National Laboratories, Albuquerque, NM, 1991.

9. Greene, G. A. and R. A. Bari, International Standard Problem No. 24, SURC-4 Experiment on Core-Concrete Interactions, Vol. 2: Workshop Summary Report, Prepared by Brookhaven National Laboratory for the OECD Committee on the Safety of Nuclear Installations, June 1989.

10. Powers, D. A., J. E. Brockmann, and A. W. Shiver, VANESA: A Mechanistic Model of Radionuclide Release and Aerosol Generation During Core Debris Interactions With Concrete, NUREG/CR-4308, SAND85-1370, Sandia National Laboratories, Albuquerque, NM, 1986.

11. Light Water Reactor Safety Research Program Quarterly (or Semiannual) Report, Nuclear Fuel Cycle Program, Sandia National Laboratories, Albuquerque, NM.

    a. January - March 1976 — SAND76-0369
       September 1976
    b. October - December 1978 — SAND79-0820
       July 1979
    c. April - June 1979 — SAND79-2057
       April 1980
    d. January - March 1980 — SAND80-1304
       July 1980 — (1 of 4)
    e. January - March 1981 — SAND81-1214
       July 1981 — (1 of 4)
    f. April - September 1981 — SAND81-0006
       February 1992
    g. Oct 1981 - March 1982 — SAND82-1572
       December 1982
    h. April - September 1982 — SAND83-1576
       October 1983

12. Powers, D. A., et al., Exploratory Study of Molten Core Material/Concrete Interactions July 1975 - March 1977, SAND77-2042, Sandia National Laboratories, Albuquerque, NM, 1978.

13. Greene, G. A., "Heat, Mass, and Momentum Transfer in a Multi-Fluid Bubbling Pool," Advances in Heat Transfer, Vol. 21, pp. 270-345, 1991.

14. Nelson, L. S., M. J. Eatough, and K. P. Guay, Explosive Interactions Between Molten Aluminum and Aqueous Coolants, SAND88-2959, Sandia National Laboratories, Albuquerque, NM, 1989.

15. Blose, R. E., J. E. Gronager, A. J. Suo-Antilla, and J. E. Brockmann, SWISS: Sustained Heated Metallic Melt/Concrete Interactions With Overlying Water Pools, NUREG/CR-4727, SAND85-1546, Sandia National Laboratories, Albuquerque, NM, 1987.

16. Spencer, B. W., et al., MACE Scoping Test Data Report, MACE-TR-D03, Argonne National Laboratory, Argonne, IL, 1991.

17. Copus, E. R., et al., Simultaneous Interactions Between Molten Aluminum, Siliceous Concrete, and Overlying Water Pools: The SRL-3 Experiment, SAND92-0443, Sandia National Laboratories, Albuquerque, NM.

18. Greene, G. A., et al., "Some Observations on Simulated Molten Debris-Coolant Layer Dynamics," International Meeting on Light Water Reactor Severe Accident Evaluation, Cambridge, MA, September 1983.

19. Fauske & Associates, Inc., Technical Support for the Debris Coolability Requirements for Advanced Light Water Reactors in the Utility/EPRI Light Water Reactor Requirements Document, DOE/ID-10278, June 1990.

20. Thompson, D. H., and J. K. Fink, ACE MCCI Test L6 Test Data Report, Vols. 1 and 2, ACE-TR-C26 v.1 and v.2, Argonne National Laboratory, Argonne, IL, 1991.

21. Bennett, D. E., SANDIA-ORIGEN User's Manual, NUREG/CR-0987, SAND79-0299, Sandia National Laboratories, Albuquerque, NM, 1979.

22. Blottner, F. G., Hydrodynamics and Heat Transfer Characteristics of Liquid Pools with Bubble Agitation, NUREG/CR-0944, SAND79-1132, Sandia National Laboratories, Albuquerque, NM, 1979.

23. Konsetov, V. V., "Heat Transfer during Bubbling of Gas Through Liquid," International Journal of Heat Mass Transfer, Vol. 9, pp. 1103-1108, 1966.

24. Ginsberg, T. and G. A. Greene, "BNL Program in Support of LWR Degraded Core Accident Analysis," Proceedings of the 10th Water Reactor Safety Research Information Meeting, Vol. 2, NUREG/CP-0041, pp. 364-395, 1983.

25. Bradley, D. R., "Modeling of Heat Transfer Between Core Debris and Concrete," in ANS Proceedings of the 1988 National Heat Transfer Conference, Houston, TX, pp. 37-49, July 24-27, 1988.

26. Kutateladze, S. S., and I. G. Malenkov, "Boiling and Bubbling Heat Transfer Under Conditions of Free and Forced Convection," 6th International Heat Transfer Conference, Toronto, Canda, 1978.

27. Sokolov, V. N., and A. D. Salamakin, "Heat Exchange Between a Gas-Liquid System and a Heat Exchange Element," Zhurnal Prikladnoi Khimii (Journal of Applied Chemistry of the USSR), Vol. 35, No. 11, 1962.

28. Greene, G. A., and T. F. Irvine, "Heat Transfer Between Stratified Immiscible Liquid Layers Driven by Gas Bubbling Across the Interface," in ANS Proceedings of the 1988 National Heat Transfer Conference, Houston, TX, July 24-27, 1988.

29. Farmer, M. T., J. J. Sienicki, and B. W. Spencer, "CORQUENCH: A Model for Gas Sparging-Enhanced Melt-Water, Film Boiling Heat Transfer," ANS Special Session on Thermal Hydraulics of Severe Accidents, November 11-15, 1990.

30. McAdams, W. H., Heat Transmission, McGraw-Hill Book Co., New York, NY, 1954.

31. Kulacki, F. A., and R. J. Goldstein, "Thermal Convection in a Horizontal Fluid Layer with Uniform Volumetric Energy Source," Journal of Fluid Mechanics, Vol. 55, No. 2, p. 271, 1975.

32. Kulacki, F. A., and M. E. Nagle, Journal of Heat Transfer, Vol. 97, p. 204, 1975.

33. Kulacki, F. A., and A. A. Emara, Trans ANS, Vol. 22, p. 447, 1975.

34. Epstein, M., "Heat Conduction in the UO_2-Cladding Composite Body with Simultaneous Solidification and Melting," Nuclear Science and Engineering, Vol. 51, 1973.

35. Alsmeyer, H., and M. Reimann, "On the Heat and Mass Transport Processes of a Horizontal Melting or Decomposing Layer Under a Molten Pool," Nuclear Reactor Safety Heat Transfer, Winter Annual Meeting ASME, Atlanta, GA, pp. 47-53, 1977.

36. Berenson, P. J., "Transition Boiling Heat Transfer From a Horizontal Surface," Journal of Heat Transfer, Vol. 83, pp. 351-358, 1961.

37. Bergles, A. E., et al., Two-Phase Flow and Heat Transfer in the Power and Process Industries, McGraw Hill, New York, NY, 1981.

38. Keenan, J. H., et al., Steam Tables, Thermodynamic Properties of Water Including Vapor, Liquid, and Solid Phases (International System of Units-S.I.), John Wiley and Sons, New York, NY, 1978.

39. Rohsenow, W. M., "A Method of Correlating Heat Transfer for Surface Boiling of Liquids," Trans. ASME, Vol. 74, pp. 979-976, 1952.

40. Zuber, N., "On Stability of Boiling Heat Transfer," Trans. ASME, Vol. 80, pp. 711-720, 1958.

41. Zuber, N., et al., "The Hydrodynamic Crisis in Pool Boiling of Saturated and Subcooled Liquids," in International Developments in Heat Transfer, Part II, ASME, New York, NY, pp. 230-235, 1961.

42. Rohsenow, W. H., "Boiling," in Handbook of Heat Transfer, McGraw-Hill, New York, NY, pp. 13-28, 1973.

43. Ivey, H. J., "Acceleration and the Critical Heat Flux in Pool Boiling," Chartered Mechanical Engineering, Vol. 9, pp. 413-427, 1962.

44. Duignan, M. R., and G. A. Greene, "Enhanced Convective and Film Boiling Heat Transfer by Surface Injection," Diss., State University of New York at Stony Brook, NY, 1989.

45. Siviour, J. B., and A. J. Ede, "Heat Transfer in Subcooled Film Boiling," paper B3.12, in Proceedings of the Fourth International Heat Transfer Conference, Paris-Versailles, France, 1970.

46. Dhir, V. K. and G. P. Purohit, "Subcooled Film Voiling Heat Transfer from Spheres," Nuclear Engr. and Design, Vol. 47, 1978, pp. 49-66.

47. Toda, S., and M. Mori, "Subcooled Film Boiling and the Behavior of Vapor Film on a Horizontal Wire and Sphere," 7th International Heat Transfer Conference, Munich, Germany, pp. 173-178, 1982.

48. Bradfield, W. S., "On the Effect of Subcooling on Wall Superheat in Pool Boiling," Journal of Heat Transfer, pp. 269-270, 1967.

49. Cole, Jr., R. K., "A Crust Formation and Refreezing Model for Molten-Fuel/Concrete Interactions Codes," Paper 12.5, in Proceedings, International Meeting on Light Water Reactor Severe Accident Evaluation, Cambridge, MA, 1983.

50. Clift, R., J. R. Grace, and M. E. Weber, Bubbles, Drops, and Particles, Academic Press, New York, NY, 1978.

51. Mendelson, H. D., Journal of the American Institute of Chemical Engineering, Vol. 13, p. 250, 1967.

52. Davies, R. M., and G. I. Taylor, Proceedings of the Royal Society of London A, Vol. 200, p. 375, 1950.

53. Wallis, G. B., One-Dimensional, Two-Phase Flow, McGraw-Hill, New York, NY, 1969.

54. Brockmann, J. E., Validation of Models of Gas Holdup in the CORCON Code, NUREG/CR-5433, SAND89-1951, Sandia National Laboratories, Albuquerque, NM, 1989.

55. Davidson, J. F., and B. O. G. Schuler, Transactions of the Institute of Chemical Engineers, Vol. 38, pp. 144, 335, 1960.

56. Hosler, E. R., and J. W. Westwater, "Film Boiling on a Horizontal Plate," ARS Journal, pp. 553-558, April 1962.

57. Greene, G. A., J. C. Chen, and M. T. Conklin, "Onset of Entrainment Between Immiscible Liquid Layers Due to Rising Gas Bubbles," International Journal of Heat and Mass Transfer, Vol. 31, p. 1309, 1988.

58. Greene, G. A., J. C. Chen, and M. T. Conklin, "Bubble-Induced Entrainment Between Stratified Liquid Layers," International Journal of Heat and Mass Transfer, Vol. 34, p. 149, 1990.

59. Beard, K. V., and H. R. Pruppacher, "A Determination of the Terminal Velocity and Drag of Small Water Drops by Means of a Wind Tunnel," Journal of Atmospheric Science, Vol. 26, p. 1066, 1969.

60. Cheung, F. B., S. H. Chan, T. C. Chawla, and D. H. Cho, "Radiative Heat Transfer in a Heat Generating and Turbulent Convecting Fluid Layer," International Journal of Heat Mass Transfer, Vol. 23, pp. 1313-1323, 1980.

61. Kwong, K. C., R. A. S. Beck, and T. C. Derbidge, CORCON Program Assistance, FR-79-10/AS, ACUREX Corporation/Aerotherm Aerospace Systems Division, Mt. View, CA, 1979.

62. Van Zeggeren, F. H., and S. H. Storey, The Computation of Chemical Equilibrium, Cambridge University Press, Cambridge, 1970.

63. Bottinga, Y., D. F. Weill, and P. Richert, "Thermodynamic Modeling of Silicate Melts," Thermodynamics of Minerals and Melts, R. C. Newton, A. Navrotsky, and B. J. Wood, eds., Springer-Verlag, 1981.

64. Scheibel, E. G., "Physical Chemistry in Chemical Engineering," Ind. Eng. Chem., Vol. 46, p. 2007, 1954.

65. Wilke, C. R., and P. Chang, "Correlations of Diffusion Coefficients in Dilute Solutions," AICHE Journal, Vol. 1, p. 264, 1955.

66. Ziemniak, S. E., "A Study of Interfacial Resistance to Mass Transfer at High Evaporation Rates," Diss., Rennesselaer Polytechnic Institute, 1968.

67. Singh, P. C., and S. Singh, "Development of a New Correlation for Binary Gas Phase Diffusion Coefficients," International Commission on Heat Mass Transfer, Vol. 10, p. 123, 1983.

68. Kataoka, I, and M. Ishii, "Mechanistic Modeling of Pool Entrainment Phenomenon," International Journal of Heat Mass Transfer, Vol. 27, p. 1999, 1984.

69. Azbel, D. S., et al., "Acoustic Resonance Theory for the Rupture of Film Cap of a Gas Bubble at a Horizontal Gas-Liquid Interface," Two Phase Momentum, Heat and Mass Transfer in Chemical Process and Energy Engineering Systems, Vol. 1, Hemisphere Publishing Co., pp. 159-170, 1978.

70. Fuchs, N. A., The Mechanics of Aerosols, Pergamon Press, 1964.

71. Powers, D. A., and A. W. Frazier, VISRHO: A Computer Subroutine for Estimating the Viscosity and Density of Complex Silicate Melts, SAND76-0649, Sandia National Laboratories, Albuquerque, NM, 1977.

72. SNL, Core-Meltdown Experimental Review, NUREG-0205, SAND74-0382, Sandia National Laboratories, Albuquerque, NM, 1977.

73. Weast, R. C., Ed., Handbook of Chemistry and Physics, CRC Press, Cleveland, OH, 1976.

74. JANAF Thermochemical Tables, Physicochemical Studies, DOW Chemical USA, Midland, MI (including supplements).

75. Samsonov, G. V., ed., The Oxide Handbook, translated from Russian by C. N. Turton and T. I. Turton, IFI/Plenum Press, New York, NY, 1973.

76. Robie, R. A., B. S. Hemingway, and J. R. Fisher, Thermodynamic Properties of Minerals, Geological Survey Bulletin 1452, U. S. Department of Interior, U. S. Government Printing Office, Washington, DC, 1978.

77. Touloukian, Y. S., ed., Thermophysical Properties of Matter, The TPRC Data Series, Vols. 1-8, IFI/Plenum Press, New York, NY, 1970.

78. Kendell, J., and K. P. Monroe, "The Viscosity of Liquids, III Ideal Solution of Solids in Liquids," Journal of the American Chem. Soc., Vol. 39, No. 9, p. 1802, September 1917.

79. Shaw, H. R., "Viscosities of Magmatic Silicate Liquids: An Empirical Method of Prediction," American Journal of Science, Vol. 272, pp. 870-893, 1972.

80. Bottinga, Y., and D. F. Weill, "The Viscosity of Magmatic Silicate Liquids: A Model for Calculation," American Journal of Science, Vol. 272, pp. 438-475, 1972.

81. Ogino, Y., F. O. Borgmann, and M. G. Frohberg, "On the Viscosity of Liquid Iron," Japan Inst. of Metals Journ., Vol. 37, p. 1230, 1973.

82. Kunitz, M., Journal of General Physiology, Vol. 9, p. 715, 1926.

83. Parrott, J. E., and A. D. Stuckes, Thermal Conductivity of Solids, Pion Limited, London, England, 1975.

84. Nause, R. C., and M. T. Leonard, Thermophysical Property Assessment for Savannah River Site Production Reactor Materials, 89/6507, Science Applications International Corporation, Albuquerque, NM, 1989.

85. Speich, G. R., "Cr-Fe-Ni (Chromium-Iron Nickel), "Metals Handbook, Vol. 8, American Society for Metals, Metals Park, OH, p. 424, 1973.

DISTRIBUTION LIST

External Distribution:

25 U.S. Nuclear Regulatory Commission
Office of Nuclear Regulatory Research
Washington, DC 20555
Attn: B. W. Sheron, NLS-007
C. G. Tinkler, Jr. NLN-344
G. R. Marino, NLS-007
A. M. Rubin, NLN-344
R. B. Foulds, NLN-344
A. Notafrancesco, NLN-344
J. A. Murphy, NLS-007
S. Basu, NLN-344
E. S. Beckjord, NLS-007
F. Eltawila, NLN-344
T. P. Speis, NLS-007

5 U.S. Nuclear Regulatory Commission
Office of Nuclear Reactor Regulation
Washington, DC 20555
Attn: T. C. Murley, 12G18
F. P. Gillespie
A. C. Thadani, 8E2 (3)

2 U.S. Department of Energy
Albuquerque, New Mexico
P.O. 5400
Albuquerque, NM 87185
Attn: C. E. Garcia, Director

2 Electric Power Research Institute
3412 Hillview Avenue
Palo Alto, CA 94303
Attn: A. Machiel

3 Brookhaven National Laboratory
130 BNL
Upton, NY 11973
Attn: T. Pratt

3 Oak Ridge National Laboratory
P.O. Box Y
Oak Ridge, TN 37830
Attn: T. Kress

3 Argonne National Laboratory
9700 S. Cass Avenue
Argonne, IL 60439
Attn: B. Spencer

1 Nuclear Safety Oversight Commission
1133 15th Street, NW
Room 307
Washington, DC 20005
Attn: Cathy Anderson

1 Battelle Columbus Laboratory
505 King Avenue
Columbus, OH 43201
Attn: P. Cybulskis

1 UCLA Nuclear Energy Laboratory
405 Hilgaard Avenue
Los Angeles, CA 90024
Attn: I. Catton

1 Los Alamos National Laboratories
P.O. Box 1663
Los Alamos, NM 87545
Attn: M. Stevenson

1 University of Wisconsin
Nuclear Engineering Department
1500 Johnson Drive
Madison, WI 53706
Attn: M. L. Corradini

1 EG&G Idaho
Willo Creek Building, W-3
P.O. Box 1625
Idaho Falls, ID 83415
Attn: R. Hobbins

1 Battelle Pacific Northwest Laboratory
P.O. Box 999
Richland, WA 99352
Attn: M. Freshley

1 Department of Energy
Scientific and Tech. Info. Center
P.O. Box 62
Oak Ridge, TN 37831

1 Fauske and Associates, Inc.
16W070 West 83rd Street
Burr Ridge, IL 60952
Attn: R. Henry

1 IAEA
Division of Nuclear Reactor Safety
Wagranesrstrasse 5
P.O. Box 100
A/1400 Vienna
AUSTRIA
Attn: M. Jankowski

1 Department LWR Fuel
Belgonuucleaire
Rue de Champde Mars. 25
B-1050 Brussels
BELGIUM
Attn: Mr. H. Bairiot, Chief

1 U.S. Nuclear Regulatory Commission
Advising Comm. on Reactor Safeguard
Washington, DC 20555
Attn: M. D. Houston, P-315

1 Atomic Energy Canada, Ltd.
Chalk River, Ontario
CANADA KOJ IJO
Attn: R. D. MacDonald

1 Institute of Nuclear Energy Research
P.O. Box 3
Lungtan
Taiwan 325
REPUBLIC OF CHINA
Attn: Sen-I Chang

1 Department of Nuclear Safety
Finnish Center for Radiation
and Nuclear Safety
P.O. Box 268
SF-00181 Helsinki
FINLAND
Attn: Jorma V. Sandberg

1 CEN Cadarache
18108 Saint Paul Lez Durance
FRANCE
Attn: A. Meyer-Heine

1 Energy Research Inc.
P. O. Box 2034
Rockville, MD 20847-2034
Attn: Dr. Mohsen Khatib Rahbar

1 Centre d'Estudes Nuclearies (IPSN-DAS)
Commisariat a l'Energie Atomique
Boite Postale No. 6
F-92265 Fontenay-aux-Roses Cedex
FRANCE
Attn: Jacques Duco

2 Gesellschaft fur Reaktorsicherheit
(GRS)
Postfach 101650
Glockengrasse 2
5000 Koeln 1
GERMANY
Attn: Dr. Ing. Manfred Fimhaber

1 Kraftwerk Union
Hammerbacher Strasse 1214
Postfach 3220
D-8520 Erlangen 2
GERMANY
Attn: Dr. M. Peeks

2 Kernforschungszentrum Karlsruhe
Postfach 3640
75 Karlsruhe
GERMANY
Attn: S. Hagen

2 Japan Atomic Energy Research Institute
Tokai-Mura, Naka-Gun
Ibaraki-Ken 319-11
JAPAN
Attn: K. Soda

1 Reactor Centrum Nederland
1755 ZG Petten
THE NETHERLANDS
Attn: Dr. K. J. Brinkman

1 I. V. Kurchatov Institute
of Atomic Energy
Nuclear Safety Department
Moscow, 123182
RUSSIA
Attn: V. Asmalov

1 Sub. Emplazamientos y Programas
Consejo de Seguridad Nuclear
Justo Dorado II
28040 Madrid
SPAIN
Attn: Jose Angel Martinez

1 Consejo de Seguridad Nuckan
SOR Angela de la Cruz No. 3
Madrid
SPAIN
Attn: Juan Bagues

1 Nucleare e della Protezione
Sanitaria (DISP)
Ente Nazionnle Energie
Alternative 7 (ENEA)
Viale Regina Margherita, 125
Casella Postale M. 2358
I-00100 Roma A.D.
ITALY
Attn: Mr. G. Petrangeli

1 Thermodynamics & Rad. Physics
CEC Joint Research Center, Ispra
I-21020 Ispra (Varese)
ITALY
Attn: Alan V. Jones

2 Statens Karnkraftinspektion
P.O. Box 27106
S-10252 Stockholm
SWEDEN
Attn: W. Frid

1 E.T.S. Ingenieros Industriales
Jost Gutierrez Abascal, 2
28006 Madrid
SPAIN
Attn: Professor Agustin Alonso

1 Department of Nuclear Power Safety
Royal Institute of Technology
S-100 11 Stockholm
SWEDEN
Attn: B. Raj Sehgal

1 UKAEA Culham Laboratory
Abingdon
Oxfordshire OX14 3DB
UNITED KINGDOM
Attn: B. D. Turland E5.157

1 Light Water Reactor Safety Program
Paul Scherrer Institute
CH-5232 Villigen PSI
SWITZERLAND
Attn: J. Peter Hosemann

1 Swiss Federal Nuclear Safety Directorate
CH-5303 Wurenlingen
SWITZERLAND
Attn: S. Chakraborty

1 Korea Atomic Energy Research Inst.
Korea Adv. Energy Research Inst.
P.O. Box 7
Daeduk-Danji
TAEJAN 305-606
Attn: Mr. Hee Dong Kim

2 UKAEA
Winfrith, Dorchester
Dorset DT2 8DH
UNITED KINGDOM
Attn: A. Nichols 102/A50
S. Kinnersly 204/A32

Sandia Distribution:

1810 D. W. Schaeffer
6400 N. R. Ortiz
6403 W. A. von Riesemann
6404 D. A. Powers
6418 R. K. Cole
6418 S. L. Thompson
6422 M. D. Allen
6422 R. E. Blose
6422 J. E. Brockmann
6422 M. Pilch
6423 K. O. Reil
6429 R. O. Griffith
6429 K. K. Murata
6429 K. E. Washington (5)
7141 Technical Library (5)
7151 Technical Publications
7613 Document Processing for DOE/OSTI (10)
8523-2 Central Technical Files

DATE
FILMED
1/7/94
END